

A security framework for quantum key distribution with imperfect sources

Guillermo Currás-Lorenzo,^{1, 2, 3, 4,*} Margarida Pereira,^{1, 2, 3, 4} Go Kato,⁵ Marcos Curty,^{2, 3, 4} and Kiyoshi Tamaki¹

¹Faculty of Engineering, University of Toyama, Gofuku 3190, Toyama 930-8555, Japan

²Vigo Quantum Communication Center, University of Vigo, Vigo E-36310, Spain

³Escuela de Ingeniería de Telecomunicación, Department of Signal

Theory and Communications, University of Vigo, Vigo E-36310, Spain

⁴atlanTTic Research Center, University of Vigo, Vigo E-36310, Spain

⁵National Institute of Information and Communications Technology, Nukui-kita, Koganei, Tokyo 184-8795 Japan

Imperfect bit-and-basis encoders compromise the security of quantum key distribution (QKD) systems via modulation flaws, side channels and inter-pulse correlations, which invalidate standard security proofs. Existing results addressing such imperfections suffer from critical limitations: they either consider only specific flaws, offer an unreasonably poor performance, or require the protocol to be run very slowly. Here, we present a finite-key security proof approach against coherent attacks that incorporates general bit-and-basis encoding imperfections (including modulation flaws, side channels and inter-pulse correlations) while achieving significantly better performances than previous approaches and requiring only partial characterization.

I. INTRODUCTION

Quantum key distribution (QKD) can theoretically achieve the Holy Grail of cryptography, unconditional security against eavesdropping. However, in practice, discrepancies between the mathematical models assumed in security proofs and the actual functioning of the devices used in implementations prevent it from reaching this goal. Device-independent QKD [1–3] is currently not a satisfactory solution to this problem, as its performance is extremely poor [4–7] and, in any case, its security proofs assume that the user devices leak absolutely no information to the outside [8, 9]. On the other hand, measurement-device-independent (MDI) QKD [10] provides a practical approach to guarantee security with arbitrarily flawed receivers while achieving high performance. Thus, the remaining challenge is ensuring the security of QKD with imperfect sources, such as sources that suffer from imperfections and side channels in the encoding of bit-and-basis information.

So far, all efforts in this regard [11–16] have come at a price; some proofs are suitable only for particular encoding imperfections such as qubit flaws [14], while others severely compromise the system’s performance, i.e., its repetition rate [15–18] and maximum achievable distance [11–13] (see *Discussion*). Here, we overcome these crucial problems by presenting a security proof in the finite-key regime against coherent attacks that can incorporate bit-and-basis encoding imperfections and side channels while achieving much higher performances than previous approaches. Our approach unifies ideas from the quantum coin [11–13] and loss-tolerant [14] security analyses in a way that naturally preserves their respective advantages—including their validity against the most general attacks allowed by quantum mechanics without any sequential restrictions—while overcoming their re-

spective limitations. Moreover, our proof requires only partial state characterization, which facilitates its application to real-life implementations.

II. RESULTS

A. Partial state characterization assumption

For ease of discussion, in the main text, we present our security proof approach by considering its application to an imperfect BB84 [19] protocol; in the Supplementary Information, we provide a general description of our approach, and explicitly show how to apply it to other schemes. More precisely, here we consider that, in each round k , the sender (Alice) probabilistically selects a setting $j \in \{0_Z, 1_Z, 0_X, 1_X\}$ and sends a signal in the state $\rho_j^{(k)}$ to the receiver (Bob). The states $\rho_j^{(k)}$ are partially characterized: they are known to be ϵ -close (in terms of fidelity) to some characterized states $\{|\phi_j\rangle_B\}_j$, i.e.,

$$\langle \phi_j | \rho_j^{(k)} | \phi_j \rangle_B \geq 1 - \epsilon, \quad (1)$$

for known $0 \leq \epsilon \leq 1$, which could more generally depend on j . In this discussion, for concreteness, we will assume that $\{|\phi_j\rangle_B\}_j$ is any set of qubit states, including flawed versions of the eigenstates $|j\rangle_B$ of the Pauli operators. We remark, however, that $\{|\phi_j\rangle_B\}_j$ could more generally be *any* set of characterized states (see Appendix A 4).

We refer to the deviation between $|\phi_j\rangle_B$ and $|j\rangle_B$ as the qubit flaw, and to the deviation between $\rho_j^{(k)}$ and $|\phi_j\rangle_B$ as the side channel. Equation (1) is general in that it is not necessary to specify the cause for a non-zero ϵ ; it can cover *any* kind of practical passive information leakage, such as those due to mode dependencies [20–22], electromagnetic or acoustic radiation [23], or power consumption [24]; and *any* kind of practical active information leakage, such as those due to Trojan-horse attacks (THAs) [15, 16, 25–27]. The partial state characterization assumed by our security proof is useful because some

* gcurras@vqcc.uvigo.es

imperfections could in principle live in arbitrarily high-dimensional spaces, making it extremely challenging to fully characterize them in practice.

In our main text discussion, for concreteness, we will consider that the emitted states are pure, and we will not mark their possible dependence on the round k , i.e., we will assume that $\rho_j^{(k)} = |\psi_j\rangle\langle\psi_j|_B$. However, we remark that our security proof is directly applicable even if the emitted states are mixed and/or different for different rounds k , as long as Eq. (1) holds (see Appendix A 1). We also remark that our security proof is applicable even if the emitted states are correlated, although in this case, one needs to consider a modification to Eq. (1) and to the post-processing step of the protocol (see Appendix A 3).

Due to Eq. (1), the emitted states $|\psi_j\rangle_B$, which we denote by $|\psi_j(\epsilon_j)\rangle_B$ hereafter, can be expressed as [15]

$$|\psi_j(\epsilon_j)\rangle_B = \sqrt{1 - \epsilon_j} |\phi_j\rangle_B + \sqrt{\epsilon_j} |\phi_j^\perp\rangle_B, \quad (2)$$

which is simply a state expansion in the basis $\{|\phi_j\rangle_B, |\phi_j^\perp\rangle_B\}$. Here, $0 \leq \epsilon_j \leq \epsilon$, and $|\phi_j^\perp\rangle_B$ could be *any* state orthogonal to $|\phi_j\rangle_B$, which implies that $\{|\psi_j(\epsilon_j)\rangle_B\}_j$ could be linearly independent when $\epsilon \neq 0$. Importantly, this fact makes the system inherently vulnerable to channel loss, as Eve could exploit it to enhance the distinguishability of the emitted states caused by the side channels. For example, she could perform an unambiguous state discrimination (USD) [28] measurement and ensure that conclusive (inconclusive) events result (do not result) in detections. This implies that, if ϵ and the observed channel loss are high enough, Eve could have learned Alice's setting choices for all detected rounds without introducing any errors, and no security proof can provide a positive key rate. On the other hand, qubit flaws do not cause this vulnerability, as in their presence $\{|\psi_j(0)\rangle_B\}_j$ remain linearly dependent, and there is no USD measurement for linearly dependent qubit states.

Side channels and qubit flaws are thus qualitatively different, and to achieve the best possible performance, security proofs should treat them differently. However, so far, no security proof achieves this satisfactorily. The loss-tolerant (LT) analysis [14] deals with qubit flaws tightly, and in fact shows that they have almost no impact on the secret-key rate, but cannot be applied in the presence of side channels, i.e., when $\epsilon > 0$. Conversely, the quantum coin analysis [11–13] can be applied in the presence of both qubit flaws and side channels, but does not take into account their qualitative difference, and thus offers an extremely pessimistic performance for the former. Meanwhile, recent attempts to combine the strengths of both analyses, such as the reference technique (RT) [16] (see also [15]), require an additional sequential assumption [17, 25, 29] that restricts the repetition rate at which the protocol can be run, severely reducing the secret-key rate obtainable in practice.

B. Security analysis

Here, we introduce a security proof approach that solves all of these drawbacks. To illustrate how, in this discussion, we consider a particular instance in which the qubit components can be expressed as

$$|\psi_j(0)\rangle_B = |\phi_j\rangle_B = \cos(\theta_j) |0_Z\rangle_B + \sin(\theta_j) |1_Z\rangle_B, \quad (3)$$

where $\theta_j = (1 + \delta/\pi)\varphi_j/2$, $\varphi_j \in \{0, \pi, \pi/2, 3\pi/2\}$ for $j \in \{0_Z, 1_Z, 0_X, 1_X\}$, and $\delta \in [0, \pi)$ represents the magnitude of the qubit flaws. We emphasize that this is just a specific example for illustration purposes, and that our general security proof, presented in the Supplementary Information, can be applied regardless of the specific form of the states $\{|\phi_j\rangle_B\}_j$. Moreover, without loss of generality (see Supplementary Information), we consider that $\epsilon_j = \epsilon$ for all j . The sifted key is generated from the detected key rounds, i.e., the rounds in which both Alice and Bob select the Z basis and Bob obtains a bit value. In these rounds, instead of emitting $|\psi_{0_Z}(\epsilon)\rangle_B$ and $|\psi_{1_Z}(\epsilon)\rangle_B$ randomly, Alice could have generated the entangled state

$$|\Psi_Z(\epsilon)\rangle_{AB} = \frac{1}{\sqrt{2}} (|0_Z\rangle_A |\psi_{0_Z}(\epsilon)\rangle_B + |1_Z\rangle_A |\psi_{1_Z}(\epsilon)\rangle_B), \quad (4)$$

and measured the ancillary system A in the Z basis. The amount of privacy amplification that needs to be applied to turn the sifted key into a secret key is directly related to the phase-error rate e_{ph} , which is defined as the error rate that Alice and Bob would have observed if, in the detected key rounds, Alice had measured system A in the X basis (X_A), complementary to the Z basis, and Bob had used his actual X -basis measurement (X_B). This is the case for security proofs based on the leftover hashing lemma with the entropic uncertainty relation [30–34], and for those based on phase-error correction [13, 35–37], which have been shown to be essentially equivalent [38].

The phase-error rate cannot be observed directly, and the goal of the security proof is to estimate it using the data obtained in the experiment. A common approach is to use the observed X -basis bit-error rate e_X . By noting that Alice could have replaced her X -basis emissions by the generation of

$$|\Psi_X(\epsilon)\rangle_{AB} = \frac{1}{\sqrt{2}} (|0_X\rangle_A |\psi_{0_X}(\epsilon)\rangle_B - |1_X\rangle_A |\psi_{1_X}(\epsilon)\rangle_B), \quad (5)$$

one can define e_{ph} and e_X as the error rates associated to the measurement of X_A and X_B on the detected rounds in which Alice prepares $|\Psi_Z(\epsilon)\rangle_{AB}$ and $|\Psi_X(\epsilon)\rangle_{AB}$, respectively. If δ and ϵ are close to zero, $|\Psi_Z(\epsilon)\rangle_{AB}$ and $|\Psi_X(\epsilon)\rangle_{AB}$ are close to each other, implying that e_{ph} and e_X should also be relatively similar. This intuition was formalized in [11–13] by introducing the quantum coin state

$$\frac{1}{\sqrt{2}} (|0_Z\rangle_C |\Psi_Z(\epsilon)\rangle_{AB} + |1_Z\rangle_C |\Psi_X(\epsilon)\rangle_{AB}), \quad (6)$$

and then considering that Alice probabilistically selects one of the complementary bases Z_C or X_C to measure the coin C . In particular, these works showed that the deviation between e_{ph} and e_X can be bounded by a function of the fraction of events in which Alice obtained $X_C = 1$ amongst the detected events in which she selected X_C . Of course, since in the real protocol Alice's coin is actually classical, this fraction cannot be observed. Instead, it can be upper bounded by considering the *a priori* probability that Alice obtains $X_C = 1$, given by $\frac{1}{2}(1 - \text{Re} \langle \Psi_Z(\epsilon) | \Psi_X(\epsilon) \rangle_{AB})$, and assuming the worst-case scenario in which all events such that $X_C = 1$ are detected. However, the need to assume this scenario leads to a bound on e_{ph} whose tightness deteriorates as the channel loss increases. The speed at which this occurs depends on the probability to obtain $X_C = 1$, which grows with both δ and ϵ . In the case of ϵ , this behaviour is expected, as the effect of the side channels can be enhanced by Eve in the presence of loss. However, as previously discussed, this is not the case for qubit flaws, leading to a very loose bound when $\delta > 0$. The solution to this limitation is the key to our security proof, and to understand it, it is helpful to first review the LT analysis, which is tight for $\delta > 0$ but only valid when $\epsilon = 0$.

The main idea of the LT analysis is to consider the state resulting from the measurement of X_A on $|\Psi_Z(0)\rangle_{AB}$ by re-expressing $|\Psi_Z(0)\rangle_{AB} = \sqrt{1-q_0}|0_X\rangle_A|\psi_{\text{vir}0}(0)\rangle_B + \sqrt{q_0}|1_X\rangle_A|\psi_{\text{vir}1}(0)\rangle_B$ with $q_0 = \frac{1}{2}(1 - \text{Re} \langle \psi_{0Z}(0) | \psi_{1Z}(0) \rangle_B)$; we call $|\psi_{\text{vir}\beta}(0)\rangle_B$ ($\beta \in \{0, 1\}$) the virtual states. That is, Alice emits $|\psi_{\text{vir}0}(0)\rangle_B$ ($|\psi_{\text{vir}1}(0)\rangle_B$) with probability $1 - q_0$ (q_0), and the estimation of the phase-error rate is reduced to the task of estimating the X_B detection statistics of these virtual states. By using the fact that when $\epsilon = 0$ the emitted states are qubit states, one can always find an operator form linear relationship between the actual states and the virtual states. We remark that these linear relationships can always be derived regardless of the form of the qubit states $\{|\psi_j(0)\rangle_B\}_j$; the general procedure to do so can be found in [39, Appendix B] and is discussed in our Supplementary Information. When the qubit states have the particular form in Eq. (3), one such linear relationship is given by

$$|\psi_{\text{vir}0}(0)\rangle\langle\psi_{\text{vir}0}(0)|_B = |\psi_{0X}(0)\rangle\langle\psi_{0X}(0)|_B, \quad (7)$$

$$\begin{aligned} c_1 |\psi_{0Z}(0)\rangle\langle\psi_{0Z}(0)|_B + |\psi_{\text{vir}1}(0)\rangle\langle\psi_{\text{vir}1}(0)|_B \\ = c_2 |\psi_{1Z}(0)\rangle\langle\psi_{1Z}(0)|_B + c_3 |\psi_{1X}(0)\rangle\langle\psi_{1X}(0)|_B, \end{aligned} \quad (8)$$

where

$$\begin{aligned} c_1 &:= \frac{\cos(\kappa\pi/2)}{\cos(\kappa\pi) - \cos(\kappa\pi/2)}, \\ c_2 &:= \frac{\cos(\kappa\pi/2)}{\cos(\kappa\pi/2) - 1}, \\ c_3 &:= \frac{1 + \cos(\kappa\pi/2)}{\cos(\kappa\pi/2) - \cos(\kappa\pi)}. \end{aligned} \quad (9)$$

with $\kappa = 1 + \delta/\pi$. The existence of such linear relationships implies that the X_B detection statistics of the virtual states can be determined *exactly* using the observed X_B detection statistics of the actual states, including basis-mismatched events. As a result, the LT analysis allows a tight estimation of e_{ph} even in the presence of high loss, and offers a key rate that is almost independent of δ when $\epsilon = 0$.

The key idea of our proof to extend this behaviour to the case $\epsilon > 0$ is to combine the quantum coin analysis and the LT analysis through the notion of the target and reference states introduced by the RT [16]. Note that, when $\epsilon > 0$, the relationships in Eqs. (7) and (8) do not hold exactly, but do still hold approximately if $\epsilon \approx 0$, irrespectively of the value of δ . We use this fact to construct a quantum coin state for which the probability to obtain $X_C = 1$ is almost independent of δ .

First of all, rather than considering $|\Psi_Z(\epsilon)\rangle_{AB}$, which is a purification of a convex combination of $|\psi_{\text{vir}0}(\epsilon)\rangle\langle\psi_{\text{vir}0}(\epsilon)|_B$ and $|\psi_{\text{vir}1}(\epsilon)\rangle\langle\psi_{\text{vir}1}(\epsilon)|_B$ taken according to the probabilities $1 - q_\epsilon$ and $q_\epsilon = \frac{1}{2}(1 - \text{Re} \langle \psi_{0Z}(\epsilon) | \psi_{1Z}(\epsilon) \rangle_B)$; we consider instead a purification of a convex combination of the LHS of Eqs. (7) and (8) taken according to these probabilities (followed by normalization), i.e.,

$$\begin{aligned} |\Psi_{\text{Tar}}(\epsilon)\rangle_{DAB} &= \frac{1}{\sqrt{1 + c_1 q_\epsilon}} \left[\sqrt{1 - q_\epsilon} |0\rangle_D |0\rangle_A |\psi_{\text{vir}0}(\epsilon)\rangle_B \right. \\ &\quad \left. + \sqrt{q_\epsilon} |1\rangle_D \left(\sqrt{c_1} |0\rangle_A |\psi_{0Z}(\epsilon)\rangle_B + |1\rangle_A |\psi_{\text{vir}1}(\epsilon)\rangle_B \right) \right]. \end{aligned} \quad (10)$$

Then, we define the target statistics as the error rate associated to the measurement $\{|0\rangle_D, |1\rangle_D\}$ and X_B on the detected rounds after Eve's attack, i.e., the statistics of the outcomes $(|0\rangle_D, X_B = 1)$ and $(|1\rangle_D, X_B = 0)$. Note that, since this measurement commutes with the measurement $\{|0\rangle_A, |1\rangle_A\}$, the target statistics can be regarded as a mixture of the phase-error statistics and the statistics of the events in which Alice emits $|\psi_{0Z}(\epsilon)\rangle_B$ and Bob obtains $X_B = 0$, with the latter being observed in the actual protocol. Therefore, if we can estimate the overall target statistics, we can estimate the phase-error rate.

To do so, we consider a purification of a similar convex combination of the RHS of Eqs. (7) and (8), i.e.,

$$\begin{aligned} |\Psi_{\text{Ref}}(\epsilon)\rangle_{DAB} &= \frac{1}{\sqrt{1 + c_1 q_\epsilon}} \left[\sqrt{1 - q_\epsilon} |0\rangle_D |0\rangle_A |\psi_{0X}(\epsilon)\rangle_B \right. \\ &\quad \left. + \sqrt{q_\epsilon} |1\rangle_D \left(\sqrt{c_2} |0'\rangle_A |\psi_{1Z}(\epsilon)\rangle_B + \sqrt{c_3} |1'\rangle_A |\psi_{1X}(\epsilon)\rangle_B \right) \right], \end{aligned} \quad (11)$$

where the orthonormal basis $\{|0'\rangle_A, |1'\rangle_A\}$ has been chosen such that $|\Psi_{\text{Tar}}(0)\rangle_{DAB} = |\Psi_{\text{Ref}}(0)\rangle_{DAB}$, which is always possible due to the equality in Eq. (8). As before, we define the reference statistics as the error rate of the measurement $\{|0\rangle_D, |1\rangle_D\}$ and X_B on the detected rounds after Eve's attack. Since this measurement commutes with the measurement $\{|0'\rangle_A, |1'\rangle_A\}$, the reference

statistics can be regarded as a mixture of the statistics of the events in which Alice emits $|\psi_{0_X}(\epsilon)\rangle_B$ and Bob obtains $X_B = 1$, and the events in which Alice emits $|\psi_{1_Z}(\epsilon)\rangle_B$ or $|\psi_{1_X}(\epsilon)\rangle_B$ and Bob obtains $X_B = 0$, all of which are observed. In other words, the reference statistics can be determined using the data acquired in the actual protocol.

Finally, we define the loss-tolerant quantum coin state as

$$|\Psi_{\text{LTcoin}}(\epsilon)\rangle_{CDAB} = \frac{1}{\sqrt{2}} (|0_Z\rangle_C |\Psi_{\text{Tar}}(\epsilon)\rangle_{DAB} + |1_Z\rangle_C |\Psi_{\text{Ref}}(\epsilon)\rangle_{DAB}), \quad (12)$$

and bound the deviation between the target and reference statistics by considering the probability to obtain $X_C = 1$, given by $\frac{1}{2}(1 - \text{Re} \langle \Psi_{\text{Tar}}(\epsilon) | \Psi_{\text{Ref}}(\epsilon) \rangle_{DAB})$. When $\delta > 0$, the resulting bound on the phase-error rate is much tighter than in the original quantum coin analysis, since $\text{Re} \langle \Psi_{\text{Tar}}(\epsilon) | \Psi_{\text{Ref}}(\epsilon) \rangle_{DAB}$ is almost independent of δ , while $\text{Re} \langle \Psi_Z(\epsilon) | \Psi_X(\epsilon) \rangle_{DAB}$ decreases rapidly as δ increases.

To turn the above argument into a full security proof against general attacks, there remains a loose end to tie up. Unlike in the original quantum coin analysis, it is not possible to assume here that Alice replaces her actual source by the generation of Eq. (12) in all rounds, since the statistics of Alice's source differ in general from those of Eq. (12). Instead, we consider that Alice randomly samples her emissions, where the sampling probabilities depend on her emitted state and are chosen such that a sampled emission is equivalent to that originating from Eq. (12). As shown in the Supplementary Information, this allows us to apply the above analysis to estimate the number of phase errors within the sampled rounds, and then extend this estimate to all rounds via known statistical results, thus obtaining a bound on the overall phase-error rate that is valid even in the finite-key regime. We note that the proof merely relies on the idea that Alice *could* in principle sample her emissions; in the actual experiment, however, Alice does not actually need to perform this sampling step, nor to decide which sampled rounds correspond to measuring the quantum coin in the Z_C or X_C bases. The latter is another improvement over the original quantum coin analysis, which requires Alice to actually assign each round of the protocol to either the Z_C or X_C basis, and discard the data of the rounds assigned to X_C [40].

A critical advantage of our security proof is that it allows the protocol to be run at high repetition rates, unlike some previous approaches that address source imperfections. In particular, the RT [16], while sharing many of the advantages of our approach (including the ability to incorporate side channels and resilience to qubit flaws), requires the assumption that the probability that Alice selects a particular bit and basis choice in round k must be independent of Bob's previous $k - 1$ measurement outcomes. This independence condition can only be

guaranteed if Eve's attack is sequential, that is, if she is prevented from correlating Bob's measurement outcomes with Alice's setting choices in later rounds. In practice, enforcing this sequential condition requires running the protocol slowly such that Alice's emitted pulses could not possibly have influenced Bob's previous outcomes, even if Eve wanted to correlate them.

In contrast, our security proof directly guarantees security against the most general attacks allowed by quantum mechanics without any sequential restrictions, thus enabling high-speed operation. The key technical insight is that our proof is based on bounding the deviation between the reference and target statistics by considering that Alice generates the quantum coin state in Eq. (12), and then deriving a quantum coin inequality through the application of the Bloch sphere bound to each coin system C . To derive this inequality, we consider that Eve performs a coherent attack on all rounds simultaneously, after which Bob performs basis-independent quantum non-demolition measurements to determine which rounds are detected, and then Alice and Bob measure the systems corresponding to the detected rounds. Crucially, the coin system C corresponding to any particular detected round k always remains a qubit system, even when conditioning on Eve's global attack, on Bob's detection outcomes for all rounds, and on all of Alice's and Bob's previous measurement outcomes in detected rounds 1 through $k - 1$. As a result, we obtain a quantum coin inequality that relates the expectation values for the outcomes on round k conditional on any outcomes in rounds 1 through $k - 1$. We then apply concentration inequalities such as Azuma's inequality or Kato's inequality [41] to relate the conditional expectations to the actual statistics observed in the protocol. Importantly, all our proof steps hold regardless of any correlations Eve might introduce between rounds.

We remark that, while in this section we have focused on the prepare-and-measure BB84 protocol for clarity, our security proof approach is broadly applicable to other QKD protocols as well. For example, it can be directly extended to standard MDI-QKD [10]. Since MDI-QKD eliminates all detector side channels while our proof addresses transmitter imperfections, combining these approaches enables security against both source and measurement device imperfections. The extension to MDI-QKD follows naturally because the bit-and-basis encoding imperfections at each transmitter can be incorporated using the same loss-tolerant quantum coin technique described above. Furthermore, our approach can be applied to other protocols, including three-state protocols and even an MDI-type protocol in which the users send non-phase-randomized coherent states [26], demonstrating the versatility of our techniques. For the full analysis of these scenarios, see Supplementary Information.

III. DISCUSSION

Now, we apply our loss-tolerant quantum coin analysis to evaluate the secret-key rate obtainable for BB84-type protocols in the presence of both qubit flaws and side channels, and discuss our findings by drawing a comparison with previous analyses. For the simulations, we assume the following parameters: error correction inefficiency $f = 1.16$, detector dark count probability $p_d = 10^{-8}$ [9, 42], detector efficiency $\eta_d = 0.73$ [42], and a repetition rate of 2.5 GHz [43].

In Fig. 1, we plot the achievable secret-key rate in bits per second for both the BB84 and three-state protocols when using our analysis. We consider $\delta = 0.063$, following the experimental results reported in [21, 44], and several values of ϵ . For both protocols, the key rate is sensitive to the value of ϵ , which is expected, as higher values of ϵ make it easier for Eve to discriminate the emitted states in the presence of channel loss. When $\epsilon = 0$, both protocols offer the same secret-key rate, as already known [14]. However, consistently with previous results [25], we find that, for $\epsilon > 0$, the additional state emitted in the BB84 protocol results in a tighter phase-error rate estimation, which translates to higher key rates.

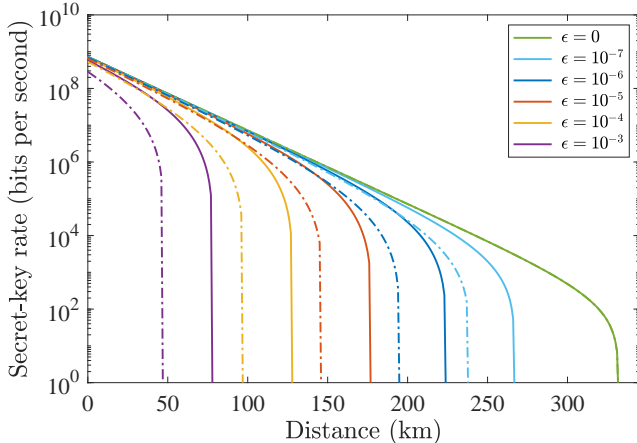


Figure 1. Asymptotic secret-key rate obtainable using our proof as a function of the distance (km) for the BB84 (solid lines) and three-state (dashed-dotted lines) protocols. We assume $\delta = 0.063$ [21, 44] and consider several values of ϵ .

In Fig. 2, we compare the secret-key rate obtainable using our proof with that of the original quantum coin analysis [11–13] and the RT analysis [16, 25]. We consider the BB84 protocol, since the original quantum coin analysis cannot provide any key for the three-state protocol. Also, we fix $\epsilon = 10^{-6}$, and consider the presence ($\delta = 0.063$) and absence ($\delta = 0$) of qubit flaws. When there are no qubit flaws, our proof converges to the original quantum coin analysis. However, in their presence, the secret-key rate offered by our proof decreases only very slightly, while that of the original quantum coin analysis decreases dramatically. As already mentioned, applying the RT requires running the protocol sequen-

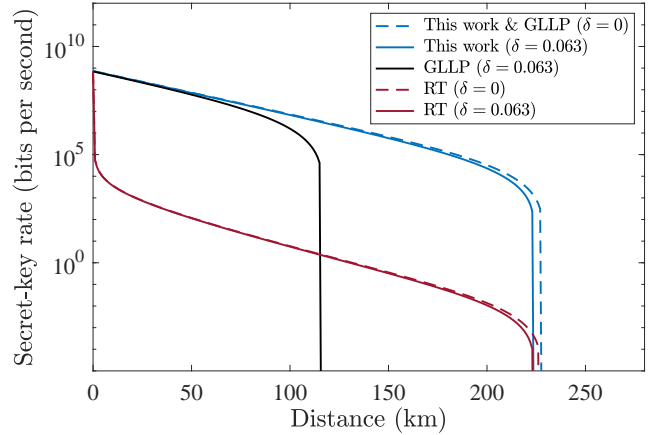


Figure 2. Asymptotic secret-key rate obtainable using our proof as a function of the distance (km) for the BB84 protocol, compared with that of the original quantum coin (GLLP) [11–13] and reference technique (RT) [16, 25] analyses. We consider the values $\epsilon = 10^{-6}$ and $\delta \in \{0, 0.063\}$.

tially, which limits the repetition rate. Therefore, for the RT, rather than using 2.5 GHz, we determine the maximum repetition rate under the restriction that Alice only emits a pulse after Bob has finished his measurement of the previous pulse. For this calculation, we assume a standard fibre in which photons travel at about 2/3 of the speed of light [45]. As can be seen in Fig. 2, this significantly restricts the secret-key rate achievable using the RT after the first few kilometers. We note that this sequential condition, which is also imposed by security proofs based on the generalized entropy accumulation theorem [17, 29], is not required by our security proof, as discussed in Section II B. In the Supplementary Information, we explain at length why this is the case.

In Figs. 1 and 2, we have assumed the asymptotic regime in which the total number of emitted pulses, N , approaches infinity. However, our security proof can be applied to secure practical QKD implementations with a finite N . In Fig. 3, we show the achievable secret-key rate for several values of this parameter. For large N , the performance approaches that of the asymptotic regime.

IV. CONCLUSION

We have introduced a security proof approach that can ensure the finite-key security of QKD protocols against the most general attacks allowed by quantum mechanics (i.e., coherent attacks) in the presence of bit-and-basis encoding imperfections. As Fig. 2 demonstrates, our analysis achieves significantly higher secret-key rates than previous results in the presence of both side channels and qubit flaws, guaranteeing the security of practical QKD setups without compromising their performance.

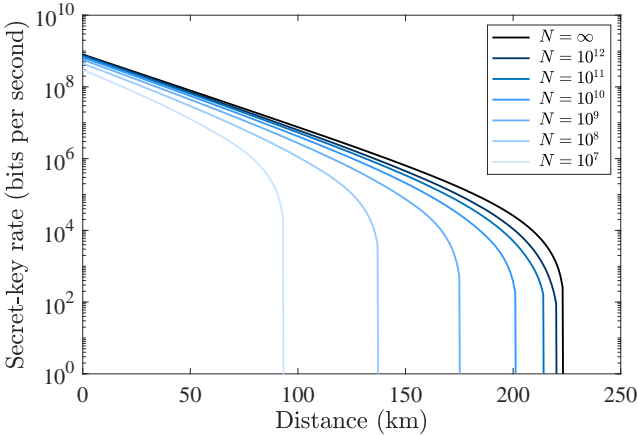


Figure 3. Finite-size secret-key rate against general attacks obtainable using our proof as a function of the total number of emitted pulses N . We consider the BB84 protocol, $\epsilon = 10^{-6}$, $\delta = 0.063$, and we set the correctness and secrecy parameters of the final key to $\epsilon_{\text{corr}} = \epsilon_{\text{secr}} = 10^{-10}$.

Moreover, it does not need any characterization of the side channels, other than an upper bound on their overall magnitude. Importantly, when applied to the BB84 protocol, the asymptotic performance of our security proof is essentially optimal given its partial characterization assumptions [46].

While our security proof represents a significant advance in addressing implementation imperfections while relaxing the need for full characterization, several important challenges remain for achieving truly secure QKD in practice. On the experimental front, accurately determining the parameter ϵ that bounds the magnitude of side channels remains a difficult task. Real QKD systems may suffer from multiple side channels simultaneously—including mode dependencies, setting-dependent correlations, electromagnetic radiation, acoustic emissions, power consumption variations, and susceptibility to Trojan-horse attacks—each requiring careful characterization, and new unexpected side channels are still being discovered [22]. The total ϵ must account for all these leakage channels combined, and obtaining tight bounds requires sophisticated measurement techniques with very high accuracy and extremely low noise. Furthermore, as we have shown, if ϵ is too large, the system becomes vulnerable to USD attacks that can completely compromise security. This places stringent requirements on experimental implementations to minimize side-channel leakage through careful engineering, shielding, and isolation techniques. Modulator-free [47] and passive QKD [48, 49] represent a promising approach to eliminate the side channels introduced by active components, and our techniques have been adapted to incorporate residual side channels in such setups [50].

On the theoretical front, while our proof addresses bit-and-basis encoding imperfections, extending it to simultaneously handle imperfections in decoy-state implemen-

tations remains an open challenge. Decoy-state QKD is crucial for practical implementations using weak coherent pulses, but decoy-state modulators can introduce their own side channels (including correlations in intensity modulation and phase randomization) that are not fully covered by our current analysis. Although we discuss in the Supplementary Information how our techniques could potentially be extended to address some of these issues, and simple imperfections like intensity fluctuations can be readily incorporated, a comprehensive treatment of general decoy-state imperfections—particularly in the finite-key regime—requires further theoretical development.

Despite these challenges, the techniques we have developed demonstrate considerable flexibility and broad applicability. While we have focused on the prepare-and-measure BB84 protocol for clarity in the main text, our security proof approach can be extended to many other QKD protocols. For example, it can be applied to MDI-QKD [10]. Since MDI-QKD eliminates all detector side channels while our proof addresses transmitter imperfections, combining these approaches enables security against both source and measurement device imperfections. The extension to MDI-QKD follows naturally because the bit-and-basis encoding imperfections at each transmitter can be incorporated using the same loss-tolerant quantum coin technique. Furthermore, our approach can be applied to other protocols, including three-state protocols and even an MDI-type protocol in which the users send non-phase-randomized coherent states [26], demonstrating the versatility of our techniques (see Appendix A and Supplementary Information for detailed analyses of these scenarios). Moreover, as shown in [51], our security proof can be combined with the result in [34] to incorporate also detection efficiency mismatches in Bob’s setup, going beyond previous attempts at simultaneously addressing source and detector imperfections [52, 53] in terms of generality and applicability in the finite-key regime. Beyond QKD, our techniques may also prove useful for other information-theoretic tasks in which information leakage must be addressed.

In short, we believe this work represents an important step toward bridging the gap between the theoretical promise of unconditional security and the practical reality of QKD implementations.

Appendix A: METHODS

1. Mixed and non-identically-distributed states

Our analysis directly applies even if the emitted states ρ_j are mixed. To see why, note that, if Eq. (1) holds, by Uhlmann’s theorem, there must exist a purification $|\psi_j\rangle_{BS}$ of ρ_j such that

$$|\langle\phi_j|\psi_j\rangle_{BS}|^2 = \langle\phi_j|\rho_j|\phi_j\rangle_B \geq 1 - \epsilon, \quad (\text{A1})$$

where we have defined $|\phi_j\rangle_{BS} := |\phi_j\rangle_B |0\rangle_S$. This implies that our analysis for pure states can be directly applied to the mixed state case simply by substituting $|\psi_j\rangle_B \rightarrow |\psi_j\rangle_{BS}$ and $|\phi_j\rangle_B \rightarrow |\phi_j\rangle_{BS}$ throughout.

Also, our security proof can be applied without any modification even if the emitted states $\rho_j^{(k)}$ are different for different rounds k , as long as Eq. (1) holds for all rounds. Note that, in this case, the target and reference states $|\Psi_{\text{Tar}}^{(k)}(\epsilon)\rangle$ and $|\Psi_{\text{Ref}}^{(k)}(\epsilon)\rangle$, and thus also the quantum coin state $|\Psi_{\text{LTcoin}}^{(k)}(\epsilon)\rangle$, depend on the round k . However, this is not a problem since one can use exactly the same procedure as in the case of identically distributed states to find a lower bound on $\text{Re} \langle \Psi_{\text{Ref}}^{(k)}(\epsilon) | \Psi_{\text{Tar}}^{(k)}(\epsilon) \rangle$ that holds for all rounds k , and apply our security proof as is.

2. Determining the value of ϵ

Any device used in a communication system can leak partial information about its internal settings to the channel. This means that any cryptosystem, including device-independent QKD [1–3], necessarily requires a degree of characterization of such potential side channels to guarantee security. For this characterization, our security proof requires only a bound on the overall combined magnitude of all side channels — the parameter ϵ . That is, unlike other security proofs (e.g., [54]), we do not need any state characterization of the side channels, which might be impossible to obtain in practice. Remarkably, this means that our proof could serve as a guideline to secure the source while significantly relaxing the need for detailed characterization. While obtaining a rigorous bound on ϵ for a given implementation is a non-trivial experimental problem that is outside the scope of this work, here, we discuss how one could combine information about various side channels in order to obtain a value for ϵ .

One critical side channel is that caused by a THA, in which Eve injects light into Alice's source and then measures the back-reflected light to learn information about Alice's setting choice. The amount of leaked information can be related to the intensity of the back-reflected light, $\mu_{\text{out}} = \gamma \mu_{\text{in}}$, where μ_{in} is the intensity of the injected light, and γ represents the optical isolation of the transmitting unit. In particular, it is straightforward to show that the back-reflected light can be expressed as

$$|\xi_j\rangle_E = \sqrt{1 - \epsilon_j} |v\rangle_E + \sqrt{\epsilon_j} |\Omega_j\rangle_E, \quad (\text{A2})$$

where $\epsilon_j \leq \mu_{\text{out}}$ [25]. Here, $|v\rangle_E$ is a vacuum state independent of Alice's setting j , and $|\Omega_j\rangle_E$ is a non-vacuum state that can in general depend on j . It has been argued [54] that, for any given implementation, one can determine a threshold μ_{in}^U above which the injected light is very likely to damage the optical components of Alice's source and be detected. Based on this, one can obtain a bound $\mu_{\text{out}}^U := \gamma \mu_{\text{in}}^U$ that can be reduced by adjusting the optical

isolation γ . If Eve's THA is the only side channel present, the emitted states are $\{|\phi_j\rangle_B \otimes |\xi_j\rangle_E\}_j$, where $\{|\phi_j\rangle_B\}_j$ are qubit states. Therefore, we can apply our proof by considering the set of qubit states $\{|\phi_j\rangle_B \otimes |v\rangle_E\}_j$ and setting $\epsilon = \epsilon_{\text{THA}} := \mu_{\text{out}}^U$. Note that, unlike other analyses [54], our proof does not need any assumption on Eve's injected light, such as it being a coherent state, other than a bound on its intensity.

Beyond THAs, Alice's source may also passively leak information through unwanted modes. For example, consider polarization mode dependencies in phase-encoding setups. While the encoded pulses should ideally maintain constant polarization (e.g., horizontal), imperfect alignment between laser and phase modulator can cause the polarization to depend slightly on the setting choice j . The generated pulse then becomes

$$|\psi_j\rangle_B = \sqrt{1 - \epsilon'_j} |\phi_j\rangle_{B_h} |v\rangle_{B_v} + \sqrt{\epsilon'_j} |v\rangle_{B_h} |\phi_j\rangle_{B_v}, \quad (\text{A3})$$

where B_h (B_v) denotes the horizontally (vertically) polarized mode. While the exact values of $\{\epsilon'_j\}_j$ may fluctuate, obtaining an upper bound $\epsilon'_j \leq \epsilon_{\text{MD}}$ should be experimentally feasible. If necessary, its value may be reduced using countermeasures such as polarizing beam splitters. In the presence of both the THA and the polarization mode dependencies, the emitted states are $\{|\psi_j\rangle_B |\xi_j\rangle_E\}_j$, and one can apply our analysis by defining the qubit states $\{|\phi_j\rangle_{B_h} |v\rangle_{B_v} |v\rangle_E\}_j$, which satisfy

$$|\langle B_h | \langle \phi_j | B_v \langle v | E \langle v | |\psi_j\rangle_B | \xi_j \rangle_E |^2 \leq \epsilon, \quad (\text{A4})$$

where $\epsilon := 1 - (1 - \epsilon_{\text{THA}})(1 - \epsilon_{\text{MD}}) \leq \epsilon_{\text{THA}} + \epsilon_{\text{MD}}$. That is, the magnitudes of the side channels simply combine additively. Other forms of information leakage, such as electromagnetic/acoustic radiation, or temporal/spectral/spatial mode dependencies, can also be written in the form of Eqs. (A2) and (A3), and thus their individual magnitudes also contribute additively towards the overall ϵ . Pulse correlations can also be essentially regarded as a form of information leakage and incorporated into ϵ in this way (see below).

Based on all the above, we consider the following to be a promising approach: (1) identify the principal source side channels affecting a particular implementation; (2) obtain an upper bound on their magnitude; (3) if necessary, apply countermeasures to reduce this magnitude; and (4) sum all the individual upper bounds. Side channels that are too small to be precisely quantified could be accounted for by conservatively increasing ϵ .

3. Pulse correlations

Pulse correlations are a special type of side channel that occurs when the state emitted in the k -th round, denoted as $|\psi_{j_k|j_{k-1}, j_{k-2}, \dots, j_{k-l_c}}\rangle_{B_k}$, depends not only on the k -th setting choice j_k , but also on the previous l_c setting choices $j_{k-1}, j_{k-2}, \dots, j_{k-l_c}$, where l_c denotes the

maximum correlation length. In this case, these states should satisfy

$$|\langle \phi_{j_k} | \psi_{j_k|j_{k-1},j_{k-2},\dots,j_{k-l_c}} \rangle_{B_k}|^2 \geq 1 - \epsilon_{\text{qubit}}, \quad (\text{A5})$$

and

$$\begin{aligned} & |\langle \psi_{j_k|j_{k-1},\dots,\tilde{j}_{k-l},\dots,j_{k-l_c}} | \psi_{j_k|j_{k-1},\dots,j_{k-l},\dots,j_{k-l_c}} \rangle_{B_k}|^2 \\ & \geq 1 - \epsilon_l, \end{aligned} \quad (\text{A6})$$

where $\{|\phi_j\rangle_{B_k}\}_j$ is a set of known qubit states, $l \in \{1, \dots, l_c\}$, and \tilde{j}_{k-l} is a setting choice that differs from j_{k-l} . Then, one can apply our security proof by setting

$$\epsilon = 1 - (1 - \epsilon_{\text{qubit}})(1 - \epsilon_{\text{correl}}) \leq \epsilon_{\text{qubit}} + \epsilon_{\text{correl}} \quad (\text{A7})$$

where

$$\epsilon_{\text{correl}} := 1 - \prod_{l=1}^{l_c} (1 - \epsilon_l) \leq \sum_{l=1}^{l_c} \epsilon_l. \quad (\text{A8})$$

Also, one needs to divide the protocol rounds into $(l_c + 1)$ groups according to the value of $k \bmod (l_c + 1)$, and apply post-processing separately for each group [16, 25, 27]. While this does not affect the asymptotic key rate, it can have an impact in the finite-key regime, as the blocksize is effectively reduced from N to $N/(l_c + 1)$ rounds. Also, although this discussion implicitly assumes a finite maximum correlation length l_c , our security proof can also be applied when the correlations have an unbounded length, as recently shown in [55] (see also [56]). For more details, see the Supplementary Information.

4. A more general form of Eq. (1)

In the main text, we have assumed that the emitted states $\rho_j^{(k)}$ are close in fidelity to some known qubit states $\{|\phi_j\rangle_{B_k}\}_j$, see Eq. (1). However, our security proof can be applied under a more general assumption; namely,

$$\langle \tilde{\phi}_j | \rho_j^{(k)} | \tilde{\phi}_j \rangle_B \geq 1 - \epsilon, \quad (\text{A9})$$

where $\{|\tilde{\phi}_j\rangle_B\}_j$ are *any* characterized states, not necessarily qubits. This is because, in our analysis, the fictitious qubit states $\{|\phi_j\rangle_B\}_j$ only serve as a blueprint to appropriately define the states $|\Psi_{\text{Tar}}\rangle_{DAB}$ and $|\Psi_{\text{Ref}}\rangle_{DAB}$. The secret-key rate obtainable primarily depends on $\text{Re}\langle \Psi_{\text{Tar}} | \Psi_{\text{Ref}} \rangle_{DAB}$, which is a linear combination of the inner products $\text{Re}\langle \psi_{j'} | \psi_j \rangle_B \forall j, j'$. Although these inner products are not known precisely, in the Supplementary Information, we show that, for any $\{|\tilde{\phi}_j\rangle_B\}_j$, the problem of finding the minimum value of $\text{Re}\langle \Psi_{\text{Tar}} | \Psi_{\text{Ref}} \rangle_{DAB}$ that is consistent with Eq. (A9) reduces to a numerically solvable semidefinite program. Our numerical simulations focus on the case $|\tilde{\phi}_j\rangle_B = |\phi_j\rangle_B$, for which Eq. (A9) becomes Eq. (1). As explained in ‘‘Determining the value of ϵ ’’ above, this corresponds

to minimal side-channel characterization, in which one knows only the overall magnitude of the side channels, but has no information on their specific form. While this minimal requirement is a key strength of our proof, given the experimental challenges of obtaining precise side-channel characterization, our proof is not *only* applicable in this scenario. Namely, if one is able to obtain a partial characterization of some side channels, one could include this information into the definition of the states $\{|\tilde{\phi}_j\rangle_B\}_j$. This would generally improve the bound on $\text{Re}\langle \Psi_{\text{Tar}} | \Psi_{\text{Ref}} \rangle_{DAB}$, potentially resulting in a significant performance improvement for many practical side channels.

5. Characterizing qubit flaws

In addition to ϵ , the proof also requires knowledge of the qubit states $\{|\phi_j\rangle\}_j$, which can be acquired by testing the source. Methods to characterize this imperfection have been proposed and implemented, see e.g., [21, 57]. In practice, these characterization tests could be subject to small inaccuracies. The simplest way to take these into account would be to incorporate any deviation between the estimated $\{|\phi_j\rangle\}_j$ and the actual qubit components of the emitted states into the parameter ϵ . However, this is in general pessimistic, since Eve cannot enhance the effect of this deviation in the presence of loss.

A tighter approach would be to define $\{|\phi_j\rangle\}_j$ as the actual qubit components of the emitted states. This requires a slight modification to our security proof, as the states $\{|\phi_j\rangle\}_j$ would no longer be fully characterized. Consequently, the coefficients in Eqs. (7) and (8), which appear in the definition of the target and reference states in Eqs. (10) and (11), are no longer known precisely. However, as shown in [25], one can calculate the maximum possible range for these coefficients and find the worst case scenario within those ranges. For more information on this approach, we refer the reader to [25].

6. Protection against detector imperfections side channels

Our security proof is designed to protect QKD implementations from source imperfections. When applied to BB84—or other prepare-and-measure (P&M) scenarios—our security proof’s only requirement for Bob’s measurement is that it satisfies the basis-independent detection efficiency condition, i.e., that the probability that he obtains a successful bit outcome is independent of his choice of basis. While this requirement relaxes the need for an exact characterization of Bob’s setup and can tolerate certain imperfections (such as the measurement bases not being mutually unbiased), it is still a stringent condition that is only met in practice if all of Bob’s detectors have the same efficiency. However, we remark that, as recently shown in [51], our security

proof can be readily combined with the result in [34] to incorporate detection efficiency mismatches.

Still, detector control attacks [58–61] constitute a significant threat to the security of BB84 and other P&M protocols, and no solution at the security proof level is known to comprehensively deal with these [8, 9]. That being said, our approach is compatible with MDI-QKD [10], which eliminates all detector-related security vulnerabilities by delegating measurements to an untrusted intermediary node. When applied to MDI protocols, our analysis secures both Alice’s and Bob’s sources against general imperfections, providing robust protection against both source and detector side channels. For details on applying our security proof to MDI-type protocols, see Supplementary Information.

7. Weak coherent sources

Our security proof can also be applied when the users emit intensity-modulated phase-randomized weak coherent pulses, rather than single photons. In this case, assuming ideal intensity modulation and phase randomization, the emitted signals can be regarded as a statistical mixture of photon-number states, and our proof is directly applicable to obtain a bound on the number of phase errors within the single-photon events. The quantities needed to evaluate this bound are not directly observable, since the users do not know which events correspond to single photons. Nevertheless, one can simply obtain bounds for these quantities using the decoy-state method [62–64].

For decoy-state QKD protocols, our security proof can directly incorporate general imperfections and side-channels in the bit-and-basis encoder, which addresses a major practical security concern. Our proof can also straightforwardly incorporate fluctuations in the intensity modulation, since in their presence the emitted states can still be regarded as a mixture of photon-number states. For scenarios with imperfect intensity modulation (beyond simple fluctuations) and/or imperfect phase randomization, additional considerations are needed since the emitted signals may no longer be perfectly described as a statistical mixture of photon-number states independent of the intensity choice. As explained in the Supplementary Information, the techniques introduced in our work could find applications in incorporating such decoy imperfections into security proofs while considering the finite-key regime and general attacks. This represents a promising research avenue, since previous works addressing such imperfections [65–71] have considered the asymptotic regime and/or collective attacks.

An alternative approach to circumvent the security vulnerabilities associated with these imperfections is the MDI-type protocol proposed in [26], which employs coherent light but requires neither intensity modulation nor phase randomization. Our security analysis is directly compatible with this protocol, and offers significant en-

hancements in both security and performance compared with its original security proof [26] based on the RT [16]. In particular, while the original proof is only valid against sequential attacks, ours can defend against the most general attacks allowed by quantum mechanics. The combination of our approach with this protocol constitutes a practical solution that offers an unprecedented level of implementation security and performance. For more details, including a comprehensive security analysis and numerical results, see the Supplementary Information.

8. Choice of target and reference states

We note that Eqs. (10) and (11) are not the only possible choice for $|\Psi_{\text{Tar}}(\epsilon)\rangle_{DAB}$ and $|\Psi_{\text{Ref}}(\epsilon)\rangle_{DAB}$. Essentially, these states need to satisfy two conditions: (1) when $\epsilon = 0$, $|\Psi_{\text{Tar}}(0)\rangle_{DAB} = |\Psi_{\text{Ref}}(0)\rangle_{DAB}$, as this ensures the resilience of the phase-error rate bound against qubit flaws; (2) the coefficient of the state $|\psi_{\text{vir0}}(\epsilon)\rangle_B$ ($|\psi_{\text{vir1}}(\epsilon)\rangle_B$) inside $|\Psi_{\text{Tar}}(\epsilon)\rangle_{DAB}$ should be proportional to $\sqrt{1 - q_\epsilon}$ ($\sqrt{q_\epsilon}$), as in $|\Psi_Z(\epsilon)\rangle_{AB}$, which is needed to ensure that phase errors are correctly defined. To compute the results in Figs. 1 to 3, we have used a slightly different choice of target and reference states than that in Eqs. (10) and (11). The reason why this different choice is advantageous is explained in the Supplementary Information.

9. Comparison with side-channel-secure QKD

Both our work and side-channel-secure (SCS) QKD [72] aim to address source imperfections in QKD systems, but they take fundamentally different approaches. The main idea behind SCS-QKD is to design a variant of twin-field QKD [73] that is inherently immune to mode dependencies by having each user send only two states: a vacuum state and a non-vacuum state. Since the vacuum state is “mode independent”, the protocol becomes immune to mode dependencies in the sense that, regardless of which mode the non-vacuum state occupies, this does not allow Eve to better distinguish between the two states. However, despite its name, SCS-QKD is not immune to other side channels that leak key information through systems different from the intended signal, such as unintended electromagnetic radiation, back-reflected light due to Trojan-horse attacks, or correlations between consecutive pulses.

Recently, a refined version of the protocol was proposed [74] to address a limitation of the original proposal—the requirement to generate perfect vacuum states—by demanding only a lower bound on the fidelity between the two emitted states. Although this is not discussed in [74], we believe this new assumption could be exploited to incorporate side channels beyond mode dependencies (including pulse correlations through the approach described in Appendix A 3) after bounding their overall

magnitude, by introducing a parameter ϵ as in our work. Thus, certain aspects of our work, such as our state characterization (see Appendix A 2), may be relevant for SCS-QKD as well.

A limitation of SCS-QKD is that its key idea is fundamentally restricted to protocol designs where each user sends only two different states. In contrast, our work develops general techniques to incorporate source imperfections into security proofs of QKD, and is thus broader in scope. Our state characterization can incorporate general imperfections directly into the state used in the security proof, making it highly useful for the security analysis of QKD protocol in general. Although we focus mainly on BB84-type protocols, in the Supplementary Information, we demonstrate the versatility of our techniques by applying them to a MDI-type scenario in which the users send non-phase-randomized coherent states [26]. This latter scenario differs from SCS-QKD mainly in that three states are emitted rather than two, and thus the approach we take to prove security is necessarily different.

ACKNOWLEDGEMENTS

We thank Koji Azuma, Akihiro Mizutani, Álvaro Navarrete and Víctor Zapatero for valuable discussions. This work was supported by the Galician Regional Government (consolidation of research units: atlanTIC), the Spanish Ministry of Economy and Competitiveness (MINECO), the Fondo Europeo de Desarrollo Regional (FEDER) through the grant No. PID2020-118178RB-C21, MICIN with funding from the European Union NextGenerationEU (PRTRC17.II) and the Galician Regional Government with own funding through the “Planes Complementarios de I+D+I con las Comunidades Autónomas” in Quantum Communication, the “Hub Nacional de Excelencia en Comunicaciones Cuánticas” funded by the Spanish Ministry for Digital Transformation and the Public Service and the European Union NextGenerationEU, the European Union’s

Horizon Europe Framework Programme under the Marie Skłodowska-Curie Grant No. 101072637 (Project QSI), the project “Quantum Security Networks Partnership” (QSNP, grant agreement No 101114043) and the European Union via the European Health and Digital Executive Agency (HADEA) under the Project QuTechSpace (grant 101135225).. G.C.-L. and M.P. acknowledge support from JSPS Postdoctoral Fellowships for Research in Japan. G.C.-L. acknowledges funding from the European Union’s Horizon Europe research and innovation programme under the Marie Skłodowska-Curie Postdoctoral Fellowship grant agreement No. 101149523. G.K. acknowledges support from JSPS Kakenhi (C) No.20K03779 and 21K03388. K.T. acknowledges support from JSPS KAKENHI Grant Numbers JP18H05237 and 23H01096, and JST-CREST JPMJCR 1671.

AUTHOR CONTRIBUTIONS

G.C.-L. identified the need for the research project, and K.T. conceived the fundamental idea behind the security proof, with help from all the authors. K.T., G.C.-L. and M.P. developed the majority of the security proof, with contributions from G.K. and M.C. M.P. and G.C.-L. performed the calculations and the numerical simulations. G.C.-L., M.P. and K.T. wrote the manuscript, and all the authors contributed towards improving it and checking the validity of the results.

COMPETING INTERESTS

The authors declare no competing interests.

DATA AVAILABILITY STATEMENT

All data generated and analyzed during this study is available from the corresponding author on reasonable request.

[1] D. Mayers and A. Yao, Quantum cryptography with imperfect apparatus, in *Proceedings 39th Annual Symposium on Foundations of Computer Science (Cat. No.98CB36280)* (1998) pp. 503–509.

[2] J. Barrett, L. Hardy, and A. Kent, No Signaling and Quantum Key Distribution, *Phys. Rev. Lett.* **95**, 010503 (2005).

[3] A. Acín, N. Brunner, N. Gisin, S. Massar, S. Pironio, and V. Scarani, Device-Independent Security of Quantum Cryptography against Collective Attacks, *Phys. Rev. Lett.* **98**, 230501 (2007).

[4] D. P. Nadlinger, P. Drmota, B. C. Nichol, G. Araneda, D. Main, R. Srinivas, D. M. Lucas, C. J. Ballance, K. Ivanov, E. Y.-Z. Tan, P. Sekatski, R. L. Urbanke, R. Renner, N. Sangouard, and J.-D. Bancal, Experimental quantum key distribution certified by Bell’s theorem, *Nature* **607**, 682 (2022).

[5] W. Zhang, T. van Leent, K. Redeker, R. Garthoff, R. Schwonnek, F. Fertig, S. Eppelt, W. Rosenfeld, V. Scarani, C. C.-W. Lim, and H. Weinfurter, A device-independent quantum key distribution system for distant users, *Nature* **607**, 687 (2022).

[6] W.-Z. Liu, Y.-Z. Zhang, Y.-Z. Zhen, M.-H. Li, Y. Liu, J. Fan, F. Xu, Q. Zhang, and J.-W. Pan, Toward a Photonic Demonstration of Device-Independent Quantum Key Distribution, *Phys. Rev. Lett.* **129**, 050502 (2022).

[7] V. Zapatero, T. van Leent, R. Arnon-Friedman, W.-Z. Liu, Q. Zhang, H. Weinfurter, and M. Curty, Advances in device-independent quantum key distribution, *npj Quantum Inf* **9**, 1 (2023).

[8] V. Zapatero, Á. Navarrete, and M. Curty, Implementation Security in Quantum Key Distribution, *Advanced Quantum Technologies* **7**, 2300380 (2023).

[9] F. Xu, X. Ma, Q. Zhang, H.-K. Lo, and J.-W. Pan, Secure quantum key distribution with realistic devices, *Rev. Mod. Phys.* **92**, 025002 (2020).

[10] H.-K. Lo, M. Curty, and B. Qi, Measurement-Device-Independent Quantum Key Distribution, *Phys. Rev. Lett.* **108**, 130503 (2012).

[11] D. Gottesman, H.-K. Lo, N. Lütkenhaus, and J. Preskill, Security of quantum key distribution with imperfect devices, *Quantum Inf. Comput.* **4**, 325 (2004).

[12] H.-K. Lo and J. Preskill, Security of quantum key distribution using weak coherent states with nonrandom phases, *Quantum Inf. Comput.* **7**, 431 (2007).

[13] M. Koashi, Simple security proof of quantum key distribution based on complementarity, *New J. Phys.* **11**, 045018 (2009).

[14] K. Tamaki, M. Curty, G. Kato, H.-K. Lo, and K. Azuma, Loss-tolerant quantum cryptography with imperfect sources, *Phys. Rev. A* **90**, 052314 (2014).

[15] M. Pereira, M. Curty, and K. Tamaki, Quantum key distribution with flawed and leaky sources, *npj Quantum Inf* **5**, 62 (2019).

[16] M. Pereira, G. Kato, A. Mizutani, M. Curty, and K. Tamaki, Quantum key distribution with correlated sources, *Sci. Adv.* **6**, eaaz4487 (2020).

[17] T. Metger and R. Renner, Security of quantum key distribution from generalised entropy accumulation, *Nat Commun* **14**, 5272 (2023).

[18] M. Sandfuchs, M. Haberland, V. Vilasini, and R. Wolf, Security of differential phase shift QKD from relativistic principles, *Quantum* **9**, 1611 (2025).

[19] C. H. Bennett and G. Brassard, Quantum cryptography: Public key distribution and coin tossing, in *Proceedings of IEEE International Conference on Computers, Systems, and Signal Processing* (1984) pp. 175–179.

[20] S. Nauerth, M. Fürst, T. Schmitt-Manderbach, H. Weier, and H. Weinfurter, Information leakage via side channels in freespace BB84 quantum cryptography, *New J. Phys.* **11**, 065001 (2009).

[21] F. Xu, K. Wei, S. Saeed, S. Kaiser, S. Sun, Z. Tang, L. Qian, V. Makarov, and H.-K. Lo, Experimental quantum key distribution with source flaws, *Phys. Rev. A* **92**, 032305 (2015).

[22] A. Gnanapandithan, L. Qian, and H.-K. Lo, Hidden Multidimensional Modulation Side Channels in Quantum Protocols, *Phys. Rev. Lett.* **134**, 130802 (2025).

[23] K. Gandolfi, C. Mourtel, and F. Olivier, Electromagnetic Analysis: Concrete Results, in *Cryptographic Hardware and Embedded Systems — CHES 2001*, Lecture Notes in Computer Science, edited by Ç. K. Koç, D. Naccache, and C. Paar (Springer, Berlin, Heidelberg, 2001) pp. 251–261.

[24] P. Kocher, J. Jaffe, and B. Jun, Differential Power Analysis, in *Advances in Cryptology — CRYPTO' 99*, Lecture Notes in Computer Science, edited by M. Wiener (Springer, Berlin, Heidelberg, 1999) pp. 388–397.

[25] M. Pereira, G. Currás-Lorenzo, Á. Navarrete, A. Mizutani, G. Kato, M. Curty, and K. Tamaki, Modified BB84 quantum key distribution protocol robust to source imperfections, *Phys. Rev. Res.* **5**, 023065 (2023).

[26] Á. Navarrete, M. Pereira, M. Curty, and K. Tamaki, Practical Quantum Key Distribution That is Secure Against Side Channels, *Phys. Rev. Applied* **15**, 034072 (2021).

[27] A. Mizutani and G. Kato, Security of round-robin differential-phase-shift quantum-key-distribution protocol with correlated light sources, *Phys. Rev. A* **104**, 062611 (2021).

[28] I. D. Ivanovic, How to differentiate between non-orthogonal states, *Physics Letters A* **123**, 257 (1987).

[29] M. Sandfuchs, M. Haberland, V. Vilasini, and R. Wolf, Security of differential phase shift QKD from relativistic principles (2023), arXiv:2301.11340 [quant-ph].

[30] R. Renner, *Security of Quantum Key Distribution*, Ph.D. thesis, ETH Zurich (2005).

[31] M. Tomamichel and R. Renner, Uncertainty Relation for Smooth Entropies, *Phys. Rev. Lett.* **106**, 110506 (2011).

[32] M. Tomamichel, C. C. W. Lim, N. Gisin, and R. Renner, Tight finite-key analysis for quantum cryptography, *Nat Commun* **3**, 634 (2012).

[33] G. Currás-Lorenzo, Á. Navarrete, K. Azuma, G. Kato, M. Curty, and M. Razavi, Tight finite-key security for twin-field quantum key distribution, *npj Quantum Inf* **7**, 22 (2021).

[34] D. Tupkary, S. Nahar, P. Sinha, and N. Lütkenhaus, Phase error rate estimation in QKD with imperfect detectors (2024), arXiv:2408.17349.

[35] D. Mayers, Quantum key distribution and string oblivious transfer in noisy channels, in *Advances in Cryptology — CRYPTO '96*, edited by N. Koblitz (Springer Berlin Heidelberg, Berlin, Heidelberg, 1996) pp. 343–357.

[36] P. W. Shor and J. Preskill, Simple Proof of Security of the BB84 Quantum Key Distribution Protocol, *Phys. Rev. Lett.* **85**, 441 (2000).

[37] M. Hayashi and T. Tsurumaru, Concise and tight security analysis of the Bennett–Brassard 1984 protocol with finite key lengths, *New Journal of Physics* **14**, 093014 (2012).

[38] T. Tsurumaru, Leftover hashing from quantum error correction: Unifying the two approaches to the security proof of quantum key distribution, *IEEE Transactions on Information Theory* **66**, 3465 (2020).

[39] G. Currás-Lorenzo, Á. Navarrete, M. Pereira, and K. Tamaki, Finite-key analysis of loss-tolerant quantum key distribution based on random sampling theory, *Phys. Rev. A* **104**, 012406 (2021).

[40] W. Wang, K. Tamaki, and M. Curty, Finite-key security analysis for quantum key distribution with leaky sources, *New J. Phys.* **20**, 083027 (2018).

[41] G. Kato, Concentration inequality using unconfirmed knowledge (2020), arXiv:2002.04357 [quant-ph].

[42] M. Pittaluga, M. Minder, M. Lucamarini, M. Sanzaro, R. I. Woodward, M.-J. Li, Z. Yuan, and A. J. Shields, 600-km repeater-like quantum communications with dual-band stabilization, *Nat. Photon.* **15**, 530 (2021).

[43] A. Boaron, G. Boso, D. Rusca, C. Vulliez, C. Autebert, M. Caloz, M. Perrenoud, G. Gras, F. Bussières, M.-J. Li, D. Nolan, A. Martin, and H. Zbinden, Secure Quantum

Key Distribution over 421 km of Optical Fiber, *Phys. Rev. Lett.* **121**, 190502 (2018).

[44] T. Honjo, K. Inoue, and H. Takahashi, Differential-phase-shift quantum key distribution experiment with a planar light-wave circuit Mach-Zehnder interferometer, *Opt. Lett.* **29**, 2797 (2004).

[45] G. P. Agrawal, *Fiber-Optic Communication Systems* (John Wiley & Sons, 2021).

[46] G. Currás-Lorenzo, Á. Navarrete, J. Núñez-Bon, M. Pereira, and M. Curty, Numerical security analysis for quantum key distribution with partial state characterization, *Quantum Sci. Technol.* **10**, 035031 (2025).

[47] T. K. Paraíso, I. De Marco, T. Roger, D. G. Marangon, J. F. Dynes, M. Lucamarini, Z. Yuan, and A. J. Shields, A modulator-free quantum key distribution transmitter chip, *npj Quantum Inf.* **5**, 42 (2019).

[48] W. Wang, R. Wang, C. Hu, V. Zapatero, L. Qian, B. Qi, M. Curty, and H.-K. Lo, Fully Passive Quantum Key Distribution, *Phys. Rev. Lett.* **130**, 220801 (2023).

[49] V. Zapatero, W. Wang, and M. Curty, A fully passive transmitter for decoy-state quantum key distribution, *Quantum Sci. Technol.* **8**, 025014 (2023).

[50] Á. Navarrete, V. Zapatero, and M. Curty, Security of practical modulator-free quantum key distribution (2024), arXiv:2411.15777 [quant-ph].

[51] G. Currás-Lorenzo, M. Pereira, S. Nahar, and D. Tukary, Security of quantum key distribution with source and detector imperfections through phase-error estimation (2025), arXiv:2507.03549 [quant-ph].

[52] S. Sun and F. Xu, Security of quantum key distribution with source and detection imperfections, *New J. Phys.* **23**, 023011 (2021).

[53] A. Marcomini, A. Mizutani, F. Grünenfelder, M. Curty, and K. Tamaki, Loss-tolerant quantum key distribution with detection efficiency mismatch (2024), arXiv:2412.09684 [quant-ph].

[54] M. Lucamarini, I. Choi, M. B. Ward, J. F. Dynes, Z. L. Yuan, and A. J. Shields, Practical Security Bounds Against the Trojan-Horse Attack in Quantum Key Distribution, *Phys. Rev. X* **5**, 031030 (2015).

[55] M. Pereira, G. Currás-Lorenzo, A. Mizutani, D. Rusca, M. Curty, and K. Tamaki, Quantum key distribution with unbounded pulse correlations, *Quantum Sci. Technol.* **10**, 015001 (2024).

[56] A. Agulleiro, F. Grünenfelder, M. Pereira, G. Currás-Lorenzo, H. Zbinden, M. Curty, and D. Rusca, Modeling and Characterization of Arbitrary Order Pulse Correlations for Quantum Key Distribution (2025), arXiv:2506.18684 [quant-ph].

[57] A. Huang, A. Mizutani, H.-K. Lo, V. Makarov, and K. Tamaki, Characterization of State-Preparation Uncertainty in Quantum Key Distribution, *Phys. Rev. Appl.* **19**, 014048 (2023).

[58] L. Lydersen, C. Wiechers, C. Wittmann, D. Elser, J. Skaar, and V. Makarov, Hacking commercial quantum cryptography systems by tailored bright illumination, *Nature Photon.* **4**, 686 (2010).

[59] I. Gerhardt, Q. Liu, A. Lamas-Linares, J. Skaar, C. Kurt-siefer, and V. Makarov, Full-field implementation of a perfect eavesdropper on a quantum cryptography system, *Nat Commun.* **2**, 349 (2011).

[60] V. Makarov, Controlling passively quenched single photon detectors by bright light, *New J. Phys.* **11**, 065003 (2009).

[61] C. Wiechers, L. Lydersen, C. Wittmann, D. Elser, J. Skaar, C. Marquardt, V. Makarov, and G. Leuchs, After-gate attack on a quantum cryptosystem, *New J. Phys.* **13**, 013043 (2011).

[62] W.-Y. Hwang, Quantum key distribution with high loss: Toward global secure communication, *Physical Review Letters* **91**, 057901 (2003).

[63] H.-K. Lo, X. Ma, and K. Chen, Decoy State Quantum Key Distribution, *Phys. Rev. Lett.* **94**, 230504 (2005).

[64] X.-B. Wang, Beating the Photon-Number-Splitting Attack in Practical Quantum Cryptography, *Phys. Rev. Lett.* **94**, 230503 (2005).

[65] K. Tamaki, M. Curty, and M. Lucamarini, Decoy-state quantum key distribution with a leaky source, *New J. Phys.* **18**, 065008 (2016).

[66] V. Zapatero, Á. Navarrete, K. Tamaki, and M. Curty, Security of quantum key distribution with intensity correlations, *Quantum* **5**, 602 (2021).

[67] X. Sixto, V. Zapatero, and M. Curty, Security of Decoy-State Quantum Key Distribution with Correlated Intensity Fluctuations, *Phys. Rev. Applied* **18**, 044069 (2022).

[68] G. Currás-Lorenzo, S. Nahar, N. Lütkenhaus, K. Tamaki, and M. Curty, Security of quantum key distribution with imperfect phase randomisation, *Quantum Sci. Technol.* **9**, 015025 (2023).

[69] S. Nahar, T. Upadhyaya, and N. Lütkenhaus, Imperfect phase randomization and generalized decoy-state quantum key distribution, *Phys. Rev. Appl.* **20**, 064031 (2023).

[70] X. Sixto, G. Currás-Lorenzo, K. Tamaki, and M. Curty, Secret key rate bounds for quantum key distribution with faulty active phase randomization, *EPJ Quantum Technol.* **10**, 1 (2023).

[71] X. Sixto, Á. Navarrete, M. Pereira, G. Currás-Lorenzo, K. Tamaki, and M. Curty, Quantum key distribution with imperfectly isolated devices, *Quantum Sci. Technol.* **10**, 035034 (2025).

[72] X.-B. Wang, X.-L. Hu, and Z.-W. Yu, Practical Long-Distance Side-Channel-Free Quantum Key Distribution, *Phys. Rev. Applied* **12**, 054034 (2019).

[73] M. Lucamarini, Z. Yuan, J. Dynes, and A. Shields, Overcoming the rate-distance limit of quantum key distribution without quantum repeaters, *Nature* **557**, 400 (2018).

[74] C. Jiang, X.-L. Hu, Z.-W. Yu, and X.-B. Wang, Side-channel security of practical quantum key distribution, *Phys. Rev. Res.* **6**, 013266 (2024).

SUPPLEMENTARY INFORMATION

Supplementary Methods	S3
SM1. Security proof for prepare-and-measure protocols	S3
A. Protocol description, assumptions, and security framework	S3
1. Protocol description	S3
2. Assumptions	S4
3. Security framework	S5
B. Security proof for a particular three-state scenario	S6
1. Constructing the loss-tolerant quantum coin state	S6
2. Overview of the next steps in the security proof	S7
3. Tag assignment	S8
4. Coin Protocol	S11
C. Security proof for a particular BB84 scenario	S14
1. Security analysis	S14
2. Investigating how tight is our security proof	S16
3. Reduction to the original quantum coin analysis when there are no qubit flaws	S17
D. General analysis for prepare-and-measure protocols	S18
E. General finite-key analysis for prepare-and-measure protocols	S22
1. Concentration inequalities	S22
2. Analysis for a general prepare-and-measure protocol	S23
3. Secret-key rate for a particular BB84 scenario	S25
SM2. Security proof for MDI-type protocols	S25
A. Protocol description, assumptions and security framework	S26
1. Protocol description	S26
2. Assumptions	S27
3. Security framework	S27
B. Constructing the reference and target states, and the Virtual Protocol with tag assignment	S28
C. Coin protocol	S30
D. General finite-key analysis for MDI protocols	S31
SM3. Security analysis for non-IID sources	S32
A. Independent but not identical pure states	S32
B. Independent but not identical mixed states	S32
C. Setting-independent pulse correlations	S33
D. Setting-dependent pulse correlations	S33
SM4. Security with WCP light sources	S35
A. Coherent-light-based MDI protocol	S36
1. Protocol description	S36
2. Security analysis	S37
3. Finite-key analysis	S43
B. Decoy-state protocols	S45
1. Ideal PR-WCP light sources	S45
2. Realistic PR-WCP light sources	S46
SM5. Why our security proof does not require the sequential assumption	S47
A. Ensuring sequentiality by restricting the repetition rate	S48
SM6. Recipe for experimentalists	S50
Supplementary Equations	S51
SE1. Proof of the quantum coin inequality	S51
A. Prepare-and-measure scenario	S51
B. Measurement-device-independent scenario	S54

SE2. Obtaining a bound on the coin imbalance parameter Δ	S54
A. Three-state protocol	S55
1. Numerical bound using SDP techniques	S55
2. Analytical bound with an additional assumption	S56
3. Comparison between the numerical and analytical bounds	S56
B. Coherent-light-based MDI protocol	S56
SE3. Channel model	S58
A. Prepare-and-measure protocol	S58
B. Coherent-light-based MDI protocol	S59
SE4. High-level description of the code	S60

Supplementary Tables	S61
-----------------------------	-----

References	S63
-------------------	-----

Supplementary Methods

In the Supplementary Methods, we present our security proof in detail. In Section [SM1](#), we consider prepare-and-measure (P&M) protocols and in Section [SM2](#), we consider measurement-device-independent (MDI) protocols. In Section [SM3](#), we show how our security proof can be applied to scenarios in which the pulses emitted by the source are mixed and even correlated across different rounds, and in Section [SM4](#), how it can be applied to scenarios in which the sources emit weak coherent pulses. In Section [SM5](#), we present a key feature of our security proof, namely, why, unlike other analyses [[S1](#), [S2](#)], it does not require the sequential assumption. Finally, in Section [SM6](#), we present a simple step-by-step instruction list to apply our security proof to a practical QKD implementation. We remark that, for simplicity, throughout the Supplementary Information we denote the emitted quantum states by $|\psi_j\rangle_B$ rather than $|\psi_j(\epsilon)\rangle_B$, the notation used in the Main Text.

SM1. SECURITY PROOF FOR PREPARE-AND-MEASURE PROTOCOLS

A. Protocol description, assumptions, and security framework

1. Protocol description

As explained in the Main Text, our security proof is applicable irrespectively of whether Alice emits three or four different states $\{|\psi_j\rangle_B\}_j$. Without loss of generality, in the former (latter) case, we label these states as $j \in \{0_Z, 1_Z, 0_X\}$ ($j \in \{0_Z, 1_Z, 0_X, 1_X\}$). States such that $j \in \{0_Z, 1_Z\}$ ($j \notin \{0_Z, 1_Z\}$) are considered Z -basis (X -basis) states. For simplicity, the Z -basis states are assumed to be selected with probability $p_{Z_A}/2$ each (see Section [SE3 A](#) in Supplementary Tables for a list of all probabilities). Also, in the three-state scenario, Alice selects the X -basis state $j = 0_X$ with probability $p_{X_A} := 1 - p_{Z_A}$; while in the four-state scenario, we assume that the X -basis states $j \in \{0_X, 1_X\}$ are selected with probability $p_{X_A}/2$ each.

Actual Protocol

- Quantum communication:** For each of the N rounds: (a) Alice probabilistically chooses a state $\{|\psi_j\rangle_B\}_j$ and sends it to Bob through a quantum channel. (b) Bob chooses the positive operator-valued measure (POVM) \mathcal{Z} (\mathcal{X}) with probability p_{Z_B} (p_{X_B}), measures the incoming state and, if he obtains a detection (i.e., a bit value, rather than an inconclusive outcome), he announces this fact.
- Basis and bit announcement:** Alice and Bob reveal their basis choices in the detected rounds. Then, they define the detected key rounds as the detected rounds in which both chose the Z basis, and their sifted keys as the bit outcomes of these rounds. Also, they evaluate its length $N_{\text{key}}^{\text{det}}$. Then, they define the detected test rounds as the detected rounds in which Bob used the X basis. For each of these rounds, Bob reveals his bit outcome, and Alice reveals her setting choice j .
- Parameter estimation:** Alice and Bob quantify the number of events $N_j^{\beta_X}$ for $\beta \in \{0, 1\}$, i.e., the number of instances in which Alice emitted the state $|\psi_j\rangle_B$ and Bob obtained the measurement result β_X . Then, they use this information to obtain an upper bound on the phase-error rate e_{ph} of the sifted key.
- Data post-processing:** Alice sends Bob syndrome information about her sifted key through an authenticated classical channel for him to correct his own sifted key. After, Alice and Bob perform error verification by computing a hash of their corrected keys using a random two-universal hash function and then check whether they are identical. If so, Alice and Bob perform privacy amplification by employing a random two-universal hash function to extract a secure key pair from the corrected keys. Otherwise, they abort the protocol.

For simplicity, we assume that, in Step 4, Alice and Bob perform error correction for a predetermined bit-error rate, which is inferred from *a priori* knowledge of the channel. After, they perform error verification, learning whether or not the actual bit-error rate exceeded the predetermined one. Alternatively, Alice and Bob could sacrifice a small fraction of their sifted key to estimate its bit-error rate, and then select an appropriate error correcting code. This would require minor changes in the security proof, but its essence would remain the same. Also, we remark that during Step 1 of the Actual Protocol, Eve can perform the most general attack allowed by quantum mechanics on all of the transmitted signals at once. Indeed, our security proof does not rely on an independent and identically distributed (IID) assumption or on a sequential assumption. For more details on why this is the case, see Section [SM5](#).

2. Assumptions

(A1) *Bounded fidelity to qubit states:* Alice's emitted states $\{|\psi_j\rangle_B\}_j$ are ϵ -close (in terms of fidelity) to some characterized qubit states $\{|\phi_j\rangle_B\}_j$, i.e., for all j ,

$$|\langle\phi_j|\psi_j\rangle_B|^2 \geq 1 - \epsilon, \quad (\text{S1})$$

where ϵ is known¹. For notational simplicity, we consider throughout the proof that the states emitted by Alice are pure and identical for all rounds. However, as explained in the Main Text and Appendix A, our security analysis can be trivially extended without any modifications to the scenario in which Alice's states are mixed and/or different for different rounds (see Eq. (1) in the Main Text). Moreover, with a simple modification to Eq. (S1) and to the post-processing step of the protocol, our analysis can be applied in the presence of setting-dependent pulse correlations i.e., when the state emitted in a given round depends on the setting choices made in previous rounds. For more information, see Section SM3.

Claim. As a consequence of Eq. (S1), we can assume that the emitted states are

$$|\psi_j\rangle_B = \sqrt{1-\epsilon}|\phi_j\rangle_B + \sqrt{\epsilon}|\phi_j^\perp\rangle_B, \quad (\text{S2})$$

where $|\phi_j^\perp\rangle_B$ is a state such that $\langle\phi_j|\phi_j^\perp\rangle_B = 0$, since this never underestimates the information available to Eve.

Proof of Claim. Without loss of generality, Eq. (S1) implies that the emitted states can be expressed as

$$|\psi_j\rangle_B = e^{i\varphi_j}(\sqrt{1-\epsilon_j}|\phi_j\rangle_B + \sqrt{\epsilon_j}|\phi_j^\perp\rangle_B), \quad (\text{S3})$$

where $\epsilon_j \leq \epsilon$ and $\varphi_j \in [0, 2\pi)$. However, since the global phases φ_j have no physical meaning, we can take $\varphi_j = 0$ and write Eq. (S3) as

$$|\psi_j\rangle_B = \sqrt{1-\epsilon_j}|\phi_j\rangle_B + \sqrt{\epsilon_j}|\phi_j^\perp\rangle_B. \quad (\text{S4})$$

Now, we show that, in Eq. (S4), we can simply consider that $\epsilon_j = \epsilon$. For this, suppose that instead of preparing $\{|\psi_j\rangle_B\}_j$ in Eq. (S4), Alice first generates the states $\{|\psi_j\rangle_{BF}\}_j$:

$$|\psi_j\rangle_{BF} = |\psi_j\rangle_B \otimes \left[\frac{\sqrt{1-\epsilon}}{\sqrt{1-\epsilon_j}}|0\rangle_F + \sqrt{1 - \frac{1-\epsilon}{1-\epsilon_j}}|1\rangle_F \right], \quad (\text{S5})$$

where $\{|0\rangle_F, |1\rangle_F\}$ forms an orthonormal basis, and then emits system B . In both scenarios, the states that Eve observes are the same, and therefore they are equivalent. We can then rewrite Eq. (S5) as

$$|\psi_j\rangle_{BF} = \sqrt{1-\epsilon}|\phi_j\rangle_{BF} + \sqrt{\epsilon}|\phi_j^\perp\rangle_{BF}, \quad (\text{S6})$$

where we have defined $|\phi_j\rangle_{BF} := |\phi_j\rangle_B|0\rangle_F$ and $\langle\phi_j|\phi_j^\perp\rangle_{BF} = 0$. If we assume that Eve also has access to the fictitious system F , which never underestimates her side information, and rename systems BF as simply B , we obtain Eq. (S2), as required. The advantage of Eq. (S2) with respect to Eq. (S4) is that, in the former, the coefficient of the qubit state $|\phi_j\rangle_B$ is known exactly, which is needed to run the semidefinite program (SDP) in Section SE2. \square

(A2) *Basis-independent detection efficiency:* Bob's POVMs can be expressed as $\mathcal{Z} := \{\hat{m}_{0Z}, \hat{m}_{1Z}, \hat{m}_f\}$ and $\mathcal{X} := \{\hat{m}_{0X}, \hat{m}_{1X}, \hat{m}_f\}$, where \hat{m}_f is associated with an inconclusive outcome. That is, the probability that Bob obtains a successful detection is independent of his basis choice, regardless of the state that arrives to his measurement device. For later convenience, we define $\hat{m}_{\text{det}} = \hat{1} - \hat{m}_f$. Also, we assume that there are no side channels on Bob's devices. We remark that, due to the feasibility of attacks that can control the behavior of the detectors [S3–S6], no existing security analysis can achieve information-theoretic security against general detector side channels, and in fact achieving this at the security-proof level may be an unrealistic goal. Fortunately, this issue can be avoided by considering an MDI-type protocol [S7], for which our analysis can be applied to close vulnerabilities and side channels for both Alice and Bob's sources (see Section SM2).

¹ For simplicity, we have considered that ϵ is independent of j , but our security proof can be equally applied when its value is different for different j . Also, as explained in Appendix A, our security proof can be applied under the more general assumption that $|\langle\tilde{\phi}_j|\psi_j\rangle_B|^2 \geq 1 - \epsilon$, where $\{|\tilde{\phi}_j\rangle_B\}_j$ are characterized states, not necessarily qubits.

3. Security framework

The sifted key is generated from the detected key rounds, i.e., the detected rounds in which both Alice and Bob selected the Z basis. Note that, in these rounds, instead of emitting $\{|\psi_{0Z}\rangle_B, |\psi_{1Z}\rangle_B\}$, Alice could have generated the entangled state

$$|\Psi_Z\rangle_{AB} = \frac{1}{\sqrt{2}} (|0_Z\rangle_A |\psi_{0Z}\rangle_B + e^{i\omega} |1_Z\rangle_A |\psi_{1Z}\rangle_B), \quad (\text{S7})$$

where $\omega = [0, 2\pi)$ can be freely chosen, and then measured the ancillary system A in the Z basis. Due to Assumption (A2), the amount of privacy amplification that needs to be applied to the sifted key to turn it into a secret key can be directly related to the error rate that Alice and Bob would have observed if, in these rounds, Alice had measured system A in the X basis and Bob had used the \mathcal{X} POVM, i.e., the phase-error rate e_{ph} . For this estimation, it is useful to rewrite Eq. (S7) as

$$|\Psi_Z\rangle_{AB} = \sqrt{q_{\text{vir0}}^\psi} |0_X\rangle_A |\psi_{\text{vir0}}\rangle_B + e^{i\omega} \sqrt{q_{\text{vir1}}^\psi} |1_X\rangle_A |\psi_{\text{vir1}}\rangle_B, \quad (\text{S8})$$

where

$$\begin{aligned} |\psi_{\text{vir0}}\rangle_B &= \frac{1}{2\sqrt{q_{\text{vir0}}^\psi}} (|\psi_{0Z}\rangle_B + e^{i\omega} |\psi_{1Z}\rangle_B), \\ |\psi_{\text{vir1}}\rangle_B &= \frac{1}{2\sqrt{q_{\text{vir1}}^\psi}} (|\psi_{0Z}\rangle_B - e^{i\omega} |\psi_{1Z}\rangle_B), \end{aligned} \quad (\text{S9})$$

with

$$\begin{aligned} q_{\text{vir0}}^\psi &= \frac{1}{4} \|\psi_{0Z}\rangle_B + e^{i\omega} |\psi_{1Z}\rangle_B\|^2 = \frac{1}{2} (1 + \text{Re} e^{i\omega} \langle \psi_{0Z} | \psi_{1Z} \rangle_B), \\ q_{\text{vir1}}^\psi &= \frac{1}{4} \|\psi_{0Z}\rangle_B - e^{i\omega} |\psi_{1Z}\rangle_B\|^2 = \frac{1}{2} (1 - \text{Re} \{e^{i\omega}\} \langle \psi_{0Z} | \psi_{1Z} \rangle_B). \end{aligned} \quad (\text{S10})$$

Thus, the scenario described above is equivalent to a protocol in which, in the key rounds, Alice emits the *virtual* states $|\psi_{\text{vir0}}\rangle_B$ ($|\psi_{\text{vir1}}\rangle_B$) with probability q_{vir0}^ψ (q_{vir1}^ψ), and Bob uses the \mathcal{X} POVM; we refer to this scenario as the Virtual Protocol (see full description below). We remark that, for clarity, throughout the Supplementary Information we use q_{vir0}^ψ (q_{vir1}^ψ) to denote the probability $1 - q_\epsilon$ (q_ϵ), the notation used in the Main Text.

In this Virtual Protocol, the phase-error rate can be expressed as $e_{\text{ph}} := N_{\text{ph}}/N_{\text{key}}^{\text{det}}$, where $N_{\text{ph}} := N_{\text{vir0}}^{1X} + N_{\text{vir1}}^{0X}$ is the number of phase errors, and $N_{\text{vir}\alpha}^{\beta_X}$ is the number of events in which Alice emits $|\psi_{\text{vir}\alpha}\rangle_B$ and Bob obtains the measurement result β_X , with $\alpha, \beta \in \{0, 1\}$ (see Table S1 in Supplementary Tables for a list of all random variables). The objective of our security analysis is then to find a bound of the form

$$N_{\text{ph}} \leq f(\{N_j^{\beta_X}\}_{j,\beta}, N_{\text{key}}^{\text{det}}) =: N_{\text{ph}}^{\text{U}}, \quad (\text{S11})$$

with a failure probability approaching zero exponentially fast as the number of detected rounds increases, and consequently be able to upper bound the phase-error rate as $e_{\text{ph}}^{\text{U}} := N_{\text{ph}}^{\text{U}}/N_{\text{key}}^{\text{det}}$.

Virtual Protocol

- 1. Quantum communication:** For each of the N rounds: (a) With probability $p_{ZA}p_{ZB}$, the round is a key round. If so, Alice emits $|\psi_{\text{vir0}}\rangle_B$ ($|\psi_{\text{vir1}}\rangle_B$) with probability q_{vir0}^ψ (q_{vir1}^ψ), and Bob uses the \mathcal{X} POVM to measure the incoming signal. (b) With probability p_{XB} , the round is a test round. If so, Alice emits $\{|\psi_j\rangle_B\}_j$ with the same probabilities as in the Actual Protocol and Bob uses the \mathcal{X} POVM to measure the incoming signal. (c) With probability $p_{ZA}p_{ZB}$, Alice emits some state $|\psi_j\rangle_B$ such that $j \notin \{0_Z, 1_Z\}$ and Bob measures the incoming signal using the \mathcal{Z} POVM. As in the Actual Protocol (see Section SM1 A 1), whenever Bob obtains a successful detection, he announces it.
- 2. Basis and bit announcement:** Alice and Bob reveal their basis choices in the detected rounds. In particular, for the key rounds, Bob announces the Z basis even though he uses the \mathcal{X} POVM. This ensures that the announcements in the Virtual Protocol match those in the Actual Protocol. For the test rounds, Bob reveals his bit outcome, and Alice reveals her setting choice j .

Note that, from Eve's perspective, the Virtual Protocol is completely equivalent to Steps 1 and 2 in the Actual Protocol. This is because all quantum and classical information available to her is identical in both protocols². Also, note that the Virtual Protocol is merely a mathematical tool that is used to prove security, and there is no need to implement it in reality.

B. Security proof for a particular three-state scenario

As explained in the Main Text, our approach to obtain e_{ph}^{U} relies on the construction of a loss-tolerant quantum coin state. The exact form of this quantum coin state, and the resulting phase-error rate bound, depends on the form of the states $\{|\phi_j\rangle_B\}_j$. In this Section, we explain all the ideas in our security proof in detail by applying it to a particular three-state scenario in which these states are

$$|\phi_j\rangle_B = \cos(\theta_j) |0_Z\rangle_B + \sin(\theta_j) |1_Z\rangle_B, \quad (\text{S12})$$

for $j \in \{0_Z, 1_Z, 0_X\}$. Here, $\{|0_Z\rangle_B, |1_Z\rangle_B\}$ forms a qubit basis, and

$$\theta_{0_Z} = 0, \quad \theta_{1_Z} = \kappa\pi/2, \quad \theta_{0_X} = \kappa\pi/4, \quad (\text{S13})$$

with $\kappa = 1 + \delta/\pi$, and where $\delta \in [0, \pi)$ quantifies the magnitude of the qubit flaws. Also, for simplicity, in this Section, we assume the asymptotic regime. In Section SM1 D, we present a general analysis that is valid for any $\{|\phi_j\rangle_B\}_j$ and in Section SM1 E, we extend it to the finite-key regime. However, we recommend reading this Section first, as the ideas behind our security proof are explained in much more detail here.

1. Constructing the loss-tolerant quantum coin state

To construct the quantum coin state, we need to appropriately define the target and reference states. For this, we first consider the scenario $\epsilon = 0$ and employ the loss-tolerant (LT) analysis [S14] to find relationships between the virtual and qubit states. For the states in Eq. (S12), these are [S15]

$$|\phi_{\text{vir}0}\rangle\langle\phi_{\text{vir}0}|_B = |\phi_{0_X}\rangle\langle\phi_{0_X}|_B, \quad (\text{S14})$$

$$c_2 |\phi_{0_X}\rangle\langle\phi_{0_X}|_B + |\phi_{\text{vir}1}\rangle\langle\phi_{\text{vir}1}|_B = c_1 |\phi_{0_Z}\rangle\langle\phi_{0_Z}|_B + c_1 |\phi_{1_Z}\rangle\langle\phi_{1_Z}|_B, \quad (\text{S15})$$

where

$$\begin{aligned} c_1 &:= \frac{1}{2\sin^2(\kappa\pi/4)} \in (1/2, 1], \\ c_2 &:= 2c_1 - 1 \in (0, 1], \end{aligned} \quad (\text{S16})$$

and

$$\begin{aligned} |\phi_{\text{vir}0}\rangle_B &= \frac{1}{2\sqrt{q_{\text{vir}0}^\phi}} (|\phi_{0_Z}\rangle_B + |\phi_{1_Z}\rangle_B), \\ |\phi_{\text{vir}1}\rangle_B &= \frac{1}{2\sqrt{q_{\text{vir}1}^\phi}} (|\phi_{0_Z}\rangle_B - |\phi_{1_Z}\rangle_B), \end{aligned} \quad (\text{S17})$$

with

$$\begin{aligned} q_{\text{vir}0}^\phi &= \frac{1}{2} (1 + \text{Re} \langle \phi_{0_Z} | \phi_{1_Z} \rangle_B) = \frac{1}{2c_1}, \\ q_{\text{vir}1}^\phi &= \frac{1}{2} (1 - \text{Re} \langle \phi_{0_Z} | \phi_{1_Z} \rangle_B) = \frac{2c_1 - 1}{2c_1}. \end{aligned} \quad (\text{S18})$$

² Although the Virtual Protocol cannot output the information that is available to Eve in Step 4 of the Actual Protocol, the parameter estimation (i.e., the phase-error rate estimation) established in the Virtual Protocol can be directly used to determine the amount of privacy amplification required in the Actual Protocol [S8–S13].

Note that Eqs. (S17) and (S18) are analogous to Eqs. (S9) and (S10) after taking $\omega = 0$ and substituting the actual Z basis states $|\psi_{0Z}\rangle_B$ and $|\psi_{1Z}\rangle_B$ by their respective qubit components $|\phi_{0Z}\rangle_B$ and $|\phi_{1Z}\rangle_B$. We remark that, for clarity, throughout the Supplementary Information we use $q_{\text{vir}0}^\phi$ ($q_{\text{vir}1}^\phi$) to denote the probability $1 - q_0$ (q_0), the notation used in the Main Text.

When $\epsilon \gtrapprox 0$, namely, in the presence of side channels, the equalities in Eqs. (S14) and (S15) do not hold exactly, but still hold approximately, i.e.,

$$|\psi_{\text{vir}0}\rangle\langle\psi_{\text{vir}0}|_B \approx |\psi_{0X}\rangle\langle\psi_{0X}|_B, \quad (\text{S19})$$

$$c_2 |\psi_{0X}\rangle\langle\psi_{0X}|_B + |\psi_{\text{vir}1}\rangle\langle\psi_{\text{vir}1}|_B \approx c_1 |\psi_{0Z}\rangle\langle\psi_{0Z}|_B + c_1 |\psi_{1Z}\rangle\langle\psi_{1Z}|_B. \quad (\text{S20})$$

Taking advantage of this fact, we define $|\Psi_{\text{Tar}}\rangle_{DAB}$ and $|\Psi_{\text{Ref}}\rangle_{DAB}$ in the following way

$$|\Psi_{\text{Tar}}\rangle_{DAB} = \frac{1}{\sqrt{1 + c_2 q_{\text{vir}1}^\phi}} \left[\sqrt{q_{\text{vir}0}^\psi} |0\rangle_D |0\rangle_A |\psi_{\text{vir}0}\rangle_B + |1\rangle_D \left(\sqrt{c_2 q_{\text{vir}1}^\phi} |0'\rangle_A |\psi_{0X}\rangle_B + \sqrt{q_{\text{vir}1}^\psi} |1'\rangle_A |\psi_{\text{vir}1}\rangle_B \right) \right], \quad (\text{S21})$$

$$|\Psi_{\text{Ref}}\rangle_{DAB} = \frac{1}{\sqrt{1 + c_2 q_{\text{vir}1}^\phi}} \left[\sqrt{q_{\text{vir}0}^\phi} |0\rangle_D |0\rangle_A |\psi_{0X}\rangle_B + \sqrt{c_1 q_{\text{vir}1}^\phi} |1\rangle_D (|0\rangle_A |\psi_{0Z}\rangle_B + |1\rangle_A |\psi_{1Z}\rangle_B) \right]. \quad (\text{S22})$$

In Eq. (S21), the orthonormal basis $\{|0'\rangle_A, |1'\rangle_A\}$ has been chosen such that

$$\sqrt{c_2} |0'\rangle_A |\phi_{0X}\rangle_B + |1'\rangle_A |\phi_{\text{vir}1}\rangle_B = \sqrt{c_1} (|0\rangle_A |\phi_{0Z}\rangle_B + |1\rangle_A |\phi_{1Z}\rangle_B), \quad (\text{S23})$$

which must exist due to the equality in Eq. (S15) and Uhlmann's theorem, and can be calculated to be

$$\begin{aligned} |0'\rangle_A &= \frac{1}{\sqrt{2}} (|0\rangle_A + |1\rangle_A), \\ |1'\rangle_A &= \frac{1}{\sqrt{2}} (|0\rangle_A - |1\rangle_A). \end{aligned} \quad (\text{S24})$$

Note that $|\Psi_{\text{Tar}}\rangle_{DAB} = |\Psi_{\text{Ref}}\rangle_{DAB}$ when $\epsilon = 0$, which ensures the robustness of our phase-error rate bound against qubit flaws; and that, in Eq. (S21), the coefficient of the state $|\psi_{\text{vir}0}\rangle_B$ ($|\psi_{\text{vir}1}\rangle_B$) is proportional to $\sqrt{q_{\text{vir}0}^\psi}$ ($\sqrt{q_{\text{vir}1}^\psi}$). Therefore, the target and reference states in Eq. (S21) and Eq. (S22) fulfill the requirements described in Appendix A for the definition of these states. Our particular choice in Eqs. (S21) and (S22) uses $q_{\text{vir}\alpha}^\phi$ rather than $q_{\text{vir}\alpha}^\psi$ everywhere except in the coefficients of the virtual states. This is advantageous because it will lead to a phase-error rate bound that depends on $q_{\text{vir}\alpha}^\phi$, which is known exactly, rather than $q_{\text{vir}\alpha}^\psi$, which is not (see Eq. (S46) below). This avoids having to use numerical optimization to find the worst-case scenario for $q_{\text{vir}\alpha}^\psi$ in this expression. Finally, we define the loss-tolerant quantum coin state as (see the Main Text for more details)

$$|\Psi_{\text{coin}}\rangle_{CDAB} = \frac{1}{\sqrt{2}} (|0_Z\rangle_C |\Psi_{\text{Tar}}\rangle_{DAB} + |1_Z\rangle_C |\Psi_{\text{Ref}}\rangle_{DAB}), \quad (\text{S25})$$

where system C is held by Alice, and therefore inaccessible to Eve.

2. Overview of the next steps in the security proof

Let us assume that Alice generates many copies of Eq. (S25), sends all systems B to Bob through the Eve-controlled quantum channel, and then probabilistically decides whether to measure each coin system C in the Z basis or X basis. Also, Alice and Bob perform a joint POVM containing the element $\hat{m}_{\text{err}} = |0\rangle\langle 0|_D \otimes \hat{m}_{1X} + |1\rangle\langle 1|_D \otimes \hat{m}_{0X}$. Let $N_{Z_C=0}^{\text{err}}$ ($N_{Z_C=1}^{\text{err}}$) be the number of events in which Alice chooses the Z basis to measure the coin system C , obtains the result $Z_C = 0$ ($Z_C = 1$), and Alice and Bob obtain the outcome associated to \hat{m}_{err} . Note that $N_{Z_C=0}^{\text{err}}$ contains events in which Alice emits $|\psi_{\text{vir}0}\rangle_B$ ($|\psi_{\text{vir}1}\rangle_B$) and Bob obtains measurement outcome 1_X (0_X), i.e., phase errors; and that both $N_{Z_C=0}^{\text{err}}$ and $N_{Z_C=1}^{\text{err}}$ contain events in which Alice emits some actual state $|\psi_j\rangle_B$ and Bob obtains a measurement outcome β_X , whose detection statistics can be observed in the Actual Protocol. These facts allow us to use the quantum coin idea to obtain a bound on the number of phase errors in the Virtual Protocol. More precisely, using the quantum coin inequality (see Section SE1 for more details), we can bound the deviation between $N_{Z_C=0}^{\text{err}}$ and $N_{Z_C=1}^{\text{err}}$

by a function of $N_{X_C=1}$, the overall number of events, detected or not, in which Alice obtained $X_C = 1$. In turn, $N_{X_C=1}$ can be estimated by bounding the *a priori* probability that Alice obtains $X_C = 1$ in her measurement of the quantum coin, as discussed in the Main Text.

However, to use the quantum coin idea, we first need to deal with the fact that the generation of the quantum coin state in Eq. (S25) is not directly equivalent to Alice's state preparation in the Virtual Protocol, and therefore the quantum coin inequality is not directly applicable to the latter scenario. This is because the probability that Alice emits a particular state in the Virtual Protocol differs from the probability that Alice "emits" this state when she generates the quantum coin. For example, the probability that Alice emits the state $|\psi_{0Z}\rangle_B$ in the Virtual Protocol is $p_{Z_A}p_{X_B}/2$, while the probability that Alice "emits" $|\psi_{0Z}\rangle_B$ when she generates the quantum coin is $q_{\text{vir1}}^\phi c_1/(2 + 2c_2q_{\text{vir1}}^\phi)$. In general, it is not possible to select p_{Z_A} and p_{Z_B} such that these probabilities coincide for all states. To address this, we consider a slight modification to the Virtual Protocol. Namely, we consider that, after the quantum communication step, Alice probabilistically assigns tags to her emissions, in such a way that emissions that receive a tag can be regarded as equivalent to those originating from the quantum coin state in Eq. (S25). This allows us to draw an equivalence between the Virtual Protocol and a scenario in which Alice sometimes generates this quantum coin state, which we denote as the Coin Protocol. More specifically, tagged rounds in the former scenario correspond to coin rounds (i.e., rounds in which the quantum coin state is generated) in the latter, see Fig. S1. Thanks to this correspondence, we are able to apply the quantum coin inequality described above to obtain a bound on the number of phase errors within the tagged rounds. Finally, by using the fact that Alice's tag assignment is independent between rounds, and is independent of Bob's measurement outcomes (because it does not affect the emitted quantum state), we combine this result with known random sampling inequalities to obtain a bound on the total number of phase errors. We note that, since the outcomes of the tag assignment step are statistically estimated, Alice does not actually need to perform this tag assignment step in the Actual Protocol; the mere fact that she could have done so is enough for the idea to work.

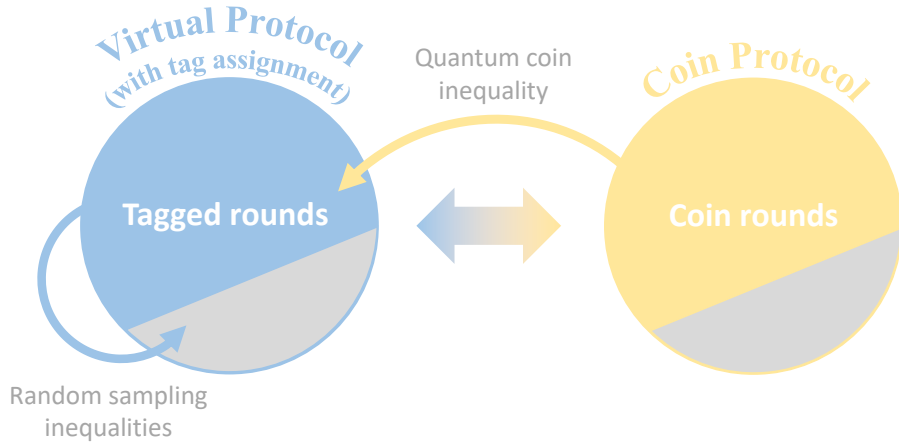


Figure S1. Overview of the phase-error rate estimation. After adding a fictitious tag assignment step to the Virtual Protocol, the tagged rounds can be seen as equivalent to the generation of the quantum coin state $|\Psi_{\text{coin}}\rangle_{CDAB}$ in Eq. (S25). This allows us to use the quantum coin inequality to derive a bound on the number of phase errors within the tagged rounds. Then, we obtain a bound on the total number of phase errors by combining this result with random sampling inequalities.

3. Tag assignment

As explained in Section SM1 B 2, to find an equivalence between the Virtual Protocol and the Coin Protocol, we consider the addition of a fictitious tag assignment step to the former, such that tagged emissions can be regarded as equivalent to those originating from the loss-tolerant quantum coin state in Eq. (S25). Let $l \in \{\text{vir0}, \text{vir1}, 0_Z, 1_Z, 0_X, 0_X^*\}$ denote Alice and Bob's joint selection in Step 1 of the Virtual Protocol, where $l = 0_X$ (0_X^*) denotes an event in which Alice emits $|\psi_{0X}\rangle_B$ and Bob chooses the X (Z) basis, and the rest of the events are self-descriptive. The probability p_l associated to each event in the Virtual Protocol is

$$\begin{aligned}
p_{\text{vir0}} &= q_{\text{vir0}}^\psi p_{Z_A} p_{Z_B}, \\
p_{\text{vir1}} &= q_{\text{vir1}}^\psi p_{Z_A} p_{Z_B}, \\
p_{0_Z} &= p_{1_Z} = \frac{1}{2} p_{Z_A} p_{X_B}, \\
p_{0_X} &= p_{X_A} p_{X_B}, \\
p_{0_X^*} &= p_{X_A} p_{Z_B}.
\end{aligned} \tag{S26}$$

The events $l = 0_X^*$ are irrelevant for the analysis, because Bob's Z -basis measurement results do not help to estimate the phase-error rate, and in the following we assume $l \in \{\text{vir0}, \text{vir1}, 0_Z, 1_Z, 0_X\}$. We can define the additional tag assignment step, which is performed after Step 1 of the Virtual Protocol, as:

1.5. **Tag assignment:** For each event $l \in \{\text{vir0}, \text{vir1}, 0_Z, 1_Z, 0_X\}$, Alice assigns it a single tag $t \in \{\text{TAR}, \text{REF}\}$ with probability $p_{t|l}$, or no tag with probability $1 - \sum_t p_{t|l}$. Then, for the tagged events, Alice marks (i.e., takes note of) each emission as Z_C (X_C) with probability p_{Z_C} ($p_{X_C} = 1 - p_{Z_C}$).

The conditional tag assignment probabilities $\{p_{t|l}\}$ should be chosen carefully, such that an emission with a tag **TAR** (**REF**) is equivalent to that originating from the state $|\Psi_{\text{TAR}}\rangle_{DAB}$ ($|\Psi_{\text{REF}}\rangle_{DAB}$). Also, since the coefficients associated with $|\Psi_{\text{Tar}}\rangle_{DAB}$ and $|\Psi_{\text{Ref}}\rangle_{DAB}$ in Eq. (S25) are identical, the overall probability of assigning both tags must also be identical, i.e., $p_{\text{TAR}} = p_{\text{REF}}$. By doing so, an emission with a tag **TAR** or **REF** can be regarded as equivalent to that originating from the state $|\Psi_{\text{coin}}\rangle_{CDAB}$. In addition, Alice probabilistically marks each tagged emission as Z_C or X_C . These correspond to rounds in which, in the Coin Protocol, Alice measures the quantum coin system C in the Z_C or X_C basis, respectively. In Fig. S2, we depict the Virtual Protocol before and after the tag assignment step. For the latter, we have reordered emissions according to their tag t and mark (Z_C or X_C), which helps represent its equivalence with the Coin Protocol, shown on the right.

Let us rewrite the states $|\Psi_{\text{Tar}}\rangle_{DAB}$ and $|\Psi_{\text{Ref}}\rangle_{DAB}$ in Eqs. (S21) and (S22) as

$$\begin{aligned}
|\Psi_{\text{Tar}}\rangle_{DAB} &= \sqrt{p_{\text{vir0}|\text{TAR}}} |0\rangle_D |0\rangle_A |\psi_{\text{vir0}}\rangle_B + |1\rangle_D (\sqrt{p_{0_X|\text{TAR}}} |0'\rangle_A |\psi_{0_X}\rangle_B + \sqrt{p_{\text{vir1}|\text{TAR}}} |1'\rangle_A |\psi_{\text{vir1}}\rangle_B), \\
|\Psi_{\text{Ref}}\rangle_{DAB} &= \sqrt{p_{0_X|\text{REF}}} |0\rangle_D |0\rangle_A |\psi_{0_X}\rangle_B + |1\rangle_D (\sqrt{p_{0_Z|\text{REF}}} |0\rangle_A |\psi_{0_Z}\rangle_B + \sqrt{p_{1_Z|\text{REF}}} |1\rangle_A |\psi_{1_Z}\rangle_B),
\end{aligned} \tag{S27}$$

where

$$\begin{aligned}
p_{\text{vir0}|\text{TAR}} &= \frac{q_{\text{vir0}}^\psi}{1 + c_2 q_{\text{vir1}}^\phi}, \\
p_{0_X|\text{TAR}} &= \frac{c_2 q_{\text{vir1}}^\phi}{1 + c_2 q_{\text{vir1}}^\phi}, \\
p_{\text{vir1}|\text{TAR}} &= \frac{q_{\text{vir1}}^\psi}{1 + c_2 q_{\text{vir1}}^\phi}, \\
p_{0_X|\text{REF}} &= \frac{q_{\text{vir0}}^\phi}{1 + c_2 q_{\text{vir1}}^\phi}, \\
p_{0_Z|\text{REF}} &= p_{1_Z|\text{REF}} = \frac{c_1 q_{\text{vir1}}^\phi}{1 + c_2 q_{\text{vir1}}^\phi}.
\end{aligned} \tag{S28}$$

The tag assignment probabilities $p_{t|l}$ should be chosen appropriately such that the probability that an emission with tag t originated from event l , $p_{l|t}$, matches Eq. (S28). By Bayes' Theorem, we can express

$$p_{t|l} = \frac{p_t p_{l|t}}{p_l}, \tag{S29}$$

where p_l is the probability of event l and p_t is the overall probability to assign tag t . Note that the sets $\{p_l\}$ and $\{p_{l|t}\}$ are fixed and given by Eqs. (S26) and (S28), respectively. Therefore, the conditional tag assignment probabilities $\{p_{t|l}\}$ become fixed once we fix p_{TAR} and p_{REF} , which should be such that $p_{\text{TAR}} = p_{\text{REF}}$, as explained above. Taking the

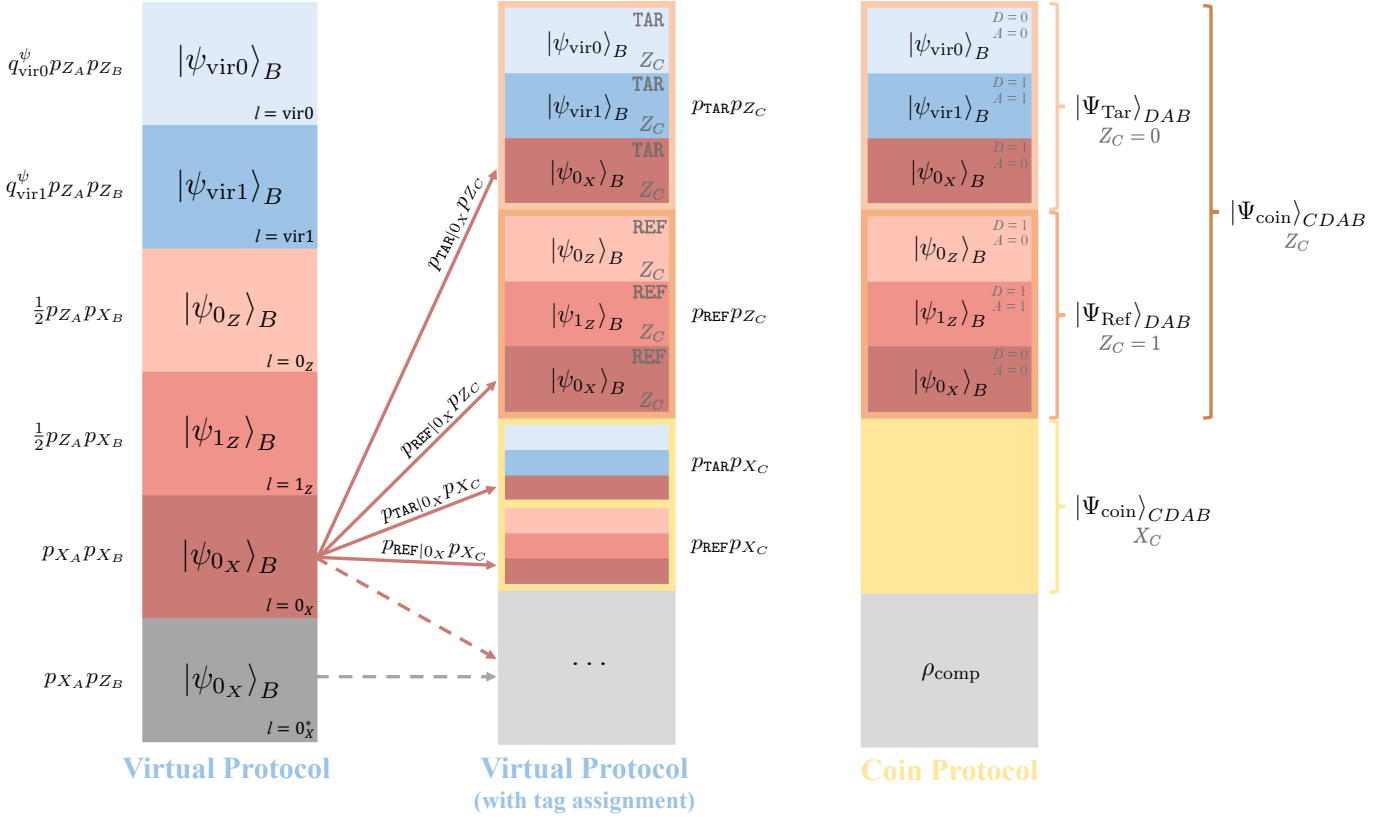


Figure S2. Equivalence between the Virtual Protocol and the Coin Protocol, after adding a fictitious tag assignment step to the former. As an example, this assignment is illustrated for the events $l = 0_X$ using arrows, which are either tagged as $t \in \{\text{TAR, REF}\}$ and marked as Z_C (X_C) with probability $p_{t|0_X}p_{ZC}$ ($p_{t|0_X}p_{XC}$) (solid lines) or receive no tag (dashed line). The emissions with a tag TAR (REF) and marked with Z_C , which are enclosed by an orange square, are equivalent to those originating from the state $|\Psi_{\text{Tar}}\rangle_{DAB}$ ($|\Psi_{\text{Ref}}\rangle_{DAB}$). Also, when considered together, the two orange squares in the Virtual Protocol with tag assignment are equivalent to the generation of the quantum coin state $|\Psi_{\text{coin}}\rangle_{CDAB}$; the same is true for the two yellow squares. Note that, in the Z_C rounds, Alice and Bob learn the same information in both protocols, while in the X_C rounds, they learn different information. The untagged rounds, and their equivalent compensation rounds, are marked in light gray.

sum over $t \in \{\text{TAR, REF}\}$ on both sides of Eq. (S29) and using the fact that $p_{\text{TAR}|l} + p_{\text{REF}|l} \leq 1$, we derive the following constraints,

$$p_{\text{TAR}}p_{l|\text{TAR}} + p_{\text{REF}}p_{l|\text{REF}} \leq p_l, \quad \forall l. \quad (\text{S30})$$

The selected value of $p_{\text{TAR}} = p_{\text{REF}}$ should be consistent with the above inequalities, i.e.,

$$p_{\text{TAR}} = p_{\text{REF}} \leq \min_l \frac{p_l}{p_{l|\text{TAR}} + p_{l|\text{REF}}}. \quad (\text{S31})$$

Substituting Eq. (S26) and Eq. (S28) into Eq. (S31) and simplifying, we obtain

$$p_{\text{TAR}} = p_{\text{REF}} \leq (1 + c_2 q_{\text{vir1}}^\phi) \min \left\{ p_{Z_A} p_{Z_B}, \frac{p_{X_A} p_{X_B}}{1 - (1 - c_2) q_{\text{vir1}}^\phi}, \frac{p_{Z_A} p_{X_B}}{2c_1 q_{\text{vir1}}^\phi} \right\}, \quad (\text{S32})$$

and we can simply select p_{TAR} as the right-hand side of Eq. (S32). Also, substituting Eq. (S28) into Eq. (S29) and using the fact that $p_{\text{TAR}} = p_{\text{REF}}$, we obtain

$$\begin{aligned}
p_{\text{TAR}|\text{vir}} &:= p_{\text{TAR}|\text{vir}0} = p_{\text{TAR}|\text{vir}1} = \frac{p_{\text{TAR}}}{p_{Z_A}p_{Z_B}(1+c_2q_{\text{vir}1}^\phi)}, \\
p_{\text{TAR}|0_X} &= \frac{p_{\text{TAR}}c_2q_{\text{vir}1}^\phi}{p_{X_A}p_{X_B}(1+c_2q_{\text{vir}1}^\phi)}, \\
p_{\text{REF}|0_X} &= \frac{p_{\text{TAR}}q_{\text{vir}0}}{p_{X_A}p_{X_B}(1+c_2q_{\text{vir}1}^\phi)}, \\
p_{\text{REF}|0_Z} &= p_{\text{REF}|1_Z} = \frac{2p_{\text{TAR}}c_1q_{\text{vir}1}^\phi}{p_{Z_A}p_{X_B}(1+c_2q_{\text{vir}1}^\phi)}.
\end{aligned} \tag{S33}$$

Note that these probabilities do not depend on $q_{\text{vir}0}^\psi$, and therefore their exact value is known. This is a consequence of our choice of target and reference states in Eqs. (S21) and (S22).

Random sampling relationships

Let $N_l^{\beta_X}$ be the number of events l in which Bob obtained the measurement result $\beta_X \in \{0_X, 1_X\}$, and let $N_{l,t,Z_C}^{\beta_X}$ be the number of events l with tag t marked as Z_C in which Bob obtained β_X . The probability that a given event l is assigned a tag t must be independent of Bob's measurement result for that round, since the tag assignment does not change the emitted quantum state, and Eve has no tag information. The same is true for the probability that the event is marked as Z_C . Therefore, $N_{l,t,Z_C}^{\beta_X}$ is a random sample of a population of $N_l^{\beta_X}$ events, where each event is selected with probability $p_{Z_C}p_{t|l}$. By the Chernoff bound [S16],

$$N_{l,t,Z_C}^{\beta_X} \simeq p_{Z_C}p_{t|l}N_l^{\beta_X}, \tag{S34}$$

where the symbol “ \simeq ” denotes that the ratio between the left- and right-hand sides approaches one as $N \rightarrow \infty$ (see Section SM1 E for the analysis with a finite N). Similarly, if we denote $N_l^{\text{det}} = N_l^{0_X} + N_l^{1_X}$ and $N_{l,t,Z_C}^{\text{det}} = N_{l,t,Z_C}^{0_X} + N_{l,t,Z_C}^{1_X}$, we have that

$$N_{l,t,Z_C}^{\text{det}} \simeq p_{Z_C}p_{t|l}N_l^{\text{det}}. \tag{S35}$$

4. Coin Protocol

We are now ready to provide a full definition for the Coin Protocol. We remark that, in addition to coin rounds, this scenario also contains rounds in which the quantum coin state is not generated, which correspond to the untagged rounds in the Virtual Protocol with tag assignment. In these rounds, which we denote as compensation rounds, Alice prepares a state ρ_{comp} that is equivalent to the average state emitted in an untagged round, see Fig. S2. This ensures the overall equivalence between the Coin Protocol and the Virtual Protocol with tag assignment.

Coin Protocol

- 1. State preparation:** (a) With probability $p_C := p_{\text{TAR}} + p_{\text{REF}} = 2p_{\text{TAR}}$, the round is a coin round. Alice prepares $|\Psi_{\text{coin}}\rangle_{CDAB}$, and sends system B through a quantum channel. (b) With probability $1 - p_C$, the round is a compensation round. Alice prepares ρ_{comp} and sends it through the quantum channel.
- 2. Detection:** For each round, Bob performs the POVM $\{\hat{m}_{0_X}, \hat{m}_{1_X}, \hat{m}_f\}$. If he obtains a successful detection, which is associated to the outcome $\hat{m}_{\text{det}} := \hat{\mathbb{I}} - \hat{m}_f$, he announces this information.
- 3. Coin measurement:** For each coin round, Alice chooses the basis Z_C (X_C) with probability p_{Z_C} (p_{X_C}), and measures system C in the chosen basis. Let $N_{Z_C=0}^{\text{det}}$ ($N_{Z_C=1}^{\text{det}}$) be the number of detected rounds in which Alice chose Z_C and obtained the outcome $Z_C = 0$ ($Z_C = 1$).
- 4. Ancilla measurement:** For each detected coin round in which Alice chose Z_C , she measures system D in the basis $\{|0\rangle_D, |1\rangle_D\}$, whose measurement outcome we denote by $D = d$ for $d \in \{0, 1\}$. Note that the outcome of this measurement, together with the outcome of Bob's measurement in Step 2, associates each of these rounds to one of $\{\hat{m}_{\text{err}}, \hat{\mathbb{I}} - \hat{m}_{\text{err}}\}$, where $\hat{m}_{\text{err}} = |0\rangle\langle 0|_D \otimes \hat{m}_{1_X} + |1\rangle\langle 1|_D \otimes \hat{m}_{0_X}$. Then, if she obtained $D = 0$, or if she obtained $D = 1$ and $Z_C = 1$, she measures system A in the $\{|0\rangle_A, |1\rangle_A\}$ basis; if she

obtained $D = 1$ and $Z_C = 0$, she measures system A in the $\{|0\rangle_A, |1\rangle_A\}$ basis. In either case, we denote the outcome of this measurement as $A = a$, with $a \in \{0, 1\}$. Also, let $N_{Z_C=z, D=d, A=a}^{\beta_X}$ be the number of rounds in which Alice obtained $Z_C = z, D = d, A = a$ and Bob obtained the outcome associated to \hat{m}_{β_X} , and let $N_{Z_C=z, D=d, A=a}^{\det} = N_{Z_C=z, D=d, A=a}^{0_X} + N_{Z_C=z, D=d, A=a}^{1_X}$.

Note that, in the coin rounds in which Alice chooses Z_C , Alice and Bob learn the same information as in the tagged rounds marked as Z_C in the Virtual Protocol with tag assignment. This allows us to draw an equivalence between the random variables associated to these rounds in the two scenarios. For example, in the Coin Protocol in Fig. S2, if Alice obtains $Z_C = 0, d = 0$ and $a = 0$, she has learned that she emitted $|\psi_{\text{vir0}}\rangle_B$. The number of these events in which Bob obtains a measurement outcome of, say, $1_X, N_{Z_C=0, d=0, a=0}^{1_X}$, is equivalent to the number of events in which, in the Virtual Protocol with tag assignment, Alice emits $|\psi_{\text{vir0}}\rangle_B$, assigns it a tag $t = \text{TAR}$, marks it as Z_C , and Bob obtains the outcome $1_X, N_{\text{vir0,TAR}, Z_C}^{1_X}$. We represent this equivalence as $N_{Z_C=0, d=0, a=0}^{1_X} \equiv N_{\text{vir0,TAR}, Z_C}^{1_X}$. Moreover, in the Coin Protocol, due to the form of the operator \hat{m}_{err} and Eqs. (S21), (S22) and (S25), we have relationships of the form $N_{Z_C=0}^{\text{err}} = N_{Z_C=0, d=0, a=0}^{1_X} + N_{Z_C=0, d=1, a=1}^{0_X} + N_{Z_C=0, d=1, a=0}^{0_X}$, and so on. Putting it all together, we have that

$$\begin{aligned} N_{Z_C=0}^{\text{err}} &= N_{Z_C=0, d=0, a=0}^{1_X} + N_{Z_C=0, d=1, a=1}^{0_X} + N_{Z_C=0, d=1, a=0}^{0_X} \equiv N_{\text{vir0,TAR}, Z_C}^{1_X} + N_{\text{vir1,TAR}, Z_C}^{0_X} + N_{0_X, \text{TAR}, Z_C}^{0_X}, \\ N_{Z_C=1}^{\text{err}} &= N_{Z_C=1, d=0, a=0}^{1_X} + N_{Z_C=1, d=1, a=0}^{0_X} + N_{Z_C=1, d=1, a=1}^{0_X} \equiv N_{0_X, \text{REF}, Z_C}^{1_X} + N_{0_Z, \text{REF}, Z_C}^{0_X} + N_{1_Z, \text{REF}, Z_C}^{0_X}, \\ N_{Z_C=0}^{\det} &= N_{Z_C=0, d=0, a=0}^{\det} + N_{Z_C=0, d=1, a=1}^{\det} + N_{Z_C=0, d=1, a=0}^{\det} \equiv N_{\text{vir0,TAR}, Z_C}^{\det} + N_{\text{vir1,TAR}, Z_C}^{\det} + N_{0_X, \text{TAR}, Z_C}^{\det}, \\ N_{Z_C=1}^{\det} &= N_{Z_C=1, d=0, a=0}^{\det} + N_{Z_C=1, d=1, a=0}^{\det} + N_{Z_C=1, d=1, a=1}^{\det} \equiv N_{0_X, \text{REF}, Z_C}^{\det} + N_{0_Z, \text{REF}, Z_C}^{\det} + N_{1_Z, \text{REF}, Z_C}^{\det}. \end{aligned} \quad (\text{S36})$$

Substituting the random sampling relations in Eqs. (S34) and (S35) into Eq. (S36), we obtain

$$\begin{aligned} N_{Z_C=0}^{\text{err}} &\simeq p_{Z_C} (p_{\text{TAR}|\text{vir0}} N_{\text{vir0}}^{1_X} + p_{\text{TAR}|\text{vir1}} N_{\text{vir1}}^{0_X} + p_{\text{TAR}|0_X} N_{0_X}^{0_X}) \stackrel{(1)}{=} p_{Z_C} (p_{\text{TAR}|\text{vir}} N_{\text{ph}} + p_{\text{TAR}|0_X} N_{0_X}^{0_X}), \\ N_{Z_C=1}^{\text{err}} &\simeq p_{Z_C} (p_{\text{REF}|0_X} N_{0_X}^{1_X} + p_{\text{REF}|0_Z} N_{0_Z}^{0_X} + p_{\text{REF}|1_Z} N_{1_Z}^{0_X}), \\ N_{Z_C=0}^{\det} &\simeq p_{Z_C} (p_{\text{TAR}|\text{vir0}} N_{\text{vir0}}^{\det} + p_{\text{TAR}|\text{vir1}} N_{\text{vir1}}^{\det} + p_{\text{TAR}|0_X} N_{0_X}^{\det}) \stackrel{(2)}{=} p_{Z_C} (p_{\text{TAR}|\text{vir}} N_{\text{key}}^{\det} + p_{\text{TAR}|0_X} N_{0_X}^{\det}), \\ N_{Z_C=1}^{\det} &\simeq p_{Z_C} (p_{\text{REF}|0_X} N_{0_X}^{\det} + p_{\text{REF}|0_Z} N_{0_Z}^{\det} + p_{\text{REF}|1_Z} N_{1_Z}^{\det}). \end{aligned} \quad (\text{S37})$$

In the equalities marked by (1) and (2), we have used $p_{\text{TAR}|\text{vir}} := p_{\text{TAR}|\text{vir0}} = p_{\text{TAR}|\text{vir1}}$; in the equality marked by (1), we have used $N_{\text{ph}} := N_{\text{vir0}}^{1_X} + N_{\text{vir1}}^{0_X}$; and in the equality marked by (2), we have used the fact that $N_{\text{vir0}}^{\det} + N_{\text{vir1}}^{\det}$ equals the length of the sifted key, N_{key}^{\det} .

As explained in Section SMI B 2, using the quantum coin idea, we can find a statistical relationship — the quantum coin inequality — between the random variables $\{N_{Z_C=0}^{\text{err}}, N_{Z_C=1}^{\text{err}}, N_{Z_C=0}^{\det}, N_{Z_C=1}^{\det}, N_{X_C=1}\}$. Namely, in Section SE1, we show that,

$$N_{Z_C=0}^{\text{err}} \lesssim N_{Z_C=0}^{\det} G_+ \left(\frac{N_{Z_C=1}^{\text{err}}}{N_{Z_C=1}^{\det}}, 1 - \frac{2p_{Z_C} N_{X_C=1}}{p_{X_C} (N_{Z_C=0}^{\det} + N_{Z_C=1}^{\det})} \right), \quad (\text{S38})$$

where the symbol \lesssim means that, in the limit $N \rightarrow \infty$, the ratio between the left and right-hand sides is less or equal to one; and where

$$G_+(y, z) = \begin{cases} y + (1 - z^2)(1 - 2y) + 2\sqrt{z^2(1 - z^2)y(1 - y)} & \text{if } 0 \leq y < z^2 \leq 1, \\ 1 & \text{otherwise.} \end{cases} \quad (\text{S39})$$

Moreover, note that the event “Alice generates the quantum coin, chooses the X_C basis and obtains the result $X_C = 1$ ” is independently and identically distributed for the N rounds of the Coin Protocol, because Alice’s measurement on each coin system C commutes with any other measurement in any other system. Therefore, using the Chernoff bound, we have that

$$N_{X_C=1} \simeq N p_C p_{X_C} \frac{1 - \text{Re} \langle \Psi_{\text{Ref}} | \Psi_{\text{Tar}} \rangle_{DAB}}{2}. \quad (\text{S40})$$

In Section SE2, we show how to obtain a bound

$$1 - \text{Re} \langle \Psi_{\text{Ref}} | \Psi_{\text{Tar}} \rangle_{DAB} \leq \Delta, \quad (\text{S41})$$

numerically using SDP techniques, and analytically with an additional assumption on the form of the states $\{|\psi_j\rangle_B\}_j$. Combining Eqs. (S40) and (S41), we arrive at

$$N_{X_C=1} \lesssim \frac{N p_C p_{X_C} \Delta}{2} =: N_{X_C=1}^U. \quad (\text{S42})$$

Substituting Eq. (S42) into Eq. (S38), and using $p_C := p_{\text{TAR}} + p_{\text{REF}} = 2p_{\text{TAR}}$, we obtain

$$N_{Z_C=0}^{\text{err}} \lesssim N_{Z_C=0}^{\text{det}} G_+ \left(\frac{N_{Z_C=1}^{\text{err}}}{N_{Z_C=1}^{\text{det}}}, 1 - \frac{2p_{Z_C} p_{\text{TAR}} N \Delta}{N_{Z_C=0}^{\text{det}} + N_{Z_C=1}^{\text{det}}} \right). \quad (\text{S43})$$

Finally, substituting Eqs. (S33) and (S37) into Eq. (S43), and taking into account that $N_l^{\text{det}} = N_l^{0x} + N_l^{1x}$ for $l \in \{0_Z, 1_Z, 0_X\}$, we obtain a bound of the form

$$N_{\text{ph}} \lesssim f(N_{0_Z}^{0x}, N_{0_Z}^{1x}, N_{1_Z}^{0x}, N_{1_Z}^{1x}, N_{0_X}^{0x}, N_{0_X}^{1x}, N_{\text{key}}^{\text{det}}) =: N_{\text{ph}}^U, \quad (\text{S44})$$

and, as desired, the bound on the phase-error rate is given by

$$e_{\text{ph}} \lesssim \frac{N_{\text{ph}}^U}{N_{\text{key}}^{\text{det}}} =: e_{\text{ph}}^U. \quad (\text{S45})$$

Note that, in the Coin Protocol defined in this Section, Alice and Bob do not make any basis and bit announcements. Therefore, strictly speaking, the Coin Protocol is only equivalent to the Virtual Protocol *before* the basis and bit announcement step of the latter. In other words, we have proven that Eq. (S45) holds *before* this basis and bit announcement step. However, note that e_{ph}^U is a function of the random variables $\{N_{0_Z}^{0x}, N_{0_Z}^{1x}, N_{1_Z}^{0x}, N_{1_Z}^{1x}, N_{0_X}^{0x}, N_{0_X}^{1x}, N_{\text{key}}^{\text{det}}\}$, whose distribution depends only on Eve's attack, which she can no longer modify after Bob has finished all his measurements in the quantum communication phase of the protocol. Thus, if Eq. (S45) holds *before* the basis and bit announcement step, it must also hold *after* this step, which concludes the proof.

Because of the above, a corollary of our result is that, in security proofs based on the quantum coin idea, including our proof, one can extract key from both the instances in which Alice selects Z_C and the instances in which she selects X_C . In fact, in the Actual Protocol, Alice does not even need to decide which instances belong to Z_C or X_C . This decision only needs to be made in the fictitious tag assignment step, allowing us to obtain a statistical statement for the rounds marked as Z_C , and then extending it to the rest of rounds via random sampling arguments. A key reason why this is allowed is that, in the Coin Protocol, Alice does not make any postselection or perform any operation that depends on the outcome of her X_C measurements. Moreover, our statistical bound on the number of phase errors does not depend on these outcomes, since the random variable $N_{X_C=1}$ is replaced by its upper bound $N_{X_C=1}^U$, where both $N_{X_C=1}^U$ and the failure probability of the bound $\Pr[N_{X_C=1} > N_{X_C=1}^U]$ are constants that can be calculated and set before running the protocol. Therefore, the estimation remains valid even if, in the rounds marked as X_C , Alice does not actually perform the X_C measurement, or even if she performs the Z_C measurement instead. Moreover, since her measurement on the rounds marked as X_C does not change the reduced density operator on the rounds marked as Z_C , and the rounds marked as Z_C and X_C are identical, the statistical statement obtained for the rounds marked as Z_C can be extended to the rounds marked as X_C via the random sampling argument. This is another improvement over previous security proofs based on the quantum coin idea, in which, in the actual protocol, Alice actually needed to probabilistically mark each detected round as either Z_C or X_C and discard those marked as X_C [S17–S19].

Throughout this Section, for simplicity, we have assumed the asymptotic regime ($N \rightarrow \infty$), in which the phase-error rate bound can be expressed as

$$e_{\text{ph}}^U \simeq \left(1 + \frac{c_2 q_{\text{vir1}}^\phi Y_{0_X}}{Y_Z} \right) G_+ \left(\frac{q_{\text{vir0}}^\phi Y_{0_X}^{1x} + c_1 q_{\text{vir1}}^\phi (Y_{0_Z}^{0x} + Y_{1_Z}^{0x})}{q_{\text{vir0}}^\phi Y_{0_X} + c_1 q_{\text{vir1}}^\phi Y_Z}, 1 - \frac{2\Delta(1 + c_2 q_{\text{vir1}}^\phi)}{Y_Z + q_{\text{vir0}}^\phi Y_{0_X} + q_{\text{vir1}}^\phi (c_2 Y_{0_X} + c_1 Y_Z)} \right) - \frac{c_2 q_{\text{vir1}}^\phi Y_{0_X}^{0x}}{Y_Z}, \quad (\text{S46})$$

where we have used that $N_j^{\beta_X} \simeq N p_j Y_j^{\beta_X}$ and $N_{\text{key}}^{\text{det}} \simeq N p_{Z_A} p_{Z_B} Y_Z$, with p_j for $j \in \{0_Z, 1_Z, 0_X\}$ defined in Eq. (S26), $Y_j^{\beta_X}$ is the observed rate at which Bob obtains β_X conditioned on Alice selecting the setting j , and Y_Z is the rate at which Bob obtains a detection event conditioned on Alice choosing the Z basis. Also, in Eq. (S46), we have used the fact that $Y_Z = Y_Z^{0z} + Y_Z^{1z} = Y_Z^{0x} + Y_Z^{1x}$ (see Assumption A2). Using e_{ph}^U , we can finally obtain a lower bound on the asymptotic secret-key rate:

$$R \geq p_{Z_A} p_{Z_B} Y_Z [1 - h(e_{\text{ph}}^U) - f h(e_Z)], \quad (\text{S47})$$

where $h(x) = -x \log_2 x - (1-x) \log_2(1-x)$ is the binary entropy function, f is the error correction inefficiency and e_Z is the bit-error rate. We remark that it is straightforward to apply our analysis in the finite-key regime by taking into account the deviation terms and failure probabilities associated to the concentration inequalities employed in the analysis. In Section SM1 E, we explicitly show how to derive a bound on the phase-error rate that takes into account finite-key effects and how to calculate the secret-key length.

C. Security proof for a particular BB84 scenario

1. Security analysis

Here, we apply our security proof to the BB84 scenario considered in the Main Text. This scenario only differs from the one in the previous section in that Alice sends an additional state $|\psi_{1x}\rangle_B$ whose qubit component $|\phi_{1x}\rangle_B$ is given by Eq. (S12) with $\theta_{1x} = 3\kappa\pi/4$.

Similarly to Section SM1 B 1, we can use the LT analysis to obtain the following expressions

$$|\phi_{\text{vir}0}\rangle\langle\phi_{\text{vir}0}|_B = |\phi_{0x}\rangle\langle\phi_{0x}|_B, \quad (\text{S48})$$

$$c_1 |\phi_{0z}\rangle\langle\phi_{0z}|_B + |\phi_{\text{vir}1}\rangle\langle\phi_{\text{vir}1}|_B = c_2 |\phi_{1z}\rangle\langle\phi_{1z}|_B + c_3 |\phi_{1x}\rangle\langle\phi_{1x}|_B, \quad (\text{S49})$$

where

$$\begin{aligned} c_1 &:= \frac{\cos(\kappa\pi/2)}{\cos(\kappa\pi) - \cos(\kappa\pi/2)}, \\ c_2 &:= \frac{\cos(\kappa\pi/2)}{\cos(\kappa\pi/2) - 1}, \\ c_3 &:= \frac{1 + \cos(\kappa\pi/2)}{\cos(\kappa\pi/2) - \cos(\kappa\pi)}. \end{aligned} \quad (\text{S50})$$

We remark that, for this scenario, Eqs. (S48) and (S49) are just one of the possible ways to write the virtual states as a linear function of qubit states. Indeed, to find these expressions, we have to solve two systems of three linear equations with four unknowns, which have infinitely many solutions. This is in contrast with the three-state scenario considered in Section SM1 B, whose two systems of three linear equations have three unknowns and thus have a unique solution each. Here, we select the solution given by Eqs. (S48) and (S49) because it provides the tightest bound on the phase-error rate [S20]. When $\epsilon \gtrless 0$, these equations do not hold exactly, but still hold approximately, i.e.,

$$|\psi_{\text{vir}0}\rangle\langle\psi_{\text{vir}0}|_B \approx |\psi_{0x}\rangle\langle\psi_{0x}|_B, \quad (\text{S51})$$

$$c_1 |\psi_{0z}\rangle\langle\psi_{0z}|_B + |\psi_{\text{vir}1}\rangle\langle\psi_{\text{vir}1}|_B \approx c_2 |\psi_{1z}\rangle\langle\psi_{1z}|_B + c_3 |\psi_{1x}\rangle\langle\psi_{1x}|_B. \quad (\text{S52})$$

Taking into account the relationships in Eqs. (S51) and (S52), we define the following target and reference states

$$|\Psi_{\text{Tar}}\rangle_{DAB} = \frac{1}{\sqrt{1 + c_1 q_{\text{vir}1}^\phi}} \left[\sqrt{q_{\text{vir}0}^\psi} |0\rangle_D |0\rangle_A |\psi_{\text{vir}0}\rangle_B + |1\rangle_D \left(\sqrt{c_1 q_{\text{vir}1}^\phi} |0'\rangle_A |\psi_{0z}\rangle_B + \sqrt{q_{\text{vir}1}^\psi} |1'\rangle_A |\psi_{\text{vir}1}\rangle_B \right) \right], \quad (\text{S53})$$

$$|\Psi_{\text{Ref}}\rangle_{DAB} = \frac{1}{\sqrt{1 + c_1 q_{\text{vir}1}^\phi}} \left[\sqrt{q_{\text{vir}0}^\phi} |0\rangle_D |0\rangle_A |\psi_{0x}\rangle_B + \sqrt{q_{\text{vir}1}^\phi} |1\rangle_D \left(\sqrt{c_2} |0\rangle_A |\psi_{1z}\rangle_B + \sqrt{c_3} |1\rangle_A |\psi_{1x}\rangle_B \right) \right], \quad (\text{S54})$$

where $q_{\text{vir}\alpha}^\phi$ and $q_{\text{vir}\alpha}^\psi$ are defined in Eq. (S18) and Eq. (S10), respectively. In Eq. (S54), the orthonormal basis $\{|0'\rangle_A, |1'\rangle_A\}$ has been chosen such that

$$\sqrt{c_1} |0'\rangle_A |\phi_{0z}\rangle_B + |1'\rangle_A |\phi_{\text{vir}1}\rangle_B = \sqrt{c_2} |0\rangle_A |\phi_{1z}\rangle_B + \sqrt{c_3} |1\rangle_A |\phi_{1x}\rangle_B, \quad (\text{S55})$$

which must exist due to Eq. (S49), and can be calculated to be

$$\begin{aligned} |0'\rangle_A &= \sqrt{\frac{\cos(\kappa\pi) - \cos(\kappa\pi/2)}{\cos(\kappa\pi/2) - 1}} |0\rangle_A - \sqrt{-2 \cos(\kappa\pi/2)} |1\rangle_A, \\ |1'\rangle_A &= -\sqrt{-2 \cos(\kappa\pi/2)} |0\rangle_A - \sqrt{\frac{\cos(\kappa\pi) - \cos(\kappa\pi/2)}{\cos(\kappa\pi/2) - 1}} |1\rangle_A. \end{aligned} \quad (\text{S56})$$

Note that the definitions in Eqs. (S53) and (S54) are slightly different from those in Eqs. (9) and (10) of the Main Text, i.e., the coefficients associated with the actual states depend on $q_{\text{vir}\alpha}^\phi$ rather than on $q_{\text{vir}\alpha}^\psi$. As explained in Appendix A, one can make different choices of target and reference states given that they satisfy the required conditions. The states in Eqs. (S53) and (S54) do so because: (1) $|\Psi_{\text{Tar}}\rangle_{DAB} = |\Psi_{\text{Ref}}\rangle_{DAB}$ when $\epsilon = 0$ due to our choice in Eq. (S56), and (2) the coefficient of the state $|\psi_{\text{vir}0}\rangle_B$ ($|\psi_{\text{vir}1}\rangle_B$) is proportional to $\sqrt{q_{\text{vir}0}^\psi} \left(\sqrt{q_{\text{vir}1}^\psi} \right)$. The advantage of Eqs. (S53) and (S54) over Eqs. (9) and (10) is that our final bound on e_{ph} is independent of $q_{\text{vir}\alpha}^\psi$ (see Eq. (S63) below), and therefore no numerical optimization is needed. Using Eqs. (S53) and (S54), we can then define the loss-tolerant quantum coin state as

$$|\Psi_{\text{coin}}\rangle_{CDAB} = \frac{1}{\sqrt{2}} (|0_Z\rangle_C |\Psi_{\text{Tar}}\rangle_{DAB} + |1_Z\rangle_C |\Psi_{\text{Ref}}\rangle_{DAB}). \quad (\text{S57})$$

The rest of the analysis is essentially the same as for the three-state protocol. First, as in Section SM1 B 3, we add a fictitious tag assignment to the Virtual Protocol, such that the tagged rounds can be regarded as equivalent to generating the quantum coin state in Eq. (S57). The only difference is the definition of l , which for the BB84 protocol is $l \in \{\text{vir}0, \text{vir}1, 0_Z, 1_Z, 0_X, 1_X\}$. Then, as in Section SM1 B 4, we consider a Coin Protocol and obtain that, in the limit $N \rightarrow \infty$,

$$\begin{aligned} N_{Z_C=0}^{\text{err}} &\simeq p_{Z_C} (p_{\text{TAR}|\text{vir}} N_{\text{ph}} + p_{\text{TAR}|0_Z} N_{0_Z}^{0_X}), \\ N_{Z_C=1}^{\text{err}} &\simeq p_{Z_C} (p_{\text{REF}|0_X} N_{0_X}^{1_X} + p_{\text{REF}|1_Z} N_{1_Z}^{0_X} + p_{\text{REF}|1_X} N_{1_X}^{0_X}), \\ N_{Z_C=0}^{\text{det}} &\simeq p_{Z_C} (p_{\text{TAR}|\text{vir}} N_{\text{key}}^{\text{det}} + p_{\text{TAR}|0_Z} N_{0_Z}^{\text{det}}), \\ N_{Z_C=1}^{\text{det}} &\simeq p_{Z_C} (p_{\text{REF}|0_X} N_{0_X}^{\text{det}} + p_{\text{REF}|1_Z} N_{1_Z}^{\text{det}} + p_{\text{REF}|1_X} N_{1_X}^{\text{det}}), \end{aligned} \quad (\text{S58})$$

where

$$\begin{aligned} p_{\text{TAR}|\text{vir}} &:= p_{\text{TAR}|\text{vir}0} = p_{\text{TAR}|\text{vir}1} = \frac{p_{\text{TAR}}}{p_{Z_A} p_{Z_B} (1 + c_1 q_{\text{vir}1}^\phi)}, \\ p_{\text{TAR}|0_Z} &= \frac{2p_{\text{TAR}} c_1 q_{\text{vir}1}^\phi}{p_{Z_A} p_{X_B} (1 + c_1 q_{\text{vir}1}^\phi)}, \\ p_{\text{REF}|0_X} &= \frac{2p_{\text{TAR}} q_{\text{vir}0}^\phi}{p_{X_A} p_{X_B} (1 + c_1 q_{\text{vir}1}^\phi)}, \\ p_{\text{REF}|1_Z} &= \frac{2p_{\text{TAR}} c_2 q_{\text{vir}1}^\phi}{p_{Z_A} p_{X_B} (1 + c_1 q_{\text{vir}1}^\phi)}, \\ p_{\text{REF}|1_X} &= \frac{2p_{\text{TAR}} c_3 q_{\text{vir}1}^\phi}{p_{X_A} p_{X_B} (1 + c_1 q_{\text{vir}1}^\phi)}, \end{aligned} \quad (\text{S59})$$

and

$$p_{\text{TAR}} \leq (1 + c_1 q_{\text{vir}1}^\phi) \min \left\{ p_{Z_A} p_{Z_B}, \frac{p_{Z_A} p_{X_B}}{2c_1 q_{\text{vir}1}^\phi}, \frac{p_{Z_A} p_{X_B}}{2c_2 q_{\text{vir}1}^\phi}, \frac{p_{X_A} p_{X_B}}{2q_{\text{vir}10}^\phi}, \frac{p_{X_A} p_{X_B}}{2c_3 q_{\text{vir}1}^\phi} \right\}. \quad (\text{S60})$$

Finally, using the quantum coin inequality (see Section SE1 for more details), we have that

$$N_{Z_C=0}^{\text{err}} \lesssim N_{Z_C=0}^{\text{det}} G_+ \left(\frac{N_{Z_C=1}^{\text{err}}}{N_{Z_C=1}^{\text{det}}}, 1 - \frac{2p_{Z_C} p_{\text{TAR}} N \Delta}{N_{Z_C=0}^{\text{det}} + N_{Z_C=1}^{\text{det}}} \right), \quad (\text{S61})$$

where $\Delta \geq 1 - \text{Re} \langle \Psi_{\text{Ref}} | \Psi_{\text{Tar}} \rangle_{DAB}$. As before, we can obtain Δ by using SDP techniques, as described in Section SE2. Then, by substituting Eqs. (S58) and (S59) into Eq. (S61), and by taking into account that $N_l^{\text{det}} = N_l^{0_X} + N_l^{1_X}$ for $l \in \{0_Z, 1_Z, 0_X, 1_X\}$, we obtain a bound of the form

$$N_{\text{ph}} \lesssim f(N_{0_Z}^{0_X}, N_{0_Z}^{1_X}, N_{1_Z}^{0_X}, N_{1_Z}^{1_X}, N_{0_X}^{0_X}, N_{0_X}^{1_X}, N_{0_X}^{0_Z}, N_{0_X}^{1_Z}, N_{1_X}^{0_X}, N_{1_X}^{1_X}, N_{\text{key}}^{\text{det}}) =: N_{\text{ph}}^{\text{U}}, \quad (\text{S62})$$

as desired. Our bound on the phase-error rate is then $e_{\text{ph}}^{\text{U}} \simeq N_{\text{ph}}^{\text{U}} / N_{\text{key}}^{\text{det}}$, and in the asymptotic regime, it can be expressed as

$$e_{\text{ph}}^{\text{U}} \simeq \left(1 + \frac{c_1 q_{\text{vir1}}^{\phi} Y_{0Z}}{Y_Z}\right) G_+ \left(\frac{q_{\text{vir0}}^{\phi} Y_{0X}^{1X} + q_{\text{vir1}}^{\phi} (c_2 Y_{1Z}^{0X} + c_3 Y_{1X}^{0X})}{q_{\text{vir0}}^{\phi} Y_{0X} + q_{\text{vir1}}^{\phi} (c_2 Y_{1Z} + c_3 Y_{1X})}, 1 - \frac{2\Delta(1 + c_1 q_{\text{vir1}}^{\phi})}{Y_Z + q_{\text{vir0}}^{\phi} Y_{0X} + q_{\text{vir1}}^{\phi} (c_1 Y_{0Z} + c_2 Y_{1Z} + c_3 Y_{1X})} \right) - \frac{c_1 q_{\text{vir1}}^{\phi} Y_{0Z}^{0X}}{Y_Z}. \quad (\text{S63})$$

Finally, by substituting Eq. (S63) into Eq. (S47) we obtain the secret-key rate of the protocol. We remark that this analysis can be extended to the finite-key regime using the procedure in Section SM1 E below.

2. Investigating how tight is our security proof

The analysis for the BB84 protocol presented in the previous section was used to plot Fig. 1 in the Main Text. As one can see in that figure, to achieve non-zero key rates at reasonable distances, one needs to guarantee that ϵ is fairly small. However, here, we highlight that this is, for the most part, a fundamental limitation of QKD protocols, rather than a specific drawback of our analysis. More specifically, here we show that, if the only information available about the emitted states $\{|\psi_j\rangle_B\}_j$ is that their overlap with some other states $\{|\phi_j\rangle_B\}_j$ is bounded by a certain threshold, i.e., $|\langle\phi_j|\psi_j\rangle_B|^2 \geq 1 - \epsilon$, no security proof can achieve any key rate when the detection rate η is such that $\eta \leq \epsilon$, which is not so far off from what our security proof achieves.

Remember that the emitted states can be expressed as in Eq. (S2), where the only information known about the side-channel states $\{|\phi_j^\perp\rangle_B\}_j$ is that $\langle\phi_j^\perp|\phi_j\rangle_B = 0$ for all j . This implies that the side-channel states might be in a high-dimensional space and completely distinguishable for different j , enabling very powerful attacks by Eve based on unambiguous state discrimination [S21]. To define a simple attack of this type, let us assume for simplicity that $\langle\phi_k^\perp|\phi_j\rangle_B = 0$ and $\langle\phi_k^\perp|\phi_j^\perp\rangle_B = 0$ for all $j \neq k$, and consider that, in each protocol round, Eve applies the POVM $\{\hat{E}_{0Z}, \hat{E}_{1Z}, \hat{E}_{0X}, \hat{E}_{1X}, \hat{E}_{\text{inc}}\}$, where $\hat{E}_j = |\phi_j^\perp\rangle\langle\phi_j^\perp|_B$ and $\hat{E}_{\text{inc}} = \mathbb{I} - \sum_j \hat{E}_j$. By doing so, Eve will either unambiguously discriminate Alice's setting choice j with probability ϵ or obtain an inconclusive result with probability $1 - \epsilon$. Then, if she gets a conclusive result, she resends the identified state to Bob; otherwise, she sends a vacuum state. This attack allows Eve to learn Alice's setting choices for all detected rounds without introducing any errors, and results in an observed detection rate $\eta = \epsilon$. This implies that, if the observed η is such that $\eta \leq \epsilon$, distilling a secret key is impossible, which can be used as a crude upper bound on the maximum distance at which any security proof could achieve a non-zero key rate, as illustrated by the dashed lines in Fig. S3. When $\epsilon = 10^{-3}$, it is impossible to obtain any key after 143 km, less than half the maximum distance that the standard BB84 protocol can achieve for $\epsilon = 0$, which is not so far off from the 100 km achievable using our security proof. We remark that this crude upper bound does not use any information about Bob's measurement results other than his overall detection rate, and a tighter bound may be obtained by taking into account his detailed observed statistics, including the observed bit-error rate.

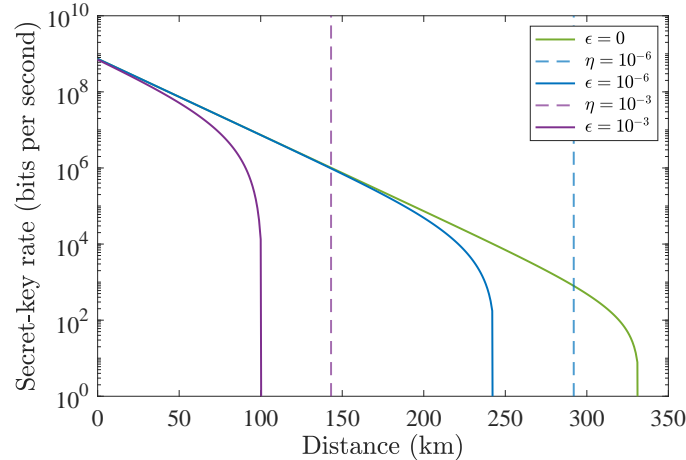


Figure S3. Asymptotic secret-key rate achievable when using our analysis for different values of ϵ , under the assumption that $\langle\phi_k^\perp|\phi_j\rangle_B = 0$ and $\langle\phi_k^\perp|\phi_j^\perp\rangle_B = 0$ for $j \neq k$ (solid lines), compared with a crude upper bound on the maximum distance at which a non-zero secret-key rate could be generated (dashed lines).

Hence, to achieve non-zero key rates at reasonable distances, there are only two possible experimental avenues: (1) ensuring that the overall magnitude of the side channels ϵ is low enough, or (2) obtaining a (full or partial) characterization of the side-channel states $\{|\phi_j^\perp\rangle\}_j$ (this could guarantee, for example, that $\langle\phi_k^\perp|\phi_j^\perp\rangle_B \neq 0$, thus ruling out the specific attack we have considered above). As we have argued in Appendix A, obtaining a characterization of the side-channel states appears to be significantly harder than simply obtaining a bound on ϵ , and for this reason, when evaluating the performance of our security proof, we have assumed that no information is known about them. If some information is known, however, one could incorporate it into the SDP used to bound the inner product between the states $|\Psi_{\text{Tar}}\rangle_{DAB}$ and $|\Psi_{\text{Ref}}\rangle_{DAB}$ (see Section SE2), potentially resulting in a significant secret-key rate increase³. This highlights the flexibility and potential of our security proof to achieve good performances regardless of the information that is experimentally available.

3. Reduction to the original quantum coin analysis when there are no qubit flaws

Here, we show that our security proof reduces to the original quantum coin analysis when there are no qubit flaws (i.e., when $\delta = 0$). In this case, we have that $q_{\text{vir}0}^\phi = q_{\text{vir}1}^\phi = 1/2$ (see Eq. (S18)) and the coefficients in Eq. (S50) satisfy $c_1 = c_2 = 0$ and $c_3 = 1$. Substituting these in Eq. (S63), we obtain

$$e_{\text{ph}}^{\text{U}} \simeq G_+ \left(\frac{Y_{0x}^{1x} + Y_{1x}^{0x}}{Y_{0x} + Y_{1x}}, 1 - \frac{2\Delta}{Y_Z + \frac{1}{2}(Y_{0x} + Y_{1x})} \right) = G_+ \left(e_X, 1 - \frac{2\Delta}{Y_Z + Y_X} \right) = G_+(e_X, 1 - 2\Delta'), \quad (\text{S64})$$

where in the second equality we have defined $Y_X := (Y_{0x} + Y_{1x})/2$ and $e_X := (Y_{0x}^{1x} + Y_{1x}^{0x})/(Y_{0x} + Y_{1x})$; and in the third equality we have defined $\Delta' := \Delta/(Y_Z + Y_X)$, with $\Delta \geq 1 - \text{Re} \langle \Psi_X | \Psi_Z \rangle_{AB}$. Equation (S64) is exactly the same phase-error rate bound as that of the original quantum coin analysis, see [S22]. Therefore, in Fig. 2 of the Main Text, the secret-key rate offered by the two analyses overlaps when $\delta = 0$.

To see why this is the case, let us substitute $c_1 = c_2 = 0$, $c_3 = 1$ and $q_{\text{vir}0}^\phi = q_{\text{vir}1}^\phi = 1/2$ in Eqs. (S53) and (S54). Then, the target and reference states become

$$|\Psi_{\text{Tar}}\rangle_{DAB} = \sqrt{q_{\text{vir}0}^\psi} |0\rangle_D |0\rangle_A |\psi_{\text{vir}0}\rangle_B - \sqrt{q_{\text{vir}1}^\psi} |1\rangle_D |1\rangle_A |\psi_{\text{vir}1}\rangle_B, \quad (\text{S65})$$

$$|\Psi_{\text{Ref}}\rangle_{DAB} = \frac{1}{\sqrt{2}} [|0\rangle_D |0\rangle_A |\psi_{0x}\rangle_B + |1\rangle_D |1\rangle_A |\psi_{1x}\rangle_B], \quad (\text{S66})$$

where we have used the fact that $|1'\rangle_A = -|1\rangle_A$ when $\delta = 0$. Then, by redefining $|i\rangle_D |i\rangle_A$ as $|i_X\rangle_A$ for $i \in \{0, 1\}$ in Eqs. (S65) and (S66), where $|i_X\rangle_A := (|0_Z\rangle + (-1)^i |1_Z\rangle)/\sqrt{2}$, we obtain

$$|\Psi_{\text{Tar}}\rangle_{DAB} = \frac{1}{\sqrt{2}} (|0_Z\rangle_A |\psi_{0z}\rangle_B + |1_Z\rangle_A |\psi_{1z}\rangle_B) = |\Psi_Z\rangle_{AB}, \quad (\text{S67})$$

$$|\Psi_{\text{Ref}}\rangle_{DAB} = \frac{1}{\sqrt{2}} (|0_X\rangle_A |\psi_{0x}\rangle_B - |1_X\rangle_A |\psi_{1x}\rangle_B) = |\Psi_X\rangle_{AB}. \quad (\text{S68})$$

Note that Eqs. (S67) and (S68) are equivalent to the states $|\Psi_Z(\epsilon)\rangle_{AB}$ and $|\Psi_X(\epsilon)\rangle_{AB}$ in Eqs. (4) and (5) of the Main Text. Therefore, our quantum coin state is

$$|\Psi_{\text{coin}}\rangle_{CAB} = \frac{1}{\sqrt{2}} (|0_Z\rangle_C |\Psi_Z\rangle_{AB} + |1_Z\rangle_C |\Psi_X\rangle_{AB}), \quad (\text{S69})$$

which is identical to that in Eq. (6). Therefore, our security proof reduces to the original quantum coin analysis in the absence of qubit flaws.

³ In fact, we remark that, in Fig. S3, we have computed the performance of our security analysis under the assumption that $\langle\phi_k^\perp|\phi_j\rangle_B = 0$ and $\langle\phi_k^\perp|\phi_j^\perp\rangle_B = 0$ for $j \neq k$, as this assumption is also made in the calculation of the upper bound; intuitively, this should not be very far off from the worst-case scenario, since it assumes that the side-channel states are orthogonal and thus completely distinguishable. Nevertheless, Fig. S3 already shows a slight but appreciable key-rate improvement with respect to the scenario considered in the Main Text, in which no such assumption is made.

D. General analysis for prepare-and-measure protocols

Here, we present the general version of our analysis for P&M protocols, which can be applied irrespectively of whether Alice sends three or four states, and irrespectively of the form of the qubit components $\{|\phi_j\rangle_B\}_j$. The analyses presented in Sections [SM1 B](#) and [SM1 C](#) are special cases of this general approach. However, to understand the main ideas of the security proof, we recommend reading Sections [SM1 B](#) and [SM1 C](#) first. The starting point of our general analysis is the LT expressions

$$|\phi_{\text{vir}\alpha}\rangle\langle\phi_{\text{vir}\alpha}|_B + \sum_{j \in \mathcal{C}_{\text{Tar}}^{(\alpha)}} c_j^{(\alpha)} |\phi_j\rangle\langle\phi_j|_B = \sum_{j \in \mathcal{C}_{\text{Ref}}^{(\alpha)}} c_j^{(\alpha)} |\phi_j\rangle\langle\phi_j|_B, \quad (\text{S70})$$

where $\alpha \in \{0, 1\}$, $c_j^{(\alpha)} \geq 0$ for all j, α , and $|\phi_{\text{vir}\alpha}\rangle_B$ are the qubit analogues of Eq. (S9), defined as

$$\begin{aligned} |\phi_{\text{vir}0}\rangle_B &= \frac{1}{2\sqrt{q_{\text{vir}0}^\phi}} (|\phi_{0z}\rangle_B + e^{i\omega} |\phi_{1z}\rangle_B), \\ |\phi_{\text{vir}1}\rangle_B &= \frac{1}{2\sqrt{q_{\text{vir}1}^\phi}} (|\phi_{0z}\rangle_B - e^{i\omega} |\phi_{1z}\rangle_B), \end{aligned} \quad (\text{S71})$$

with

$$\begin{aligned} q_{\text{vir}0}^\phi &= \frac{1}{2} (1 + \text{Re } e^{i\omega} \langle\phi_{0z}|\phi_{1z}\rangle_B), \\ q_{\text{vir}1}^\phi &= \frac{1}{2} (1 - \text{Re } e^{i\omega} \langle\phi_{0z}|\phi_{1z}\rangle_B). \end{aligned} \quad (\text{S72})$$

These expressions can always be obtained, although the procedure varies slightly depending on the Bloch vectors of the states $\{|\phi_j\rangle_B\}_j$, and requires setting the parameter ω appropriately:

Case 1: The end points of the Bloch vectors of the states $\{|\phi_j\rangle_B\}_j$ lie in the same plane, and this plane passes through the origin—. Without loss of generality, we can assume that this plane is the XZ plane; if it is not, one should simply redefine the Bloch sphere such that it is. For this case, one should take $\omega = 0$, and follow the procedure detailed in Appendix B.1 of [\[S15\]](#) to obtain the LT formulas in Eq. (S70). Note that the specific scenarios considered in Section [SM1 B](#) and Section [SM1 C](#) fall under this Case. If the set $\{|\phi_j\rangle_B\}_j$ contains three states (as in Section [SM1 B](#)), the LT formulas are unique, whereas if it contains four states (as in Section [SM1 C](#)), there are infinitely many expressions of the form in Eq. (S70). In general, choosing expressions with lower coefficients should result in a tighter analysis [\[S20\]](#).

Case 2: The end points of the Bloch vectors of the states $\{|\phi_j\rangle_B\}_j$ lie in the same plane, but this plane does not pass through the origin—. In this case, one should choose the parameter ω appropriately such that the end points of the Bloch vectors of the states $|\phi_{\text{vir}0}\rangle_B$ and $|\phi_{\text{vir}1}\rangle_B$ lie in the same plane as those of the states $\{|\phi_j\rangle_B\}_j$, as explained in Appendix B.2 of [\[S15\]](#). By following the procedure detailed there, one can obtain the LT formulas in Eq. (S70). As in *Case 1*, when the set $\{|\phi_j\rangle_B\}_j$ contains three states, these expressions are unique, and when it contains four states, there are infinitely many expressions to choose from.

Case 3: The end points of the Bloch vectors of the states $\{|\phi_j\rangle_B\}_j$ are not in the same plane (i.e., they form a pyramid)—. This can only occur when the set $\{|\phi_j\rangle_B\}_j$ contains four states. In this case, one can find unique expressions of the form in Eq. (S70) regardless of the value of ω ; in general, one can simply choose $\omega = 0$. This is because, in this case, the Pauli operators $\{\sigma_I, \sigma_Z, \sigma_X, \sigma_Y\}$ can be uniquely expressed as a linear combination of $\{|\phi_j\rangle\langle\phi_j|_B\}_j$, and any density operator in this qubit space, including the virtual states $|\phi_{\text{vir}\alpha}\rangle\langle\phi_{\text{vir}\alpha}|_B$, can be expressed uniquely as a linear combination of the Pauli operators. For more information, see [\[S14\]](#).

Once we have the expressions in Eq. (S70), we use them as a blueprint to construct the target and reference states

$|\Psi_{\text{Tar}}\rangle_{DAB}$ and $|\Psi_{\text{Ref}}\rangle_{DAB}$. First, we take purifications of the left- and right-hand sides of Eq. (S70),

$$|0\rangle_A |\phi_{\text{vir}\alpha}\rangle_B + \sum_{j \in \mathcal{C}_{\text{Tar}}^{(\alpha)}} \sqrt{c_j^{(\alpha)}} |k_j^{(\alpha)}\rangle_A |\phi_j\rangle_B, \quad (\text{S73})$$

$$\sum_{j \in \mathcal{C}_{\text{Ref}}^{(\alpha)}} \sqrt{c_j^{(\alpha)}} |k_j'^{(\alpha)}\rangle_A |\phi_j\rangle_B, \quad (\text{S74})$$

where $\{|0\rangle_A\} \cup \{|k_j^{(\alpha)}\rangle_A\}_{j \in \mathcal{C}_{\text{Tar}}^{(\alpha)}}$ and $\{|k_j'^{(\alpha)}\rangle_A\}_{j \in \mathcal{C}_{\text{Ref}}^{(\alpha)}}$ are orthonormal bases chosen appropriately such that Eqs. (S73) and (S74) are identical; these bases always exist due to the equality in Eq. (S70). Then, making use of Eqs. (S73) and (S74), we define the normalized states

$$|\Phi_{\text{Tar}}\rangle_{DAB} = 1/\sqrt{C} \left[\sum_{\alpha \in \{0,1\}} \sqrt{q_{\text{vir}\alpha}^\phi} |\alpha\rangle_D \left(|0\rangle_A |\phi_{\text{vir}\alpha}\rangle_B + \sum_{j \in \mathcal{C}_{\text{Tar}}^{(\alpha)}} \sqrt{c_j^{(\alpha)}} |k_j^{(\alpha)}\rangle_A |\phi_j\rangle_B \right) \right], \quad (\text{S75})$$

$$|\Phi_{\text{Ref}}\rangle_{DAB} = 1/\sqrt{C} \left[\sum_{\alpha \in \{0,1\}} \sqrt{q_{\text{vir}\alpha}^\phi} |\alpha\rangle_D \left(\sum_{j \in \mathcal{C}_{\text{Ref}}^{(\alpha)}} \sqrt{c_j^{(\alpha)}} |k_j'^{(\alpha)}\rangle_A |\phi_j\rangle_B \right) \right], \quad (\text{S76})$$

where

$$C = 1 + \sum_{\alpha \in \{0,1\}} \sum_{j \in \mathcal{C}_{\text{Tar}}^{(\alpha)}} q_{\text{vir}\alpha}^\phi c_j^{(\alpha)} = \sum_{\alpha \in \{0,1\}} \sum_{j \in \mathcal{C}_{\text{Ref}}^{(\alpha)}} q_{\text{vir}\alpha}^\phi c_j^{(\alpha)}, \quad (\text{S77})$$

is a normalization factor. Note that $|\Phi_{\text{Tar}}\rangle_{DAB} = |\Phi_{\text{Ref}}\rangle_{DAB}$. Finally, we substitute $|\phi_j\rangle_B \rightarrow |\psi_j\rangle_B$ and $|\phi_{\text{vir}\alpha}\rangle_B \rightarrow |\psi_{\text{vir}\alpha}\rangle_B$ in Eqs. (S75) and (S76), and then substitute $q_{\text{vir}\alpha}^\phi \rightarrow q_{\text{vir}\alpha}^\psi$ only in the terms multiplying the state $|\psi_{\text{vir}\alpha}\rangle_B$, obtaining

$$|\Psi_{\text{Tar}}\rangle_{DAB} = 1/\sqrt{C} \left[\sum_{\alpha \in \{0,1\}} |\alpha\rangle_D \left(\sqrt{q_{\text{vir}\alpha}^\psi} |0\rangle_A |\psi_{\text{vir}\alpha}\rangle_B + \sqrt{q_{\text{vir}\alpha}^\phi} \sum_{j \in \mathcal{C}_{\text{Tar}}^{(\alpha)}} \sqrt{c_j^{(\alpha)}} |k_j^{(\alpha)}\rangle_A |\psi_j\rangle_B \right) \right], \quad (\text{S78})$$

$$|\Psi_{\text{Ref}}\rangle_{DAB} = 1/\sqrt{C} \left[\sum_{\alpha \in \{0,1\}} \sqrt{q_{\text{vir}\alpha}^\phi} |\alpha\rangle_D \left(\sum_{j \in \mathcal{C}_{\text{Ref}}^{(\alpha)}} \sqrt{c_j^{(\alpha)}} |k_j'^{(\alpha)}\rangle_A |\psi_j\rangle_B \right) \right]. \quad (\text{S79})$$

We can then define the quantum coin state as

$$|\Psi_{\text{coin}}\rangle_{CDAB} = \frac{1}{\sqrt{2}} (|0_Z\rangle_C |\Psi_{\text{Tar}}\rangle_{DAB} + |1_Z\rangle_C |\Psi_{\text{Ref}}\rangle_{DAB}). \quad (\text{S80})$$

Let us rewrite Eqs. (S78) and (S79) as

$$|\Psi_{\text{Tar}}\rangle_{DAB} = \sum_{\alpha \in \{0,1\}} \sqrt{p_{\text{TAR}\alpha|\text{TAR}}} |\alpha\rangle_D |\Psi_{\text{Tar}\alpha}\rangle_{AB}, \quad (\text{S81})$$

$$|\Psi_{\text{Ref}}\rangle_{DAB} = \sum_{\alpha \in \{0,1\}} \sqrt{p_{\text{REF}\alpha|\text{REF}}} |\alpha\rangle_D |\Psi_{\text{Ref}\alpha}\rangle_{AB}, \quad (\text{S82})$$

where

$$p_{\text{TAR}\alpha|\text{TAR}} = \frac{q_{\text{vir}\alpha}^\psi + q_{\text{vir}\alpha}^\phi \sum_{j \in \mathcal{C}_{\text{Tar}}^{(\alpha)}} c_j^{(\alpha)}}{C}, \quad (\text{S83})$$

$$p_{\text{REF}\alpha|\text{REF}} = \frac{q_{\text{vir}\alpha}^\phi \sum_{j \in \mathcal{C}_{\text{Ref}}^{(\alpha)}} c_j^{(\alpha)}}{C}, \quad (\text{S84})$$

and

$$|\Psi_{\text{Tar}\alpha}\rangle_{AB} = \sqrt{p_{\text{vir}\alpha|\text{TAR}\alpha}} |0\rangle_A |\psi_{\text{vir}\alpha}\rangle + \sum_{j \in \mathcal{C}_{\text{Tar}}^{(\alpha)}} \sqrt{p_{j|\text{TAR}\alpha}} |k_j^{(\alpha)}\rangle_A |\psi_j\rangle_B, \quad (\text{S85})$$

$$|\Psi_{\text{Ref}\alpha}\rangle_{AB} = \sum_{j \in \mathcal{C}_{\text{Ref}}^{(\alpha)}} \sqrt{p_{j|\text{REF}\alpha}} |k_j'^{(\alpha)}\rangle_A |\psi_j\rangle_B, \quad (\text{S86})$$

with

$$p_{\text{vir}\alpha|\text{TAR}\alpha} = \frac{q_{\text{vir}\alpha}^\psi}{q_{\text{vir}\alpha}^\psi + q_{\text{vir}\alpha}^\phi \sum_{j \in \mathcal{C}_{\text{Tar}}^{(\alpha)}} c_j^{(\alpha)}}, \quad (\text{S87})$$

$$p_{j|\text{TAR}\alpha} = \frac{q_{\text{vir}\alpha}^\phi c_j^{(\alpha)}}{q_{\text{vir}\alpha}^\psi + q_{\text{vir}\alpha}^\phi \sum_{j' \in \mathcal{C}_{\text{Tar}}^{(\alpha)}} c_{j'}^{(\alpha)}} \quad \text{for } j \in \mathcal{C}_{\text{Tar}}^{(\alpha)}, \quad (\text{S88})$$

$$p_{j|\text{REF}\alpha} = \frac{c_j^{(\alpha)}}{\sum_{j' \in \mathcal{C}_{\text{Ref}}^{(\alpha)}} c_{j'}^{(\alpha)}} \quad \text{for } j \in \mathcal{C}_{\text{Ref}}^{(\alpha)}. \quad (\text{S89})$$

Tagging

Similarly to Section SM1 B 3, we consider the addition of the following fictitious tag assignment step to the Virtual Protocol:

1.5. Tag assignment: For each event l , Alice assigns it a single tag $t \in \{\text{TAR0}, \text{TAR1}, \text{REF0}, \text{REF1}\}$ with probability $p_{t|l}$, or no tag with probability $1 - \sum_t p_{t|l}$. Then, for the tagged events, Alice marks each emission as Z_C (X_C) with probability p_{Z_C} ($p_{X_C} = 1 - p_{Z_C}$).

In this general case, we need to consider the tags $\{\text{TAR0}, \text{TAR1}, \text{REF0}, \text{REF1}\}$, rather than just $\{\text{TAR}, \text{REF}\}$, because the same state could appear twice in each of Eqs. (S78) and (S79). For example, if $0_Z \in \mathcal{C}_{\text{Ref}}^{(0)}$ and $0_Z \in \mathcal{C}_{\text{Ref}}^{(1)}$, the state $|\psi_{0_Z}\rangle_B$ would appear twice in Eq. (S79), and one needs to distinguish whether an emission of $|\psi_{0_Z}\rangle_B$ is assigned to the $|0\rangle_D$ part (REF0) or the $|1\rangle_D$ part (REF1) of the state.

The conditional tag assignment probabilities $p_{t|l}$ should be chosen appropriately such that the probability that an emission with tag t originated from event l , $p_{l|t}$, matches Eqs. (S87) to (S89). As before, we can use Bayes' Theorem to obtain an expression for $p_{t|l}$ in terms of $p_{l|t}$, p_t and p_l , i.e.,

$$p_{t|l} = \frac{p_t p_{l|t}}{p_l}, \quad (\text{S90})$$

where $p_{l|t}$ is given by Eqs. (S87) to (S89),

$$\begin{aligned} p_l &= p_{Z_A} p_{Z_B} q_{\text{vir}\alpha}^\psi & \text{for } l \in \{\text{vir}\alpha\}_{\alpha \in \{0,1\}}, \\ p_l &= \frac{p_{Z_A}}{2} p_{X_B} & \text{for } l \in \{0_Z, 1_Z\}, \end{aligned} \quad (\text{S91})$$

and in the three-state scenario,

$$p_l = p_{X_A} p_{X_B} \quad \text{for } l = 0_X, \quad (\text{S92})$$

while, in the four-state scenario,

$$p_l = \frac{p_{X_A}}{2} p_{X_B} \quad \text{for } l \in \{0_X, 1_X\}. \quad (\text{S93})$$

Note that conditional tag assignment probabilities $\{p_{t|l}\}$ become fixed once we fix $\{p_t\}$. Taking the sum over $t \in \{\text{TAR0}, \text{TAR1}, \text{REF0}, \text{REF1}\}$ on both sides of Eq. (S90) and using the fact that $\sum_t p_{t|l} \leq 1$, we derive the following constraints,

$$\sum_t p_t p_{l|t} \leq p_l, \quad \forall l. \quad (\text{S94})$$

Let $p_{\text{TAR}} = p_{\text{TAR0}} + p_{\text{TAR1}}$ and $p_{\text{REF}} = p_{\text{REF0}} + p_{\text{REF1}}$. We want that

$$p_{\text{TAR}\alpha} = p_{\text{TAR}} p_{\text{TAR}\alpha|\text{TAR}}, \quad (\text{S95})$$

$$p_{\text{REF}\alpha} = p_{\text{REF}} p_{\text{REF}\alpha|\text{REF}}, \quad (\text{S96})$$

where $p_{\text{TAR}\alpha|\text{TAR}}$ and $p_{\text{REF}\alpha|\text{REF}}$ are given by Eqs. (S83) and (S84). We also want that $p_{\text{TAR}} = p_{\text{REF}}$, since the reference and target states have the same coefficient in Eq. (S80). Putting everything together, we obtain

$$\begin{aligned}
p_l &\geq \sum_t p_t p_{l|t} = \sum_{\alpha \in \{0,1\}} (p_{\text{TAR}\alpha} p_{l|\text{TAR}\alpha} + p_{\text{REF}\alpha} p_{l|\text{REF}\alpha}) \\
&= \sum_{\alpha \in \{0,1\}} (p_{\text{TAR}} p_{\text{TAR}\alpha|\text{TAR}} p_{l|\text{TAR}\alpha} + p_{\text{REF}} p_{\text{REF}\alpha|\text{REF}} p_{l|\text{REF}\alpha}) \\
&= \sum_{\alpha \in \{0,1\}} (p_{\text{TAR}} p_{\text{TAR}\alpha|\text{TAR}} p_{l|\text{TAR}\alpha} + p_{\text{TAR}} p_{\text{REF}\alpha|\text{REF}} p_{l|\text{REF}\alpha}) \\
&= p_{\text{TAR}} \sum_{\alpha \in \{0,1\}} (p_{\text{TAR}\alpha|\text{TAR}} p_{l|\text{TAR}\alpha} + p_{\text{REF}\alpha|\text{REF}} p_{l|\text{REF}\alpha}).
\end{aligned} \tag{S97}$$

The only constraint on the value of p_{TAR} is that Eq. (S97) holds for all l . Therefore, we can set its value as

$$p_{\text{TAR}} = \min_l \frac{p_l}{\sum_{\alpha \in \{0,1\}} (p_{\text{TAR}\alpha|\text{TAR}} p_{l|\text{TAR}\alpha} + p_{\text{REF}\alpha|\text{REF}} p_{l|\text{REF}\alpha})}. \tag{S98}$$

Once we set p_{TAR} , the tag selection probabilities $p_{\text{TAR}\alpha}$ and $p_{\text{REF}\alpha}$ become fixed, and so do the conditional tag assignment probabilities $p_{t|l}$. As in Section SM1 B 3, we have that, in the limit $N \rightarrow \infty$,

$$\begin{aligned}
N_{l,t,Z_C}^{\beta_X} &\simeq p_{Z_C} p_{t|l} N_l^{\beta_X}, \\
N_{l,t,Z_C}^{\text{det}} &\simeq p_{Z_C} p_{t|l} N_l^{\text{det}}.
\end{aligned} \tag{S99}$$

Coin Protocol

In the scenario described above, the tags $\{\text{TAR0}, \text{TAR1}, \text{REF0}, \text{REF1}\}$ are assigned such that an emission with a tag TAR0 is indistinguishable from the preparation of the state $|\Psi_{\text{TAR0}}\rangle_{AB}$, and similar for the others. Moreover, since the probabilities p_{TAR0} and p_{TAR1} (p_{REF0} and p_{REF1}) satisfy Eq. (S95) (Eq. (S96)), an emission with a tag $t \in \{\text{TAR0}, \text{TAR1}\}$ ($t \in \{\text{REF0}, \text{REF1}\}$) is equivalent to the preparation of the state $|\Psi_{\text{Tar}}\rangle_{DAB}$ ($|\Psi_{\text{Ref}}\rangle_{DAB}$). Finally, since $p_{\text{TAR0}} + p_{\text{TAR1}} = p_{\text{REF0}} + p_{\text{REF1}}$, an emission with a tag $t \in \{\text{TAR0}, \text{TAR1}, \text{REF0}, \text{REF1}\}$ is equivalent to that originating from the quantum coin state $|\Psi_{\text{coin}}\rangle_{CDAB}$. This equivalence allows us to define a Coin Protocol as in Section SM1 B 4, in which Alice prepares the quantum coin state with probability $p_C := p_{\text{TAR0}} + p_{\text{TAR1}} + p_{\text{REF0}} + p_{\text{REF1}} = 2p_{\text{TAR}}$. Using similar arguments as in Section SM1 B 4, due to the equivalence between the Virtual Protocol after the tag assignment and the Coin Protocol, we have that

$$\begin{aligned}
N_{Z_C=0}^{\text{err}} &\equiv \sum_{\alpha \in \{0,1\}} \left[N_{\text{vira}, \text{TAR}\alpha, Z_C}^{(\alpha \oplus 1)_X} + \sum_{j \in \mathcal{C}_{\text{Tar}}^{(\alpha)}} N_{j, \text{TAR}\alpha, Z_C}^{(\alpha \oplus 1)_X} \right], \\
N_{Z_C=1}^{\text{err}} &\equiv \sum_{\alpha \in \{0,1\}} \sum_{j \in \mathcal{C}_{\text{Ref}}^{(\alpha)}} N_{j, \text{REF}\alpha, Z_C}^{(\alpha \oplus 1)_X}, \\
N_{Z_C=0}^{\text{det}} &\equiv \sum_{\alpha \in \{0,1\}} \left[N_{\text{vira}, \text{TAR}\alpha, Z_C}^{\text{det}} + \sum_{j \in \mathcal{C}_{\text{Tar}}^{(\alpha)}} N_{j, \text{TAR}\alpha, Z_C}^{\text{det}} \right], \\
N_{Z_C=1}^{\text{det}} &\equiv \sum_{\alpha \in \{0,1\}} \sum_{j \in \mathcal{C}_{\text{Ref}}^{(\alpha)}} N_{j, \text{REF}\alpha, Z_C}^{\text{det}}.
\end{aligned} \tag{S100}$$

Substituting the random sampling relations in Eq. (S99) into Eq. (S100), we obtain that, in the limit $N \rightarrow \infty$,

$$\begin{aligned} N_{Z_C=0}^{\text{err}} &\simeq p_{Z_C} \left(p_{\text{TAR}|\text{vir}} N_{\text{ph}} + \sum_{\alpha \in \{0,1\}} \sum_{j \in \mathcal{C}_{\text{Tar}}^{(\alpha)}} p_{\text{TAR}\alpha|j} N_j^{(\alpha \oplus 1)x} \right), \\ N_{Z_C=1}^{\text{err}} &\simeq p_{Z_C} \left(\sum_{\alpha \in \{0,1\}} \sum_{j \in \mathcal{C}_{\text{Ref}}^{(\alpha)}} p_{\text{REF}\alpha|j} N_j^{(\alpha \oplus 1)x} \right), \\ N_{Z_C=0}^{\text{det}} &\simeq p_{Z_C} \left(p_{\text{TAR}|\text{vir}} N_{\text{key}}^{\text{det}} + \sum_{\alpha \in \{0,1\}} \sum_{j \in \mathcal{C}_{\text{Tar}}^{(\alpha)}} p_{\text{TAR}\alpha|j} N_j^{\text{det}} \right), \\ N_{Z_C=1}^{\text{det}} &\simeq p_{Z_C} \left(\sum_{\alpha \in \{0,1\}} \sum_{j \in \mathcal{C}_{\text{Ref}}^{(\alpha)}} p_{\text{REF}\alpha|j} N_j^{\text{det}} \right), \end{aligned} \tag{S101}$$

where we have used that $p_{\text{TAR}0|\text{vir}0} = p_{\text{TAR}1|\text{vir}1} =: p_{\text{TAR}|\text{vir}}$. The latter relationship can be derived by substituting into Eq. (S90) the definition of $p_{\text{vir}0|\text{TAR}0}$ and $p_{\text{vir}1|\text{TAR}1}$ in Eq. (S87), the definition of $p_{\text{vir}0}$ and $p_{\text{vir}1}$ in Eq. (S91), and the definition of $p_{\text{TAR}0}$ and $p_{\text{TAR}1}$ in Eq. (S95). Also, in Eq. (S101), we have used $N_{\text{key}}^{\text{det}} = N_{\text{vir}0}^{0x} + N_{\text{vir}0}^{1x} + N_{\text{vir}1}^{0x} + N_{\text{vir}1}^{1x}$, where $N_{\text{key}}^{\text{det}}$ is the total number of detected key rounds, i.e., the length of the sifted key.

As in Section SM1B4, we have that, in the Coin Protocol,

$$N_{Z_C=0}^{\text{err}} \lesssim N_{Z_C=0}^{\text{det}} G_+ \left(\frac{N_{Z_C=1}^{\text{err}}}{N_{Z_C=1}^{\text{det}}}, 1 - \frac{p_{Z_C} p_C N \Delta}{N_{Z_C=0}^{\text{det}} + N_{Z_C=1}^{\text{det}}} \right). \tag{S102}$$

Finally, substituting Eq. (S101), $p_C = 2p_{\text{TAR}}$, $N_l^{\text{det}} = N_l^{0x} + N_l^{1x}$ for $l \in \{j\}_j$, and the values of $\{p_{t|l}\}$ into Eq. (S102), and rearranging, we obtain a bound of the form

$$N_{\text{ph}} \lesssim f(\{N_j^{\beta x}\}_{j,\beta}, N_{\text{key}}^{\text{det}}) =: N_{\text{ph}}^{\text{U}}, \tag{S103}$$

as desired.

E. General finite-key analysis for prepare-and-measure protocols

Here, we extend the general analysis presented in the previous Section to the finite-key regime. First, we introduce the concentration inequalities employed and then, show how to derive an upper bound on the number of phase errors N_{ph} for a general P&M protocol. Finally, we plot the secret-key rate obtainable for the particular BB84 scenario considered in the Main Text as a function of the total number of transmitted signals N .

1. Concentration inequalities

Let $\xi_1, \xi_2, \dots, \xi_n$ be a sequence of independent Bernoulli random variables and let $\xi := \sum_{u=1}^n \xi_u$, whose expectation value is $\mu_\xi := E[\xi]$. Also, let us define the notation $L \leq_{\epsilon} R$ to mean that the event $L \leq R$ occurs except with probability at most ϵ , i.e., $\Pr[L > R] \leq \epsilon$.

- *Chernoff's bound* [S16]

This bound states that for a known μ_ξ , we have that

$$\mu_\xi - \Delta_C^-(\mu_\xi) \leq \xi \leq \mu_\xi + \Delta_C^+(\mu_\xi), \tag{S104}$$

where $\Delta_C^-(x) = \sqrt{2x \ln(1/\epsilon_C)}$ and $\Delta_C^+(x) = \sqrt{3x \ln(1/\epsilon_C)}$.

- *Hoeffding's bound* [S23]

This bound states that

$$\xi - \Delta_H(n) \leq \mu_\xi \leq \xi + \Delta_H(n), \tag{S105}$$

where $\Delta_H(n) = \sqrt{n \ln(1/\epsilon_H)/2}$.

Let us now consider $\zeta_1, \zeta_2, \dots, \zeta_n$ to be *any* (not necessarily independent) sequence of Bernoulli random variables and let $\{\mathcal{F}_l\}_{l=1}^n$ be a filtration identifying random variables, including $\zeta_1, \zeta_2, \dots, \zeta_n$. That is, \mathcal{F}_l is a σ -algebra satisfying $\mathcal{F}_{l-1} \subseteq \mathcal{F}_l$ and $E[\zeta_{l'} | \mathcal{F}_l] = \zeta_{l'}$ for $l' \leq l$. Also, let $\Lambda_l = \sum_{u=1}^l \zeta_u$, with $l \leq n$. Below, we state a specific result that can be directly derived from Azuma's inequality [S24]; for simplicity, in this paper, we refer to this as Azuma's inequality.

- *Azuma's inequality*

This bound states that

$$\Pr\left(\Lambda_n - \sum_{u=1}^n \Pr(\zeta_u = 1 | \mathcal{F}_{u-1}) > b\sqrt{n}\right) \leq \exp\left(-\frac{b^2}{2}\right), \text{ and} \quad (\text{S106})$$

$$\Pr\left(\sum_{u=1}^n \Pr(\zeta_u = 1 | \mathcal{F}_{u-1}) - \Lambda_n > b\sqrt{n}\right) \leq \exp\left(-\frac{b^2}{2}\right), \quad (\text{S107})$$

for any $b \in (0, 1)$. In particular, this means that

$$\Lambda_n - \Delta_A(n) \leq \sum_{u=1}^n \Pr(\zeta_u = 1 | \mathcal{F}_{u-1}) \leq \Lambda_n + \Delta_A(n), \quad (\text{S108})$$

where $\Delta_A(n) = \sqrt{2n \ln(1/\epsilon_A)}$.

Note that Chernoff's and Hoeffding's bounds only apply to independent random variables. However, Azuma's inequality applies to *any* random variables, including those that are correlated, and therefore it can be used to evaluate the security of our analysis against coherent attacks in the finite-key regime. Recently, another concentration inequality for sums of dependent random variables has been proposed by Kato [S25]. This result can be seen as a refined form of Azuma's inequality that is much tighter when the expected value of the sum of the random variables is low. For a complete description of the application of this inequality to QKD, see Appendix F in [S15].

2. Analysis for a general prepare-and-measure protocol

As shown in Section SE1, in the finite-key regime, the Coin Protocol inequality becomes

$$N_{Z_C=0}^{\text{err}} - \Delta_A \leq \frac{1}{6\epsilon_A} (N_{Z_C=0}^{\text{det}} + \Delta_A) G_+ \left(\frac{N_{Z_C=1}^{\text{err}} + \Delta_A}{N_{Z_C=1}^{\text{det}} - \Delta_A}, 1 - \frac{2p_{Z_C}(N_{X_C=1} + \Delta_A)}{p_{X_C}(N_{Z_C}^{\text{det}} - \Delta_A)} \right), \quad (\text{S109})$$

where we have employed Azuma's inequality using $\Delta_A := \Delta_A(N^{\text{det}})$ with N^{det} denoting the number of detected rounds. By substituting the definition of $N_{Z_C=0}^{\text{err}}$ in Eq. (S100) into Eq. (S109) and rearranging, we obtain

$$N_{\text{ph,TAR},Z_C} \leq \frac{1}{6\epsilon_A} (N_{Z_C=0}^{\text{det}} + \Delta_A) G_+ \left(\frac{N_{Z_C=1}^{\text{err}} + \Delta_A}{N_{Z_C=1}^{\text{det}} - \Delta_A}, 1 - \frac{2p_{Z_C}(N_{X_C=1} + \Delta_A)}{p_{X_C}(N_{Z_C}^{\text{det}} - \Delta_A)} \right) + \Delta_A - \sum_{\alpha \in \{0,1\}} \sum_{j \in \mathcal{C}_{\text{Tar}}^{(\alpha)}} N_{j,\text{TAR}\alpha,Z_C}^{(\alpha\oplus 1)_X}, \quad (\text{S110})$$

where we have defined $N_{\text{ph,TAR},Z_C} := \sum_{\alpha \in \{0,1\}} N_{\text{vir}\alpha,\text{TAR}\alpha,Z_C}^{(\alpha\oplus 1)_X}$. Although the values of $N_{Z_C=\alpha}^{\text{err}}$, $N_{Z_C=\alpha}^{\text{det}}$, $N_{X_C=1}$, $N_{Z_C}^{\text{det}} = \sum_{\alpha \in \{0,1\}} N_{Z_C=\alpha}^{\text{det}}$ and $N_{j,\text{TAR}\alpha,Z_C}^{(\alpha\oplus 1)_X}$ in Eq. (S110) are not directly observable in the experiment, we can apply the Chernoff bound to establish lower and upper limits for these variables, such that an upper bound on $N_{\text{ph,TAR},Z_C}$ can be obtained. In particular, we have that

$$N_{X_C=1} \leq \frac{\hat{N}_{X_C=1} + \Delta_C^+ (\hat{N}_{X_C=1})}{\epsilon_C} =: \bar{N}_{X_C=1}, \quad (\text{S111})$$

where $\hat{N}_{X_C=1} = N p_C p_{X_C} \Delta/2$. Also, we have that

$$\begin{aligned}
N_{Z_C=1}^{\text{err}} &\stackrel{v_r \epsilon_C}{\leq} \bar{N}_{Z_C=1}^{\text{err}} := \sum_{\alpha \in \{0,1\}} \sum_{j \in \mathcal{C}_{\text{Ref}}^{(\alpha)}} \bar{N}_{j,\text{REF}\alpha,Z_C}^{(\alpha \oplus 1)_X}, \\
N_{Z_C=0}^{\text{det}} &\stackrel{(v_t+1)\epsilon_C}{\leq} \bar{N}_{Z_C=0}^{\text{det}} := \bar{N}_{\text{key,TAR},Z_C}^{\text{det}} + \sum_{\alpha \in \{0,1\}} \sum_{j \in \mathcal{C}_{\text{TAR}}^{(\alpha)}} \bar{N}_{j,\text{TAR}\alpha,Z_C}^{\text{det}}, \\
N_{Z_C=0}^{\text{det}} &\stackrel{(v_t+1)\epsilon_C}{\geq} \underline{N}_{Z_C=0}^{\text{det}} := \underline{N}_{\text{key,TAR},Z_C}^{\text{det}} + \sum_{\alpha \in \{0,1\}} \sum_{j \in \mathcal{C}_{\text{TAR}}^{(\alpha)}} \underline{N}_{j,\text{TAR}\alpha,Z_C}^{\text{det}}, \\
N_{Z_C=1}^{\text{det}} &\stackrel{v_r \epsilon_C}{\geq} \underline{N}_{Z_C=1}^{\text{det}} := \sum_{\alpha \in \{0,1\}} \sum_{j \in \mathcal{C}_{\text{Ref}}^{(\alpha)}} \underline{N}_{j,\text{REF}\alpha,Z_C}^{\text{det}},
\end{aligned} \tag{S112}$$

where we have used Eq. (S100) and

$$\begin{aligned}
\underline{N}_{l,t,Z_C}^{\beta_X} &:= \hat{N}_{l,t,Z_C}^{\beta_X} - \Delta_C^-(\hat{N}_{l,t,Z_C}^{\beta_X}) \stackrel{\epsilon_C}{\leq} N_{l,t,Z_C}^{\beta_X} \stackrel{\epsilon_C}{\leq} \hat{N}_{l,t,Z_C}^{\beta_X} + \Delta_C^+(\hat{N}_{l,t,Z_C}^{\beta_X}) =: \bar{N}_{l,t,Z_C}^{\beta_X}, \\
\underline{N}_{l,t,Z_C}^{\text{det}} &:= \hat{N}_{l,t,Z_C}^{\text{det}} - \Delta_C^-(\hat{N}_{l,t,Z_C}^{\text{det}}) \stackrel{\epsilon_C}{\leq} N_{l,t,Z_C}^{\text{det}} \stackrel{\epsilon_C}{\leq} \hat{N}_{l,t,Z_C}^{\text{det}} + \Delta_C^+(\hat{N}_{l,t,Z_C}^{\text{det}}) =: \bar{N}_{l,t,Z_C}^{\text{det}}, \\
\underline{N}_{\text{key,TAR},Z_C}^{\text{det}} &:= \hat{N}_{\text{key,TAR},Z_C}^{\text{det}} - \Delta_C^-(\hat{N}_{\text{key,TAR},Z_C}^{\text{det}}) \stackrel{\epsilon_C}{\leq} N_{\text{key,TAR},Z_C}^{\text{det}} \stackrel{\epsilon_C}{\leq} \hat{N}_{\text{key,TAR},Z_C}^{\text{det}} + \Delta_C^+(\hat{N}_{\text{key,TAR},Z_C}^{\text{det}}) =: \bar{N}_{\text{key,TAR},Z_C}^{\text{det}},
\end{aligned} \tag{S113}$$

with $v_r = |\mathcal{C}_{\text{Ref}}^{(0)}| + |\mathcal{C}_{\text{Ref}}^{(1)}|$, $v_t = |\mathcal{C}_{\text{TAR}}^{(0)}| + |\mathcal{C}_{\text{TAR}}^{(1)}|$, $\hat{N}_{l,t,Z_C}^{\beta_X} = p_{Z_C} p_{t|l} N_l^{\beta_X}$, $\hat{N}_{l,t,Z_C}^{\text{det}} = p_{Z_C} p_{t|l} N_l^{\text{det}}$, $N_{\text{key,TAR},Z_C}^{\text{det}} = \sum_{\alpha \in \{0,1\}} N_{\text{vir}\alpha,\text{TAR}\alpha,Z_C}^{\text{det}}$, and $\hat{N}_{\text{key,TAR},Z_C}^{\text{det}} = p_{Z_C} p_{\text{TAR}|\text{vir}} N_{\text{key}}^{\text{det}}$. By substituting Eqs. (S111) to (S113) into Eq. (S110), we get that

$$\begin{aligned}
N_{\text{ph,TAR},Z_C} &\stackrel{6\epsilon_A + (2v_r + 3v_t + 3)\epsilon_C}{\leq} (\bar{N}_{Z_C=0}^{\text{det}} + \Delta_A) G_+ \left(\frac{\bar{N}_{Z_C=1}^{\text{err}} + \Delta_A}{\bar{N}_{Z_C=1}^{\text{det}} - \Delta_A}, 1 - \frac{2p_{Z_C}(\bar{N}_{X_C=1} + \Delta_A)}{p_{X_C}(\bar{N}_{Z_C=0}^{\text{det}} + \bar{N}_{Z_C=1}^{\text{det}} - \Delta_A)} \right) \\
&\quad + \Delta_A - \sum_{\alpha \in \{0,1\}} \sum_{j \in \mathcal{C}_{\text{TAR}}^{(\alpha)}} \underline{N}_{j,\text{TAR}\alpha,Z_C}^{(\alpha \oplus 1)_X}.
\end{aligned} \tag{S114}$$

Then, we can obtain an expression in terms of N_{ph} by using our knowledge of $N_{\text{ph,TAR},Z_C}$ and Hoeffding's bound such that

$$N_{\text{ph,TAR},Z_C} \stackrel{\epsilon_H}{\geq} p_{Z_C} p_{\text{TAR}|\text{vir}} N_{\text{ph}} - \Delta_H(N_{\text{ph}}) \geq p_{Z_C} p_{\text{TAR}|\text{vir}} N_{\text{ph}} - \Delta_H(N_{\text{key}}^{\text{det}}), \tag{S115}$$

where in the last inequality we have upper bounded $\Delta_H(N_{\text{ph}})$ by $\Delta_H(N_{\text{key}}^{\text{det}})$, where $N_{\text{key}}^{\text{det}}$ is the number of detected key rounds. Finally, by substituting Eq. (S115) into Eq. (S114) and rearranging, we obtain an upper bound on the number of phase errors:

$$\begin{aligned}
N_{\text{ph}} &\stackrel{\epsilon_{\text{tot}}}{\leq} \frac{1}{p_{Z_C} p_{\text{TAR}|\text{vir}}} \left[(\bar{N}_{Z_C=0}^{\text{det}} + \Delta_A) G_+ \left(\frac{\bar{N}_{Z_C=1}^{\text{err}} + \Delta_A}{\bar{N}_{Z_C=1}^{\text{det}} - \Delta_A}, 1 - \frac{2p_{Z_C}(\bar{N}_{X_C=1} + \Delta_A)}{p_{X_C}(\bar{N}_{Z_C=0}^{\text{det}} + \bar{N}_{Z_C=1}^{\text{det}} - \Delta_A)} \right) \right. \\
&\quad \left. - \sum_{\alpha \in \{0,1\}} \sum_{j \in \mathcal{C}_{\text{TAR}}^{(\alpha)}} \underline{N}_{j,\text{TAR}\alpha,Z_C}^{(\alpha \oplus 1)_X} + \Delta_A + \Delta_H(N_{\text{key}}^{\text{det}}) \right] =: N_{\text{ph}}^{\text{U}},
\end{aligned} \tag{S116}$$

where $\epsilon_{\text{tot}} := 6\epsilon_A + (2v_r + 3v_t + 3)\epsilon_C + \epsilon_H$ is the sum of the failure probabilities of all the concentration inequalities applied. After performing error correction, error verification and privacy amplification, Alice and Bob obtain a secret key of length

$$N_{\text{sec}} = N_{\text{key}}^{\text{det}} [1 - h(e_{\text{ph}}^{\text{U}})] - \lambda_{\text{EC}} - \log_2 \frac{1}{\epsilon_{\text{corr}}} - \log_2 \frac{1}{\epsilon_{\text{PA}}}, \tag{S117}$$

where $e_{\text{ph}}^{\text{U}} := N_{\text{ph}}^{\text{U}} / N_{\text{key}}^{\text{det}}$ is the upper bound on the phase-error rate, $\lambda_{\text{EC}} = fh(e_Z)$ is the cost of error correction, with f denoting the error correction efficiency and e_Z the bit-error rate, ϵ_{corr} is the probability that the reconciled keys are not identical (due to the failure of error verification) and ϵ_{PA} is a free parameter that can be regarded as the failure

probability of privacy amplification. It is known [S26] that, if N_{ph} is bounded such that $\Pr[N_{\text{ph}}^{\text{U}} > N_{\text{ph}}] \leq \epsilon_{\text{tot}}$ and the secret-key length is set as in Eq. (S117), then the protocol is ϵ_{secr} -secret, with $\epsilon_{\text{secr}} = \sqrt{2\sqrt{\epsilon_{\text{tot}} + \epsilon_{\text{PA}}}}$. Since the protocol is also ϵ_{corr} , then it is ϵ_s -secure with $\epsilon_s = \epsilon_{\text{corr}} + \epsilon_{\text{secr}}$.

We remark that the key rate formula in Eq. (S117) assumes the phase-error correction security framework [S13, S26]. However, our security proof is compatible with the leftover hashing lemma in combination with the entropic uncertainty relation (EUR) [S8–S10]. We remark that previous works have shown that a bound on the phase-error rate such as the one derived in our work is enough to guarantee security in the variable length scenario [S27, S28].

3. Secret-key rate for a particular BB84 scenario

To evaluate the secret-key rate offered by our analysis in the finite-key regime we consider, as an example, the BB84 scenario introduced in the Main Text (see also Section SM1 C). To simulate the data that one would obtain in the Actual Protocol, we use the channel model in Section SE3 A. For this, we assume the following experimental parameters: $f = 1.16$, dark count probability $p_d = 10^{-8}$ [S29, S30] and detector efficiency $\eta_d = 0.73$ [S30]. Moreover, we select $\epsilon_{\text{secr}} = \epsilon_{\text{corr}} = 10^{-10}$ [S31] and for simplicity, we set $\epsilon_C = \epsilon_H = \epsilon_A =: \hat{\epsilon}$, from which it follows that $\epsilon_{\text{tot}} = 19\hat{\epsilon}$. For simplicity, we also assume that $\epsilon_{\text{PA}} = \epsilon_{\text{tot}}$, and therefore $\epsilon_{\text{tot}} = \epsilon_{\text{secr}}^2/4$. In the simulations, we optimize over the probabilities p_{Z_A} , p_{Z_B} and p_{Z_C} , and consider different values of the block size N , which represents the total number of emitted signals. To evaluate the achievable secret-key rate under different amounts of information leakage, we fix the qubit flaws to $\delta = 0.063$ [S32, S33] and take $\epsilon \in \{10^{-3}, 10^{-6}\}$. The results obtained are shown in Fig. S4, where a reasonable finite-key scaling is achieved for practical values of N . Also, as expected, a lower value of ϵ results in higher secret-key rates (see also Fig. 1 in the Main Text).

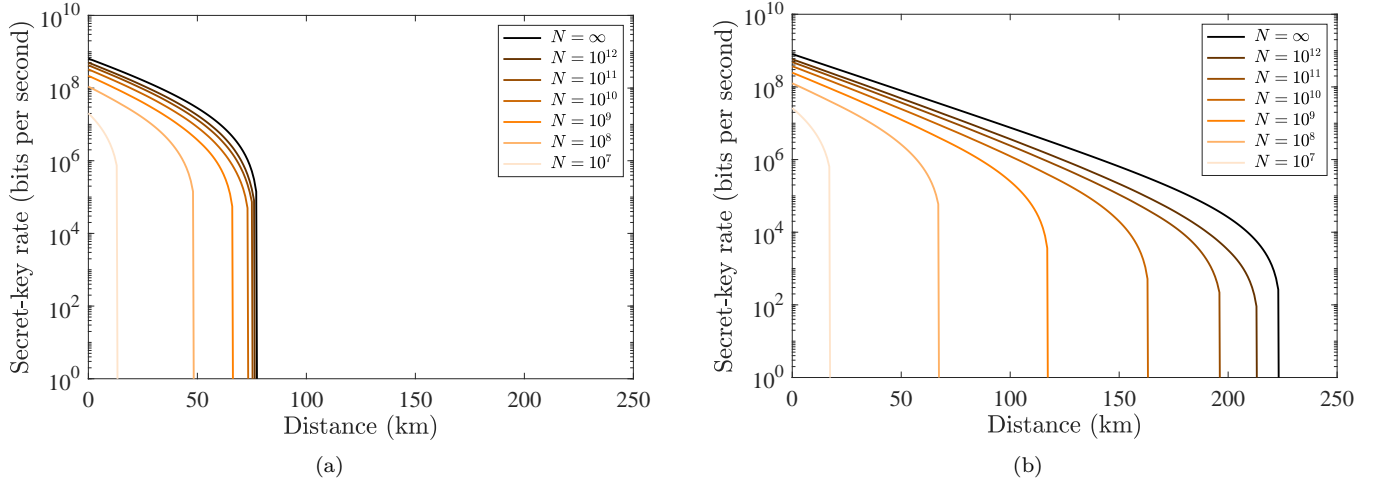


Figure S4. Finite-size secret-key rate as a function of distance when applying our analysis with Azuma's inequality for different values of the block size N . We assume that $\delta = 0.063$ and take (a) $\epsilon = 10^{-3}$ and (b) $\epsilon = 10^{-6}$.

The finite-key analysis presented in the previous Section can also be carried out using Kato's rather than Azuma's inequality. As explained above, the former can offer a tighter bound on N_{ph} , resulting in higher secret-key rates. However, we remark that its use requires an extra condition: the users need to make an attempt at predicting the results that they will obtain in the QKD session before they actually run the protocol. This inequality is tight only if these predictions are close to the actual experimental data. In Fig. S5, we present the results obtained when employing Kato's inequality under the assumption that the users make perfect predictions. This figure shows a considerable improvement in performance when compared to Fig. S4, especially for $\epsilon = 10^{-6}$ and lower values of N .

SM2. SECURITY PROOF FOR MDI-TYPE PROTOCOLS

Here, we show how the security proof approach presented in Section SM1 can be extended to MDI-type protocols. The most obvious application is to setups based on the original MDI-QKD scheme [S7], since in this scenario, the users send BB84-type states, and thus the ideas translate immediately. Still, in Section SM4 A, we also show that

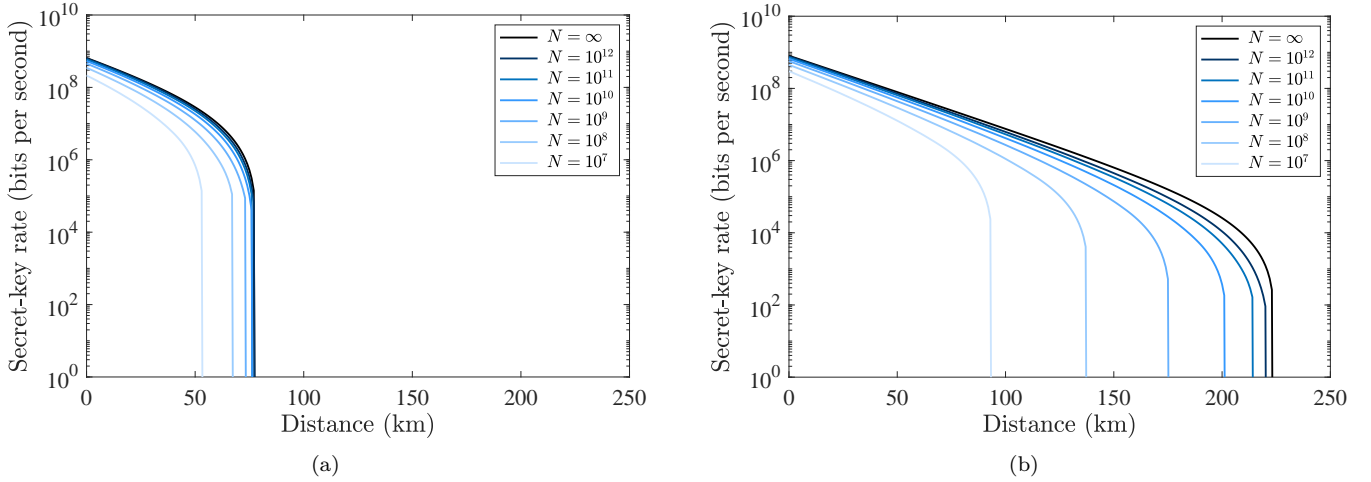


Figure S5. Finite-size secret-key rate as a function of distance when applying our analysis with Kato's inequality for different values of the block size N . We assume that $\delta = 0.063$ and take (a) $\epsilon = 10^{-3}$ and (b) $\epsilon = 10^{-6}$.

our security proof can be applied to an MDI-type scheme based on single-photon interference where the users emit non-phase-randomized coherent states [S34], and which can be considered as a simplified version of TF-QKD [S35]. This highlights the broad applicability of our techniques.

A. Protocol description, assumptions and security framework

1. Protocol description

As in the P&M case, our proof is applicable irrespectively of whether Alice and Bob emit three or four different states each. Without loss of generality, in the former (latter) case, we label these states as $j \in \{0_Z, 1_Z, 0_X\}$ ($j \in \{0_Z, 1_Z, 0_X, 1_X\}$). States such that $j \in \{0_Z, 1_Z\}$ ($j \notin \{0_Z, 1_Z\}$) are considered Z -basis (X -basis) states. For simplicity, we assume that Alice and Bob select the Z -basis states with probability $p_Z/2$ each.

MDI-type Protocol

- 1. Quantum communication:** For each of the N rounds: (a) Alice (Bob) chooses a state from the set $\{|\psi_j\rangle_{B_a}\}_j$ ($\{|\psi_j\rangle_{B_b}\}_j$) with probability p_j , and sends it to the middle node Charlie through a quantum channel. (b) Charlie performs a measurement on the incoming signals and announces the result.
- 2. Basis and bit announcement:** For each round in which Charlie announced a successful detection, Alice (Bob) announces the Z basis if her (his) setting choice was $j \in \{0_Z, 1_Z\}$, or the X basis otherwise. Then, for each detected round in which both users announced the Z basis, Alice assigns the round to “key” (“test”) with probability $p_{\text{key}|Z}$ ($p_{\text{test}|Z} = 1 - p_{\text{key}|Z}$), and announces this information. All the other detected rounds are assigned to “test”. Then, the users announce their setting choices for the rounds assigned to “test”, and define their sifted keys as the bit outcomes of the rounds assigned to “key”.
- 3. Parameter estimation:** The users quantify the number of events N_{ij}^{det} in which Alice’s (Bob’s) setting choice was i (j), Charlie announced a detection, and the round was assigned to “test”; the number of detected key events $N_{\text{key}}^{\text{det}}$ (i.e., the length of the sifted key); and the total number of detected rounds $N^{\text{det}} := N_{\text{key}}^{\text{det}} + \sum_{i,j} N_{ij}^{\text{det}}$. Then, they use this information to obtain an upper bound on the phase-error rate e_{ph} of the sifted key.
- 4. Data post-processing:** Alice sends Bob syndrome information about her sifted key through an authenticated classical channel for him to correct his own sifted key. After, Alice and Bob perform error verification by computing a hash of their corrected keys using a random two-universal hash function and then check whether they are identical. If so, Alice and Bob perform privacy amplification by employing a random two-universal hash function to extract a secure key pair from the corrected keys. Otherwise, they abort the protocol.

As for the P&M scenario, for simplicity, we assume that the users perform error correction for a predetermined bit-error rate, which is inferred from *a priori* knowledge of the channel. However, as explained in Section [SM1 A 1](#), after a few modifications, our analysis could also be applied to the case in which the users sacrifice a small fraction of the sifted key to estimate its bit-error rate.

2. Assumptions

For MDI-type protocols, our analysis only requires the following assumption:

(A1) *Bounded fidelity to qubit states:* Alice's (Bob's) emitted states $\{|\psi_j\rangle_{B_a}\}_j$ ($\{|\psi_j\rangle_{B_b}\}_j$) are ϵ -close (in terms of fidelity) to some characterized qubit states $\{|\phi_j\rangle_{B_a}\}_j$ ($\{|\phi_j\rangle_{B_b}\}_j$), i.e., for all j ,

$$|\langle\phi_j|\psi_j\rangle_{B_a(B_b)}|^2 \geq 1 - \epsilon, \quad (\text{S118})$$

where ϵ is known. Again, for notational simplicity, we consider throughout the proof that the states emitted by Alice and Bob are pure and identical for all rounds. However, as explained in the Main Text and Appendix A, our security analysis can be trivially extended without any modifications to the scenario in which the states are mixed and/or different for different rounds (see Eq. (1) in the Main Text). Moreover, with a simple modification to Eq. [\(S118\)](#) and to the post-processing step of the protocol, our analysis can be applied in the presence of setting-dependent pulse correlations i.e., when the state emitted in a given round depends on the setting choices made in previous rounds. For more information, see Section [SM3](#).

As in the P&M scenario, Eq. [\(S118\)](#) implies that we can assume that the states emitted by Alice (Bob) have the form

$$|\psi_j\rangle_{B_a(B_b)} = \sqrt{1 - \epsilon} |\phi_j\rangle_{B_a(B_b)} + \sqrt{\epsilon} |\phi_j^\perp\rangle_{B_a(B_b)}, \quad (\text{S119})$$

where $|\phi_j^\perp\rangle_{B_a(B_b)}$ is a state such that $\langle\phi_j|\phi_j^\perp\rangle_{B_a(B_b)} = 0$ (see Eq. [\(S2\)](#) for the proof of this claim).

3. Security framework

The sifted key is generated from the detected key rounds, which are a subset of the detected rounds in which both Alice and Bob selected the Z basis. Note that, in these rounds, the users could have replaced their emissions by the generation of the entangled state

$$|\Psi_Z\rangle_{A_u B_u} = \frac{1}{\sqrt{2}} (|0_Z\rangle_{A_u} |\psi_{0_Z}\rangle_{B_u} + e^{i\omega_u} |1_Z\rangle_{A_u} |\psi_{1_Z}\rangle_{B_u}), \quad (\text{S120})$$

where $\omega_u \in [0, 2\pi)$ can be freely chosen, and $u \in \{a, b\}$ indicates if the state is prepared by Alice or Bob. The amount of privacy amplification that needs to be applied to the sifted key to turn it into a secret key can be directly related to the error rate that Alice and Bob would have observed if, in these rounds, they had measured systems their A_a and A_b in the X basis, i.e., the phase-error rate e_{ph} . For simplicity, here, we will assume that a “phase error” is defined as an event in which Alice and Bob obtain the same X -basis outcome⁴, i.e., both obtain 0_X or both obtain 1_X . Note that this entanglement-based view is equivalent to a scenario in which, in the key rounds, Alice and Bob emit the virtual states

$$\begin{aligned} |\psi_{\text{vir}0}\rangle_{B_u} &= \frac{1}{2\sqrt{q_{\text{vir}0}^{\psi,u}}} (|\psi_{0_Z}\rangle_{B_u} + e^{i\omega_u} |\psi_{1_Z}\rangle_{B_u}), \\ |\psi_{\text{vir}1}\rangle_{B_u} &= \frac{1}{2\sqrt{q_{\text{vir}1}^{\psi,u}}} (|\psi_{0_Z}\rangle_{B_u} - e^{i\omega_u} |\psi_{1_Z}\rangle_{B_u}), \end{aligned} \quad (\text{S121})$$

⁴ In general, the appropriate definition of a phase error depends on the MDI protocol under consideration. In some protocols, such as the standard MDI-QKD [\[S7\]](#), the definition of a phase error actually depends on the specific announcement made by Charlie. In this case, one should define separate sifted key pairs according to the specific announcement made by Charlie, and apply our analysis to compute a bound on the phase-error rate separately for each sifted key pair. On the other hand, for scenarios in which the definition of a phase error does not depend on the specific announcement made by Charlie, such as the coherent-light-based MDI protocol [\[S34\]](#) considered in Section [SM4 A](#), this separation is not necessary.

with

$$\begin{aligned} q_{\text{vir0}}^{\psi,u} &= \frac{1}{4} \left\| \left| \psi_{0Z} \right\rangle_{B_u} + e^{i\omega_u} \left| \psi_{1Z} \right\rangle_{B_u} \right\|^2 = \frac{1}{2} (1 + \text{Re} e^{i\omega_u} \langle \psi_{0Z} | \psi_{1Z} \rangle_{B_u}), \\ q_{\text{vir1}}^{\psi,u} &= \frac{1}{4} \left\| \left| \psi_{0Z} \right\rangle_{B_u} - e^{i\omega_u} \left| \psi_{1Z} \right\rangle_{B_u} \right\|^2 = \frac{1}{2} (1 - \text{Re} \{ e^{i\omega_u} \} \langle \psi_{0Z} | \psi_{1Z} \rangle_{B_u}). \end{aligned} \quad (\text{S122})$$

B. Constructing the reference and target states, and the Virtual Protocol with tag assignment

The starting point of the analysis are the MDI loss-tolerant formulas

$$\begin{aligned} |\phi_{\text{vir00}}\rangle\langle\phi_{\text{vir00}}|_{B_a B_b} + \sum_{(i,j) \in \mathcal{C}_{\text{Tar}}^{(00)}} c_{ij}^{(00)} |\phi_{ij}\rangle\langle\phi_{ij}|_{B_a B_b} &= \sum_{(i,j) \in \mathcal{C}_{\text{Ref}}^{(00)}} c_{ij}^{(00)} |\phi_{ij}\rangle\langle\phi_{ij}|_{B_a B_b}, \\ |\phi_{\text{vir11}}\rangle\langle\phi_{\text{vir11}}|_{B_a B_b} + \sum_{(i,j) \in \mathcal{C}_{\text{Tar}}^{(11)}} c_{ij}^{(11)} |\phi_{ij}\rangle\langle\phi_{ij}|_{B_a B_b} &= \sum_{(i,j) \in \mathcal{C}_{\text{Ref}}^{(11)}} c_{ij}^{(11)} |\phi_{ij}\rangle\langle\phi_{ij}|_{B_a B_b}, \\ |\phi_{\text{vir10}}\rangle\langle\phi_{\text{vir10}}|_{B_a B_b} + \sum_{(i,j) \in \mathcal{C}_{\text{Tar}}^{(10)}} c_{ij}^{(10)} |\phi_{ij}\rangle\langle\phi_{ij}|_{B_a B_b} &= \sum_{(i,j) \in \mathcal{C}_{\text{Ref}}^{(10)}} c_{ij}^{(10)} |\phi_{ij}\rangle\langle\phi_{ij}|_{B_a B_b}, \\ |\phi_{\text{vir01}}\rangle\langle\phi_{\text{vir01}}|_{B_a B_b} + \sum_{(i,j) \in \mathcal{C}_{\text{Tar}}^{(01)}} c_{ij}^{(01)} |\phi_{ij}\rangle\langle\phi_{ij}|_{B_a B_b} &= \sum_{(i,j) \in \mathcal{C}_{\text{Ref}}^{(01)}} c_{ij}^{(01)} |\phi_{ij}\rangle\langle\phi_{ij}|_{B_a B_b}, \end{aligned} \quad (\text{S123})$$

with $c_{ij}^{(\alpha\beta)} \geq 0$ for all i, j, α, β , and where we have defined $|\phi_{ij}\rangle_{B_a B_b} = |\phi_i\rangle_{B_a} \otimes |\phi_j\rangle_{B_b}$ and $|\phi_{\text{vir}\alpha\beta}\rangle_{B_a B_b} = |\phi_{\text{vir}\alpha}\rangle_{B_a} \otimes |\phi_{\text{vir}\beta}\rangle_{B_b}$. To obtain these expressions, one should compute the P&M loss-tolerant formulas in Eq. (S70) for both Alice and Bob, isolate the terms $|\phi_{\text{vir}\alpha}\rangle\langle\phi_{\text{vir}\alpha}|_{B_u}$, take the tensor products of the resulting left- and right-hand sides, and reorganize terms.

Using the formulas in Eq. (S123) and following a similar approach to that described in Section SM1 D, we construct the following reference and target states:

$$|\Psi_{\text{Tar}}\rangle_{DAB} = 1/\sqrt{C} \left[\sum_{\alpha, \beta} |\alpha\beta\rangle_{D_a D_b} \left(\sqrt{q_{\text{vir}\alpha\beta}^{\psi}} |0\rangle_A |\psi_{\text{vir}\alpha\beta}\rangle_{B_a B_b} + \sqrt{q_{\text{vir}\alpha\beta}^{\phi}} \sum_{(i,j) \in \mathcal{C}_{\text{Tar}}^{(\alpha\beta)}} \sqrt{c_{ij}^{(\alpha\beta)}} |k_{ij}^{(\alpha\beta)}\rangle_A |\psi_{ij}\rangle_{B_a B_b} \right) \right], \quad (\text{S124})$$

$$|\Psi_{\text{Ref}}\rangle_{DAB} = 1/\sqrt{C} \left[\sum_{\alpha, \beta} \sqrt{q_{\text{vir}\alpha\beta}^{\phi}} |\alpha\beta\rangle_{D_a D_b} \left(\sum_{(i,j) \in \mathcal{C}_{\text{Ref}}^{(\alpha\beta)}} \sqrt{c_{ij}^{(\alpha\beta)}} |k_{ij}^{(\alpha\beta)}\rangle_A |\psi_{ij}\rangle_{B_a B_b} \right) \right], \quad (\text{S125})$$

where we have defined $D := D_a D_b$, $B := B_a B_b$, $|\psi_{ij}\rangle_{B_a B_b} := |\psi_i\rangle_{B_a} \otimes |\psi_j\rangle_{B_b}$, $|\psi_{\text{vir}\alpha\beta}\rangle_{B_a B_b} := |\psi_{\text{vir}\alpha}\rangle_{B_a} \otimes |\psi_{\text{vir}\beta}\rangle_{B_b}$, $q_{\text{vir}\alpha\beta}^{\psi} := q_{\text{vir}\alpha}^{\psi} q_{\text{vir}\beta}^{\psi}$, $q_{\text{vir}\alpha\beta}^{\phi} := q_{\text{vir}\alpha}^{\phi} q_{\text{vir}\beta}^{\phi}$, and

$$C = 1 + \sum_{\alpha, \beta} \sum_{(i,j) \in \mathcal{C}_{\text{Tar}}^{(\alpha\beta)}} q_{\text{vir}\alpha\beta}^{\phi} c_{ij}^{(\alpha\beta)} = \sum_{\alpha, \beta} \sum_{(i,j) \in \mathcal{C}_{\text{Ref}}^{(\alpha\beta)}} q_{\text{vir}\alpha\beta}^{\phi} c_{ij}^{(\alpha\beta)}. \quad (\text{S126})$$

The sets $\{|0\rangle_A\} \cup \{|k_{ij}^{(\alpha\beta)}\rangle_A\}_{ij \in \mathcal{C}_{\text{Tar}}^{(\alpha\beta)}}$ and $\{|k_{ij}^{(\alpha\beta)}\rangle_A\}_{ij \in \mathcal{C}_{\text{Ref}}^{(\alpha\beta)}}$ are two orthonormal bases that should be appropriately chosen such that $|\Psi_{\text{Tar}}\rangle_{DAB} = |\Psi_{\text{Ref}}\rangle_{DAB}$ when $\epsilon = 0$. These orthonormal bases must exist due to the equalities in Eq. (S123). As in the P&M scenario, the quantum coin can then be defined as

$$|\Psi_{\text{coin}}\rangle_{CDAB} = \frac{1}{\sqrt{2}} (|0_Z\rangle_C |\Psi_{\text{Tar}}\rangle_{DAB} + |1_Z\rangle_C |\Psi_{\text{Ref}}\rangle_{DAB}). \quad (\text{S127})$$

Now, let us rewrite Eqs. (S124) and (S125) as

$$|\Psi_{\text{Tar}}\rangle_{DAB} = \sum_{\alpha, \beta} \sqrt{p_{\text{tar}\alpha\beta|\text{tar}}^{\text{tar}}} |\alpha\beta\rangle_{D_a D_b} |\Psi_{\text{tar}\alpha\beta}\rangle_{AB}, \quad (\text{S128})$$

$$|\Psi_{\text{Ref}}\rangle_{DAB} = \sum_{\alpha, \beta} \sqrt{p_{\text{ref}\alpha\beta|\text{ref}}^{\text{ref}}} |\alpha\beta\rangle_{D_a D_b} |\Psi_{\text{ref}\alpha\beta}\rangle_{AB}, \quad (\text{S129})$$

where

$$p_{\text{TAR}\alpha\beta|\text{TAR}} = \frac{q_{\text{vir}\alpha\beta}^\psi + q_{\text{vir}\alpha\beta}^\phi \sum_{(i,j) \in \mathcal{C}_{\text{Tar}}^{(\alpha\beta)}} c_{ij}^{(\alpha\beta)}}{C}, \quad (\text{S130})$$

$$p_{\text{REF}\alpha\beta|\text{REF}} = \frac{q_{\text{vir}\alpha\beta}^\phi \sum_{(i,j) \in \mathcal{C}_{\text{Ref}}^{(\alpha\beta)}} c_{ij}^{(\alpha\beta)}}{C}, \quad (\text{S131})$$

and

$$|\Psi_{\text{TAR}\alpha\beta}\rangle_{AB} = \sqrt{p_{\text{vir}\alpha\beta|\text{TAR}\alpha\beta}} |0\rangle_A |\psi_{\text{vir}\alpha\beta}\rangle + \sum_{(i,j) \in \mathcal{C}_{\text{Tar}}^{(\alpha\beta)}} \sqrt{p_{ij|\text{TAR}\alpha\beta}} |k_{ij}^{(\alpha\beta)}\rangle_A |\psi_{ij}\rangle_{B_a B_b}, \quad (\text{S132})$$

$$|\Psi_{\text{REF}\alpha\beta}\rangle_{AB} = \sum_{(i,j) \in \mathcal{C}_{\text{Ref}}^{(\alpha\beta)}} \sqrt{p_{ij|\text{REF}\alpha\beta}} |k_{ij}^{(\alpha\beta)}\rangle_A |\psi_{ij}\rangle_{B_a B_b}, \quad (\text{S133})$$

with

$$p_{\text{vir}\alpha\beta|\text{TAR}\alpha\beta} = \frac{q_{\text{vir}\alpha\beta}^\psi}{q_{\text{vir}\alpha\beta}^\psi + q_{\text{vir}\alpha\beta}^\phi \sum_{(i,j) \in \mathcal{C}_{\text{Tar}}^{(\alpha\beta)}} c_{ij}^{(\alpha\beta)}}, \quad (\text{S134})$$

$$p_{ij|\text{TAR}\alpha\beta} = \frac{q_{\text{vir}\alpha\beta}^\phi c_{ij}^{(\alpha\beta)}}{q_{\text{vir}\alpha\beta}^\psi + q_{\text{vir}\alpha\beta}^\phi \sum_{(i',j') \in \mathcal{C}_{\text{Tar}}^{(\alpha\beta)}} c_{i'j'}^{(\alpha\beta)}} \quad \text{for } (i,j) \in \mathcal{C}_{\text{Tar}}^{(\alpha\beta)}, \quad (\text{S135})$$

$$p_{ij|\text{REF}\alpha\beta} = \frac{c_{ij}^{(\alpha\beta)}}{\sum_{(i',j') \in \mathcal{C}_{\text{Ref}}^{(\alpha\beta)}} c_{i'j'}^{(\alpha\beta)}} \quad \text{for } (i,j) \in \mathcal{C}_{\text{Ref}}^{(\alpha\beta)}. \quad (\text{S136})$$

In the Virtual Protocol, we can label the emissions in the key rounds by $l \in \{\text{vir}\alpha\beta\}_{\alpha\beta}$ and the emissions in the test rounds by $l \in \{ij\}_{ij}$. Each emission with label l should be assigned a tag $t \in \{\text{TAR00}, \text{TAR01}, \text{TAR10}, \text{TAR11}, \text{REF00}, \text{REF01}, \text{REF10}, \text{REF11}\}$ with probability

$$p_{t|l} = \frac{p_t p_{l|t}}{p_l}, \quad (\text{S137})$$

where $p_{l|t}$ is given by Eqs. (S134) to (S136) and p_t is the overall probability to assign tag t . Also, for $l \in \{0_Z 0_Z, 0_Z 1_Z, 1_Z 0_Z, 1_Z 1_Z\}$, p_l corresponds to the probability that in the Actual Protocol Alice and Bob emit these states and the round is a test round, i.e., $p_{0_Z 0_Z} = p_{0_Z 1_Z} = p_{1_Z 0_Z} = p_{1_Z 1_Z} = p_Z^2 p_{\text{test}|Z}/4$. Similarly, for $l \in \{\text{vir}\alpha\beta\}_{\alpha\beta}$, we have that $p_{\text{vir}\alpha\beta} = p_Z^2 p_{\text{key}|Z} q_{\text{vir}\alpha\beta}^\psi$. Taking the sum over t on both sides of Eq. (S137) and using the fact that $\sum_t p_{t|l} \leq 1$, we derive the following constraints,

$$\sum_t p_t p_{l|t} \leq p_l, \quad \forall l. \quad (\text{S138})$$

Now, let $p_{\text{TAR}} = \sum_{\alpha\beta} p_{\text{TAR}\alpha\beta}$ and $p_{\text{REF}} = \sum_{\alpha\beta} p_{\text{REF}\alpha\beta}$. We want that

$$p_{\text{TAR}\alpha\beta} = p_{\text{TAR}} p_{\text{TAR}\alpha\beta|\text{TAR}}, \quad (\text{S139})$$

$$p_{\text{REF}\alpha\beta} = p_{\text{REF}} p_{\text{REF}\alpha\beta|\text{REF}}, \quad (\text{S140})$$

where $p_{\text{TAR}\alpha\beta|\text{TAR}}$ and $p_{\text{REF}\alpha\beta|\text{REF}}$ are given by Eqs. (S130) and (S131). We also want that $p_{\text{TAR}} = p_{\text{REF}}$. Putting everything together, we obtain

$$\begin{aligned} p_l &\geq \sum_t p_t p_{l|t} = \sum_{t \in \{\text{TAR}\alpha\beta\}_{\alpha\beta}} p_t p_{l|t} + \sum_{t \in \{\text{REF}\alpha\beta\}_{\alpha\beta}} p_t p_{l|t} \\ &= \sum_{\alpha\beta} (p_{\text{TAR}} p_{\text{TAR}\alpha\beta|\text{TAR}} p_{l|\text{TAR}\alpha\beta} + p_{\text{REF}} p_{\text{REF}\alpha\beta|\text{REF}} p_{l|\text{REF}\alpha\beta}) \\ &= \sum_{\alpha\beta} (p_{\text{TAR}} p_{\text{TAR}\alpha\beta|\text{TAR}} p_{l|\text{TAR}\alpha\beta} + p_{\text{TAR}} p_{\text{REF}\alpha\beta|\text{REF}} p_{l|\text{REF}\alpha\beta}) \\ &= p_{\text{TAR}} \sum_{\alpha\beta} (p_{\text{TAR}\alpha\beta|\text{TAR}} p_{l|\text{TAR}\alpha\beta} + p_{\text{REF}\alpha\beta|\text{REF}} p_{l|\text{REF}\alpha\beta}). \end{aligned} \quad (\text{S141})$$

The only constraint on the value of p_{TAR} is that Eq. (S141) holds for all l . Therefore, we can set its value as

$$p_{\text{TAR}} = \min_l \frac{p_l}{\sum_{\alpha\beta} (p_{\text{TAR}\alpha\beta|\text{TAR}} p_{l|\text{TAR}\alpha\beta} + p_{\text{REF}\alpha\beta|\text{REF}} p_{l|\text{REF}\alpha\beta})}. \quad (\text{S142})$$

Once we set p_{TAR} , the tag selection probabilities $p_{\text{TAR}\alpha\beta}$ and $p_{\text{REF}\alpha\beta}$ become fixed, and so do the conditional tag assignment probabilities $p_{t|l}$.

Finally, as before, we assume that the users randomly mark each tagged emission as Z_C with probability p_{Z_C} , or as X_C otherwise. By the Chernoff bound [S16], in the limit $N \rightarrow \infty$, we have that

$$N_{l,t,Z_C}^{\text{det}} \simeq p_{Z_C} p_{t|l} N_l^{\text{det}}, \quad (\text{S143})$$

where N_{l,t,Z_C}^{det} is the total number of emissions with label l and tag t that are marked as Z_C .

C. Coin protocol

Similarly to the P&M scenario, after the tag assignments explained above, the Virtual Protocol becomes equivalent to the Coin Protocol, in which Alice and Bob generate the quantum coin state $|\Psi_{\text{coin}}\rangle_{CDAB}$ with probability $p_C = 2p_{\text{TAR}}$, and then measure the coin system C in the Z_C or X_C bases with probabilities p_{Z_C} and p_{X_C} , respectively. For the rounds in which they measured the coin system C in Z_C , they measure their systems D_a and D_b in the computational basis, obtaining the measurement outcomes α and β , respectively, and check whether or not their result is such that $\alpha = \beta$ (error) or $\alpha \neq \beta$ (no error). Also, if $Z_C = 0$, they measure system A in the $\{|0\rangle_A\} \cup \{|k_{ij}^{(\alpha\beta)}\rangle_A\}_{ij \in \mathcal{C}_{\text{Tar}}^{(\alpha\beta)}}$ basis, and if $Z_C = 1$, they measure system A in the $\{|k_{ij}^{(\alpha\beta)}\rangle_A\}_{ij \in \mathcal{C}_{\text{Ref}}^{(\alpha\beta)}}$; thereby learning the label l that the emission corresponds to. Due to the equivalence between the Coin Protocol and the Virtual Protocol with tag assignment, we have that

$$\begin{aligned} N_{Z_C=0}^{\text{err}} &\equiv \sum_{\alpha=\beta} \left(N_{\text{vir}\alpha\beta, \text{TAR}\alpha\beta, Z_C}^{\text{det}} + \sum_{(i,j) \in \mathcal{C}_{\text{Tar}}^{(\alpha\beta)}} N_{ij, \text{TAR}\alpha\beta, Z_C}^{\text{det}} \right), \\ N_{Z_C=1}^{\text{err}} &\equiv \sum_{\alpha=\beta} \sum_{(i,j) \in \mathcal{C}_{\text{Ref}}^{(\alpha\beta)}} N_{ij, \text{REF}\alpha\beta, Z_C}^{\text{det}}, \\ N_{Z_C=0}^{\text{det}} &\equiv \sum_{\alpha,\beta} \left(N_{\text{vir}\alpha\beta, \text{TAR}\alpha\beta, Z_C}^{\text{det}} + \sum_{(i,j) \in \mathcal{C}_{\text{Tar}}^{(\alpha\beta)}} N_{ij, \text{TAR}\alpha\beta, Z_C}^{\text{det}} \right), \\ N_{Z_C=1}^{\text{det}} &\equiv \sum_{\alpha,\beta} \sum_{(i,j) \in \mathcal{C}_{\text{Ref}}^{(\alpha\beta)}} N_{ij, \text{REF}\alpha\beta, Z_C}^{\text{det}}, \end{aligned} \quad (\text{S144})$$

where $N_{Z_C=z}^{\text{det}}$ is the number of detected rounds in which Alice and Bob obtained outcome $z \in \{0, 1\}$ when measuring the coin system C in the Z_C basis, and $N_{Z_C=z}^{\text{err}}$ is the number of these rounds in which the outcome of their measurement on systems D_a and D_b is such that $\alpha = \beta$. Substituting Eq. (S143) into Eq. (S144), we have that, in the asymptotic regime,

$$\begin{aligned} N_{Z_C=0}^{\text{err}} &\simeq p_{Z_C} \left(p_{\text{TAR}|\text{vir}} N_{\text{ph}} + \sum_{\alpha=\beta} \sum_{(i,j) \in \mathcal{C}_{\text{Tar}}^{(\alpha\beta)}} p_{\text{TAR}\alpha\beta|ij} N_{ij}^{\text{det}} \right), \\ N_{Z_C=1}^{\text{err}} &\simeq p_{Z_C} \left(\sum_{\alpha=\beta} \sum_{(i,j) \in \mathcal{C}_{\text{Ref}}^{(\alpha\beta)}} p_{\text{REF}\alpha\beta|ij} N_{ij}^{\text{det}} \right), \\ N_{Z_C=0}^{\text{det}} &\simeq p_{Z_C} \left(p_{\text{TAR}|\text{vir}} N_{\text{key}}^{\text{det}} + \sum_{\alpha,\beta} \sum_{(i,j) \in \mathcal{C}_{\text{Tar}}^{(\alpha\beta)}} p_{\text{TAR}\alpha\beta|ij} N_{ij}^{\text{det}} \right), \\ N_{Z_C=1}^{\text{det}} &\simeq p_{Z_C} \left(\sum_{\alpha,\beta} \sum_{(i,j) \in \mathcal{C}_{\text{Ref}}^{(\alpha\beta)}} p_{\text{REF}\alpha\beta|ij} N_{ij}^{\text{det}} \right). \end{aligned} \quad (\text{S145})$$

In Eq. (S145), we have used that $p_{\text{TAR}|\text{vir}} := p_{\text{TAR00}|\text{vir00}} = p_{\text{TAR01}|\text{vir01}} = p_{\text{TAR10}|\text{vir10}} = p_{\text{TAR11}|\text{vir11}}$, $N_{\text{ph}} := N_{\text{vir00}}^{\text{det}} + N_{\text{vir11}}^{\text{det}}$ and $N_{\text{key}}^{\text{det}} = N_{\text{vir00}}^{\text{det}} + N_{\text{vir01}}^{\text{det}} + N_{\text{vir10}}^{\text{det}} + N_{\text{vir11}}^{\text{det}}$, where $N_{\text{key}}^{\text{det}}$ is the total number of detected key rounds, i.e., the size of the sifted key. Finally, substituting Eq. (S145) into the quantum coin inequality, Eq. (S43), and isolating N_{ph} , we obtain a bound on the number of phase errors in terms of the observables of the actual protocol.

D. General finite-key analysis for MDI protocols

Here, we extend the previous analysis to the finite-key regime, using the same approach as in Section SM1 E. As shown in Section SE1, in the finite-key regime, the Coin Protocol inequality becomes

$$N_{Z_C=0}^{\text{err}} - \Delta_A \underset{6\epsilon_A}{\leq} (N_{Z_C=0}^{\text{det}} + \Delta_A) G_+ \left(\frac{N_{Z_C=1}^{\text{err}} + \Delta_A}{N_{Z_C=1}^{\text{det}} - \Delta_A}, 1 - \frac{2p_{Z_C}(N_{X_C=1} + \Delta_A)}{p_{X_C}(N_{Z_C}^{\text{det}} - \Delta_A)} \right), \quad (\text{S146})$$

where we have employed Azuma's inequality using $\Delta_A := \Delta_A(N^{\text{det}})$ with N^{det} denoting the total number of detected rounds. By substituting the definition of $N_{Z_C=0}^{\text{err}}$ in Eq. (S144) into Eq. (S146) and rearranging, we obtain

$$N_{\text{ph,TAR},Z_C} \underset{6\epsilon_A}{\leq} (N_{Z_C=0}^{\text{det}} + \Delta_A) G_+ \left(\frac{N_{Z_C=1}^{\text{err}} + \Delta_A}{N_{Z_C=1}^{\text{det}} - \Delta_A}, 1 - \frac{2p_{Z_C}(N_{X_C=1} + \Delta_A)}{p_{X_C}(N_{Z_C}^{\text{det}} - \Delta_A)} \right) + \Delta_A - \sum_{\alpha=\beta} \sum_{(i,j) \in \mathcal{C}_{\text{Tar}}^{(\alpha\beta)}} N_{ij,\text{TAR}\alpha\beta,Z_C}^{\text{det}}, \quad (\text{S147})$$

where we have defined $N_{\text{ph,TAR},Z_C} := \sum_{\alpha=\beta} N_{\text{vir}\alpha\beta,\text{TAR}\alpha\beta,Z_C}^{\text{det}}$. Also, by the Chernoff bound, we have that

$$N_{X_C=1} \underset{\epsilon_C}{\leq} \hat{N}_{X_C=1} + \Delta_C^+(\hat{N}_{X_C=1}) =: \bar{N}_{X_C=1}, \quad (\text{S148})$$

where $\hat{N}_{X_C=1} = N p_C p_{X_C} \Delta / 2$, and that

$$\begin{aligned} \underline{N}_{l,t,Z_C}^{\text{det}} &:= \hat{N}_{l,t,Z_C}^{\text{det}} - \Delta_C^-(\hat{N}_{l,t,Z_C}^{\text{det}}) \underset{\epsilon_C}{\leq} N_{l,t,Z_C}^{\text{det}} \underset{\epsilon_C}{\leq} \hat{N}_{l,t,Z_C}^{\text{det}} + \Delta_C^+(\hat{N}_{l,t,Z_C}^{\text{det}}) =: \bar{N}_{l,t,Z_C}^{\text{det}}, \\ \underline{N}_{\text{key,TAR},Z_C}^{\text{det}} &:= \hat{N}_{\text{key,TAR},Z_C}^{\text{det}} - \Delta_C^-(\hat{N}_{\text{key,TAR},Z_C}^{\text{det}}) \underset{\epsilon_C}{\leq} N_{\text{key,TAR},Z_C}^{\text{det}} \underset{\epsilon_C}{\leq} \hat{N}_{\text{key,TAR},Z_C}^{\text{det}} + \Delta_C^+(\hat{N}_{\text{key,TAR},Z_C}^{\text{det}}) =: \bar{N}_{\text{key,TAR},Z_C}^{\text{det}}, \end{aligned} \quad (\text{S149})$$

where $\hat{N}_{l,t,Z_C}^{\text{det}} = p_{Z_C} p_{t|l} N_l^{\text{det}}$, $N_{\text{key,TAR},Z_C}^{\text{det}} = \sum_{\alpha,\beta} N_{\text{vir}\alpha\beta,\text{TAR}\alpha\beta,Z_C}^{\text{det}}$ and $\hat{N}_{\text{key,TAR},Z_C}^{\text{det}} = p_{Z_C} p_{\text{TAR}|\text{vir}} N_{\text{key}}^{\text{det}}$. Also, by Hoeffding's bound, we have that

$$N_{\text{ph,TAR},Z_C} \underset{\epsilon_H}{\geq} p_{Z_C} p_{\text{TAR}|\text{vir}} N_{\text{ph}} - \Delta_H(N_{\text{ph}}) \geq p_{Z_C} p_{\text{TAR}|\text{vir}} N_{\text{ph}} - \Delta_H(N_{\text{key}}^{\text{det}}), \quad (\text{S150})$$

where in the last inequality we have upper bounded $\Delta_H(N_{\text{ph}})$ by $\Delta_H(N_{\text{key}}^{\text{det}})$, where $N_{\text{key}}^{\text{det}}$ is the number of detected key rounds. Substituting Eq. (S149) into Eq. (S144), we obtain

$$\begin{aligned} N_{Z_C=1}^{\text{err}} &\underset{\# \epsilon_C}{\leq} \bar{N}_{Z_C=1}^{\text{err}} := \sum_{\alpha=\beta} \sum_{(i,j) \in \mathcal{C}_{\text{Ref}}^{(\alpha\beta)}} \bar{N}_{ij,\text{REF}\alpha\beta,Z_C}^{\text{det}}, \\ \underline{N}_{Z_C=0}^{\text{det}} &\underset{\# \epsilon_C}{\leq} \bar{N}_{Z_C=0}^{\text{det}} := \bar{N}_{\text{key,TAR},Z_C}^{\text{det}} + \sum_{\alpha,\beta} \sum_{(i,j) \in \mathcal{C}_{\text{Tar}}^{(\alpha\beta)}} \bar{N}_{ij,\text{TAR}\alpha\beta,Z_C}^{\text{det}}, \\ \underline{N}_{Z_C=0}^{\text{det}} &\underset{\# \epsilon_C}{\geq} \underline{N}_{Z_C=0}^{\text{det}} := \underline{N}_{\text{key,TAR},Z_C}^{\text{det}} + \sum_{\alpha,\beta} \sum_{(i,j) \in \mathcal{C}_{\text{Tar}}^{(\alpha\beta)}} \underline{N}_{ij,\text{TAR}\alpha\beta,Z_C}^{\text{det}}, \\ \underline{N}_{Z_C=1}^{\text{det}} &\underset{\# \epsilon_C}{\geq} \underline{N}_{Z_C=1}^{\text{det}} := \sum_{\alpha,\beta} \sum_{(i,j) \in \mathcal{C}_{\text{Ref}}^{(\alpha\beta)}} \underline{N}_{ij,\text{REF}\alpha\beta,Z_C}^{\text{det}}, \end{aligned} \quad (\text{S151})$$

where by, e.g., $\underset{\# \epsilon_C}{\leq}$, we mean that the probability that the inequality fails is a factor times ϵ_C , and for simplicity we will only calculate the total factor in the final formula. Substituting Eqs. (S148) to (S151) into Eq. (S147), we obtain an upper bound on the number of phase errors

$$\begin{aligned} N_{\text{ph}} &\leq \frac{1}{p_{Z_C} p_{\text{TAR}|\text{vir}}} \left[(\bar{N}_{Z_C=0}^{\text{det}} + \Delta_A) G_+ \left(\frac{\bar{N}_{Z_C=1}^{\text{err}} + \Delta_A}{\bar{N}_{Z_C=1}^{\text{det}} - \Delta_A}, 1 - \frac{2p_{Z_C}(\bar{N}_{X_C=1} + \Delta_A)}{p_{X_C}(\bar{N}_{Z_C=0}^{\text{det}} + \bar{N}_{Z_C=1}^{\text{det}} - \Delta_A)} \right) \right. \\ &\quad \left. - \sum_{\alpha=\beta} \sum_{(i,j) \in \mathcal{C}_{\text{Tar}}^{(\alpha\beta)}} \underline{N}_{ij,\text{TAR}\alpha\beta,Z_C}^{\text{det}} + \Delta_A + \Delta_H(N_{\text{key}}^{\text{det}}) \right] =: N_{\text{ph}}^{\text{U}}, \end{aligned} \quad (\text{S152})$$

where $\epsilon_{\text{tot}} := 6\epsilon_A + (2(|\mathcal{C}_{\text{Tar}}^{(00)}| + |\mathcal{C}_{\text{Tar}}^{(01)}| + |\mathcal{C}_{\text{Tar}}^{(10)}| + |\mathcal{C}_{\text{Tar}}^{(11)}| + |\mathcal{C}_{\text{Ref}}^{(00)}| + |\mathcal{C}_{\text{Ref}}^{(01)}| + |\mathcal{C}_{\text{Ref}}^{(10)}| + 3)\epsilon_C + \epsilon_H$ is the sum of the failure probabilities of all the concentration inequalities applied. After performing error correction, error verification and privacy amplification, Alice and Bob obtain an $(\epsilon_{\text{corr}} + \epsilon_{\text{sec}})$ -secure key of length

$$N_{\text{sec}} = N_{\text{key}}^{\text{det}} [1 - h(e_{\text{ph}}^{\text{U}})] - \lambda_{\text{EC}} - \log_2 \frac{1}{\epsilon_{\text{corr}}} - \log_2 \frac{1}{\epsilon_{\text{PA}}}, \quad (\text{S153})$$

where $e_{\text{ph}}^{\text{U}} := N_{\text{ph}}^{\text{U}}/N_{\text{key}}^{\text{det}}$ is the upper bound on the phase-error rate, $\lambda_{\text{EC}} = fh(e_Z)$ is the cost of error correction, with f denoting the error correction efficiency and e_Z the observed bit-error rate, ϵ_{corr} is the probability that the reconciled keys are not identical (due to the failure of error verification), ϵ_{PA} is a free parameter that can be regarded as the failure probability of privacy amplification, and $\epsilon_{\text{sec}} = \sqrt{2\sqrt{\epsilon_{\text{tot}} + \epsilon_{\text{PA}}}}$.

SM3. SECURITY ANALYSIS FOR NON-IID SOURCES

For simplicity, in both the Main Text and Sections **SM1** and **SM2**, we have implicitly assumed that the emitted states are pure, independent and identical across rounds. Here, we show how to apply our security analysis to scenarios in which this is not the case. For simplicity, we focus on the P&M scenario, although all results apply equally to MDI-type scenarios.

A. Independent but not identical pure states

As explained in Appendix A, our security proof can be applied without any modification when the emitted states are independent but different for different rounds, as long as Eq. (S1) holds for all rounds. That is, as long as the state emitted in the k -th round, which we can denote as $|\psi_{j_k}^{(k)}\rangle_{B_k}$, satisfies

$$|\langle\phi_{j_k}|\psi_{j_k}^{(k)}\rangle_{B_k}|^2 \geq 1 - \epsilon, \quad (\text{S154})$$

for all k , where $\{|\phi_j\rangle\}_j$ are a set of known qubit states. Note that, in this case, the target and reference states $|\Psi_{\text{Tar}}^{(k)}\rangle_{D_k A_k B_k}$ and $|\Psi_{\text{Ref}}^{(k)}\rangle_{D_k A_k B_k}$, and thus also the quantum coin state $|\Psi_{\text{coin}}^{(k)}\rangle_{C_k D_k A_k B_k}$, depend on the round k . However, this does not cause any problem in the security analysis presented in Section **SM1** (and similarly for Section **SM2**), as the derivation of the coin protocol inequality in Section **SE1** still holds, and the procedure in Section **SE2** can still be used to obtain a bound on $\text{Re}\langle\Psi_{\text{Ref}}^{(k)}|\Psi_{\text{Tar}}^{(k)}\rangle_{D_k A_k B_k}$ that holds for all k .

B. Independent but not identical mixed states

Also, as explained in Appendix A, our security proof can be applied without any modification when the emitted states $\rho_j^{(k)}$ are mixed, as long as Eq. (1) of the Main Text is satisfied, i.e.,

$$\langle\phi_j|\rho_j^{(k)}|\phi_j\rangle_{B_k} \geq 1 - \epsilon. \quad (\text{S155})$$

This is because, by Uhlmann's theorem, there must exist a purification $|\psi_j^{(k)}\rangle_{B_k S_k}$ of $\rho_j^{(k)}$ such that

$$|\langle\phi_j|\psi_j^{(k)}\rangle_{B_k S_k}|^2 = \langle\phi_j|\rho_j|\phi_j\rangle_{B_k} \geq 1 - \epsilon, \quad (\text{S156})$$

where we have defined $|\phi_j\rangle_{B_k S_k} := |\phi_j\rangle_{B_k} |0\rangle_{S_k}$. This implies that our analysis can be applied to the mixed state case simply by substituting $|\psi_j^{(k)}\rangle_{B_k} \rightarrow |\psi_j^{(k)}\rangle_{B_k S_k}$ and $|\phi_j^{(k)}\rangle_{B_k} \rightarrow |\phi_j^{(k)}\rangle_{B_k S_k}$ in the scenario just described in Section **SM3 A**.

Moreover, we remark that our proof can be applied even if Eq. (S155) does not hold for *all* rounds of the protocol, as long as one can obtain a bound on the number of rounds for which it does not hold. In this scenario, one can apply the *tagging* idea introduced in [S36]; namely, one simply assumes that all rounds that violate Eq. (S155) are detected and *tagged* (i.e., its outcomes are assumed to be known to Eve), and then applies our security proof to the non-tagged rounds.

C. Setting-independent pulse correlations

Our analysis is also directly applicable in a scenario that previous works have described as *setting-independent pulse correlations* [S37], i.e., when the emitted pulses are correlated but are independent of the setting choices made in previous rounds. Without loss of generality, in this case, we can consider that there exists a sequence of arbitrarily correlated random variables $G_1 \dots G_N$ such that the states emitted in different rounds are independent given a particular sequence of outcomes $g_1 \dots g_N$ of $G_1 \dots G_N$. That is, the global state emitted conditional on $g_1 \dots g_N$ and a particular sequence of setting choices $j_1 \dots j_N$ can be written as

$$\rho_{j_1}^{(g_1)} \otimes \dots \otimes \rho_{j_N}^{(g_N)}. \quad (\text{S157})$$

In this case, our security analysis is applicable as long as

$$\langle \phi_{j_k} | \rho_{j_k}^{(g_k)} | \phi_{j_k} \rangle_{B_k} \geq 1 - \epsilon, \quad (\text{S158})$$

for all k , j_k and g_k . This is because, as shown in [S20], we can prove security by assuming a fictitious but mathematically equivalent scenario in which, in the very beginning of the protocol, Alice learns the sequence of outcomes g_1, \dots, g_N of G_1, \dots, G_N . Then, we have that, conditioned on a particular outcome g_1, \dots, g_N , the resulting scenario is equivalent to that discussed in Section SM3 B above, which directly implies that we can use our analysis to obtain a bound of the form

$$\Pr[N_{\text{ph}}^{\text{U}} > N_{\text{ph}} | G_1 = g_1, \dots, G_N = g_N] \leq \epsilon_{\text{tot}}. \quad (\text{S159})$$

However, since this bound holds for any g_1, \dots, g_N , it follows that

$$\Pr[N_{\text{ph}}^{\text{U}} > N_{\text{ph}}] \leq \epsilon_{\text{tot}}, \quad (\text{S160})$$

which is what we need to guarantee security.

D. Setting-dependent pulse correlations

With some modifications, our security proof can also be applied in the presence of setting-dependent pulse correlations, i.e., when the state emitted in a particular round depends also on the setting choices made in previous rounds. For this, it is useful to first examine the entangled state generated by Alice in the entanglement-based view of the protocol, for both the uncorrelated and correlated cases. In the former case, the state emitted in any round k , denoted as $|\psi_{j_k}\rangle_{B_k}$, depends solely on the k -th setting choice j_k , and Alice's state preparation is equivalent to the generation of the global entangled state

$$|\Psi_{\text{indep}}\rangle_{\mathbf{AB}} = \bigotimes_k \sum_{j_k} \sqrt{p_{j_k}} |j_k\rangle_{A_k} |\psi_{j_k}\rangle_{B_k}, \quad (\text{S161})$$

where $\{|j_k\rangle_{A_k}\}_{j_k}$ forms an orthonormal basis for the ancillary system A_k , $\mathbf{A} := A_1 \dots A_N$ and $\mathbf{B} := B_1 \dots B_N$. Note that, in Eq. (S161), the state of systems $A_k B_k$ and the state of systems $A_{k'} B_{k'}$ is separable for all $k \neq k'$.

Now, let us consider correlated sources, starting with the simplest case: nearest-neighbor pulse correlations. In this scenario, the state emitted in the k -th round, denoted as $|\psi_{j_k|j_{k-1}}\rangle_{B_k}$, depends not only on the k -th setting choice j_k but also on the previous setting choice j_{k-1} . This situation is equivalent to Alice preparing the global entangled state⁵

$$|\Psi_{\text{correl}}\rangle_{\mathbf{AB}} = \sum_{j_1} \sqrt{p_{j_1}} |j_1\rangle_{A_1} |\psi_{j_1}\rangle_{B_1} \otimes \sum_{j_2} \sqrt{p_{j_2}} |j_2\rangle_{A_2} |\psi_{j_2|j_1}\rangle_{B_2} \otimes \dots \otimes \sum_{j_N} \sqrt{p_{j_N}} |j_N\rangle_{A_N} |\psi_{j_N|j_{N-1}}\rangle_{B_N}. \quad (\text{S162})$$

Importantly, the state of the systems A_k and B_{k+1} is now entangled, and thus $|\Psi_{\text{correl}}\rangle_{\mathbf{AB}}$ lacks the separable structure of $|\Psi_{\text{indep}}\rangle_{\mathbf{AB}}$ in Eq. (S161). At first glance, this presents an impediment to applying our security proof. However, we can overcome this problem by following the approach introduced in [S2, S20, S38, S39], which involves dividing the

⁵ Note that, more generally, the emitted states may depend on the round k , and may be mixed rather than pure. However, as just shown in Sections SM3 A to SM3 C, this can be easily accommodated in our security proof, and for simplicity, we do not reflect this in the notation used here.

protocol rounds into even and odd subgroups, and separately proving the security of the key generated within each subgroup.

Say that we want to prove the security of the even subkey. To do so, we consider that Alice first measures all odd ancillas $A_1 A_3 A_5 \dots$ in the computational basis, obtaining some measurement results j'_1, j'_3, j'_5, \dots , and the post-measurement state

$$|\Psi_{j'_1, j'_3, j'_5, \dots} \rangle_{\mathbf{AB}} = |j'_1 j'_3 j'_5 \dots\rangle_{A_1 A_3 A_5 \dots} |\psi_{j'_1}\rangle_{B_1} \bigotimes_{k \text{ even}} \sum_{j_k} \sqrt{p_{j_k}} |j_k\rangle_{A_k} |\psi_{j_k|j'_{k-1}}\rangle_{B_k} |\psi_{j'_{k+1}|j_k}\rangle_{B_{k+1}}. \quad (\text{S163})$$

Our goal is to establish that a secure even subkey can be obtained from the entangled state in Eq. (S163) irrespectively of the sequence j'_1, j'_3, j'_5, \dots . This implies that the even subkey is also secure in the actual scenario independently of Alice's setting choices in the odd rounds.

Since we are considering the security of the even subkey, the state of systems $A_1 A_3 A_5 \dots$ and B_1 in Eq. (S163) is irrelevant and they can be traced out, resulting in the redefined state

$$|\Psi_{j'_1, j'_3, j'_5, \dots} \rangle_{\mathbf{AB}} = \bigotimes_{k \text{ even}} \sum_{j_k} \sqrt{p_{j_k}} |j_k\rangle_{A_k} |\psi_{j_k|j'_{k-1}}\rangle_{B_k} |\psi_{j'_{k+1}|j_k}\rangle_{B_{k+1}}. \quad (\text{S164})$$

Note that Eq. (S164) has essentially the same structure as Eq. (S161), with the only differences being that in the former formula the tensor product is over even values of k only, and that the role played by $|\psi_{j_k}\rangle_{B_k}$ in the latter formula is played by the combined state $|\psi_{j_k|j'_{k-1}}\rangle_{B_k} |\psi_{j'_{k+1}|j_k}\rangle_{B_{k+1}}$ in the former. This takes into account the fact that, in the presence of nearest-neighbor pulse correlations, information about the k -th setting choice j_k is not only encoded into system B_k but also into system B_{k+1} . The equivalence between Eq. (S164) and Eq. (S161) directly implies that one can apply our analysis to prove the security of the even subkey by considering that the states emitted in the k -th round are $\{|\psi_{j_k|j'_{k-1}}\rangle_{B_k} |\psi_{j'_{k+1}|j_k}\rangle_{B_{k+1}}\}_{j_k}$. In particular, to apply our security proof, these states must satisfy

$$|\langle \phi_{j_k} | \psi_{j_k|j'_{k-1}} \rangle_{B_k} \langle \lambda_{j'_{k+1}} | \psi_{j'_{k+1}|j_k} \rangle_{B_{k+1}}|^2 \geq 1 - \epsilon, \quad (\text{S165})$$

for any setting choices j'_{k-1}, j_k, j'_{k+1} , where $\{|\phi_{j_k}\rangle_{B_k}\}_{j_k}$ are known qubit states and $|\lambda_{j'_{k+1}}\rangle_{B_{k+1}}$ is an arbitrary state on system B_{k+1} that is independent of j_k . This condition is the analogue to Eq. (S1) for the case of nearest-neighbor pulse correlations.

More generally, let us assume a maximum correlation length of l_c rounds and the knowledge that, for any setting choices $j'_{k-l_c}, j'_{k-l_c+1}, \dots, j'_{k-1}, j_k, j'_{k+1}, \dots, j'_{k+l_c-1}, j'_{k+l_c}$,

$$|\langle \phi_{j_k} | \psi_{j_k|j'_{k-1}, j'_{k-2}, \dots, j'_{k-l_c}} \rangle_{B_k} \langle \lambda_{j'_{k-l_c+1}, \dots, j'_{k-1}, j'_{k+1}, \dots, j'_{k+l_c}} | \psi_{j'_{k-l_c+1}, \dots, j'_{k-1}, j_k, j'_{k+1}, \dots, j'_{k+l_c}} \rangle_{B_{k+1} B_{k+2} \dots B_{k+l_c}}|^2 \geq 1 - \epsilon, \quad (\text{S166})$$

where

$$|\psi_{j'_{k-l_c+1}, \dots, j'_{k-1}, j_k, j'_{k+1}, \dots, j'_{k+l_c}}\rangle_{B_{k+1} B_{k+2} \dots B_{k+l_c}} := |\psi_{j'_{k+1}|j_k, j'_{k-1}, \dots, j'_{k-l_c+1}}\rangle_{B_{k+1}} \dots |\psi_{j'_{k+l_c}|j'_{k+l_c-1}, j'_{k+l_c-2}, \dots, j_k}\rangle_{B_{k+l_c}}, \quad (\text{S167})$$

represents the state of systems $B_{k+1} B_{k+2} \dots B_{k+l_c}$ for a given list of setting choices $j'_{k-l_c+1}, \dots, j'_{k-1}, j_k, j'_{k+1}, \dots, j'_{k+l_c}$, and $|\lambda_{j'_{k-l_c+1}, \dots, j'_{k-1}, j'_{k+1}, \dots, j'_{k+l_c}}\rangle_{B_{k+1} B_{k+2} \dots B_{k+l_c}}$ denotes an arbitrary state on systems $B_{k+1} B_{k+2} \dots B_{k+l_c}$ that is independent of j_k . Then, if these conditions are met, one can divide the protocol rounds into $(l_c + 1)$ subgroups and apply our analysis to prove the security of the key extracted from each individual subgroup.

In practice, it may be useful to decompose the bound in Eq. (S166) into two, i.e.,

$$|\langle \phi_{j_k} | \psi_{j'_{k-1}, j'_{k-2}, \dots, j'_{k-l_c}} \rangle_{B_k}|^2 \geq 1 - \epsilon_{\text{qubit}}, \quad (\text{S168})$$

and

$$|\langle \lambda_{j'_{k-l_c+1}, \dots, j'_{k-1}, j'_{k+1}, \dots, j'_{k+l_c}} | \psi_{j'_{k-l_c+1}, \dots, j'_{k-1}, j_k, j'_{k+1}, \dots, j'_{k+l_c}} \rangle_{B_{k+1} B_{k+2} \dots B_{k+l_c}}|^2 \geq 1 - \epsilon_{\text{correl}}, \quad (\text{S169})$$

with $\epsilon = 1 - (1 - \epsilon_{\text{qubit}})(1 - \epsilon_{\text{correl}}) \leq \epsilon_{\text{qubit}} + \epsilon_{\text{correl}}$. Similarly to Eq. (S1), the bound in Eq. (S168) evaluates how close the emitted state in each round is to a known qubit state, and should incorporate the effect of other side channels beyond pulse correlations. In contrast, the bound in Eq. (S169) depends only on the magnitude of the pulse correlations; in general, to evaluate it one needs knowledge on how this magnitude decreases as the pulse separation $l \in \{1, \dots, l_c\}$ increases. For example, let us assume that we are able to obtain a bound on the maximum deviation

that the state emitted in a given round can undergo when varying the setting choice made l rounds ago, i.e., obtain a bound ϵ_l such that, for $j_{k-l} \neq \tilde{j}_{k-l}$

$$|\langle \psi_{j_k|j_{k-1}, \dots, j_{k-l+1}, \tilde{j}_{k-l}, j_{k-l-1}, \dots, j_{k-l_c}} | \psi_{j_k|j_{k-1}, \dots, j_{k-l+1}, j_{k-l}, j_{k-l-1}, \dots, j_{k-l_c}} \rangle_{B_k}|^2 \geq 1 - \epsilon_l. \quad (\text{S170})$$

Then, following a similar approach to that in the Methods Section of [S2], one can mathematically define a state $|\lambda_{j'_{k-l_c+1}, \dots, j'_{k-1}, j'_{k+1}, \dots, j'_{k+l_c}}\rangle_{B_{k+1}B_{k+2}\dots B_{k+l_c}}$ that is independent of j_k by considering the state of systems $B_{k+1}B_{k+2}\dots B_{k+l_c}$ when the k -th setting choice has been fixed to a particular value $j_k = \gamma$, i.e.,

$$\begin{aligned} |\lambda_{j'_{k-l_c+1}, \dots, j'_{k-1}, j'_{k+1}, \dots, j'_{k+l_c}}\rangle_{B_{k+1}B_{k+2}\dots B_{k+l_c}} &:= |\psi_{j'_{k-l_c+1}, \dots, j'_{k-1}, \gamma, j'_{k+1}, \dots, j'_{k+l_c}}\rangle_{B_{k+1}B_{k+2}\dots B_{k+l_c}} \\ &= |\psi_{j'_{k+1}|\gamma, j'_{k-1}, \dots, j'_{k-l_c+1}}\rangle_{B_{k+1}} \dots |\psi_{j'_{k+l_c}|j'_{k+l_c-1}, j'_{k+l_c-2}, \dots, \gamma}\rangle_{B_{k+l_c}}, \end{aligned} \quad (\text{S171})$$

and it immediately follows that

$$\epsilon_{\text{correl}} = 1 - \prod_{l=1}^{l_c} (1 - \epsilon_l) \leq \sum_{l=1}^{l_c} \epsilon_l. \quad (\text{S172})$$

Note that the above analysis implicitly assumes that the correlations have a finite maximum correlation length l_c , i.e., that there is a certain l such that the setting choice made in the k -th round has absolutely no influence on the signal emitted in the $(k+l)$ -th round for $l > l_c$. In practice, while it seems reasonable to assume that the correlation magnitude ϵ_l should decrease rapidly with the length l , the expectation that this magnitude will drop to exactly zero for any finite value of l may not be justified. Nevertheless, as recently shown in [S40], security proofs such as ours can still be rigorously applied even if the length of the correlations is unbounded, using the following approach: (1) consider an effective maximum correlation length l_e , which should be such that the combined magnitude of the correlations between pulses separated by more than l_e rounds is extremely small; (2) apply our security proof assuming that the true correlation length l_c equals l_e ; and (3) rigorously account for the neglected long-range correlations by slightly increasing the security parameter of the final key ϵ_{sec} by an amount that can be made as small as desired by increasing l_e .

We emphasize that, in this section, we have focused on *classical* pulse correlations, i.e., the scenario in which the classical setting choices made in a particular round influence the quantum states emitted in subsequent rounds. This effect is well-documented and widely recognized as a significant threat to the security of QKD systems, particularly those run at high speeds [S41, S42]. Theoretically, another type of correlations, referred to as *quantum* correlations, could also be considered. These would occur if the photonic systems emitted in different rounds were entangled.

For standard weak coherent pulse sources used in most practical QKD implementations, inter-round entanglement is extremely unlikely since these sources do not involve entanglement generation processes. However, it is perhaps conceivable that sources based on parametric down-conversion or quantum dots could potentially produce residual entanglement between consecutive rounds. While such sources would ideally be engineered to produce independent photons across rounds (e.g., by measuring one photon from an entangled pair locally and sending the other), their fundamental reliance on entanglement generation processes makes it plausible that small amounts of inter-round entanglement could persist.

Even if such entanglement occurred, we expect its magnitude would be minimal, providing negligible advantage to an eavesdropper. In this context, we remark that our security proof could incorporate these quantum correlations by applying the results of [S40] in a similar way as described in the previous paragraph for residual long-range correlations: (1) obtain a bound on the trace distance d between the actual global state emitted by the source, which contains a minimal amount of quantum correlations, and the global state that would be emitted if these correlations did not exist; (2) apply our security proof assuming that these quantum correlations do not exist; and (3) increment the security parameter of the final key by $2d$. Whether any residual entanglement from such sources would be small enough for this approach to be practical remains to be determined experimentally, and developing more direct methods to incorporate such correlations into security proofs represents an interesting direction for future work.

SM4. SECURITY WITH WCP LIGHT SOURCES

In this Section, we discuss how our security proof can be applied to scenarios in which the light source emits weak coherent pulses (WCPs) rather than single photons. First, in Section SM4 A, we show how to directly apply our analysis to a coherent-light-based MDI protocol [S34] that does not require either intensity modulation or phase randomization, and thus avoids the security loopholes introduced by imperfections in these processes, achieving a

very high degree of implementation security in a straightforward manner. Then, in Section SM4B, we show how our analysis can be combined with the decoy-state method [S43–S45] to guarantee security in the more common scenario in which the light source is an intensity-modulated phase-randomized WCP source, and discuss how our techniques can be applied to take into account imperfections in both the intensity modulation and phase randomization processes.

A. Coherent-light-based MDI protocol

Here, we apply our general security proof for MDI-type protocols, presented in Section SM2, to prove the security of the coherent-light-based MDI scheme proposed in [S34]. By doing so, we introduce two important improvements with respect to its existing security proof in [S34]: (1) the proof in [S34] is based on the reference technique (RT) [S2], and therefore requires a sequential assumption that may be especially difficult to guarantee for MDI-type protocols (see Section SM5 for more information); and (2) our security proof achieves significantly higher secret-key rates than that of [S34], even in terms of bits per pulse.

1. Protocol description

In this scheme, Alice (Bob) tries to prepare the states $\{|\sqrt{\mu}\rangle_{B_a(B_b)}, |-\sqrt{\mu}\rangle_{B_a(B_b)}, |\text{vac}\rangle_{B_a(B_b)}\}$, where $|\sqrt{\mu}\rangle_{B_a(B_b)}$ and $|-\sqrt{\mu}\rangle_{B_a(B_b)}$ are coherent states of intensity μ and opposite phases associated with bit values 0 and 1, respectively, and $|\text{vac}\rangle_{B_a(B_b)}$ is a vacuum state that is used for parameter estimation. However, we assume that, due to various imperfections and side channels, the states that she (he) actually prepares, $\{|\psi_{0Z}\rangle_{B_a(B_b)}, |\psi_{1Z}\rangle_{B_a(B_b)}, |\psi_{0X}\rangle_{B_a(B_b)}\}$, are only ϵ -close to these, i.e., they satisfy

$$\begin{aligned} |\langle \sqrt{\mu} | \psi_{0Z} \rangle_{B_u}|^2 &\geq 1 - \epsilon, \\ |\langle -\sqrt{\mu} | \psi_{1Z} \rangle_{B_u}|^2 &\geq 1 - \epsilon, \\ |\langle \text{vac} | \psi_{0X} \rangle_{B_u}|^2 &\geq 1 - \epsilon, \end{aligned} \quad (\text{S173})$$

where $u \in \{a, b\}$. The setup for this scheme is depicted in Fig. S6, and the full protocol is described below.

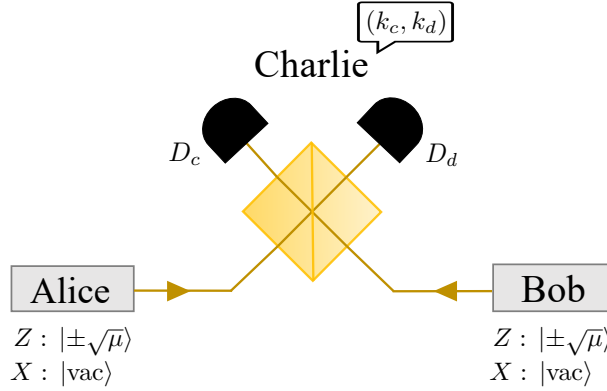


Figure S6. Illustration of the coherent-light-based MDI setup [S34]. In every round, Alice and Bob attempt to prepare a state in the set $\{|\sqrt{\mu}\rangle, |-\sqrt{\mu}\rangle, |\text{vac}\rangle\}$ and send it to the middle node Charlie through a quantum channel. Charlie measures the incoming signals by interfering them with a 50:50 beamsplitter, followed by two threshold detectors D_c and D_d , which are associated with constructive and destructive interference, respectively; and announces the outcome (k_c, k_d) , where $k_c = 1$ ($k_d = 1$) if detector D_c (D_d) clicks, and $k_c = 0$ ($k_d = 0$) otherwise. We note that although the protocol schematic resembles twin-field QKD [S35], the secret-key rate scales linearly with the overall Alice-Bob channel transmittance, as in the original MDI-QKD scheme, rather than with the square root of the transmittance as in twin-field QKD.

Coherent-light-based MDI protocol

1. **Quantum communication:** For each of the N rounds: (a) Alice (Bob) chooses a state from the set $\{|\psi_{0Z}\rangle_{B_a(B_b)}, |\psi_{1Z}\rangle_{B_a(B_b)}, |\psi_{0X}\rangle_{B_a(B_b)}\}$ with probabilities $\{p_Z/2, p_Z/2, p_X\}$, where $p_X := 1 - p_Z$, and sends

it to the middle node Charlie through a quantum channel. (b) If Charlie is honest (he could be completely dishonest and under Eve's control), he measures Alice and Bob's signals by interfering them at a 50:50 beam-splitter, followed by threshold detectors D_c and D_d placed at the output ports corresponding to constructive and destructive interference, respectively. After the measurement, Charlie reports the pair (k_c, k_d) , where $k_c = 1$ ($k_d = 1$) if detector D_c (D_d) clicks and $k_c = 0$ ($k_d = 0$) otherwise. A round is considered detected (undetected) if $k_c \neq k_d$ ($k_c = k_d$).

2. **Basis and bit announcement:** For each detected round, Alice (Bob) announces the Z basis if her (his) setting choice was $j \in \{0_Z, 1_Z\}$, or the X basis otherwise. Then, for each detected round in which both users announced the Z basis, Alice assigns the round to "key" ("test") with probability $p_{\text{key}|Z}$ ($p_{\text{test}|Z} = 1 - p_{\text{key}|Z}$), and announces this information. All the other detected rounds are assigned to "test". Then, the users announce their setting choices for the rounds assigned to "test", and define their sifted keys as the bit outcomes of the rounds assigned to "key". For the key rounds in which $k_c = 0$ and $k_d = 1$, Bob flips his sifted key bit⁶.
3. **Parameter estimation:** The users quantify the number of events N_{ij}^{det} in which Alice's (Bob's) setting choice was i (j), Charlie announced a detection, and the round was assigned to "test"; the number of detected key events $N_{\text{key}}^{\text{det}}$ (i.e., the length of the sifted key); and the total number of detected rounds $N^{\text{det}} := N_{\text{key}}^{\text{det}} + \sum_{i,j} N_{ij}^{\text{det}}$. Then, they use this information to obtain an upper bound on the phase-error rate e_{ph} of the sifted key.
4. **Data post-processing:** Alice sends Bob syndrome information about her sifted key through an authenticated classical channel for him to correct his own sifted key. After, Alice and Bob perform error verification by computing a hash of their corrected keys using a random two-universal hash function and then check whether they are identical. If so, Alice and Bob perform privacy amplification by employing a random two-universal hash function to extract a secure key pair from the corrected keys. Otherwise, they abort the protocol.

2. Security analysis

To apply our security analysis, we need to select some qubit states $\{|\phi_{0Z}\rangle_{B_u}, |\phi_{1Z}\rangle_{B_u}, |\phi_{0X}\rangle_{B_u}\}$ that are close to the actual states $\{|\psi_{0Z}\rangle_{B_u}, |\psi_{1Z}\rangle_{B_u}, |\psi_{0X}\rangle_{B_u}\}$. As in Ref. [S34], we select the first two to be

$$\begin{aligned} |\phi_{0Z}\rangle_{B_u} &= |\sqrt{\mu}\rangle_{B_u}, \\ |\phi_{1Z}\rangle_{B_u} &= |-\sqrt{\mu}\rangle_{B_u}, \end{aligned} \quad (\text{S174})$$

and for the third, $|\phi_{0X}\rangle_{B_u}$, we pick the projection of $|\text{vac}\rangle_{B_u}$ onto the subspace spanned by $\{|\sqrt{\mu}\rangle_{B_u}, |-\sqrt{\mu}\rangle_{B_u}\}$.

Now let us define

$$|\Phi_Z\rangle_{A_u B_u} = \frac{1}{\sqrt{2}} (|0_Z\rangle_{A_u} |\phi_{0Z}\rangle_{B_u} + |1_Z\rangle_{A_u} |\phi_{1Z}\rangle_{B_u}) = \sqrt{q_{\text{vir0}}^\phi} |0_X\rangle_{A_u} |\phi_{\text{vir0}}\rangle_{B_u} + \sqrt{q_{\text{vir1}}^\phi} |1_X\rangle_{A_u} |\phi_{\text{vir1}}\rangle_{B_u}, \quad (\text{S175})$$

where

$$\begin{aligned} |\phi_{\text{vir0}}\rangle_{B_u} &= \frac{1}{2\sqrt{q_{\text{vir0}}^\phi}} (|\phi_{0Z}\rangle_{B_u} + |\phi_{1Z}\rangle_{B_u}), \\ |\phi_{\text{vir1}}\rangle_{B_u} &= \frac{1}{2\sqrt{q_{\text{vir1}}^\phi}} (|\phi_{0Z}\rangle_{B_u} - |\phi_{1Z}\rangle_{B_u}), \end{aligned} \quad (\text{S176})$$

and

$$\begin{aligned} q_{\text{vir0}}^\phi &= \frac{1 + e^{-2\mu}}{2}, \\ q_{\text{vir1}}^\phi &= \frac{1 - e^{-2\mu}}{2}. \end{aligned} \quad (\text{S177})$$

⁶ This conditional bit flip is performed in the Actual Protocol to ensure that the bit-error rate of the sifted key is kept low. However, when considering the security of the sifted key this bit flip is irrelevant, and in the security proof, we only consider whether a round has been reported as detected ($k_c \neq k_d$) or undetected ($k_c = k_d$).

It is straightforward to show that $|C_{\text{vir0}}\rangle_{B_u} = |C_{\text{even}}\rangle_{B_u}$ and $|C_{\text{vir1}}\rangle_{B_u} = |C_{\text{odd}}\rangle_{B_u}$, where $|C_{\text{even}}\rangle_{B_u}$ and $|C_{\text{odd}}\rangle_{B_u}$ are even and odd cat states, respectively, given by

$$|C_{\text{even}}\rangle_{B_u} \propto |\sqrt{\mu}\rangle_{B_u} + |-\sqrt{\mu}\rangle_{B_u}, \quad |C_{\text{odd}}\rangle_{B_u} \propto |\sqrt{\mu}\rangle_{B_u} - |-\sqrt{\mu}\rangle_{B_u}. \quad (\text{S178})$$

Since $\{|\phi_{0Z}\rangle_{B_u}, |\phi_{1Z}\rangle_{B_u}, |\phi_{0X}\rangle_{B_u}\}$ is a set of three qubit states, we can obtain unique LT expressions for them (see Section SM1D for more information), and in this case these can be calculated to be

$$\begin{aligned} |\phi_{\text{vir0}}\rangle\langle\phi_{\text{vir0}}|_{B_u} &= |\phi_{0X}\rangle\langle\phi_{0X}|_{B_u}, \\ |\phi_{\text{vir1}}\rangle\langle\phi_{\text{vir1}}|_{B_u} &= c_1 |\phi_{0Z}\rangle\langle\phi_{0Z}|_{B_u} + c_1 |\phi_{1Z}\rangle\langle\phi_{1Z}|_{B_u} - c_2 |\phi_{0X}\rangle\langle\phi_{0X}|_{B_u}, \end{aligned} \quad (\text{S179})$$

where

$$\begin{aligned} c_1 &= \frac{1 + \coth(\mu)}{2} = \frac{e^{2\mu}}{e^{2\mu} - 1} \geq 0, \\ c_2 &= \coth(\mu) = \frac{e^{2\mu} + 1}{e^{2\mu} - 1} \geq 1. \end{aligned} \quad (\text{S180})$$

Taking the tensor products of the expressions in Eq. (S179), and passing all negative terms to the left-hand side, we obtain the following MDI loss-tolerant expressions

$$\begin{aligned} |\phi_{\text{vir00}}\rangle\langle\phi_{\text{vir00}}|_{B_a B_b} &= |\phi_{0X0X}\rangle\langle\phi_{0X0X}|_{B_a B_b}, \\ |\phi_{\text{vir01}}\rangle\langle\phi_{\text{vir01}}|_{B_a B_b} + c_2 |\phi_{0X0X}\rangle\langle\phi_{0X0X}|_{B_a B_b} &= c_1 |\phi_{0X0Z}\rangle\langle\phi_{0X0Z}|_{B_a B_b} + c_1 |\phi_{0X1Z}\rangle\langle\phi_{0X1Z}|_{B_a B_b}, \\ |\phi_{\text{vir10}}\rangle\langle\phi_{\text{vir10}}|_{B_a B_b} + c_2 |\phi_{0X0X}\rangle\langle\phi_{0X0X}|_{B_a B_b} &= c_1 |\phi_{0Z0X}\rangle\langle\phi_{0Z0X}|_{B_a B_b} + c_1 |\phi_{1Z0X}\rangle\langle\phi_{1Z0X}|_{B_a B_b}, \\ |\phi_{\text{vir11}}\rangle\langle\phi_{\text{vir11}}|_{B_a B_b} + c_1 c_2 |\phi_{0Z0X}\rangle\langle\phi_{0Z0X}|_{B_a B_b} + c_1 c_2 |\phi_{1Z0X}\rangle\langle\phi_{1Z0X}|_{B_a B_b} &+ c_1 c_2 |\phi_{0X0Z}\rangle\langle\phi_{0X0Z}|_{B_a B_b} + c_1 c_2 |\phi_{0X1Z}\rangle\langle\phi_{0X1Z}|_{B_a B_b} \\ + c_1 c_2 |\phi_{0X1Z}\rangle\langle\phi_{0X1Z}|_{B_a B_b} &= c_1^2 |\phi_{0Z0Z}\rangle\langle\phi_{0Z0Z}|_{B_a B_b} + c_1^2 |\phi_{0Z1Z}\rangle\langle\phi_{0Z1Z}|_{B_a B_b} + c_1^2 |\phi_{1Z0Z}\rangle\langle\phi_{1Z0Z}|_{B_a B_b} \\ + c_1^2 |\phi_{1Z1Z}\rangle\langle\phi_{1Z1Z}|_{B_a B_b} + c_2^2 |\phi_{0X0X}\rangle\langle\phi_{0X0X}|_{B_a B_b}. \end{aligned} \quad (\text{S181})$$

Then, we construct some states $|\Phi_{\text{Tar}\alpha\beta}\rangle_{AB}$ and $|\Phi_{\text{Ref}\alpha\beta}\rangle_{AB}$, with $B := B_a B_b$, by taking purifications of the left- and right-hand sides of Eq. (S181). We choose purifications such that $|\Phi_{\text{Tar}\alpha\beta}\rangle_{AB} = |\Phi_{\text{Ref}\alpha\beta}\rangle_{AB}$, which exist due to the equalities in Eq. (S181), and can be shown to be

$$\begin{aligned} |\Phi_{\text{Tar00}}\rangle_{AB} &= |0\rangle_A |\phi_{\text{vir00}}\rangle_{B_a B_b}, \\ |\Phi_{\text{Ref00}}\rangle_{AB} &= |0\rangle_A |\phi_{0X0X}\rangle_{B_a B_b}, \\ |\Phi_{\text{Tar01}}\rangle_{AB} &\propto |0\rangle_A |\phi_{\text{vir01}}\rangle_{B_a B_b} + \sqrt{c_2} |1\rangle_A |\phi_{0X0X}\rangle_{B_a B_b}, \\ |\Phi_{\text{Ref01}}\rangle_{AB} &\propto \sqrt{c_1} |0'\rangle_A |\phi_{0X0Z}\rangle_{B_a B_b} + \sqrt{c_1} |1'\rangle_A |\phi_{0X1Z}\rangle_{B_a B_b}, \\ |\Phi_{\text{Tar10}}\rangle_{AB} &\propto |0\rangle_A |\phi_{\text{vir10}}\rangle_{B_a B_b} + \sqrt{c_2} |1\rangle_A |\phi_{0X0X}\rangle_{B_a B_b}, \\ |\Phi_{\text{Ref10}}\rangle_{AB} &\propto \sqrt{c_1} |0'\rangle_A |\phi_{0Z0X}\rangle_{B_a B_b} + \sqrt{c_1} |1'\rangle_A |\phi_{1Z0X}\rangle_{B_a B_b}, \\ |\Phi_{\text{Tar11}}\rangle_{AB} &\propto |0\rangle_A |\phi_{\text{vir11}}\rangle_{B_a B_b} + \sqrt{c_1 c_2} |1\rangle_A |\phi_{0Z0X}\rangle_{B_a B_b} + \sqrt{c_1 c_2} |2\rangle_A |\phi_{1Z0X}\rangle_{B_a B_b} + \sqrt{c_1 c_2} |3\rangle_A |\phi_{0X0Z}\rangle_{B_a B_b} \\ + \sqrt{c_1 c_2} |4\rangle_A |\phi_{0X1Z}\rangle_{B_a B_b}, \\ |\Phi_{\text{Ref11}}\rangle_{AB} &\propto c_1 |0''\rangle_A |\phi_{0Z0Z}\rangle_{B_a B_b} + c_1 |1''\rangle_A |\phi_{0Z1Z}\rangle_{B_a B_b} + c_1 |2''\rangle_A |\phi_{1Z0Z}\rangle_{B_a B_b} + c_1 |3''\rangle_A |\phi_{1Z1Z}\rangle_{B_a B_b} \\ + c_2 |4''\rangle_A |\phi_{0X0X}\rangle_{B_a B_b}, \end{aligned} \quad (\text{S182})$$

where

$$\begin{aligned} |0'\rangle_A &= \frac{1}{\sqrt{2}}(|0\rangle_A + |1\rangle_A), \\ |1'\rangle_A &= \frac{1}{\sqrt{2}}(-|0\rangle_A + |1\rangle_A), \end{aligned} \quad (\text{S183})$$

and

$$\begin{aligned}
|0''\rangle_A &= \frac{1}{2} |0\rangle_A + \frac{1}{2\sqrt{2}} |1\rangle_A - \frac{1}{2\sqrt{2}} |2\rangle_A + \frac{1}{\sqrt{2}} |3\rangle_A, \\
|1''\rangle_A &= -\frac{1}{2} |0\rangle_A + \frac{1}{2\sqrt{2}} |1\rangle_A - \frac{1}{2\sqrt{2}} |2\rangle_A + \frac{1}{\sqrt{2}} |4\rangle_A, \\
|2''\rangle_A &= -\frac{1}{2} |0\rangle_A - \frac{1}{2\sqrt{2}} |1\rangle_A + \frac{1}{2\sqrt{2}} |2\rangle_A + \frac{1}{\sqrt{2}} |3\rangle_A, \\
|3''\rangle_A &= \frac{1}{2} |0\rangle_A - \frac{1}{2\sqrt{2}} |1\rangle_A + \frac{1}{2\sqrt{2}} |2\rangle_A + \frac{1}{\sqrt{2}} |4\rangle_A, \\
|4''\rangle_A &= \frac{1}{\sqrt{2}} |1\rangle_A + \frac{1}{\sqrt{2}} |2\rangle_A.
\end{aligned} \tag{S184}$$

To obtain Eq. (S184), for example, we first define the following state with real coefficients

$$|m''\rangle_A = d_0^{(m)} |0\rangle_A + d_1^{(m)} |1\rangle_A + d_2^{(m)} |2\rangle_A + d_3^{(m)} |3\rangle_A + d_4^{(m)} |4\rangle_A, \tag{S185}$$

such that $(d_0^{(m)})^2 + (d_1^{(m)})^2 + (d_2^{(m)})^2 + (d_3^{(m)})^2 + (d_4^{(m)})^2 = 1$ for all $m \in \{0, 1, 2, 3, 4\}$, and substitute Eq. (S185) and the definition of $|\phi_{\text{vir11}}\rangle_{B_a B_b} := |\phi_{\text{vir1}}\rangle_{B_a} \otimes |\phi_{\text{vir1}}\rangle_{B_b}$ in Eq. (S176) into Eq. (S182). Then, we use the condition $|\Phi_{\text{Tar11}}\rangle_{AB} = |\Phi_{\text{Ref11}}\rangle_{AB}$ to construct a system of equations for the variables $\{d_0^{(m)}, d_1^{(m)}, d_2^{(m)}, d_3^{(m)}, d_4^{(m)}\}_{m=0}^4$, and solve this system.

Using Eq. (S182) as a blueprint, we define the states $|\Psi_{\text{Tar}\alpha\beta}\rangle_{AB}$ and $|\Psi_{\text{Ref}\alpha\beta}\rangle_{AB}$ as

$$\begin{aligned}
|\Psi_{\text{Tar00}}\rangle_{AB} &= \sqrt{p_{\text{vir00}|\text{TAR00}}} |0\rangle_A |\psi_{\text{vir00}}\rangle_{B_a B_b}, \\
|\Psi_{\text{Ref00}}\rangle_{AB} &= \sqrt{p_{0_X 0_X|\text{REF00}}} |0\rangle_A |\psi_{0_X 0_X}\rangle_{B_a B_b}, \\
|\Psi_{\text{Tar01}}\rangle_{AB} &= \sqrt{p_{\text{vir01}|\text{TAR01}}} |0\rangle_A |\psi_{\text{vir01}}\rangle_{B_a B_b} + \sqrt{p_{0_X 0_X|\text{TAR01}}} |1\rangle_A |\psi_{0_X 0_X}\rangle_{B_a B_b}, \\
|\Psi_{\text{Ref01}}\rangle_{AB} &= \sqrt{p_{0_X 0_Z|\text{REF01}}} |0'\rangle_A |\psi_{0_X 0_Z}\rangle_{B_a B_b} + \sqrt{p_{0_X 1_Z|\text{REF01}}} |1'\rangle_A |\psi_{0_X 1_Z}\rangle_{B_a B_b}, \\
|\Psi_{\text{Tar10}}\rangle_{AB} &= \sqrt{p_{\text{vir10}|\text{TAR10}}} |0\rangle_A |\psi_{\text{vir10}}\rangle_{B_a B_b} + \sqrt{p_{0_X 0_X|\text{TAR10}}} |1\rangle_A |\psi_{0_X 0_X}\rangle_{B_a B_b}, \\
|\Psi_{\text{Ref10}}\rangle_{AB} &= \sqrt{p_{0_Z 0_X|\text{REF10}}} |0'\rangle_A |\psi_{0_Z 0_X}\rangle_{B_a B_b} + \sqrt{p_{1_Z 0_X|\text{REF10}}} |1'\rangle_A |\psi_{1_Z 0_X}\rangle_{B_a B_b}, \\
|\Psi_{\text{Tar11}}\rangle_{AB} &= \sqrt{p_{\text{vir11}|\text{TAR11}}} |0\rangle_A |\psi_{\text{vir11}}\rangle_{B_a B_b} + \sqrt{p_{0_Z 0_X|\text{TAR11}}} |1\rangle_A |\psi_{0_Z 0_X}\rangle_{B_a B_b} + \sqrt{p_{1_Z 0_X|\text{TAR11}}} |2\rangle_A |\psi_{1_Z 0_X}\rangle_{B_a B_b} \\
&+ \sqrt{p_{0_X 0_Z|\text{TAR11}}} |3\rangle_A |\psi_{0_X 0_Z}\rangle_{B_a B_b} + \sqrt{p_{0_X 1_Z|\text{TAR11}}} |4\rangle_A |\psi_{0_X 1_Z}\rangle_{B_a B_b}, \\
|\Psi_{\text{Ref11}}\rangle_{AB} &= \sqrt{p_{0_Z 0_Z|\text{REF11}}} |0''\rangle_A |\psi_{0_Z 0_Z}\rangle_{B_a B_b} + \sqrt{p_{0_Z 1_Z|\text{REF11}}} |1''\rangle_A |\psi_{0_Z 1_Z}\rangle_{B_a B_b} + \sqrt{p_{1_Z 0_Z|\text{REF11}}} |2''\rangle_A |\psi_{1_Z 0_Z}\rangle_{B_a B_b} \\
&+ \sqrt{p_{1_Z 1_Z|\text{REF11}}} |3''\rangle_A |\psi_{1_Z 1_Z}\rangle_{B_a B_b} + \sqrt{p_{0_X 0_X|\text{REF11}}} |4''\rangle_A |\psi_{0_X 0_X}\rangle_{B_a B_b},
\end{aligned} \tag{S186}$$

where

$$\begin{aligned}
p_{\text{vir}00|\text{TAR}00} &= p_{0_X 0_X|\text{REF}00} = 1, \\
p_{\text{vir}01|\text{TAR}01} &= \frac{q_{\text{vir}01}^\psi}{q_{\text{vir}01}^\psi + c_2 q_{\text{vir}01}^\phi}, \\
p_{0_X 0_X|\text{TAR}01} &= \frac{c_2 q_{\text{vir}01}^\phi}{q_{\text{vir}01}^\psi + c_2 q_{\text{vir}01}^\phi}, \\
p_{0_X 0_Z|\text{REF}01} &= p_{0_X 1_Z|\text{REF}01} = p_{0_Z 0_X|\text{REF}10} = p_{1_Z 0_X|\text{REF}10} = \frac{c_1}{2c_1} = \frac{1}{2}, \\
p_{\text{vir}10|\text{TAR}10} &= \frac{q_{\text{vir}10}^\psi}{q_{\text{vir}10}^\psi + c_2 q_{\text{vir}10}^\phi}, \\
p_{0_X 0_X|\text{TAR}10} &= \frac{c_2 q_{\text{vir}10}^\phi}{q_{\text{vir}10}^\psi + c_2 q_{\text{vir}10}^\phi}, \\
p_{\text{vir}11|\text{TAR}11} &= \frac{q_{\text{vir}11}^\psi}{q_{\text{vir}11}^\psi + 4c_1 c_2 q_{\text{vir}11}^\phi}, \\
p_{0_Z 0_X|\text{TAR}11} &= p_{1_Z 0_X|\text{TAR}11} = p_{0_X 0_Z|\text{TAR}11} = p_{0_X 1_Z|\text{TAR}11} = \frac{c_1 c_2 q_{\text{vir}11}^\phi}{q_{\text{vir}11}^\psi + 4c_1 c_2 q_{\text{vir}11}^\phi}, \\
p_{0_Z 0_Z|\text{REF}11} &= p_{1_Z 0_Z|\text{REF}11} = p_{0_Z 1_Z|\text{REF}11} = p_{1_Z 1_Z|\text{REF}11} = \frac{c_1^2}{4c_1^2 + c_2^2}, \\
p_{0_X 0_X|\text{REF}11} &= \frac{c_2^2}{4c_1^2 + c_2^2}.
\end{aligned} \tag{S187}$$

Then, we define $|\Psi_{\text{Tar}}\rangle_{DAB}$ and $|\Psi_{\text{Ref}}\rangle_{DAB}$, with $D := D_a D_b$, as

$$|\Psi_{\text{Tar}}\rangle_{DAB} = \sum_{\alpha, \beta} \sqrt{p_{\text{TAR}\alpha\beta|\text{TAR}}} |\alpha\beta\rangle_{D_a D_b} |\Psi_{\text{Tar}\alpha\beta}\rangle_{AB}, \tag{S188}$$

$$|\Psi_{\text{Ref}}\rangle_{DAB} = \sum_{\alpha, \beta} \sqrt{p_{\text{REF}\alpha\beta|\text{REF}}} |\alpha\beta\rangle_{D_a D_b} |\Psi_{\text{Ref}\alpha\beta}\rangle_{AB}, \tag{S189}$$

where

$$\begin{aligned}
p_{\text{TAR}00|\text{TAR}} &= \frac{q_{\text{vir}00}^\psi}{C}, \\
p_{\text{REF}00|\text{REF}} &= \frac{q_{\text{vir}00}^\phi}{C}, \\
p_{\text{TAR}01|\text{TAR}} &= \frac{q_{\text{vir}01}^\psi + c_2 q_{\text{vir}01}^\phi}{C}, \\
p_{\text{REF}01|\text{REF}} &= \frac{2c_1 q_{\text{vir}01}^\phi}{C}, \\
p_{\text{TAR}10|\text{TAR}} &= \frac{q_{\text{vir}10}^\psi + c_2 q_{\text{vir}10}^\phi}{C}, \\
p_{\text{REF}10|\text{REF}} &= \frac{2c_1 q_{\text{vir}10}^\phi}{C}, \\
p_{\text{TAR}11|\text{TAR}} &= \frac{q_{\text{vir}11}^\psi + 4c_1 c_2 q_{\text{vir}11}^\phi}{C}, \\
p_{\text{REF}11|\text{REF}} &= \frac{(4c_1^2 + c_2^2) q_{\text{vir}11}^\phi}{C},
\end{aligned} \tag{S190}$$

with

$$C = q_{\text{vir}00}^\phi + 2c_1 q_{\text{vir}01}^\phi + 2c_1 q_{\text{vir}10}^\phi + (4c_1^2 + c_2^2) q_{\text{vir}11}^\phi. \tag{S191}$$

Now, applying Bayes' Theorem (see Eq. (S137)), and using $p_{\text{TAR}} = \sum_{\alpha, \beta} p_{\text{TAR}\alpha\beta}$, $p_{\text{REF}} = \sum_{\alpha, \beta} p_{\text{REF}\alpha\beta}$, $p_{\text{TAR}} = p_{\text{REF}}$, $p_{\text{TAR}\alpha\beta} = p_{\text{TAR}} p_{\text{TAR}\alpha\beta|\text{TAR}}$, and $p_{\text{REF}\alpha\beta} = p_{\text{REF}} p_{\text{REF}\alpha\beta|\text{REF}}$ (see Eqs. (S139) and (S140)), we obtain the fictitious tag assignment probabilities

$$\begin{aligned}
p_{\text{TAR}|\text{vir}} &:= p_{\text{TAR}00|\text{vir}00} = p_{\text{TAR}01|\text{vir}01} = p_{\text{TAR}10|\text{vir}10} = p_{\text{TAR}11|\text{vir}11} = \frac{p_{\text{TAR}}}{p_Z^2 p_{\text{key}|Z} C}, \\
p_{\text{REF}00|0_X 0_X} &= \frac{p_{\text{TAR}} q_{\text{vir}00}^\phi}{p_X^2 C}, \\
p_{\text{TAR}01|0_X 0_X} &= p_{\text{TAR}10|0_X 0_X} = \frac{p_{\text{TAR}} c_2 q_{\text{vir}01}^\phi}{p_X^2 C}, \\
p_{\text{REF}01|0_X 0_Z} &= p_{\text{REF}01|0_X 1_Z} = p_{\text{REF}10|0_Z 0_X} = p_{\text{REF}10|1_Z 0_X} = \frac{2p_{\text{TAR}} c_1 q_{\text{vir}01}^\phi}{p_X p_Z C}, \\
p_{\text{TAR}11|0_Z 0_X} &= p_{\text{TAR}11|1_Z 0_X} = p_{\text{TAR}11|0_X 0_Z} = p_{\text{TAR}11|0_X 1_Z} = \frac{2p_{\text{TAR}} c_1 c_2 q_{\text{vir}11}^\phi}{p_X p_Z C}, \\
p_{\text{REF}11|0_Z 0_Z} &= p_{\text{REF}11|1_Z 0_Z} = p_{\text{REF}11|0_Z 1_Z} = p_{\text{REF}11|1_Z 1_Z} = \frac{4p_{\text{TAR}} c_1^2 q_{\text{vir}11}^\phi}{p_Z^2 p_{\text{test}|Z} C}, \\
p_{\text{REF}11|0_X 0_X} &= \frac{p_{\text{TAR}} c_2^2 q_{\text{vir}11}^\phi}{p_X^2 C},
\end{aligned} \tag{S192}$$

where (see Eq. (S142))

$$p_{\text{TAR}} = C \min \left\{ p_Z^2 p_{\text{key}|Z}, \frac{p_Z p_X}{2(c_1 c_2 q_{\text{vir}11}^\phi + c_1 q_{\text{vir}01}^\phi)}, \frac{p_Z^2 p_{\text{test}|Z}}{4c_1^2 q_{\text{vir}11}^\phi}, \frac{p_X^2}{q_{\text{vir}00}^\phi + 2c_2 q_{\text{vir}01}^\phi + c_2^2 q_{\text{vir}11}^\phi} \right\}, \tag{S193}$$

with $p_X := 1 - p_Z$ and $p_{\text{test}|Z} := 1 - p_{\text{key}|Z}$.

After making all these definitions, one can directly use the analysis in Section SM2 to obtain our bound on N_{ph} . In this scenario, Eq. (S144) becomes

$$\begin{aligned}
N_{Z_C=0}^{\text{err}} &= N_{\text{ph}, \text{TAR}, Z_C} + N_{0_Z 0_X, \text{TAR}11, Z_C}^{\text{det}} + N_{1_Z 0_X, \text{TAR}11, Z_C}^{\text{det}} + N_{0_X 0_Z, \text{TAR}11, Z_C}^{\text{det}} + N_{0_X 1_Z, \text{TAR}11, Z_C}^{\text{det}}, \\
N_{Z_C=1}^{\text{err}} &= N_{0_X 0_X, \text{REF}00, Z_C}^{\text{det}} + N_{0_Z 0_Z, \text{REF}11, Z_C}^{\text{det}} + N_{0_Z 1_Z, \text{REF}11, Z_C}^{\text{det}} + N_{1_Z 0_Z, \text{REF}11, Z_C}^{\text{det}} + N_{1_Z 1_Z, \text{REF}11, Z_C}^{\text{det}} + N_{0_X 0_X, \text{REF}11, Z_C}^{\text{det}}, \\
N_{Z_C=0}^{\text{det}} &= N_{\text{key}, \text{TAR}, Z_C}^{\text{det}} + N_{0_Z 0_X, \text{TAR}11, Z_C}^{\text{det}} + N_{1_Z 0_X, \text{TAR}11, Z_C}^{\text{det}} + N_{0_X 0_Z, \text{TAR}11, Z_C}^{\text{det}} + N_{0_X 1_Z, \text{TAR}11, Z_C}^{\text{det}} \\
&\quad + N_{0_X 0_X, \text{TAR}01, Z_C}^{\text{det}} + N_{0_X 0_X, \text{TAR}10, Z_C}^{\text{det}}, \\
N_{Z_C=1}^{\text{det}} &= N_{0_X 0_X, \text{REF}00, Z_C}^{\text{det}} + N_{0_Z 0_Z, \text{REF}11, Z_C}^{\text{det}} + N_{0_Z 1_Z, \text{REF}11, Z_C}^{\text{det}} + N_{1_Z 0_Z, \text{REF}11, Z_C}^{\text{det}} + N_{1_Z 1_Z, \text{REF}11, Z_C}^{\text{det}} \\
&\quad + N_{0_X 0_X, \text{REF}11, Z_C}^{\text{det}} + N_{0_X 0_Z, \text{REF}01, Z_C}^{\text{det}} + N_{0_X 1_Z, \text{REF}01, Z_C}^{\text{det}} + N_{0_Z 0_X, \text{REF}10, Z_C}^{\text{det}} + N_{1_Z 0_X, \text{REF}10, Z_C}^{\text{det}},
\end{aligned} \tag{S194}$$

and Eq. (S145) becomes

$$\begin{aligned}
N_{Z_C=0}^{\text{err}} &\simeq p_{Z_C} \left(p_{\text{TAR}|\text{vir}} N_{\text{ph}} + p_{\text{TAR11}|0_Z0_X} N_{0_Z0_X}^{\text{det}} + p_{\text{TAR11}|1_Z0_X} N_{1_Z0_X}^{\text{det}} + p_{\text{TAR11}|0_X0_Z} N_{0_X0_Z}^{\text{det}} + p_{\text{TAR11}|0_X1_Z} N_{0_X1_Z}^{\text{det}} \right), \\
N_{Z_C=1}^{\text{err}} &\simeq p_{Z_C} \left(p_{\text{REF00}|0_X0_X} N_{0_X0_X}^{\text{det}} + p_{\text{REF11}|0_Z0_Z} N_{0_Z0_Z}^{\text{det}} + p_{\text{REF11}|0_Z1_Z} N_{0_Z1_Z}^{\text{det}} + p_{\text{REF11}|1_Z0_Z} N_{1_Z0_Z}^{\text{det}} \right. \\
&\quad \left. + p_{\text{REF11}|1_Z1_Z} N_{1_Z1_Z}^{\text{det}} + p_{\text{REF11}|0_X0_X} N_{0_X0_X}^{\text{det}} \right), \\
N_{Z_C=0}^{\text{det}} &\simeq p_{Z_C} \left(p_{\text{TAR}|\text{vir}} N_{\text{key}}^{\text{det}} + p_{\text{TAR11}|0_Z0_X} N_{0_Z0_X}^{\text{det}} + p_{\text{TAR11}|1_Z0_X} N_{1_Z0_X}^{\text{det}} + p_{\text{TAR11}|0_X0_Z} N_{0_X0_Z}^{\text{det}} + p_{\text{TAR11}|0_X1_Z} N_{0_X1_Z}^{\text{det}} \right. \\
&\quad \left. + p_{\text{TAR01}|0_X0_X} N_{0_X0_X}^{\text{det}} + p_{\text{TAR10}|0_X0_X} N_{0_X0_X}^{\text{det}} \right), \\
N_{Z_C=1}^{\text{det}} &\simeq p_{Z_C} \left(p_{\text{REF00}|0_X0_X} N_{0_X0_X}^{\text{det}} + p_{\text{REF11}|0_Z0_Z} N_{0_Z0_Z}^{\text{det}} + p_{\text{REF11}|0_Z1_Z} N_{0_Z1_Z}^{\text{det}} + p_{\text{REF11}|1_Z0_Z} N_{1_Z0_Z}^{\text{det}} + p_{\text{REF11}|1_Z1_Z} N_{1_Z1_Z}^{\text{det}} \right. \\
&\quad \left. + p_{\text{REF11}|0_X0_X} N_{0_X0_X}^{\text{det}} + p_{\text{REF01}|0_X0_Z} N_{0_X0_Z}^{\text{det}} + p_{\text{REF01}|0_X1_Z} N_{0_X1_Z}^{\text{det}} + p_{\text{REF10}|0_Z0_X} N_{0_Z0_X}^{\text{det}} + p_{\text{REF10}|1_Z0_X} N_{1_Z0_X}^{\text{det}} \right), \tag{S195}
\end{aligned}$$

where $p_{t|ij}$ and $p_{\text{TAR}|\text{vir}}$ are given by Eq. (S192). After substituting these expressions in the coin protocol inequality (Eq. (S43)) and isolating N_{ph} , we obtain the desired bound. Note that, to evaluate this bound, one needs an upper bound on the coin imbalance parameter $\Delta := 1 - \text{Re} \langle \Psi_{\text{Tar}} | \Psi_{\text{Ref}} \rangle_{DAB}$. Using Eqs. (S188), (S189) and related definitions, we can derive the inner product $\langle \Psi_{\text{Tar}} | \Psi_{\text{Ref}} \rangle_{DAB}$ to be

$$\begin{aligned}
\langle \Psi_{\text{Tar}} | \Psi_{\text{Ref}} \rangle_{DAB} &= \frac{q_{\text{vir}0}^\phi}{4C} \left[\langle \psi_{0_X0_X} | \psi_{0_Z0_Z} \rangle_{B_aB_b} + \langle \psi_{0_X0_X} | \psi_{0_Z1_Z} \rangle_{B_aB_b} + \langle \psi_{0_X0_X} | \psi_{1_Z0_Z} \rangle_{B_aB_b} + \langle \psi_{0_X0_X} | \psi_{1_Z1_Z} \rangle_{B_aB_b} \right] \\
&\quad + \frac{\sqrt{2c_1 q_{\text{vir}01}^\phi}}{2C} \left[\frac{1}{4} \left(\langle \psi_{0_X0_Z} | \psi_{0_Z0_Z} \rangle_{B_aB_b} - \langle \psi_{0_X0_Z} | \psi_{0_Z1_Z} \rangle_{B_aB_b} + \langle \psi_{0_X0_Z} | \psi_{1_Z0_Z} \rangle_{B_aB_b} - \langle \psi_{0_X0_Z} | \psi_{1_Z1_Z} \rangle_{B_aB_b} \right. \right. \\
&\quad - \langle \psi_{0_X1_Z} | \psi_{0_Z0_Z} \rangle_{B_aB_b} + \langle \psi_{0_X1_Z} | \psi_{0_Z1_Z} \rangle_{B_aB_b} - \langle \psi_{0_X1_Z} | \psi_{1_Z0_Z} \rangle_{B_aB_b} + \langle \psi_{0_X1_Z} | \psi_{1_Z1_Z} \rangle_{B_aB_b} + \langle \psi_{0_Z0_X} | \psi_{0_Z0_Z} \rangle_{B_aB_b} \\
&\quad + \langle \psi_{0_Z0_X} | \psi_{0_Z1_Z} \rangle_{B_aB_b} - \langle \psi_{0_Z0_X} | \psi_{1_Z0_Z} \rangle_{B_aB_b} - \langle \psi_{0_Z0_X} | \psi_{1_Z1_Z} \rangle_{B_aB_b} - \langle \psi_{1_Z0_X} | \psi_{0_Z0_Z} \rangle_{B_aB_b} - \langle \psi_{1_Z0_X} | \psi_{0_Z1_Z} \rangle_{B_aB_b} \\
&\quad \left. \left. + \langle \psi_{1_Z0_X} | \psi_{1_Z0_Z} \rangle_{B_aB_b} + \langle \psi_{1_Z0_X} | \psi_{1_Z1_Z} \rangle_{B_aB_b} \right) + \sqrt{c_2 q_{\text{vir}01}^\phi} \left(\langle \psi_{0_X0_Z} | \psi_{0_X0_X} \rangle_{B_aB_b} + \langle \psi_{0_X1_Z} | \psi_{0_X0_X} \rangle_{B_aB_b} \right. \right. \\
&\quad \left. \left. + \langle \psi_{0_Z0_X} | \psi_{0_X0_X} \rangle_{B_aB_b} + \langle \psi_{1_Z0_X} | \psi_{0_X0_X} \rangle_{B_aB_b} \right) \right] + \frac{c_1 q_{\text{vir}11}^\phi}{4C} \left(2 - \langle \psi_{0_Z0_Z} | \psi_{0_Z1_Z} \rangle_{B_aB_b} - \langle \psi_{0_Z0_Z} | \psi_{1_Z0_Z} \rangle_{B_aB_b} \right. \\
&\quad + \langle \psi_{0_Z0_Z} | \psi_{1_Z1_Z} \rangle_{B_aB_b} + \langle \psi_{0_Z1_Z} | \psi_{1_Z0_Z} \rangle_{B_aB_b} - \langle \psi_{0_Z1_Z} | \psi_{1_Z1_Z} \rangle_{B_aB_b} - \langle \psi_{1_Z0_Z} | \psi_{1_Z1_Z} \rangle_{B_aB_b} \left. \right) + \frac{q_{\text{vir}11}^\phi \sqrt{c_1 c_2}}{2\sqrt{2}C} \\
&\quad \times \left[c_1 \left(\langle \psi_{0_Z0_Z} | \psi_{0_Z0_X} \rangle_{B_aB_b} - \langle \psi_{0_Z0_Z} | \psi_{1_Z0_X} \rangle_{B_aB_b} + 2 \langle \psi_{0_Z0_Z} | \psi_{0_X0_Z} \rangle_{B_aB_b} + \langle \psi_{0_Z1_Z} | \psi_{0_Z0_X} \rangle_{B_aB_b} - \langle \psi_{0_Z1_Z} | \psi_{1_Z0_X} \rangle_{B_aB_b} \right. \right. \\
&\quad + 2 \langle \psi_{0_Z1_Z} | \psi_{0_X1_Z} \rangle_{B_aB_b} - \langle \psi_{1_Z0_Z} | \psi_{0_Z0_X} \rangle_{B_aB_b} + \langle \psi_{1_Z0_Z} | \psi_{1_Z0_X} \rangle_{B_aB_b} + 2 \langle \psi_{1_Z0_Z} | \psi_{0_X0_Z} \rangle_{B_aB_b} - \langle \psi_{1_Z1_Z} | \psi_{0_Z0_X} \rangle_{B_aB_b} \\
&\quad \left. \left. + \langle \psi_{1_Z1_Z} | \psi_{1_Z0_X} \rangle_{B_aB_b} + 2 \langle \psi_{1_Z1_Z} | \psi_{0_X1_Z} \rangle_{B_aB_b} \right) + 2c_2 \left(\langle \psi_{0_X0_X} | \psi_{0_Z0_X} \rangle_{B_aB_b} + \langle \psi_{0_X0_X} | \psi_{1_Z0_X} \rangle_{B_aB_b} \right) \right]. \tag{S196}
\end{aligned}$$

Using this expression and the assumption on the emitted states in Eq. (S173), one can obtain an upper bound on Δ by solving an SDP; see Section SE2 B for the full construction of this SDP.

In Fig. S7, we evaluate the asymptotic secret-key rate obtainable using our analysis. For the simulations, we use the channel model in Section SE3 B, set $p_Z = p_{\text{key}|Z} = p_{Z_C} = 0.9$ and consider the following experimental parameters: error correction inefficiency $f = 1.16$ and dark count probability $p_d = 10^{-8}$ [S29, S30]. For comparison, we also plot the secret-key rate obtainable using the previous analysis [S34]. Remarkably, despite considering a more general class of attacks, our proof can actually obtain considerably higher key rates than that of [S34], even in terms of secret bits per pulse. We note that, in practice, to apply the proof in [S34] rigorously, one would need to run the protocol at a low repetition rate to ensure sequentiality (see Section SM5), and therefore the performance advantage offered by our security proof would be even more pronounced if plotted in terms of bits per second⁷.

⁷ As discussed at the end of Section SM5, ensuring sequentiality for MDI protocols is not as straightforward as for P&M protocols. For this reason, we do not include a comparison in terms of secret-key bits per second for this protocol.

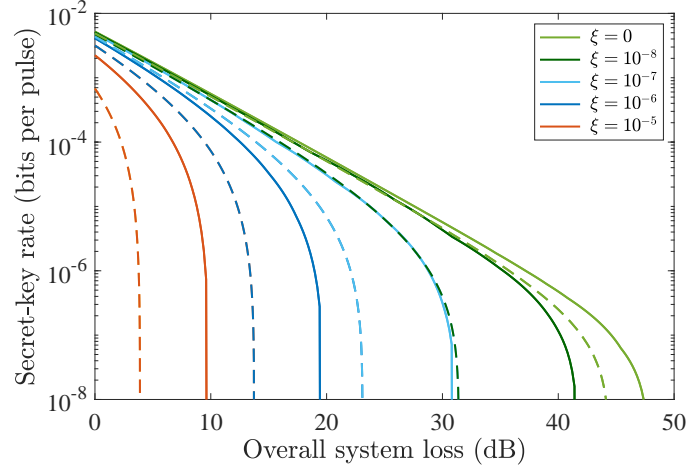


Figure S7. Asymptotic secret-key rate (in bits per pulse) for the coherent-light-based MDI scheme for several values of $\xi = 1 - (1 - \epsilon)^2 \approx 2\epsilon$ using our analysis (solid lines), compared with the previous analysis in [S34] (dashed lines). For each value of the system loss, we have optimized the intensity μ of the emitted coherent states. We note that the previous analysis is only valid against sequential attacks, while our analysis can protect against the most general attacks allowed by quantum mechanics.

3. Finite-key analysis

In the finite-key regime, we can simply apply the general analysis for MDI-type scenarios in Section SM2 D. Precisely, let us define

$$\begin{aligned} \overline{N}_{ij,t,Z_C}^{\det} &= p_{Z_C} p_{t|ij} N_{ij}^{\det} \pm \Delta_C^{\pm}(p_{Z_C} p_{t|ij} N_{ij}^{\det}), \\ \overline{N}_{\text{key},\text{TAR},Z_C}^{\det} &= p_{Z_C} p_{\text{TAR}|\text{vir}} N_{\text{key}}^{\det} \pm \Delta_C^{\pm}(p_{Z_C} p_{\text{TAR}|\text{vir}} N_{\text{key}}^{\det}), \\ \overline{N}_{X_C=1} &= N p_{\text{TAR}} p_{X_C} \Delta + \Delta_C^+(N p_{\text{TAR}} p_{X_C} \Delta), \end{aligned} \quad (\text{S197})$$

where $p_{Z_C} \in (0, 1)$ is a fictitious probability that affects the statistical deviation terms and should be optimized for best performance, $p_{X_C} := 1 - p_{Z_C}$, $i, j \in \{0_Z, 1_Z, 0_X\}$, $t \in \{\text{TAR00}, \text{TAR01}, \text{TAR10}, \text{TAR11}, \text{REF00}, \text{REF01}, \text{REF10}, \text{REF11}\}$, $p_{t|ij}$ and $p_{\text{TAR}|\text{vir}}$ are given by Eq. (S192); p_{TAR} is given by Eq. (S193); $\Delta_C^-(x) = \sqrt{2x \ln(1/\epsilon_C)}$ and $\Delta_C^+(x) = \sqrt{3x \ln(1/\epsilon_C)}$ (see Eq. (S104)); N_{ij}^{\det} is the observed number of detected events in which Alice emitted $|\psi_i\rangle_{B_a}$, Bob emitted $|\psi_j\rangle_{B_b}$, Charlie announced a detection, and the round was assigned to ‘‘test’’; N_{key}^{\det} is the size of the sifted key, i.e., the number of rounds in which $i, j \in \{0_Z, 1_Z\}$, Charlie announced a detection and the round was assigned to ‘‘key’’; and Δ is the coin imbalance parameter. Also, let us define

$$\begin{aligned} \overline{N}_{Z_C=1}^{\text{err}} &:= \overline{N}_{0_X 0_X, \text{REF00}, Z_C}^{\det} + \overline{N}_{0_Z 0_Z, \text{REF11}, Z_C}^{\det} + \overline{N}_{0_Z 1_Z, \text{REF11}, Z_C}^{\det} + \overline{N}_{1_Z 0_Z, \text{REF11}, Z_C}^{\det} \\ &\quad + \overline{N}_{1_Z 1_Z, \text{REF11}, Z_C}^{\det} + \overline{N}_{0_X 0_X, \text{REF11}, Z_C}^{\det}, \\ \overline{N}_{Z_C=0}^{\det} &:= \overline{N}_{\text{key}, \text{TAR}, Z_C}^{\det} + \overline{N}_{0_Z 0_Z, \text{TAR11}, Z_C}^{\det} + \overline{N}_{1_Z 0_X, \text{TAR11}, Z_C}^{\det} + \overline{N}_{0_X 0_Z, \text{TAR11}, Z_C}^{\det} + \overline{N}_{0_X 1_Z, \text{TAR11}, Z_C}^{\det} \\ &\quad + \overline{N}_{0_X 0_X, \text{TAR01}, Z_C}^{\det} + \overline{N}_{0_X 0_X, \text{TAR10}, Z_C}^{\det}, \\ \overline{N}_{Z_C=1}^{\det} &:= \overline{N}_{0_X 0_X, \text{REF00}, Z_C}^{\det} + \overline{N}_{0_Z 0_Z, \text{REF11}, Z_C}^{\det} + \overline{N}_{0_Z 1_Z, \text{REF11}, Z_C}^{\det} + \overline{N}_{1_Z 0_Z, \text{REF11}, Z_C}^{\det} + \overline{N}_{1_Z 1_Z, \text{REF11}, Z_C}^{\det} \\ &\quad + \overline{N}_{0_X 0_X, \text{REF11}, Z_C}^{\det} + \overline{N}_{0_X 0_Z, \text{REF01}, Z_C}^{\det} + \overline{N}_{0_X 1_Z, \text{REF01}, Z_C}^{\det} + \overline{N}_{0_Z 0_X, \text{REF10}, Z_C}^{\det} + \overline{N}_{1_Z 0_X, \text{REF10}, Z_C}^{\det}. \end{aligned} \quad (\text{S198})$$

Then, we have the following statistical bound on the number of phase errors

$$\begin{aligned} N_{\text{ph}} &\leq \frac{1}{p_{Z_C} p_{\text{TAR}|\text{vir}}} \left[(\overline{N}_{Z_C=0}^{\det} + \Delta_A) G_+ \left(\frac{\overline{N}_{Z_C=1}^{\text{err}} + \Delta_A}{\overline{N}_{Z_C=1}^{\det} - \Delta_A}, 1 - \frac{2p_{Z_C}(\overline{N}_{X_C=1} + \Delta_A)}{p_{X_C}(\overline{N}_{Z_C=0}^{\det} + \overline{N}_{Z_C=1}^{\det} - \Delta_A)} \right) \right. \\ &\quad \left. - \overline{N}_{0_Z 0_X, \text{TAR11}, Z_C}^{\det} - \overline{N}_{1_Z 0_X, \text{TAR11}, Z_C}^{\det} - \overline{N}_{0_X 0_Z, \text{TAR11}, Z_C}^{\det} - \overline{N}_{0_X 1_Z, \text{TAR11}, Z_C}^{\det} + \Delta_A + \Delta_H \right] =: N_{\text{ph}}^U, \end{aligned} \quad (\text{S199})$$

where $\epsilon_{\text{tot}} = 6\epsilon_A + 31\epsilon_C + \epsilon_H$, $\Delta_A := \sqrt{2N_{\text{key}}^{\text{det}} \ln(1/\epsilon_A)}$ and $\Delta_H := \sqrt{N_{\text{key}}^{\text{det}} \ln(1/\epsilon_H)/2}$ (see Section SM1 E 1 for more details), and the function $G_+(y, z)$ is defined in Eq. (S39).

In Fig. S8, we show the secret-key rate offered by our analysis in the finite-key regime. For the simulations, we have used the channel model in Section SE3 B, the same experimental parameters as in Fig. S7, and have optimized over the probabilities p_Z , $p_{\text{key}|Z}$ and p_{Z_C} , and over the intensity of the coherent pulses μ . Moreover, we have selected $\epsilon_{\text{secr}} = \epsilon_{\text{corr}} = 10^{-10}$ [S31] and for simplicity, we have set $\epsilon_C = \epsilon_H = \epsilon_A =: \hat{\epsilon}$, from which it follows that $\epsilon_{\text{tot}} = 38\hat{\epsilon}$. For simplicity, we have also assumed that $\epsilon_{\text{PA}} = \epsilon_{\text{tot}}$, and therefore $\epsilon_{\text{tot}} = \epsilon_{\text{secr}}^2/4$. To evaluate the achievable secret-key rate under different amounts of information leakage, we have considered $\epsilon \in \{10^{-6}, 10^{-8}\}$. The figures show that our security analysis achieves a reasonable finite-key scaling for practical values of N , and in fact compares favorably with that of other MDI protocols (see, e.g., [S46]).

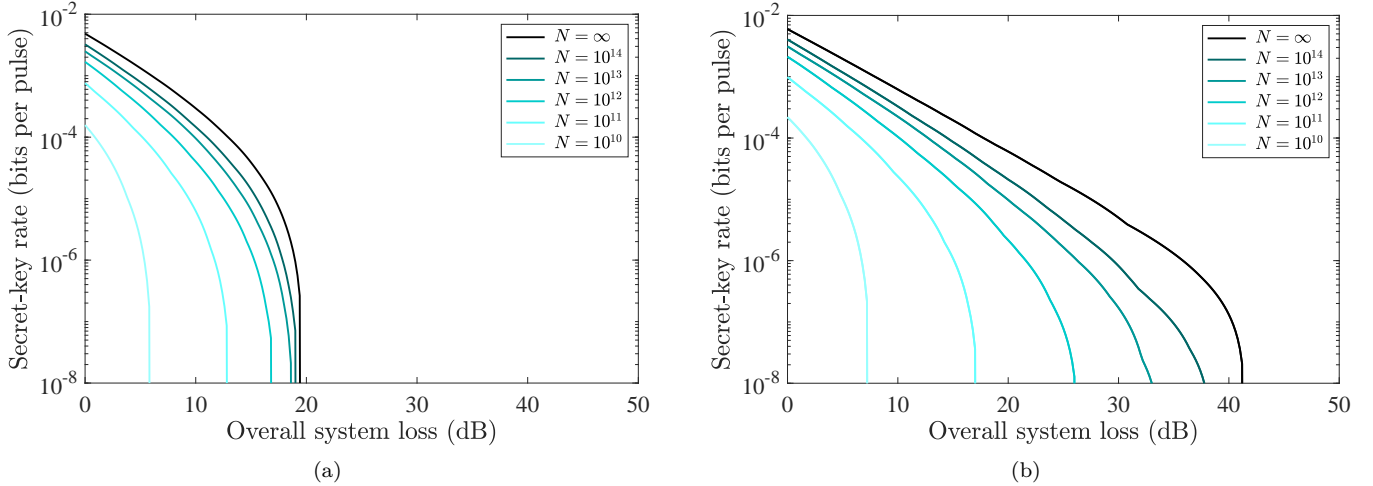


Figure S8. Finite-size secret-key rate (in bits per pulse) as a function of the overall system loss when applying our analysis to the coherent-light-based MDI scheme proposed by [S34] and using Azuma's inequality to derive the quantum coin inequality. We consider different values of the block size N and take (a) $\xi = 10^{-6}$ and (b) $\xi = 10^{-8}$.

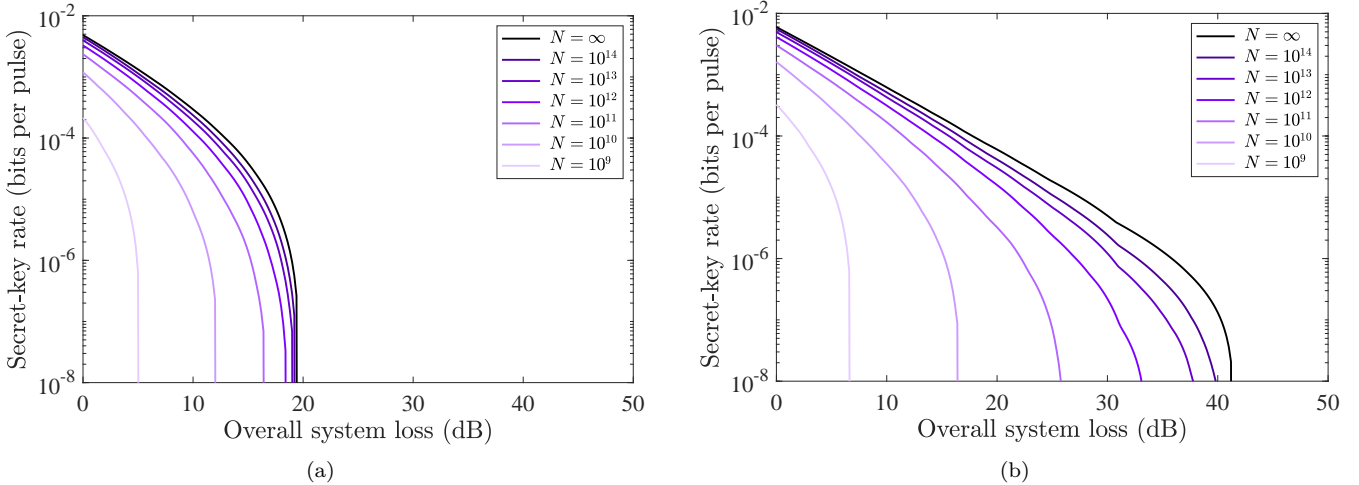


Figure S9. Finite-size secret-key rate (in bits per pulse) as a function of the overall system loss when applying our analysis to the coherent-light-based MDI scheme proposed by [S34] and using Kato's inequality to derive the quantum coin inequality. We consider different values of the block size N and take (a) $\epsilon = 10^{-6}$ and (b) $\epsilon = 10^{-8}$.

To generate the results in Fig. S8, we have used the phase-error rate bound in Eq. (S199), which was derived using Azuma's inequality. As explained in Section SM1 E, one can also substitute Azuma's inequality by Kato's inequality [S25], which requires the users to make a prediction about the experimental results that they expect to obtain after

running the protocol. If the predictions are close to the actual observed outcomes, using this inequality improves the finite-key scaling, as can be seen in Fig. S9, which assumes optimal predictions. In particular, using Kato's inequality, a positive secret-key rate could be achieved even with a block size of just 10^9 transmitted signals.

B. Decoy-state protocols

Here, we discuss how our security proof can be combined with the decoy-state method [S43–S45] and applied to the scenario in which the light source emits intensity-modulated phase-randomized (PR) WCPs. First, in Section SM4B1, we explain how the standard decoy-state analysis can be incorporated into our proof under the typical assumption that the intensity modulation and phase randomization processes are ideal. Then, in Section SM4B2, we show how our techniques could also be used to address the more realistic scenario in which these processes suffer from imperfections, including side channels.

1. Ideal PR-WCP light sources

Under the assumption of perfect intensity modulation and phase randomization, given that the intensity μ has been chosen, the state produced by a weak laser source is

$$\rho_\mu = \frac{1}{2\pi} \int_0^{2\pi} |\sqrt{\mu} e^{i\theta}\rangle \langle \sqrt{\mu} e^{i\theta}| d\theta = \sum_{n=0}^{\infty} p_{n|\mu} |n\rangle \langle n|, \quad (\text{S200})$$

where $|n\rangle$ is the n -th Fock state and $p_{n|\mu}$ follows a Poisson distribution of mean μ . The state ρ_μ produced by the laser source then goes through an imperfect modulator that encodes the bit-and-basis setting choice j into it. The action of this modulator can, without loss of generality, be represented as an isometric operator \hat{V}_j , resulting in

$$\rho_{j,\mu} = \hat{V}_j \rho_\mu \hat{V}_j^\dagger = \sum_{n=0}^{\infty} p_{n|\mu} |\psi_j^{(n)}\rangle \langle \psi_j^{(n)}|_B, \quad (\text{S201})$$

where the eigenstates of $\rho_{j,\mu}$, $|\psi_j^{(n)}\rangle_B := \hat{V}_j |n\rangle$, are independent of the intensity choice μ . In this scenario, we can apply our security proof as long as Eq. (S1) holds for the single-photon emissions, i.e., as long as

$$|\langle \phi_j^{(1)} | \psi_j^{(1)} \rangle_B|^2 \geq 1 - \epsilon, \quad (\text{S202})$$

where $\{|\phi_j^{(1)}\rangle_B\}_j$ is a set of characterized qubit states. To determine the amount of privacy amplification that needs to be applied to the sifted key pair to turn it into a secure key pair, we need to obtain the following: (1) a lower bound on the number of bits in the sifted key that originate from single-photon emissions, $N_{\text{key}}^{\text{det},(1)}$; (2) an upper bound on the number of phase errors within these bits, $N_{\text{ph}}^{(1)}$.

Let us start by discussing the second term. The set of single-photon emissions effectively constitutes a subprotocol that is indistinguishable from a scenario in which the light source is a single-photon source. Therefore, our existing analysis can be applied to obtain a bound on the number of phase errors within this subprotocol, $N_{\text{ph}}^{(1)}$, in terms of the outcomes of the test rounds within the subprotocol, $N_j^{\beta_X,(1)}$. Specifically, Eq. (S116) applies to this scenario after making the substitutions $N_{\text{ph}} \rightarrow N_{\text{ph}}^{(1)}$ and $N_j^{\beta_X} \rightarrow N_j^{\beta_X,(1)}$. The only difference with the single-photon source case is that now the quantities $N_j^{\beta_X,(1)}$ cannot be directly observed, since the users do not know the photon number of each pulse. Nevertheless, one can simply use the observed values of $N_{j,\mu}^{\beta_X}$ in combination with the standard decoy-state analysis to obtain appropriate lower or upper bounds on these quantities. Assuming first the asymptotic regime for simplicity of discussion, we have that $N_{j,\mu}^{\beta_X} \simeq N p_\mu p_j Q_{j,\mu}^{\beta_X}$ and $N_j^{\beta_X,(1)} \simeq N p_j Y_j^{\beta_X,(1)}$, and a bound on $Y_j^{\beta_X,(1)}$ can be expressed as the linear program

$$\begin{aligned} & \min / \max Y_j^{\beta_X,(1)} \\ & \text{s.t. } Q_{j,\mu}^{\beta_X} = \sum_n p_{n|\mu} Y_j^{\beta_X,(n)}, \quad \forall \mu. \end{aligned} \quad (\text{S203})$$

In an actual finite-key implementation, one needs to modify this linear program by applying concentration inequalities to take into account statistical fluctuations, as shown in [S47]. Similarly, a lower bound on $N_{\text{key}}^{\text{det},(1)}$ can also be obtained using linear programming. Analogously to Eq. (S117), the length of the secret key obtainable can then be expressed as

$$N_{\text{sec}} = N_{\text{key}}^{\text{det},(1),\text{L}} \left[1 - h\left(\frac{N_{\text{ph}}^{(1),\text{U}}}{N_{\text{key}}^{\text{det},(1),\text{L}}}\right) \right] - \lambda_{\text{EC}} - \log_2 \frac{1}{\epsilon_{\text{corr}}} - \log_2 \frac{1}{\epsilon_{\text{PA}}}, \quad (\text{S204})$$

and this key is $(\epsilon_{\text{corr}} + \epsilon_{\text{secr}})$ -secure with $\epsilon_{\text{secr}} = \sqrt{2\sqrt{\epsilon_{\text{tot}} + \epsilon_{\text{PA}}}}$, where ϵ_{tot} now refers to the sum of all concentration inequalities applied, both in our analysis and in the decoy-state analysis.

We remark that this approach is not only applicable with “ideal” PR-WCPs, but also in the presence of a common imperfection: intensity fluctuations. This occurs when the intensity of the emitted pulses does not correspond exactly to the intensity setting selected by Alice, but fluctuates from this value. Here, there are two possibilities. The first is that these fluctuations are identically distributed across rounds, and completely characterized. In this case, the approach above can actually be directly applied, since one has a full characterization of the photon number distribution of Alice’s signal conditional on her intensity symbol choice μ , i.e., $p_{n|\mu}$. The only difference is that this distribution will in general no longer be exactly Poissonian of mean μ , but it may be, e.g., a mixture of Poissonian distributions. However, this does not change anything in the analysis presented above.

The second possibility is that these fluctuations may not have an identical distribution in all rounds and/or may not be fully characterized. In this case, the photon-number distribution $p_{n|\mu}^{(k)}$ of a given round k is not fully known. Still, one should be able to obtain lower and upper bounds $p_{n|\mu}^{\text{L}}$ and $p_{n|\mu}^{\text{U}}$ on this distribution, such that it is guaranteed that $p_{n|\mu}^{(k)} \in [p_{n|\mu}^{\text{L}}, p_{n|\mu}^{\text{U}}]$. To address this latter case, one simply needs to substitute the equality constraint in Eq. (S203) by two inequality constraints, i.e.,

$$\begin{aligned} & \text{min/max } Y_j^{\beta_X,(1)} \\ \text{s.t. } & Q_{j,\mu}^{\beta_X} \geq \sum_n p_{n|\mu}^{\text{L}} Y_j^{\beta_X,(n)}, \quad \forall \mu \\ & Q_{j,\mu}^{\beta_X} \leq \sum_n p_{n|\mu}^{\text{U}} Y_j^{\beta_X,(n)}, \quad \forall \mu, \end{aligned} \quad (\text{S205})$$

and this extends naturally to the finite-key scenario as well.

2. Realistic PR-WCP light sources

In practice, both the intensity modulation and the phase randomization processes may be imperfect beyond the simple case of (uncorrelated) intensity fluctuations studied above. Previous works have looked at many of these imperfections, such as information leakage of the intensity setting [S17], intensity correlations [S48, S49], non-uniform phase randomization [S50, S51], and correlations between the phases of consecutive laser pulses [S52]. These imperfections, although distinct in nature, have a similar impact in the security of the protocol. Namely, in their presence, the eigenstates of the pulses generated by the light source are no longer perfect Fock states that are independent of the intensity setting μ , i.e., Eq. (S200) now becomes

$$\rho_\mu = \sum_n p_{n|\mu} |n_\mu\rangle\langle n_\mu|. \quad (\text{S206})$$

Due to the dependence of the eigenstates on the intensity μ , the standard decoy-state method presented in the previous Section cannot be directly applied. Still, given that the overall magnitude of the imperfections is not too large, we should have that $|n_\mu\rangle \approx |n\rangle$, and by quantifying the magnitude of the imperfections, one should be able to obtain a bound of the form

$$|\langle n|n_\mu\rangle|^2 \geq 1 - \epsilon_n. \quad (\text{S207})$$

Note that Eq. (S207) has a similar form to Eq. (S1). In what follows, we show how the ideas and formalism introduced by our security proof can also be used to prove security in this scenario.

After the pulse ρ_μ goes through the (imperfect) modulation process, it becomes

$$\rho_{j,\mu} = \hat{V}_j \rho_\mu \hat{V}_j^\dagger = \sum_n p_{n|\mu} |\psi_{j,\mu}^{(n)}\rangle\langle\psi_{j,\mu}^{(n)}|_B, \quad (\text{S208})$$

where the eigenstates of $\rho_{j,\mu}$, $|\psi_{j,\mu}^{(n)}\rangle_B \coloneqq \hat{V}_j |n_\mu\rangle$, now depend on the intensity choice μ . Still, due to Eq. (S207), we must have that

$$|\langle \psi_j^{(n)} | \psi_{j,\mu}^{(n)} \rangle_B|^2 \geq 1 - \epsilon_n, \quad (\text{S209})$$

where $|\psi_j^{(n)}\rangle_B \coloneqq \hat{V}_j |n\rangle$ is a state that does not depend on the intensity setting μ .

Let us first assume the asymptotic regime for clarity. If ϵ_n is small, the difference between the detection statistics of the states $|\psi_{j,\mu}^{(n)}\rangle_B$ and $|\psi_{j,\nu}^{(n)}\rangle_B$ for $\mu \neq \nu$ cannot be very large. In particular, similarly to our security proof, one can consider a quantum coin state of the form

$$|\Psi_{j,\mu,\nu}^{(n)}\rangle_{CB} = \frac{1}{\sqrt{2}}(|0\rangle_C |\psi_{j,\mu}^{(n)}\rangle_B + |1\rangle_C |\psi_{j,\nu}^{(n)}\rangle_B), \quad (\text{S210})$$

and then evaluate the probability to obtain the outcome $X_C = 1$ if system C is measured in the X basis to derive a bound of the form $|Y_{j,\mu}^{(n)} - Y_{j,\nu}^{(n)}| \leq \Delta_{\mu,\nu}^{(n)}$. Using this bound, we can modify the linear program in Eq. (S203) as

$$\begin{aligned} & \min / \max Y_{j,\mu_s}^{\beta_X,(1)} \\ \text{s.t. } & Q_{j,\mu}^{\beta_X} = \sum_n p_{n|\mu} Y_{j,\mu}^{\beta_X,(n)}, \quad \forall \mu \\ & |Y_{j,\mu}^{(n)} - Y_{j,\nu}^{(n)}| \leq \Delta_{\mu,\nu}^{(n)}, \quad \forall \mu, \nu. \end{aligned} \quad (\text{S211})$$

This idea can be turned into a rigorous security proof against general attacks that takes into account finite-size effects by applying the methodology introduced in our analysis. For this, one needs to define a fictitious scenario in which Alice probabilistically assigns tags to her emissions of $|\psi_{j,\mu}^{(n)}\rangle_B$ and $|\psi_{j,\nu}^{(n)}\rangle_B$, in such a way that a tagged emission can be regarded as equivalent to that originating from $|\Psi_{j,\mu,\nu}^{(n)}\rangle_{CB}$. Then, by considering that Alice sometimes measures the quantum coin system C in the X basis, and deriving a bound on the maximum number of events in which she could have obtained the outcome $X_C = 1$, one can use the quantum coin inequality to bound the maximum deviation between the number of detected events in which Alice sent $|\psi_{j,\mu}^{(n)}\rangle_B$ and $|\psi_{j,\nu}^{(n)}\rangle_B$ within the tagged rounds. Finally, one can apply concentration inequalities to derive bounds on the maximum deviation between the total number of detected events in which Alice emitted these states, $N_{j,\mu}^{(n)}$ and $N_{j,\nu}^{(n)}$, and use these bounds to construct an appropriate finite-size linear program to obtain appropriate bounds on $N_{j,\mu_s}^{\beta_X,(1)}$. After these are obtained, one simply substitutes them into Eq. (S116) to get an upper bound on $N_{\text{ph}}^{(1)}$. Using very similar ideas, one can also derive a lower bound on $N_{\text{key}}^{\text{det},(1)}$, and then simply substitute these bounds into Eq. (S204) to evaluate the length of the secret key that can be distilled. In any case, the detailed analysis for this scenario is beyond the scope of this paper.

SM5. WHY OUR SECURITY PROOF DOES NOT REQUIRE THE SEQUENTIAL ASSUMPTION

In this Section, we explain why the RT [S2] (see also [S1]) requires the QKD protocol to be run sequentially, which restricts its repetition rate, and why our analysis does not need this requirement. As discussed before, the aim of these security proofs is to estimate the phase-error rate. To do so, the RT considers an entanglement-based version of the Virtual Protocol in which Alice and Bob measure their respective systems one by one. The probability that Alice obtains $l \in \{\text{vir0}, \text{vir1}, 0_Z, 1_Z, 0_X\}$ and Bob obtains $\beta_X \in \{0_X, 1_X\}$ in the k -th round, conditioned on the outcomes \vec{v}_{k-1} of their previous $k-1$ measurements, can be expressed as

$$\Pr[v_k = (l, \beta_X) | \vec{v}_{k-1}] = p_l \text{Tr} [|\psi_l\rangle\langle\psi_l| \hat{M}_{\beta_X}^{\vec{v}_{k-1}}], \quad (\text{S212})$$

where p_l is defined in Eq. (S91) and the operators $\hat{M}_{\beta_X}^{\vec{v}_{k-1}} \geq 0$ depend on Eve's attack and on the previous measurement outcomes. Note that, for simplicity, we have implicitly assumed a three-state P&M protocol, but our discussion also applies to other P&M and MDI-type scenarios. The probability to obtain a phase error in the k -th round is then

$$\Pr[v_k = (\text{vir0}, 1_X) | \vec{v}_{k-1}] + \Pr[v_k = (\text{vir1}, 0_X) | \vec{v}_{k-1}]. \quad (\text{S213})$$

To derive a bound on this quantity, the RT employs a Cauchy-Schwarz type inequality that requires the operators $\hat{M}_{\beta_X}^{\vec{v}_{k-1}}$ to satisfy $\hat{M}_{\beta_X}^{\vec{v}_{k-1}} \leq \hat{\mathbb{I}}$, which does not necessarily hold when Eve can correlate Bob's measurement outcomes

on the rounds $\{1, \dots, k-1\}$ with Alice's setting choice on round k . For example, let us suppose that Eve simply performs a SWAP gate between the photonic systems of the first and second rounds, and that Alice obtains $l = 0_X$ and Bob obtains 0_X in the first round. Because of the SWAP gate, the fact that Bob obtained 0_X in the first round makes it more likely that Alice will obtain $l = 0_X$ in the second round, and the fact that Alice obtained $l = 0_X$ in the first round makes it almost certain that Bob will obtain 0_X in the second round. Because of this, we may have that

$$\Pr[v_2 = (0_X, 0_X) | v_1 = (0_X, 0_X)] > p_{0_X}, \quad (\text{S214})$$

or equivalently,

$$\text{Tr} [|\psi_{0_X}\rangle\langle\psi_{0_X}| \hat{M}_{0_X}^{v_1}] > 1, \quad (\text{S215})$$

implying that $\hat{M}_{0_X}^{v_1} \not\leq \hat{\mathbb{I}}$.

The condition $\hat{M}_{\beta_X}^{\vec{v}_{k-1}} \leq \hat{\mathbb{I}}$ is guaranteed to hold if Eve's attack is sequential (see Appendix D in [S20] for more details), rather than fully general, i.e., when it can be described as a sequence of N unitary operators, each acting on a single photonic system and on Eve's updated ancilla, see Fig. S10. In practice, to ensure that Eve's attack is sequential, the users need to run the protocol at a restricted repetition rate, as discussed in detail below. On the other hand, the security proof presented in this work is based on the quantum coin inequality in Eq. (S38), which does not require the sequential assumption, and thus does not impose any restriction on the repetition rate of the system. The key result used to derive this inequality is Eq. (S220), which holds even if Eve performs a fully general attack, because it merely uses the fact that the quantum coin is a qubit, i.e., a two-level system.

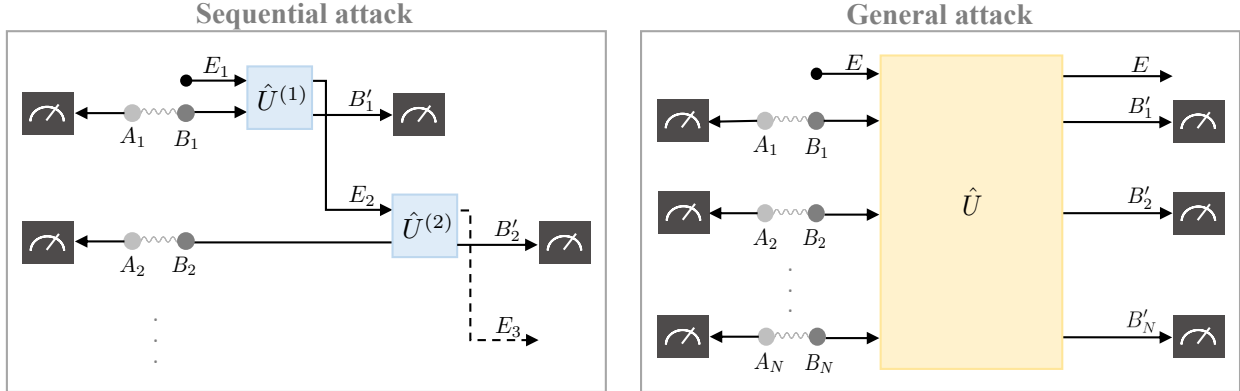


Figure S10. Diagram of the entanglement-based version of the protocol when Eve performs a sequential attack and a general attack. In the most general case, Eve can interact with all systems $B_1 \dots B_N$ at the same time. However, in the sequential case, Eve must act on system B_k before she has access to system B_{k+1} . A sequential attack can be seen as an intermediate step between a collective attack and a general attack. More precisely, a collective attack is a special case of a sequential attack in which Alice and Bob's measurement results are guaranteed to be independent and identically distributed for different rounds of the protocol.

We note that the LT analysis [S14], which considered the case in which the emitted states are qubit states (i.e., $\epsilon = 0$), does not need the sequential assumption either. In the LT analysis, we first establish a relationship among probabilities of the form of Eq. (S212) by using a relationship between the qubit states, see Eqs. (S14) and (S15). Since this relationship between the states is linear thanks to the qubit structure, the relationship among the probabilities is also linear. Noting that this linear relationship holds even if $\hat{M}_{\beta_X}^{\vec{v}_{k-1}} \not\leq \hat{\mathbb{I}}$ and also recalling that just by taking the sum over the probabilities and applying Azuma's or Kato's inequality we can obtain a bound on the number of phase errors, we conclude that the LT analysis does not require the sequential assumption.

A. Ensuring sequentiality by restricting the repetition rate

To ensure that Eve's attack is sequential, Alice and Bob need to prevent the possibility of any signalling from Alice's k -th pulse to Bob's $(k-1)$ -th measurement result. The easiest way to achieve this is for Alice to only emit the k -th pulse after Bob has performed his $(k-1)$ -th measurement [S20]. Let l_{fib} be the length of the fibre separating Alice and Bob, r be its refractive index, and c be the speed of light in a vacuum. Alice's photons travel through the fibre

at a speed of c/r , and therefore they take a time of rl_{fib}/c to reach Bob. If Alice sends her first pulse at time $t_1^A = 0$, then Bob will measure it at a time not earlier than $t_1^B = rl_{\text{fib}}/c$. Therefore, the earliest time that Alice could send the second pulse is $t_2^A = t_1^B = rl_{\text{fib}}/c$. More generally, Alice needs to separate all her pulses by at least $t_{\Delta}^A = rl_{\text{fib}}/c$, and her repetition rate should be at most

$$f_{\max} = \frac{1}{t_{\Delta}^A} = \frac{c}{rl_{\text{fib}}}. \quad (\text{S216})$$

In Fig. 2 of the Main Text, we have computed the key rate for the RT under this constraint; more specifically, we have assumed a repetition rate of $\min(f_{\max}, 2.5 \text{ GHz})$. For example, if $r = 1.5$ and $l_{\text{fib}} = 100 \text{ km}$, we have that $f_{\max} = 2 \text{ kHz}$.

A recent work [S53] has suggested that, to achieve sequentiality, it may be enough to ensure that Bob's $(k-1)$ -th measurement is outside the future light cone of Alice's k -th pulse emission. This takes into account the fact that, irrespectively of Eve's action, information about Alice's pulse cannot travel faster than c to Bob's measurement setup. Let l_{act} be the actual physical distance separating Alice and Bob, which must be such that $l_{\text{act}} \leq l_{\text{fib}}$, with equality if and only if the fibre is laid out in a straight line. Since information about Alice's pulse must take at least l_{act}/c to reach Bob, to ensure that her second pulse cannot possibly affect Bob's first measurement result, Alice needs to emit it at a time not earlier than

$$t_2^A = t_1^B - \frac{l_{\text{act}}}{c} = \frac{rl_{\text{fib}}}{c} - \frac{l_{\text{act}}}{c} = \frac{rl_{\text{fib}} - l_{\text{act}}}{c}, \quad (\text{S217})$$

and more generally, Alice needs to separate her pulses by at least $t_{\Delta}^A = t_2^A$. In other words, her repetition rate can be at most

$$f'_{\max} = \frac{1}{t_{\Delta}^A} = \frac{c}{rl_{\text{fib}} - l_{\text{act}}}. \quad (\text{S218})$$

Assuming again a standard fibre of $r = 1.5$, we have that f'_{\max} is three times larger than f_{\max} when $l_{\text{act}} = l_{\text{fib}}$, and less than that when $l_{\text{act}} < l_{\text{fib}}$. For example, assuming that $l_{\text{act}} = l_{\text{fib}} = 100 \text{ km}$, we have that $f'_{\max} = 3f_{\max} = 6 \text{ kHz}$, which is still a considerable restriction on the repetition rate. Because of this, our security proof can achieve significantly higher key rates per second than the RT even if one uses this relaxed relativistic constraint, as shown in Fig. S11.

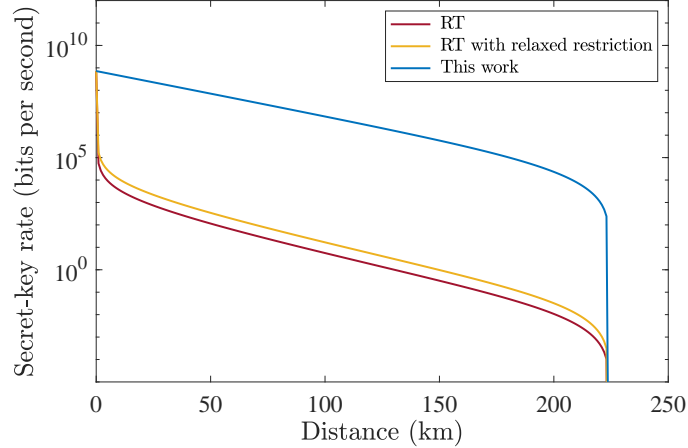


Figure S11. Secret-key rate achievable by the reference technique (RT) with the restriction that Alice emits each pulse after Bob has measured the previous pulse (red line), and with the restriction that Alice emits her pulses such that they could not have affected Bob's previous measurement result, based on relativistic arguments (yellow line); compared with that achievable by our security proof. We assume that the fibre connecting Alice and Bob is in a straight line ($l_{\text{act}} = l_{\text{fib}}$) and that its refractive index is $r = 1.5$. Moreover, for our security proof, we assume a repetition rate of 2.5 GHz, and for the RT curves, we assume repetition rates of $\min(f_{\max}, 2.5 \text{ GHz})$ and $\min(f'_{\max}, 2.5 \text{ GHz})$, respectively. Also, we consider the BB84 protocol, and the values $\delta = 0.063$ and $\epsilon = 10^{-6}$.

We note that, in the discussion above, we have assumed a P&M protocol, in which Alice and Bob can ensure that the sequential condition has been met by comparing their timestamps at the end of the protocol. In MDI-type [S7] setups, ensuring the sequential condition seems much harder because Alice and Bob cannot trust Charlie's timestamps. Therefore, they would likely have to wait until they receive Charlie's outcome announcement for the $(k-1)$ -th round before emitting their k -th pulse, which would impose even harsher restrictions on the repetition rate.

SM6. RECIPE FOR EXPERIMENTALISTS

Here, we provide a step-by-step example of the application of our security analysis to an actual finite-key QKD implementation. For this, we have chosen the coherent-light-based MDI scheme [S34] analyzed in Section SM4 A, for two main reasons: (1) its practical implementation using laser sources, and (2) the fact that for this scheme, our security proof can directly protect both Alice's and Bob's sources against any practical imperfection, including those associated to the light source itself, such as intensity fluctuations and correlations, achieving a very high level of implementation security. Still, we remark that this recipe would look fairly similar for other protocols to which our analysis is applicable, such as BB84, the three-state protocol or standard MDI-QKD.

The scheme is depicted in Fig. S6 and its protocol description is given in Section SM4 A. For each round, Alice and Bob attempt to generate a state in the set $\{|\sqrt{\mu}\rangle, |-\sqrt{\mu}\rangle, |\text{vac}\rangle\}$ and send it to an untrusted middle node Charlie, who performs an interference measurement and announces the result. We refer to the coherent states $|\pm\sqrt{\mu}\rangle$ as the Z -basis states, and these are used both for key generation and parameter estimation. The vacuum state $|\text{vac}\rangle$ is only used for parameter estimation, and we refer to it as the X -basis state. To apply our analysis, one should follow these steps:

1. Specification of Security Parameters:

- Decide the total number of emitted rounds, N .
- Specify the correctness and secrecy parameters of the final key, ϵ_{corr} and ϵ_{secr} .
- Specify the failure probabilities for the application of each concentration inequality— ϵ_C for the Chernoff bound, ϵ_H for Hoeffding's inequality, and ϵ_A for Azuma's inequality—; and the privacy amplification parameter ϵ_{PA} . These should be chosen such that $\epsilon_{\text{secr}} = \sqrt{2\sqrt{\epsilon_{\text{tot}}} + \epsilon_{\text{PA}}}$, where $\epsilon_{\text{tot}} := 6\epsilon_A + 31\epsilon_C + \epsilon_H$ is the total failure probability of the phase-error rate estimation process.
- Specify the probability that each user emits a coherent state (rather than a vacuum state), p_Z ; the probability that a detected event in which both users emitted a coherent state is used for key generation (rather than parameter estimation), $p_{\text{key}|Z}$; and a fictitious probability that does not refer to any action performed in the actual protocol (but does have an effect in the parameter estimation analysis), p_{Z_C} .

To select the parameters in the last two bullet points, one option would be simulate many runs of the protocol using different parameter combinations, and then choose the values that result in the highest secret-key rate. Another option would be to just give them some values, such as, e.g., $\epsilon_{\text{tot}} = \epsilon_{\text{PA}} = \epsilon_{\text{secr}}^2/4$, $\epsilon_A = \epsilon_C = \epsilon_H = \epsilon_{\text{tot}}/38$, and $p_Z = p_{\text{key}|Z} = p_{Z_C} = 0.7$.

2. State Characterization:

- Partially characterize Alice and Bob's sources, to ensure that the states they emit, $\{|\psi_{0Z}\rangle, |\psi_{1Z}\rangle, |\psi_{0X}\rangle\}$, are ϵ -close (in terms of fidelity) to the states $\{|\sqrt{\mu}\rangle, |-\sqrt{\mu}\rangle, |\text{vac}\rangle\}$.

3. Bound on Coin Imbalance Parameter:

- Obtain an upper bound on the coin imbalance parameter Δ using the procedure laid out in Section SE2 B.

4. Quantum Communication:

- Execute the quantum communication phase of the protocol, obtaining a sifted key pair and the value of the observables N_{ij}^{det} , $N_{\text{key}}^{\text{det}}$ and N^{det} (see protocol description in Section SM4 A).
- Substitute these values into Eqs. (S197) to (S199) to obtain an upper bound on the number of phase errors N_{ph} .

5. Error Correction and Verification:

Implement the error correction and error verification processes to ensure the ϵ_{corr} -correctness of the sifted key.

6. Privacy Amplification:

Apply privacy amplification to obtain a secure key pair of length N_{sec} , given by Eq. (S153).

After following Steps 1–6 above, the final key pair obtained is guaranteed to be $(\epsilon_{\text{corr}} + \epsilon_{\text{secr}})$ -secure.

Supplementary Equations

In the Supplementary Equations, we first prove the quantum coin inequality, which is used to derive an upper bound on the number of phase errors N_{ph} . After, in Section [SE2](#), we show how to obtain Δ in Eq. [\(S41\)](#) using numerical techniques based on SDP and then, using analytical techniques with an additional assumption. Then, in Section [SE3](#), we explain the channel model used to simulate the results for the P&M protocols and for the coherent-light-based MDI protocol considered, and list the respective equations. Finally, in Section [SE4](#), we give a high-level description of the code used to generate the figures in this work.

SE1. PROOF OF THE QUANTUM COIN INEQUALITY

A. Prepare-and-measure scenario

Here, we prove the quantum coin inequality in Eq. [\(S38\)](#). To do so, we consider that Alice and Bob run the following scenario, which is equivalent to the Coin Protocol defined in Section [SM1 B 4](#).

1. Alice prepares N copies of the state

$$|\Psi\rangle_{TCDAB} = \sqrt{p_C} |0\rangle_T |\Psi_{\text{coin}}\rangle_{CDAB} + \sqrt{1-p_C} |1\rangle_T |0\rangle_C |0\rangle_D |\rho_{\text{comp}}\rangle_{AB}, \quad (\text{S219})$$

where $|\rho_{\text{comp}}\rangle_{AB}$ is a purification of ρ_{comp} , and sends all photonic systems B through a quantum channel.

2. For each round, Bob performs the quantum nondemolition measurement $\{\hat{m}_{\text{det}}, \hat{m}_f\}$, and if he obtains a successful detection, he announces this. Let \mathcal{N}^{det} be the set of detected rounds.
3. For each round $k \in \mathcal{N}^{\text{det}}$ (i.e., each detected round), Alice measures system T in the computational basis, learning if the round is a coin round ($T = 0$) or a compensation round ($T = 1$). Also, if $T = 0$, Alice and Bob perform the POVM $\{\hat{m}_{\text{err}}, \hat{\mathbb{I}} - \hat{m}_{\text{err}}\}$, and denote by m (\bar{m}) the outcome associated to \hat{m}_{err} ($\hat{\mathbb{I}} - \hat{m}_{\text{err}}$). Then, Alice chooses Z_C (X_C) with probability p_{Z_C} (p_{X_C}) and measures the coin system C in the selected basis.
4. For each round not in \mathcal{N}^{det} , Alice measures system T in the computational basis. If $T = 0$, Alice chooses Z_C (X_C) with probability p_{Z_C} (p_{X_C}) and measures the coin system C in the selected basis.

We are interested in Alice and Bob's measurements in Step 3 above. In particular, let us consider the state of the systems corresponding to the k -th round in \mathcal{N}^{det} conditioned on Alice and Bob having obtained some overall outcome \vec{v}_{k-1} for the previous $k-1$ detected rounds, and having obtained the outcomes $T = 0$ and m for the k -th round but having not yet measured the k -th coin system C . Due to Eve's general attack and the conditioning on Alice and Bob's previous measurement results, the reduced state of the k -th system C will no longer be $\text{Tr}_{DAB}[[\Psi_{\text{coin}}\rangle\langle\Psi_{\text{coin}}|_{CDAB}]$. However, no operation has acted on this system, and its reduced state is still in the qubit space spanned by $\{|0_Z\rangle_C, |1_Z\rangle_C\}$. Because of this, and using the fact that the length of its Bloch vector cannot exceed 1, we can derive the following inequality [\[S22\]](#)

$$1 - 2P^{(k)}(X_C = 1 | X_C, T = 0, m, \vec{v}_{k-1}) \leq 2\sqrt{P^{(k)}(Z_C = 0 | Z_C, T = 0, m, \vec{v}_{k-1})P^{(k)}(Z_C = 1 | Z_C, T = 0, m, \vec{v}_{k-1})}. \quad (\text{S220})$$

Here, $P^{(k)}(Z_C = 0 | Z_C, T = 0, m, \vec{v}_{k-1})$ refers to the probability that, in the k -th round in \mathcal{N}^{det} , Alice obtains the measurement outcome $Z_C = 0$, conditional on having obtained the outcomes $T = 0$ and m , on having chosen the Z_C basis to measure the coin system for this round, and on having obtained some overall measurement result \vec{v}_{k-1} for the previous $k-1$ detected rounds. The rest of the probabilities in Eq. [\(S220\)](#) are defined analogously. Note that, when the symbols Z_C or X_C appear by themselves inside these probabilities, they refer to the selection of the Z_C or X_C basis to measure system C . However, when they appear together with an equals sign, such as $Z_C = 0$, it refers to the outcome of this measurement.

On the other hand, we have that

$$\begin{aligned}
& P^{(k)}(T = 0, m | \vec{v}_{k-1}) P^{(k)}(X_C = 1 | X_C, T = 0, m, \vec{v}_{k-1}) \\
&= P^{(k)}(T = 0, m | \vec{v}_{k-1}) \frac{P^{(k)}(X_C = 1, X_C, T = 0, m | \vec{v}_{k-1})}{P^{(k)}(X_C, T = 0, m | \vec{v}_{k-1})} \\
&= P^{(k)}(T = 0, m | \vec{v}_{k-1}) \frac{P^{(k)}(X_C = 1, X_C, T = 0, m | \vec{v}_{k-1})}{P^{(k)}(X_C | T = 0, m, \vec{v}_{k-1}) P^{(k)}(T = 0, m | \vec{v}_{k-1})} \\
&= P^{(k)}(T = 0, m | \vec{v}_{k-1}) \frac{P^{(k)}(X_C = 1, X_C, T = 0, m | \vec{v}_{k-1})}{p_{X_C} P^{(k)}(T = 0, m | \vec{v}_{k-1})} \\
&= \frac{P^{(k)}(X_C = 1, X_C, T = 0, m | \vec{v}_{k-1})}{p_{X_C}}, \tag{S221}
\end{aligned}$$

where in the third equality we have used the fact that, in a coin round (i.e., a round with an outcome $T = 0$), the probability to select the X_C basis is independent of obtaining the outcome m , and equal to p_{X_C} . In a similar way, we have that

$$\begin{aligned}
P^{(k)}(T = 0, m | \vec{v}_{k-1}) P^{(k)}(Z_C = 0 | Z_C, T = 0, m, \vec{v}_{k-1}) &= \frac{P^{(k)}(Z_C = 0, Z_C, T = 0, m | \vec{v}_{k-1})}{p_{Z_C}}, \\
P^{(k)}(T = 0, m | \vec{v}_{k-1}) P^{(k)}(Z_C = 1 | Z_C, T = 0, m, \vec{v}_{k-1}) &= \frac{P^{(k)}(Z_C = 1, Z_C, T = 0, m | \vec{v}_{k-1})}{p_{Z_C}}. \tag{S222}
\end{aligned}$$

Multiplying by $P^{(k)}(T = 0, m | \vec{v}_{k-1})$ on both sides of Eq. (S220), and using Eqs. (S221) and (S222) we obtain

$$\begin{aligned}
& P^{(k)}(T = 0, m | \vec{v}_{k-1}) - 2 \frac{P^{(k)}(X_C = 1, X_C, T = 0, m | \vec{v}_{k-1})}{p_{X_C}} \\
& \leq \frac{2}{p_{Z_C}} \sqrt{P^{(k)}(Z_C = 0, Z_C, T = 0, m | \vec{v}_{k-1}) P^{(k)}(Z_C = 1, Z_C, T = 0, m | \vec{v}_{k-1})}. \tag{S223}
\end{aligned}$$

Replacing m by \bar{m} in Eqs. (S220) to (S223), we obtain

$$\begin{aligned}
& P^{(k)}(T = 0, \bar{m} | \vec{v}_{k-1}) - 2 \frac{P^{(k)}(X_C = 1, X_C, T = 0, \bar{m} | \vec{v}_{k-1})}{p_{X_C}} \\
& \leq \frac{2}{p_{Z_C}} \sqrt{P^{(k)}(Z_C = 0, Z_C, T = 0, \bar{m} | \vec{v}_{k-1}) P^{(k)}(Z_C = 1, Z_C, T = 0, \bar{m} | \vec{v}_{k-1})} \\
& = \frac{2}{p_{Z_C}} \sqrt{P^{(k)}(Z_C = 0, Z_C, T = 0 | \vec{v}_{k-1}) - P^{(k)}(Z_C = 0, Z_C, T = 0, m | \vec{v}_{k-1})} \\
& \quad \times \sqrt{P^{(k)}(Z_C = 1, Z_C, T = 0 | \vec{v}_{k-1}) - P^{(k)}(Z_C = 1, Z_C, T = 0, m | \vec{v}_{k-1})}. \tag{S224}
\end{aligned}$$

Taking the sum of Eqs. (S223) and (S224), we obtain

$$\begin{aligned}
& P^{(k)}(T = 0 | \vec{v}_{k-1}) - 2 \frac{P^{(k)}(X_C = 1, X_C, T = 0 | \vec{v}_{k-1})}{p_{X_C}} \\
& \leq \frac{2}{p_{Z_C}} \left(\sqrt{P^{(k)}(Z_C = 0, Z_C, T = 0, m | \vec{v}_{k-1}) P^{(k)}(Z_C = 1, Z_C, T = 0, m | \vec{v}_{k-1})} \right. \\
& \quad \left. + \sqrt{P^{(k)}(Z_C = 0, Z_C, T = 0 | \vec{v}_{k-1}) - P^{(k)}(Z_C = 0, Z_C, T = 0, m | \vec{v}_{k-1})} \right. \\
& \quad \left. \times \sqrt{P^{(k)}(Z_C = 1, Z_C, T = 0 | \vec{v}_{k-1}) - P^{(k)}(Z_C = 1, Z_C, T = 0, m | \vec{v}_{k-1})} \right). \tag{S225}
\end{aligned}$$

Also, we have that,

$$P^{(k)}(T = 0 | \vec{v}_{k-1}) = \frac{P^{(k)}(T = 0 | \vec{v}_{k-1}) p_{Z_C}}{p_{Z_C}} = \frac{P^{(k)}(T = 0 | \vec{v}_{k-1}) P(Z_C | T = 0, \vec{v}_{k-1})}{p_{Z_C}} = \frac{P^{(k)}(Z_C, T = 0 | \vec{v}_{k-1})}{p_{Z_C}}. \tag{S226}$$

Substituting Eq. (S226) into Eq. (S225), taking the sum over all rounds $k \in \mathcal{N}^{\text{det}}$ on both sides of the inequality, and using the fact that \sqrt{xy} is a convex function of both x and y , we obtain

$$\begin{aligned} & \frac{\sum_k P^{(k)}(Z_C, T = 0 | \vec{v}_{k-1})}{p_{Z_C}} - 2 \frac{\sum_k P^{(k)}(X_C = 1, X_C, T = 0 | \vec{v}_{k-1})}{p_{X_C}} \\ & \leq \frac{2}{p_{Z_C}} \left(\sqrt{\sum_k P^{(k)}(Z_C = 0, Z_C, T = 0, m | \vec{v}_{k-1}) \sum_k P^{(k)}(Z_C = 1, Z_C, T = 0, m | \vec{v}_{k-1})} \right. \\ & \quad + \sqrt{\sum_k P^{(k)}(Z_C = 0, Z_C, T = 0 | \vec{v}_{k-1}) - \sum_k P^{(k)}(Z_C = 0, Z_C, T = 0, m | \vec{v}_{k-1})} \\ & \quad \left. \times \sqrt{\sum_k P^{(k)}(Z_C = 1, Z_C, T = 0 | \vec{v}_{k-1}) - \sum_k P^{(k)}(Z_C = 1, Z_C, T = 0, m | \vec{v}_{k-1})} \right). \end{aligned} \quad (\text{S227})$$

Now, let us rewrite Eq. (S227) as

$$\frac{\tilde{N}_{Z_C}^{\text{det}}}{p_{Z_C}} - \frac{2\tilde{N}_{X_C=1}^{\text{det}}}{p_{X_C}} \leq \frac{2}{p_{Z_C}} \left[\sqrt{\tilde{N}_{Z_C=0}^{\text{err}} \tilde{N}_{Z_C=1}^{\text{err}}} + \sqrt{(\tilde{N}_{Z_C=0}^{\text{det}} - \tilde{N}_{Z_C=0}^{\text{err}})(\tilde{N}_{Z_C=1}^{\text{det}} - \tilde{N}_{Z_C=1}^{\text{err}})} \right], \quad (\text{S228})$$

where we have defined $\tilde{N}_{Z_C}^{\text{det}} := \sum_k P^{(k)}(Z_C, T = 0 | \vec{v}_{k-1})$, $\tilde{N}_{X_C=1}^{\text{det}} := \sum_k P^{(k)}(X_C = 1, X_C, T = 0 | \vec{v}_{k-1})$, $\tilde{N}_{Z_C=x}^{\text{err}} := \sum_k P^{(k)}(Z_C = x, Z_C, T = 0, m | \vec{v}_{k-1})$ and $\tilde{N}_{Z_C=x}^{\text{det}} := \sum_k P^{(k)}(Z_C = x, Z_C, T = 0 | \vec{v}_{k-1})$. Then, dividing by $\tilde{N}_{Z_C}^{\text{det}}$ on both sides and using the fact that $\tilde{N}_{Z_C}^{\text{det}} = \tilde{N}_{Z_C=0}^{\text{det}} + \tilde{N}_{Z_C=1}^{\text{det}} \geq 2\sqrt{\tilde{N}_{Z_C=0}^{\text{det}} \tilde{N}_{Z_C=1}^{\text{det}}}$, we obtain

$$\begin{aligned} 1 - \frac{2p_{Z_C} \tilde{N}_{X_C=1}^{\text{det}}}{p_{X_C} \tilde{N}_{Z_C}^{\text{det}}} & \leq \frac{1}{\sqrt{\tilde{N}_{Z_C=0}^{\text{det}} \tilde{N}_{Z_C=1}^{\text{det}}}} \left[\sqrt{\tilde{N}_{Z_C=0}^{\text{err}} \tilde{N}_{Z_C=1}^{\text{err}}} + \sqrt{(\tilde{N}_{Z_C=0}^{\text{det}} - \tilde{N}_{Z_C=0}^{\text{err}})(\tilde{N}_{Z_C=1}^{\text{det}} - \tilde{N}_{Z_C=1}^{\text{err}})} \right] \\ & = \sqrt{\frac{\tilde{N}_{Z_C=0}^{\text{err}} \tilde{N}_{Z_C=1}^{\text{err}}}{\tilde{N}_{Z_C=0}^{\text{det}} \tilde{N}_{Z_C=1}^{\text{det}}}} + \sqrt{\left(1 - \frac{\tilde{N}_{Z_C=0}^{\text{err}}}{\tilde{N}_{Z_C=0}^{\text{det}}}\right) \left(1 - \frac{\tilde{N}_{Z_C=1}^{\text{err}}}{\tilde{N}_{Z_C=1}^{\text{det}}}\right)}. \end{aligned} \quad (\text{S229})$$

The inequality $z \leq \sqrt{y'y} + \sqrt{1-y'}\sqrt{1-y}$, with $z, y, y' \in [0, 1]$, is equivalent to the inequality $G_-(y, z) \leq y' \leq G_+(y, z)$, where [S2]

$$G_-(y, z) = \begin{cases} g_-(y, z) & \text{if } y > 1 - z^2 \\ 0 & \text{otherwise} \end{cases} \quad \text{and} \quad G_+(y, z) = \begin{cases} g_+(y, z) & \text{if } y < z^2 \\ 1 & \text{otherwise,} \end{cases} \quad (\text{S230})$$

and

$$g_{\pm}(y, z) = y + (1 - z^2)(1 - 2y) \pm 2\sqrt{z^2(1 - z^2)y(1 - y)}. \quad (\text{S231})$$

Therefore, Eq. (S229) implies that

$$\frac{\tilde{N}_{Z_C=0}^{\text{err}}}{\tilde{N}_{Z_C=0}^{\text{det}}} \leq G_+ \left(\frac{\tilde{N}_{Z_C=1}^{\text{err}}}{\tilde{N}_{Z_C=1}^{\text{det}}}, 1 - \frac{2p_{Z_C} \tilde{N}_{X_C=1}^{\text{det}}}{p_{X_C} \tilde{N}_{Z_C}^{\text{det}}} \right). \quad (\text{S232})$$

Then, by rearranging and applying Azuma's inequality (see Section SM1 E 1 for more details), we have that

$$N_{Z_C=0}^{\text{err}} - \Delta_A \leq (N_{Z_C=0}^{\text{det}} + \Delta_A) G_+ \left(\frac{N_{Z_C=1}^{\text{err}} + \Delta_A}{N_{Z_C=1}^{\text{det}} - \Delta_A}, 1 - \frac{2p_{Z_C} (N_{X_C=1}^{\text{det}} + \Delta_A)}{p_{X_C} (N_{Z_C}^{\text{det}} - \Delta_A)} \right), \quad (\text{S233})$$

where we have used the fact that $G_+(y, z) \leq G_+(\bar{y}, \bar{z})$ with $\bar{y} \geq y$ and $\bar{z} \leq z$. In Eq. (S233), $\Delta_A := \Delta_A(N^{\text{det}}) = \sqrt{2N^{\text{det}} \ln 1/\epsilon_A}$ where $N^{\text{det}} = |\mathcal{N}^{\text{det}}|$ is the total number of detected rounds; $N_{X_C=1}^{\text{det}}$ is the total number of detected coin events in which Alice selected the X_C basis and obtained $X_C = 1$; $N_{Z_C}^{\text{det}} := N_{Z_C=0}^{\text{det}} + N_{Z_C=1}^{\text{det}}$ is the total number of detected coin rounds in which Alice chose the Z_C basis; and $N_{Z_C=0}^{\text{err}}$, $N_{Z_C=1}^{\text{err}}$, $N_{Z_C=0}^{\text{det}}$ and $N_{Z_C=1}^{\text{det}}$ are defined in Section SM1 B 4. Note that, since we started the analysis by assuming that Bob had obtained a particular set of

detections \mathcal{N}_{det} , our formula in Eq. (S233) appears to be a statistical statement conditional on this particular set \mathcal{N}_{det} , i.e., a shorthand for a statement of the form $\Pr[L > R | \mathcal{N}_{\text{det}}] \leq 6\epsilon_A$. However, since we have shown that this statement holds for any \mathcal{N}_{det} , we can remove the conditioning on \mathcal{N}_{det} , i.e., we simply have that $\Pr[L > R] \leq 6\epsilon_A$. Finally, using the fact that $N_{X_C=1}^{\text{det}} \leq N_{X_C=1}$, where $N_{X_C=1}$ is the total number of coin events in which Alice selected the X_C basis and obtained $X_C = 1$ (detected or not), we obtain

$$N_{Z_C=0}^{\text{err}} - \Delta_A \underset{6\epsilon_A}{\leq} (N_{Z_C=0}^{\text{det}} + \Delta_A) G_+ \left(\frac{N_{Z_C=1}^{\text{err}} + \Delta_A}{N_{Z_C=1}^{\text{det}} - \Delta_A}, 1 - \frac{2p_{Z_C}(N_{X_C=1} + \Delta_A)}{p_{X_C}(N_{Z_C}^{\text{det}} - \Delta_A)} \right). \quad (\text{S234})$$

We remark that a similar expression to Eq. (S234) can be obtained by applying Kato's inequality [S25] instead of Azuma's inequality, resulting in a tighter estimation of $N_{Z_C=0}^{\text{err}}$ (see Section SM1 E).

In the asymptotic regime ($N \rightarrow \infty$), Eq. (S234) becomes

$$N_{Z_C=0}^{\text{err}} \lesssim N_{Z_C=0}^{\text{det}} G_+ \left(\frac{N_{Z_C=1}^{\text{err}}}{N_{Z_C=1}^{\text{det}}}, 1 - \frac{2p_{Z_C}N_{X_C=1}}{p_{X_C}N_{Z_C}^{\text{det}}} \right). \quad (\text{S235})$$

By substituting $N_{Z_C}^{\text{det}} := N_{Z_C=0}^{\text{det}} + N_{Z_C=1}^{\text{det}}$ in Eq. (S235), we obtain the quantum coin inequality in Eq. (S38), as desired.

B. Measurement-device-independent scenario

For MDI-type schemes, the quantum coin inequality can be derived in a similar way as for the P&M case. For this, we first define a Coin Protocol as follows.

1. Alice and Bob prepare N copies of the state

$$|\Psi\rangle_{TCDAB} = \sqrt{p_C} |0\rangle_T |\Psi_{\text{coin}}\rangle_{CDAB} + \sqrt{1-p_C} |1\rangle_T |0\rangle_C |0\rangle_D |\rho_{\text{comp}}\rangle_{AB}, \quad (\text{S236})$$

where $p_C = 2p_{\text{tar}}$ and $|\rho_{\text{comp}}\rangle_{AB}$ is a purification of ρ_{comp} . Then, they send all photonic systems B to Charlie through a quantum channel.

2. For each round, Charlie performs a measurement and announces whether the round was detected. Let \mathcal{N}^{det} be the set of detected rounds.
3. For each round $k \in \mathcal{N}^{\text{det}}$ (i.e., each detected round), Alice and Bob measure system T in the computational basis, learning if the round is a coin round ($T = 0$) or a compensation round ($T = 1$). Also, if $T = 0$, Alice and Bob perform the POVM $\{\hat{m}_{\text{err}}, \hat{\mathbb{I}} - \hat{m}_{\text{err}}\}$, where $\hat{m}_{\text{err}} = |0\rangle\langle 0|_{D_a} \otimes |0\rangle\langle 0|_{D_b} + |1\rangle\langle 1|_{D_a} \otimes |1\rangle\langle 1|_{D_b}$, and denote by m (\bar{m}) the outcome associated to \hat{m}_{err} ($\hat{\mathbb{I}} - \hat{m}_{\text{err}}$). Then, Alice and Bob choose Z_C (X_C) with probability p_{Z_C} (p_{X_C}) and measure the coin system C in the selected basis.
4. For each round not in \mathcal{N}^{det} , Alice and Bob measure system T in the computational basis. If $T = 0$, Alice and Bob choose Z_C (X_C) with probability p_{Z_C} (p_{X_C}) and measure the coin system C in the selected basis.

Then, by following the steps from Eq. (S220) to (S235), we obtain

$$N_{Z_C=0}^{\text{err}} \lesssim N_{Z_C=0}^{\text{det}} G_+ \left(\frac{N_{Z_C=1}^{\text{err}}}{N_{Z_C=1}^{\text{det}}}, 1 - \frac{2p_{Z_C}N_{X_C=1}}{p_{X_C}N_{Z_C}^{\text{det}}} \right). \quad (\text{S237})$$

SE2. OBTAINING A BOUND ON THE COIN IMBALANCE PARAMETER Δ

In this Section, we show how to obtain a bound on the coin imbalance parameter $\Delta := 1 - \text{Re} \langle \Psi_{\text{Ref}} | \Psi_{\text{tar}} \rangle_{DAB}$, which incorporates the effect of the side channels in our security proof. For concreteness, we focus on the three-state protocol considered in Section SM1 B and on the coherent-light-based MDI protocol considered in Section SM4 A. However, the methods introduced here can be easily adapted to other P&M and MDI-type protocols.

A. Three-state protocol

Here, we first explain how to obtain Δ in Eq. (S41) by using SDP techniques and then, we show that when the emitted states in Eq. (S2) satisfy the extra assumption $\langle \phi_i | \phi_j^\perp \rangle_B = 0$ for all $i, j \in \{0_Z, 1_Z, 0_X\}$ such that $i \neq j$, which is reasonable for some source imperfections, Δ can be derived analytically. Finally, we compare the secret-key rate obtainable in the general case with that obtainable under the extra assumption on the emitted states for different parameter regimes.

For this, it is useful to first rewrite the states $|\Psi_{\text{Tar}}\rangle_{DAB}$ and $|\Psi_{\text{Ref}}\rangle_{DAB}$ in Eqs. (S21) and (S22), respectively, as

$$|\Psi_{\text{Tar}}\rangle_{DAB} = \frac{1}{\sqrt{1 + c_2 q_{\text{vir1}}^\phi}} \left[\sqrt{q_{\text{vir0}}^\psi} |0\rangle_D |0\rangle_A |\psi_{\text{vir0}}\rangle_B + |1\rangle_D |0\rangle_A \left(a\sqrt{c_2 q_{\text{vir1}}^\phi} |\psi_{0_X}\rangle_B + b\sqrt{q_{\text{vir1}}^\psi} |\psi_{\text{vir1}}\rangle_B \right) \right. \quad (\text{S238})$$

$$\left. + |1\rangle_D |1\rangle_A \left(b\sqrt{c_2 q_{\text{vir1}}^\phi} |\psi_{0_X}\rangle_B - a\sqrt{q_{\text{vir1}}^\psi} |\psi_{\text{vir1}}\rangle_B \right) \right],$$

$$|\Psi_{\text{Ref}}\rangle_{DAB} = \frac{1}{\sqrt{1 + c_2 q_{\text{vir1}}^\phi}} \left[\sqrt{q_{\text{vir0}}^\phi} |0\rangle_D |0\rangle_A |\psi_{0_X}\rangle_B + \sqrt{c_1 q_{\text{vir1}}^\phi} |1\rangle_D |0\rangle_A |\psi_{0_Z}\rangle_B + \sqrt{c_1 q_{\text{vir1}}^\phi} |1\rangle_D |1\rangle_A |\psi_{1_Z}\rangle_B \right], \quad (\text{S239})$$

with $a = b = 1/\sqrt{2}$. Then, $\text{Re} \langle \Psi_{\text{Tar}} | \Psi_{\text{Ref}} \rangle_{DAB}$ can be calculated as follows

$$\begin{aligned} \text{Re} \langle \Psi_{\text{Tar}} | \Psi_{\text{Ref}} \rangle_{DAB} &= \frac{1}{1 + c_2 q_{\text{vir1}}^\phi} \left[\sqrt{q_{\text{vir0}}^\phi q_{\text{vir0}}^\psi} \text{Re} \langle \psi_{\text{vir0}} | \psi_{0_X} \rangle_B + \sqrt{c_1 q_{\text{vir1}}^\phi} \left(a\sqrt{c_2 q_{\text{vir1}}^\phi} \text{Re} \langle \psi_{0_X} | \psi_{0_Z} \rangle_B \right. \right. \\ &\quad \left. \left. + b\sqrt{q_{\text{vir1}}^\psi} \text{Re} \langle \psi_{\text{vir1}} | \psi_{0_Z} \rangle_B \right) + \sqrt{c_1 q_{\text{vir1}}^\phi} \left(b\sqrt{c_2 q_{\text{vir1}}^\phi} \text{Re} \langle \psi_{0_X} | \psi_{1_Z} \rangle_B - a\sqrt{q_{\text{vir1}}^\psi} \text{Re} \langle \psi_{\text{vir1}} | \psi_{1_Z} \rangle_B \right) \right] \\ &= \frac{1}{1 + c_2 q_{\text{vir1}}^\phi} \left[\left(\frac{\sqrt{q_{\text{vir0}}^\phi}}{2} + a\sqrt{c_1 c_2} q_{\text{vir1}}^\phi \right) \text{Re} \langle \psi_{0_Z} | \psi_{0_X} \rangle_B + \left(\frac{\sqrt{q_{\text{vir0}}^\phi}}{2} + b\sqrt{c_1 c_2} q_{\text{vir1}}^\phi \right) \text{Re} \langle \psi_{1_Z} | \psi_{0_X} \rangle_B \right. \\ &\quad \left. + (a + b) \frac{\sqrt{c_1 q_{\text{vir1}}^\phi}}{2} (1 - \text{Re} \langle \psi_{0_Z} | \psi_{1_Z} \rangle_B) \right], \end{aligned} \quad (\text{S240})$$

where in the last equality we have used the definitions of the virtual states in Eq. (S9) such that $\text{Re} \langle \psi_{\text{vir0}} | \psi_{0_X} \rangle_B = (\text{Re} \langle \psi_{0_Z} | \psi_{0_X} \rangle_B + \text{Re} \langle \psi_{1_Z} | \psi_{0_X} \rangle_B) / (2\sqrt{q_{\text{vir0}}^\psi})$ and $\text{Re} \langle \psi_{\text{vir1}} | \psi_{\alpha_Z} \rangle_B = (-1)^\alpha (1 - \text{Re} \langle \psi_{0_Z} | \psi_{1_Z} \rangle_B) / (2\sqrt{q_{\text{vir1}}^\psi})$ for $\alpha \in \{0, 1\}$, with

$$\text{Re} \langle \psi_i | \psi_j \rangle_B = \text{Re} \left[(1 - \epsilon) \langle \phi_i | \phi_j \rangle_B + \sqrt{(1 - \epsilon)\epsilon} \langle \phi_i | \phi_j^\perp \rangle_B + \sqrt{\epsilon(1 - \epsilon)} \langle \phi_i^\perp | \phi_j \rangle_B + \epsilon \langle \phi_i^\perp | \phi_j^\perp \rangle_B \right]. \quad (\text{S241})$$

1. Numerical bound using SDP techniques

To construct the SDP, let us redefine the tuple $\{0_Z, 1_Z, 0_X\}$ as $\{1, 2, 3\}$ and rename the states $|\psi_j\rangle_B$, $|\phi_j\rangle_B$ and $|\phi_j^\perp\rangle_B$ accordingly. Moreover, let us define G as the Gram matrix of the vector set $\{|\phi_1\rangle_B, |\phi_2\rangle_B, |\phi_3\rangle_B, |\phi_1^\perp\rangle_B, |\phi_2^\perp\rangle_B, |\phi_3^\perp\rangle_B\}$ such that, for example, $G[1, 1] = \langle \phi_1 | \phi_1 \rangle_B$ and $G[1, 5] = \langle \phi_1 | \phi_2^\perp \rangle_B$. That is, $G[i, j] \equiv \langle i | G | j \rangle$ denotes the coefficient in the i -th column and j -th row of G . Using this redefinition, we can rewrite Eq. (S240) as

$$\begin{aligned} \text{Re} \langle \Psi_{\text{Tar}} | \Psi_{\text{Ref}} \rangle_{DAB} &= \frac{1}{1 + c_2 q_{\text{vir1}}^\phi} \left[\left(\frac{\sqrt{q_{\text{vir0}}^\phi}}{2} + a\sqrt{c_1 c_2} q_{\text{vir1}}^\phi \right) \text{Re} \langle \psi_1 | \psi_3 \rangle_B + \left(\frac{\sqrt{q_{\text{vir0}}^\phi}}{2} + b\sqrt{c_1 c_2} q_{\text{vir1}}^\phi \right) \text{Re} \langle \psi_2 | \psi_3 \rangle_B \right. \\ &\quad \left. + (a + b) \frac{\sqrt{c_1 q_{\text{vir1}}^\phi}}{2} (1 - \text{Re} \langle \psi_1 | \psi_2 \rangle_B) \right], \end{aligned} \quad (\text{S242})$$

which is the objective function of the SDP. Note that, as required, it is guaranteed to be real and it can be expressed as a linear function of elements of G , since

$$\begin{aligned} \text{Re} \langle \psi_i | \psi_j \rangle_B &= \text{Re} \left[(1 - \epsilon) G[i, j] + \sqrt{(1 - \epsilon)\epsilon} G[i, j + 3] + \sqrt{\epsilon(1 - \epsilon)} G[i + 3, j] + \epsilon G[i + 3, j + 3] \right] \\ &= (1 - \epsilon) \text{Re} G[i, j] + \sqrt{(1 - \epsilon)\epsilon} \text{Re} G[i, j + 3] + \sqrt{\epsilon(1 - \epsilon)} \text{Re} G[i + 3, j] + \epsilon \text{Re} G[i + 3, j + 3], \end{aligned} \quad (\text{S243})$$

and $\text{Re } G[i, j] = (G[i, j] + G[j, i])/2$. The constraints of the SDP can then be listed as follows

$$\begin{aligned}
G &\geq 0; \\
G[j, j] &= \langle \phi_j | \phi_j \rangle_B = 1, & \forall j \in \{1, 2, 3\}; \\
G[j+3, j+3] &= \langle \phi_j^\perp | \phi_j^\perp \rangle_B = 1, & \forall j \in \{1, 2, 3\}; \\
G[j, j+3] &= \langle \phi_j | \phi_{j+3}^\perp \rangle_B = 0, & \forall j \in \{1, 2, 3\}; \\
G[1, 2] &= \langle \phi_1 | \phi_2 \rangle_B = \cos(\kappa\pi/2); \\
G[1, 3] &= \langle \phi_1 | \phi_3 \rangle_B = \cos(\kappa\pi/4); \\
G[2, 3] &= \langle \phi_2 | \phi_3 \rangle_B = \cos(\kappa\pi/4);
\end{aligned} \tag{S244}$$

where we have used Eqs. (S12) and (S13) to calculate the inner products $\langle \phi_i | \phi_j \rangle_B$. Note that the first inequality in Eq. (S244) is the standard positive semidefinite constraint, which holds because G is a Gram matrix, and that the others are valid SDP constraints since they can be written as a linear function of elements of G . Using the SDP we can obtain a lower bound on $\text{Re } \langle \Psi_{\text{Tar}} | \Psi_{\text{Ref}} \rangle_{DAB}$, and then directly use Eq. (S41) to define Δ .

Note that, for concreteness, we have considered the scenario in which one has knowledge on the fidelity between the actual states $\{|\psi_j\rangle_B\}_j$ and the characterized qubit states $\{|\phi_j\rangle_B\}_j$. However, as explained in the subsection “A more general form of Eq. (1)” in Appendix A, the approach presented here is also valid when one has knowledge between the actual states $\{|\psi_j\rangle_B\}_j$ and *any* characterized states $\{|\tilde{\phi}_j\rangle_B\}_j$, not necessarily qubits. In this case, one only needs to trivially substitute $|\phi_j\rangle_B \rightarrow |\tilde{\phi}_j\rangle_B$ and $|\phi_j^\perp\rangle_B \rightarrow |\tilde{\phi}_j^\perp\rangle_B$ in the SDP above, and then modify the constraints based on the knowledge of the inner products $\langle \tilde{\phi}_{j'} | \tilde{\phi}_j \rangle_B \forall j, j'$.

2. Analytical bound with an additional assumption

If the emitted states in Eq. (S2) satisfy $\langle \phi_i | \phi_j^\perp \rangle_B = 0$ for all $i, j \in \{0_Z, 1_Z, 0_X\}$ such that $i \neq j$, it is straightforward to obtain Δ by analytically deriving a lower bound on $\text{Re } \langle \Psi_{\text{Tar}} | \Psi_{\text{Ref}} \rangle_{DAB}$. First, using Eqs. (S12) and (S13) we can directly calculate the inner products $\langle \phi_i | \phi_j \rangle_B$ in Eq. (S241) to be $\langle \phi_{0_Z} | \phi_{1_Z} \rangle_B = \cos(\kappa\pi/2)$ and $\langle \phi_{0_Z} | \phi_{0_X} \rangle_B = \langle \phi_{1_Z} | \phi_{0_X} \rangle_B = \cos(\kappa\pi/4)$. Then, even though the side-channel states $|\phi_j^\perp\rangle_B$ are uncharacterized, it must be that $-1 \leq \text{Re } \langle \phi_i^\perp | \phi_j^\perp \rangle_B \leq 1$ since $\text{Re } \langle \phi_i^\perp | \phi_j^\perp \rangle_B$ is the real part of an inner product between two normalized states. Therefore, Eq. (S240) can be lower bounded by

$$\begin{aligned}
\text{Re } \langle \Psi_{\text{Tar}} | \Psi_{\text{Ref}} \rangle_{DAB} &\geq \frac{1}{1 + c_2 q_{\text{vir1}}^\phi} \left(\left[\sqrt{q_{\text{vir0}}^\phi} + (a + b) \sqrt{c_1 c_2} q_{\text{vir1}}^\phi \right] [(1 - \epsilon) \cos(\kappa\pi/4) - \epsilon] \right. \\
&\quad \left. + (a + b) \frac{\sqrt{c_1 q_{\text{vir1}}^\phi}}{2} [1 - (1 - \epsilon) \cos(\kappa\pi/2) - \epsilon] \right).
\end{aligned} \tag{S245}$$

3. Comparison between the numerical and analytical bounds

For the comparison between the numerical and analytical bounds, we evaluate the secret-key rate obtainable when employing our analysis with the SDP techniques described above, which does not assume $\langle \phi_i | \phi_j^\perp \rangle_B = 0 \forall i, j$ when $i \neq j$, and with Eq. (S245). In the simulations, we take $\delta = 0.063$ [S32, S33] and $\epsilon \in \{10^{-6}, 10^{-3}\}$. All the other experimental parameters are the same as in the Main Text.

The results are presented in Fig. S12, where the solid and dashed lines correspond to using the numerical and analytical bounds, respectively. This figure shows that these bounds provide very similar secret-key rates. In fact, when $\epsilon = 10^{-3}$, the two curves are indistinguishable to the naked eye. This suggests that, while the extra assumption helps to simplify the analysis, it does not actually result in an appreciable key-rate improvement.

B. Coherent-light-based MDI protocol

Here, we explain how to construct an SDP to find an upper bound on the coin imbalance parameter $\Delta := 1 - \text{Re } \langle \Psi_{\text{Tar}} | \Psi_{\text{Ref}} \rangle_{DAB}$ for the coherent-light-based MDI protocol analyzed in Section SM4 A. Using Eq. (S173) and

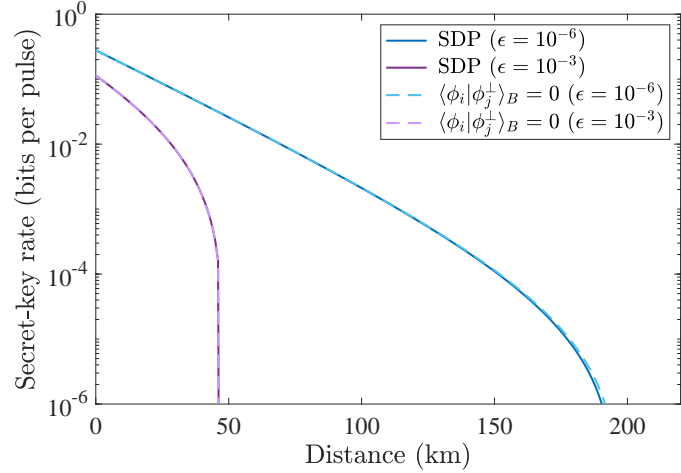


Figure S12. Secret-key rate per pulse as a function of the distance (km) for $\delta = 0.063$ and different values of ϵ when using our numerical bound based on SDP and our analytical bound that assumes $\langle \phi_i | \phi_j^\perp \rangle_B = 0$.

Eq. (S2), we can express the states emitted by Alice and Bob as

$$|\psi_j\rangle_{B_u} = \sqrt{1-\epsilon}|\tilde{\phi}_j\rangle_{B_u} + \sqrt{\epsilon}|\tilde{\phi}_j^\perp\rangle_{B_u}, \quad (\text{S246})$$

where $j \in \{0_Z, 1_Z, 0_X\}$, $u \in \{a, b\}$, $|\tilde{\phi}_0\rangle_{B_u} = |\sqrt{\mu}\rangle_{B_u}$, $|\tilde{\phi}_1\rangle_{B_u} = |-\sqrt{\mu}\rangle_{B_u}$, $|\tilde{\phi}_0\rangle_{B_u} = |\text{vac}\rangle_{B_u}$, and $\langle \tilde{\phi}_j^\perp | \tilde{\phi}_j \rangle_{B_u} = 0$ ⁸. Taking the tensor product of Eq. (S246) for $u = a$ and $u = b$, we obtain the following expression for Alice and Bob's joint states,

$$|\psi_{ij}\rangle_B := |\psi_i\rangle_{B_a} \otimes |\psi_j\rangle_{B_b} = \sqrt{1-\xi}|\tilde{\phi}_{ij}\rangle_B + \sqrt{\xi}|\tilde{\phi}_{ij}^\perp\rangle_B, \quad (\text{S247})$$

where we have defined $\xi := 1 - (1 - \epsilon)^2$, $|\tilde{\phi}_{ij}\rangle_B := |\tilde{\phi}_i\rangle_{B_a} \otimes |\tilde{\phi}_j\rangle_{B_b}$, and $|\tilde{\phi}_{ij}^\perp\rangle_B$ is a normalized state that can be easily shown to satisfy $\langle \tilde{\phi}_{ij}^\perp | \tilde{\phi}_{ij} \rangle_B = 0$. Now, let us define an ordering for Alice and Bob's joint setting choices $ij \in \{0_Z0_Z, 0_Z1_Z, 0_Z0_X, 1_Z0_Z, 1_Z1_Z, 1_Z0_X, 0_X0_Z, 0_X1_Z, 0_X0_X\}$ using the index $k \in \{1, 2, 3, 4, 5, 6, 7, 8, 9\}$, and let us define G as the Gram matrix of the union of vector sets $\{|\tilde{\phi}_{ij}\rangle_B\}_{ij}$ and $\{|\tilde{\phi}_{ij}^\perp\rangle_B\}_{ij}$, with the latter being indexed by $k \in \{10, 11, 12, 13, 14, 15, 16, 17, 18\}$. From the ordering we have defined, we have that the elements of G are, e.g., $G[1, 6] = \langle \tilde{\phi}_{0_Z0_Z} | \tilde{\phi}_{1_Z0_X} \rangle_B$, $G[10, 6] = \langle \tilde{\phi}_{0_Z0_Z}^\perp | \tilde{\phi}_{1_Z0_X} \rangle_B$, $G[3, 5] = \langle \tilde{\phi}_{0_Z0_X} | \tilde{\phi}_{1_Z1_Z} \rangle_B$, $G[3, 14] = \langle \tilde{\phi}_{0_Z0_X}^\perp | \tilde{\phi}_{1_Z1_Z} \rangle_B$, and so on. Now, let us define

$$G_\star(k, k') := (1 - \xi) \operatorname{Re} G[k, k'] + \sqrt{(1 - \xi)\xi} (\operatorname{Re} G[k + 9, k'] + \operatorname{Re} G[k, k' + 9]) + \xi \operatorname{Re} G[k + 9, k' + 9], \quad (\text{S248})$$

where $\operatorname{Re} G[k, k'] = (G[k, k'] + G[k', k]) / 2$ since G is Hermitian. Note that we have, e.g., $G_\star(1, 6) = \operatorname{Re} \langle \psi_{0_Z0_Z} | \psi_{1_Z0_X} \rangle_B$, $G_\star(3, 5) = \operatorname{Re} \langle \psi_{0_Z0_X} | \psi_{1_Z1_Z} \rangle_B$, and so on. Using the definition of $\langle \Psi_{\text{Tar}} | \Psi_{\text{Ref}} \rangle_{DAB}$ in Eq. (S196) and our definition

⁸ Note that the set of states $\{|\tilde{\phi}_0\rangle_{B_u}, |\tilde{\phi}_1\rangle_{B_u}, |\tilde{\phi}_0\rangle_{B_u}\}$ defined here is different from the set of states $\{|\phi_0\rangle_{B_u}, |\phi_1\rangle_{B_u}, |\phi_0\rangle_{B_u}\}$ defined in Section SM4 A. In particular, while $|\phi_0\rangle_{B_u} = |\tilde{\phi}_0\rangle_{B_u} = |\sqrt{\mu}\rangle_{B_u}$ and $|\phi_1\rangle_{B_u} = |\tilde{\phi}_1\rangle_{B_u} = |-\sqrt{\mu}\rangle_{B_u}$, $|\phi_0\rangle_{B_u} \neq |\tilde{\phi}_0\rangle_{B_u} = |\text{vac}\rangle_{B_u}$, since $|\phi_0\rangle_{B_u}$ was defined as the projection of $|\text{vac}\rangle_{B_u}$ onto the qubit subspace spanned by $\{|\sqrt{\mu}\rangle_{B_u}, |-\sqrt{\mu}\rangle_{B_u}\}$. The reason is that $\{|\phi_0\rangle_{B_u}, |\phi_1\rangle_{B_u}, |\phi_0\rangle_{B_u}\}$ needed to be qubit states, in order to derive the LT formulas in Eq. (S179), which are then used as a blueprint to define the reference and target states. However, here, while $\{|\tilde{\phi}_0\rangle_{B_u}, |\tilde{\phi}_1\rangle_{B_u}, |\tilde{\phi}_0\rangle_{B_u}\}$ need to be known states, they do not need to be qubit states. The reason is that we can employ any state expansion of the actual states to calculate an upper bound on Δ , and using the definition $|\tilde{\phi}_0\rangle_{B_u} = |\text{vac}\rangle_{B_u}$ results in a better bound.

in Eq. (S248), we can write our objective function as

$$\begin{aligned}
\text{Re} \langle \Psi_{\text{Tar}} | \Psi_{\text{Ref}} \rangle_{DAB} = & \frac{q_{\text{vir}0}^\phi}{4C} (G_\star(9,1) + G_\star(9,2) + G_\star(9,4) + G_\star(9,5)) + \frac{\sqrt{2c_1 q_{\text{vir}01}^\phi}}{2C} \left(\frac{1}{4} (G_\star(3,1) - G_\star(3,2) + G_\star(3,4) \right. \\
& - G_\star(3,5) - G_\star(8,1) + G_\star(8,2) - G_\star(8,4) + G_\star(8,5) + G_\star(1,7) + G_\star(2,7) - G_\star(4,7) - G_\star(5,7) - G_\star(6,1) - G_\star(6,2) \\
& + G_\star(6,4) + G_\star(6,5)) + \sqrt{c_2 q_{\text{vir}01}^\phi} (G_\star(3,9) + G_\star(8,9) + G_\star(7,9) + G_\star(6,9)) \Big) + \frac{c_1 q_{\text{vir}1}^\phi}{4C} (2 - G_\star(2,1) - G_\star(4,1) \\
& + G_\star(5,1) + G_\star(4,2) - G_\star(5,2) - G_\star(5,4)) + \frac{q_{\text{vir}11}^\phi \sqrt{c_1 c_2}}{2\sqrt{2}C} \left(c_1 (G_\star(1,7) - G_\star(4,7) + 2G_\star(1,3) + G_\star(2,7) - G_\star(5,7) \right. \\
& \left. + 2G_\star(2,8) - G_\star(4,7) + G_\star(4,6) + 2G_\star(4,3) - G_\star(5,7) + G_\star(5,6) + 2G_\star(5,8)) + 2c_2 (G_\star(9,7) + G_\star(9,6)) \right), \tag{S249}
\end{aligned}$$

which is a linear function of elements of G , and therefore a valid SDP objective function. Here, $q_{\text{vir}\alpha\beta}^\phi := q_{\text{vir}\alpha}^\phi q_{\text{vir}\beta}^\phi$ for $\alpha, \beta \in \{0, 1\}$, where $q_{\text{vir}\alpha}^\phi$ and $q_{\text{vir}\beta}^\phi$ are defined in Eq. (S177), c_1 and c_2 are defined in Eq. (S180), and C is defined in Eq. (S191). Also, using the fact that $\langle \tilde{\phi}_{ij} | \tilde{\phi}_{ij} \rangle_B = 1$, $\langle \tilde{\phi}_{ij}^\perp | \tilde{\phi}_{ij}^\perp \rangle_B = 1$ and $\langle \tilde{\phi}_{ij}^\perp | \tilde{\phi}_{ij} \rangle_B = 0$ for all i, j , and our knowledge of the states $\{|\tilde{\phi}_{ij}\rangle_B\}_{ij}$ (and thus our knowledge of the inner product between any two states in this set), we obtain the constraints

$$\begin{aligned}
G &\geq 0; \\
G[k, k] &= 1, & \forall k \in \{1, \dots, 9\}; \\
G[k+9, k] &= 0, & \forall k \in \{1, \dots, 9\}; \\
G[k+9, k+9] &= 1, & \forall k \in \{1, \dots, 9\}; \\
G[1, 2] &= G[1, 4] = G[2, 5] = G[3, 6] = G[4, 5] = G[7, 8] = \langle \sqrt{\mu} | -\sqrt{\mu} \rangle = \exp(-2\mu); \\
G[1, 3] &= G[1, 7] = G[2, 8] = G[3, 9] = G[4, 6] = G[7, 9] = \langle \sqrt{\mu} | \text{vac} \rangle = \exp(-\mu/2); \\
G[1, 5] &= G[2, 4] = (\langle \sqrt{\mu} | -\sqrt{\mu} \rangle)^2 = \exp(-4\mu); & \tag{S250} \\
G[1, 6] &= G[1, 8] = G[2, 7] = G[3, 4] = \langle \sqrt{\mu} | -\sqrt{\mu} \rangle \langle \sqrt{\mu} | \text{vac} \rangle = \exp(-5\mu/2); \\
G[1, 9] &= G[3, 7] = (\langle \sqrt{\mu} | \text{vac} \rangle)^2 = \exp(-\mu); \\
G[2, 3] &= G[4, 7] = G[5, 6] = G[5, 8] = G[6, 9] = G[8, 9] = \langle -\sqrt{\mu} | \text{vac} \rangle = \exp(-\mu/2); \\
G[2, 6] &= G[3, 5] = G[4, 8] = G[5, 7] = \langle \sqrt{\mu} | -\sqrt{\mu} \rangle \langle -\sqrt{\mu} | \text{vac} \rangle = \exp(-5\mu/2); \\
G[5, 9] &= G[6, 8] = (\langle -\sqrt{\mu} | \text{vac} \rangle)^2 = \exp(-\mu); \\
G[2, 9] &= G[3, 8] = G[4, 9] = G[6, 7] = \langle \sqrt{\mu} | \text{vac} \rangle \langle -\sqrt{\mu} | \text{vac} \rangle = \exp(-\mu);
\end{aligned}$$

all of which are valid SDP constraints. Our SDP is defined then as the optimization problem of finding the minimum of Eq. (S249) given the constraints in Eq. (S250) and the standard SDP constraint $G \geq 0$ (which holds since a Gram matrix is always positive semidefinite). By solving the dual problem of this SDP, one can obtain a rigorous lower bound on $\text{Re} \langle \Psi_{\text{Tar}} | \Psi_{\text{Ref}} \rangle_{DAB}$, and thus a rigorous upper bound on $\Delta := 1 - \text{Re} \langle \Psi_{\text{Tar}} | \Psi_{\text{Ref}} \rangle_{DAB}$.

SE3. CHANNEL MODEL

A. Prepare-and-measure protocol

For the simulations, we consider, as examples, the three-state and the BB84 protocols with a phase encoding scheme. In the presence of qubit flaws, Alice's prepared qubit states can be expressed as

$$\frac{1}{\sqrt{2}} \left(|1\rangle_r |0\rangle_s + e^{i(\varphi_j + \delta\varphi_j/\pi)} |0\rangle_r |1\rangle_s \right), \tag{S251}$$

where 0 and 1 denote the photon number, the subscript r (s) stands for reference (signal) pulse, and δ quantifies the deviation of the phase modulation from the desired phases φ_j for $j \in \{0_Z, 1_Z, 0_X, 1_X\}$. For simplicity, we assume that these phases take the values: $\varphi_{0_Z} = 0$, $\varphi_{1_Z} = \pi$, $\varphi_{0_X} = \pi/2$ and $\varphi_{1_X} = 3\pi/2$. Note that if we define $|1\rangle_r |0\rangle_s =: |0_Y\rangle_B$ and $|0\rangle_r |1\rangle_s =: |1_Y\rangle_B$, and then use the fact that $|\alpha_Y\rangle_B = (|0_Z\rangle_B + (-1)^\alpha i |1_Z\rangle_B)/\sqrt{2}$ with $\alpha \in \{0, 1\}$, it is

straightforward to obtain the states in Eq. (S12) with $\theta_j = \varphi_j \kappa/2$, after a change of global phase. The non-qubit imperfections are not considered in the calculations below because ϵ is small, and thus it does not significantly affect the estimated experimental observables.

The overall transmission efficiency of the system is defined as $\eta = \eta_c \eta_d$, where $\eta_c = 10^{-0.02l}$ is the channel transmission rate, with l denoting the length of the channel in km, and η_d is the detector efficiency. We assume, for simplicity, that there is no misalignment in the channel and that the detector dark count probability p_d is independent of Bob's basis selection. We stress that the assumption of zero misalignment is used only in the numerical analysis and is not required by the security proof. On the receiving unit, a phase $\varphi_B = 0$ ($\varphi_B = -\pi/2$) corresponds to selecting the Z (X) measurement basis, but due to an imperfect phase modulator this phase is shifted by $-\delta\varphi_B/\pi$. By neglecting the terms with p_d^2 we can then express the yields as

$$Y_j^{0x} \approx \left(1 - \frac{\eta}{2}\right) p_d + \frac{\eta}{4} \left[1 + \sin\left(\varphi_j + \frac{\delta\varphi_j}{\pi} + \frac{\delta}{2}\right)\right] \left(1 - \frac{p_d}{2}\right) + \frac{\eta}{4} \left[1 - \sin\left(\varphi_j + \frac{\delta\varphi_j}{\pi} + \frac{\delta}{2}\right)\right] \frac{p_d}{2}, \quad (\text{S252})$$

$$Y_j^{1x} \approx \left(1 - \frac{\eta}{2}\right) p_d + \frac{\eta}{4} \left[1 + \sin\left(\varphi_j + \frac{\delta\varphi_j}{\pi} + \frac{\delta}{2}\right)\right] \frac{p_d}{2} + \frac{\eta}{4} \left[1 - \sin\left(\varphi_j + \frac{\delta\varphi_j}{\pi} + \frac{\delta}{2}\right)\right] \left(1 - \frac{p_d}{2}\right), \quad (\text{S253})$$

$$Y_j^{0z} \approx \left(1 - \frac{\eta}{2}\right) p_d + \frac{\eta}{4} \left[1 + \cos\left(\varphi_j + \frac{\delta\varphi_j}{\pi}\right)\right] \left(1 - \frac{p_d}{2}\right) + \frac{\eta}{4} \left[1 - \cos\left(\varphi_j + \frac{\delta\varphi_j}{\pi}\right)\right] \frac{p_d}{2}, \quad (\text{S254})$$

$$Y_j^{1z} \approx \left(1 - \frac{\eta}{2}\right) p_d + \frac{\eta}{4} \left[1 + \cos\left(\varphi_j + \frac{\delta\varphi_j}{\pi}\right)\right] \frac{p_d}{2} + \frac{\eta}{4} \left[1 - \cos\left(\varphi_j + \frac{\delta\varphi_j}{\pi}\right)\right] \left(1 - \frac{p_d}{2}\right), \quad (\text{S255})$$

where the superscript denotes Bob's outcome. Using Eqs. (S254) and (S255), we can directly calculate the rate at which Bob obtains a detection event conditioned on Alice and Bob choosing the Z basis

$$Y_Z = \frac{1}{2} (Y_{0z}^{0z} + Y_{0z}^{1z} + Y_{1z}^{0z} + Y_{1z}^{1z}) = \frac{1}{2} \left[4 \left(1 - \frac{\eta}{2}\right) p_d + \eta\right], \quad (\text{S256})$$

and the bit-error rate

$$e_Z = \frac{Y_{1z}^{0z} + Y_{0z}^{1z}}{Y_{0z}^{0z} + Y_{1z}^{0z} + Y_{0z}^{1z} + Y_{1z}^{1z}} = \frac{2(1 - \frac{\eta}{2}) p_d + \frac{\eta}{4}(1 + p_d) + \frac{\eta}{4}(p_d - 1) \cos \delta}{4(1 - \frac{\eta}{2}) p_d + \eta}. \quad (\text{S257})$$

B. Coherent-light-based MDI protocol

Here, we present the channel model used for the simulations in Section SM4 A, which is the same as that of Ref. [S34]. We model the loss from Alice and Bob to Charlie with a beamsplitter of transmittance $\sqrt{\eta}$ and assume that there is no misalignment in the channel. Moreover, for simplicity, we assume that Charlie's detectors have the same dark count probability p_d . The conditional probability that Charlie observes a click on detector D_c and no click on detector D_d (corresponding to the announcement $k_c = 1, k_d = 0$), given that Alice and Bob have sent the states $|\psi_i\rangle_{B_a}$ and $|\psi_j\rangle_{B_b}$, respectively, is given by

$$Y_{i,j}^{k_c=1, k_d=0} = (1 - p_d)^2 \exp \left[-\sqrt{\eta} \left(\frac{|\gamma_i|^2 + |\gamma_j|^2}{2} - |\gamma_i||\gamma_j| \cos(\phi_i - \phi_j) \right) \right] \\ \times \left\{ 1 - \exp \left[-\sqrt{\eta} \left(\frac{|\gamma_i|^2 + |\gamma_j|^2}{2} + |\gamma_i||\gamma_j| \cos(\phi_i - \phi_j) \right) \right] \right\} + p_d(1 - p_d), \quad (\text{S258})$$

where $i, j \in \{0_Z, 1_Z, 0_X\}$, $\gamma_{0z} = \sqrt{\mu}$, $\gamma_{1z} = -\sqrt{\mu}$, $\gamma_{0x} = 0$, $\phi_i = \arg(\gamma_i)$ and $\phi_j = \arg(\gamma_j)$. Similarly, the probability that he observes a click on detector D_d and no click on detector D_c (corresponding to the announcement $k_c = 0, k_d = 1$) is given by

$$Y_{i,j}^{k_c=0, k_d=1} = (1 - p_d)^2 \exp \left[-\sqrt{\eta} \left(\frac{|\gamma_i|^2 + |\gamma_j|^2}{2} - |\gamma_i||\gamma_j| \cos(\phi_i - \phi_j + \pi) \right) \right] \\ \times \left\{ 1 - \exp \left[-\sqrt{\eta} \left(\frac{|\gamma_i|^2 + |\gamma_j|^2}{2} + |\gamma_i||\gamma_j| \cos(\phi_i - \phi_j + \pi) \right) \right] \right\} + p_d(1 - p_d). \quad (\text{S259})$$

Therefore, the probability that Charlie obtains a detection is given by

$$Y_{i,j}^{\text{det}} := Y_{i,j}^{k_c=1, k_d=0} + Y_{i,j}^{k_c=0, k_d=1}. \quad (\text{S260})$$

Also, the bit-error rate can be calculated to be

$$e_Z = \frac{p_d}{2p_d + \exp(2\mu\sqrt{\eta}) - 1}. \quad (\text{S261})$$

SE4. HIGH-LEVEL DESCRIPTION OF THE CODE

In this Section, we provide a high-level description of the code written to perform the simulations. We note that our SDP optimization (see Section [SE2](#)) was performed using MATLAB, in conjunction with the YALMIP toolbox and the MOSEK solver. Nonetheless, alternative programming languages, toolboxes, and solvers could also be employed to attain equivalent results. For ease of discussion, we consider the asymptotic regime and the particular three-state protocol introduced in Section [SM1 B](#) to explain the code. However, it is rather straightforward to generalize it to the finite-key regime and to other P&M or MDI-type protocols.

1. Definition of the protocol parameters

- Define the value of ϵ and δ .
- Define the coefficients c_1 and c_2 in Eq. [\(S16\)](#) and the probabilities $q_{\text{vir}_\alpha}^\phi$ in Eq. [\(S18\)](#).
- Define $\Delta = 1 - \text{Re} \langle \Psi_{\text{Ref}} | \Psi_{\text{Tar}} \rangle_{DAB}$: if $\epsilon = 0$, set $\Delta = 0$; otherwise, use the SDP techniques explained in Section [SE2 A 1](#) to obtain an upper bound on Δ .

2. Definition of the channel model

- Define the probabilities P_{Z_A} , P_{X_A} , P_{Z_B} and P_{X_B} . To generate Fig. 1 in the Main Text we have used $P_{Z_A} = P_{Z_B} = 0.9$ and $P_{X_A} = P_{X_B} = 0.1$.
- Define the parameters f , p_d , η_d and the repetition rate of the protocol. The values used to generate all figures in this work are stated in the Main Text.
- Define the yields Y_j^{0x} and Y_j^{1x} for $j \in \{0_Z, 1_Z, 0_X\}$ and Y_Z . To generate Fig. 1, we have used Eq. [\(S252\)](#), Eq. [\(S253\)](#), and Eq. [\(S256\)](#), respectively.
- Define the bit-error rate e_Z . To generate Fig. 1, we have used Eq. [\(S257\)](#).

3. Calculation of e_{ph}^U

- Define the conditions to apply the function $G_+(y, z)$ with

$$y = \frac{q_{\text{vir}_0}^\phi Y_{0x}^{1x} + c_1 q_{\text{vir}_1}^\phi (Y_{0z}^{0x} + Y_{1z}^{0x})}{q_{\text{vir}_0}^\phi Y_{0x} + c_1 q_{\text{vir}_1}^\phi Y_Z},$$

$$z = 1 - \frac{2\Delta(1 + c_1 q_{\text{vir}_1}^\phi)}{Y_Z + q_{\text{vir}_0}^\phi Y_{0x} + q_{\text{vir}_1}^\phi (c_1 Y_{0z} + c_2 Y_{1z} + c_3 Y_{1x})}. \quad (\text{S262})$$

Namely, if $y < z^2$, $G_+(y, z) = g_+(y, z)$, where $g_+(y, z)$ is defined in Eq. [\(S231\)](#); otherwise, $G_+(y, z) = 1$.

- Substitute the value of $G_+(y, z)$ in Eq. [\(S46\)](#) and use it to calculate e_{ph}^U .

4. Calculation of the secret-key rate R

- Calculate R using Eq. [\(S47\)](#) for each km.
- Plot R as a function of distance. To plot R in bits per second, multiply R by the repetition rate.

Supplementary Tables

Table S1. List of random variables by order of appearance in the Supplementary Information.

Variable	Protocol	Definition
N	All	Total number of transmitted rounds
N_{key}^{\det}	Actual and Virtual	Length of the sifted key
$N_j^{\beta_X}$	Actual	Number of events in which Alice selects the setting j and Bob obtains the X -basis measurement outcome β with $\beta \in \{0, 1\}$
e_{ph}	Virtual	Phase-error rate
N_{ph}	Virtual	Number of phase errors
$N_{\text{vir}\alpha}^{\beta_X}$	Virtual	Number of events in which Alice emits the state $ \psi_{\text{vir}\alpha}\rangle_B$ and Bob obtains the X -basis measurement outcome β with $\alpha, \beta \in \{0, 1\}$
$N_{Z_C=z}^{\text{err}}$	Coin	Number of events in which Alice chooses the Z basis to measure the coin system C , obtains the result $Z_C = z$ with $z \in \{0, 1\}$, and Alice and Bob obtain the outcome associated to \hat{m}_{err}
$N_{X_C=z}$	Coin	Number of events in which Alice obtains the outcome $X_C = z$ with $z \in \{0, 1\}$ in her X -basis measurement of the coin system C
$N_l^{\beta_X}$	Virtual	Number of events l in which Bob obtains the X -basis measurement outcome β with $\beta \in \{0, 1\}$
$N_{l,t,Z_C}^{\beta_X}$	Virtual (with tag assignment)	Number of events l with tag t marked as Z_C in which Bob obtains the X -basis measurement outcome β with $\beta \in \{0, 1\}$
N_l^{\det}	Virtual	Number of detected events l
N_{l,t,Z_C}^{\det}	Virtual (with tag assignment)	Number of detected events l with tag t marked as Z_C
$N_{Z_C=z}^{\det}$	Coin	Number of detected events in which Alice chooses Z_C and obtains the outcome $Z_C = z$ with $z \in \{0, 1\}$
$N_{Z_C=z, D=d, A=a}^{\beta_X}$	Coin	Number of events in which Alice obtains $Z_C = z$, $D = d$, $A = a$ and Bob obtains the X -basis measurement outcome β with $z, d, a, \beta \in \{0, 1\}$
N^{\det}	All	Number of detected rounds
N_{ij}	Actual	Number of events in which Alice (Bob) selects the setting $i(j)$
$N_{X_C=z}^{\det}$	Coin	Number of detected events in which Alice obtains the outcome $X_C = z$ with $z \in \{0, 1\}$ in her X -basis measurement of the coin system C

Table S2. List of probabilities by order of appearance in the Supplementary Information.

Variable	Protocol	Definition
p_{γ_A}	Actual	Probability that Alice selects the γ -basis with $\gamma \in \{Z, X\}$
p_{γ_B}	Actual	Probability that Bob measures in the γ -basis with $\gamma \in \{Z, X\}$
$q_{\text{vir}_\alpha}^\psi$	Virtual	Probability that Alice emits the virtual state $ \psi_{\text{vir}_\alpha}\rangle_B$ with $\alpha \in \{0, 1\}$
$q_{\text{vir}_\alpha}^\phi$	Virtual	Probability that Alice emits the virtual state $ \phi_{\text{vir}_\alpha}\rangle_B$ with $\alpha \in \{0, 1\}$
p_l	Virtual	Probability of selecting the state associated to l
$p_{t l}$	Virtual (with tag assignment)	Probability of assigning a tag t given an event l
p_{γ_C}	Coin	Probability that Alice measures the quantum coin system C in the γ_C basis with $\gamma \in \{Z, X\}$
p_t	Virtual (with tag assignment)	Probability of assigning a tag t
$p_{l t}$	Virtual (with tag assignment)	Probability of having selected the state associated to l given a tag t
p_C	Coin	Probability of selecting a coin round
$p_{\text{key} Z}$	Actual	Probability that a round is assigned to “key” given that the users announced the Z basis
$p_{\text{test} Z}$	Actual	Probability that a round is assigned to “test” given that the users announced the Z basis
$q_{\text{vir}_\alpha}^{\psi,u}$	Virtual	Probability that Alice ($u = a$)/Bob ($u = b$) emits the virtual state $ \psi_{\text{vir}_\alpha}\rangle_{B_u}$ with $\alpha \in \{0, 1\}$
$q_{\text{vir}_\alpha}^{\phi,u}$	Virtual	Probability that Alice ($u = a$)/Bob ($u = b$) emits the virtual state $ \phi_{\text{vir}_\alpha}\rangle_{B_u}$ with $\alpha \in \{0, 1\}$
$p_{t_{\alpha\beta} t}$	Virtual (with tag assignment)	Probability that a tag $t_{\alpha\beta}$ is assigned given a tag t with $\alpha, \beta \in \{0, 1\}$
$p_{\text{vir}_{\alpha\beta} t}$	Virtual (with tag assignment)	Probability of having selected the state associated to $\text{vir}_{\alpha\beta}$ given a tag t with $\alpha, \beta \in \{0, 1\}$

[S1] M. Pereira, M. Curty, and K. Tamaki, Quantum key distribution with flawed and leaky sources, *npj Quantum Inf* **5**, 62 (2019).

[S2] M. Pereira, G. Kato, A. Mizutani, M. Curty, and K. Tamaki, Quantum key distribution with correlated sources, *Sci. Adv.* **6**, eaaz4487 (2020).

[S3] L. Lydersen, C. Wiechers, C. Wittmann, D. Elser, J. Skaar, and V. Makarov, Hacking commercial quantum cryptography systems by tailored bright illumination, *Nature Photon* **4**, 686 (2010).

[S4] I. Gerhardt, Q. Liu, A. Lamas-Linares, J. Skaar, C. Kurtsiefer, and V. Makarov, Full-field implementation of a perfect eavesdropper on a quantum cryptography system, *Nat Commun* **2**, 349 (2011).

[S5] V. Makarov, Controlling passively quenched single photon detectors by bright light, *New J. Phys.* **11**, 065003 (2009).

[S6] C. Wiechers, L. Lydersen, C. Wittmann, D. Elser, J. Skaar, C. Marquardt, V. Makarov, and G. Leuchs, After-gate attack on a quantum cryptosystem, *New J. Phys.* **13**, 013043 (2011).

[S7] H.-K. Lo, M. Curty, and B. Qi, Measurement-Device-Independent Quantum Key Distribution, *Phys. Rev. Lett.* **108**, 130503 (2012).

[S8] R. Renner, *Security of Quantum Key Distribution*, Ph.D. thesis, ETH Zurich (2005).

[S9] M. Tomamichel and R. Renner, Uncertainty Relation for Smooth Entropies, *Phys. Rev. Lett.* **106**, 110506 (2011).

[S10] M. Tomamichel, C. C. W. Lim, N. Gisin, and R. Renner, Tight finite-key analysis for quantum cryptography, *Nat Commun* **3**, 634 (2012).

[S11] D. Mayers, Quantum key distribution and string oblivious transfer in noisy channels, in *Advances in Cryptology — CRYPTO '96*, edited by N. Koblitz (Springer Berlin Heidelberg, Berlin, Heidelberg, 1996) pp. 343–357.

[S12] P. W. Shor and J. Preskill, Simple Proof of Security of the BB84 Quantum Key Distribution Protocol, *Phys. Rev. Lett.* **85**, 441 (2000).

[S13] M. Koashi, Simple security proof of quantum key distribution based on complementarity, *New J. Phys.* **11**, 045018 (2009).

[S14] K. Tamaki, M. Curty, G. Kato, H.-K. Lo, and K. Azuma, Loss-tolerant quantum cryptography with imperfect sources, *Phys. Rev. A* **90**, 052314 (2014).

[S15] G. Currás-Lorenzo, Á. Navarrete, M. Pereira, and K. Tamaki, Finite-key analysis of loss-tolerant quantum key distribution based on random sampling theory, *Phys. Rev. A* **104**, 012406 (2021).

[S16] H. Chernoff, A Measure of Asymptotic Efficiency for Tests of a Hypothesis Based on the sum of Observations, *The Annals of Mathematical Statistics* **23**, 493 (1952).

[S17] K. Tamaki, M. Curty, and M. Lucamarini, Decoy-state quantum key distribution with a leaky source, *New J. Phys.* **18**, 065008 (2016).

[S18] W. Wang, K. Tamaki, and M. Curty, Finite-key security analysis for quantum key distribution with leaky sources, *New J. Phys.* **20**, 083027 (2018).

[S19] W. Wang, K. Tamaki, and M. Curty, Measurement-device-independent quantum key distribution with leaky sources, *Sci Rep* **11**, 1678 (2021).

[S20] M. Pereira, G. Currás-Lorenzo, Á. Navarrete, A. Mizutani, G. Kato, M. Curty, and K. Tamaki, Modified BB84 quantum key distribution protocol robust to source imperfections, *Phys. Rev. Res.* **5**, 023065 (2023).

[S21] I. D. Ivanovic, How to differentiate between non-orthogonal states, *Physics Letters A* **123**, 257 (1987).

[S22] H.-K. Lo and J. Preskill, Security of quantum key distribution using weak coherent states with nonrandom phases, *Quantum Inf. Comput.* **7**, 431 (2007).

[S23] W. Hoeffding, Probability inequalities for sums of bounded random variables, *J. Am. Stat. Assoc.* **58**, 13 (1963).

[S24] K. Azuma, Weighted sums of certain dependent random variables, *Tohoku Mathematical Journal* **19**, 357 (1967).

[S25] G. Kato, Concentration inequality using unconfirmed knowledge (2020), arXiv:2002.04357 [quant-ph].

[S26] M. Hayashi and T. Tsurumaru, Concise and tight security analysis of the Bennett–Brassard 1984 protocol with finite key lengths, *New Journal of Physics* **14**, 093014 (2012).

[S27] G. Currás-Lorenzo, Á. Navarrete, K. Azuma, G. Kato, M. Curty, and M. Razavi, Tight finite-key security for twin-field quantum key distribution, *npj Quantum Inf* **7**, 22 (2021).

[S28] D. Tukary, S. Nahar, P. Sinha, and N. Lütkenhaus, Phase error rate estimation in QKD with imperfect detectors (2024), arXiv:2408.17349.

[S29] F. Xu, X. Ma, Q. Zhang, H.-K. Lo, and J.-W. Pan, Secure quantum key distribution with realistic devices, *Rev. Mod. Phys.* **92**, 025002 (2020).

[S30] M. Pittaluga, M. Minder, M. Lucamarini, M. Sanzaro, R. I. Woodward, M.-J. Li, Z. Yuan, and A. J. Shields, 600-km repeater-like quantum communications with dual-band stabilization, *Nat. Photon.* **15**, 530 (2021).

[S31] Á. Navarrete and M. Curty, Improved finite-key security analysis of quantum key distribution against Trojan-horse attacks, *Quantum Sci. Technol.* **7**, 035021 (2022).

[S32] T. Honjo, K. Inoue, and H. Takahashi, Differential-phase-shift quantum key distribution experiment with a planar light-wave circuit Mach–Zehnder interferometer, *Opt. Lett.* **29**, 2797 (2004).

[S33] F. Xu, K. Wei, S. Saeed, S. Kaiser, S. Sun, Z. Tang, L. Qian, V. Makarov, and H.-K. Lo, Experimental quantum key distribution with source flaws, *Phys. Rev. A* **92**, 032305 (2015).

[S34] Á. Navarrete, M. Pereira, M. Curty, and K. Tamaki, Practical Quantum Key Distribution That is Secure Against Side Channels, *Phys. Rev. Applied* **15**, 034072 (2021).

[S35] M. Lucamarini, Z. Yuan, J. Dynes, and A. Shields, Overcoming the rate–distance limit of quantum key distribution

without quantum repeaters, *Nature* **557**, 400 (2018).

[S36] D. Gottesman, H.-K. Lo, N. Lütkenhaus, and J. Preskill, Security of quantum key distribution with imperfect devices, *Quantum Inf. Comput.* **4**, 325 (2004).

[S37] A. Mizutani, G. Kato, K. Azuma, M. Curty, R. Ikuta, T. Yamamoto, N. Imoto, H.-K. Lo, and K. Tamaki, Quantum key distribution with setting-choice-independently correlated light sources, *npj Quantum Information* **5**, 8 (2019).

[S38] A. Mizutani and G. Kato, Security of round-robin differential-phase-shift quantum-key-distribution protocol with correlated light sources, *Phys. Rev. A* **104**, 062611 (2021).

[S39] K.-i. Yoshino, M. Fujiwara, K. Nakata, T. Sumiya, T. Sasaki, M. Takeoka, M. Sasaki, A. Tajima, M. Koashi, and A. Tomita, Quantum key distribution with an efficient countermeasure against correlated intensity fluctuations in optical pulses, *npj Quantum Inf* **4**, 1 (2018).

[S40] M. Pereira, G. Currás-Lorenzo, A. Mizutani, D. Rusca, M. Curty, and K. Tamaki, Quantum key distribution with unbounded pulse correlations, *Quantum Sci. Technol.* **10**, 015001 (2024).

[S41] F. Grünenfelder, A. Boaron, D. Rusca, A. Martin, and H. Zbinden, Performance and security of 5 GHz repetition rate polarization-based quantum key distribution, *Appl. Phys. Lett.* **117**, 144003 (2020).

[S42] A. Agulleiro, F. Grünenfelder, M. Pereira, G. Currás-Lorenzo, H. Zbinden, M. Curty, and D. Rusca, Modeling and Characterization of Arbitrary Order Pulse Correlations for Quantum Key Distribution (2025), arXiv:2506.18684 [quant-ph].

[S43] W.-Y. Hwang, Quantum key distribution with high loss: Toward global secure communication, *Physical Review Letters* **91**, 057901 (2003).

[S44] H.-K. Lo, X. Ma, and K. Chen, Decoy State Quantum Key Distribution, *Phys. Rev. Lett.* **94**, 230504 (2005).

[S45] X.-B. Wang, Beating the Photon-Number-Splitting Attack in Practical Quantum Cryptography, *Phys. Rev. Lett.* **94**, 230503 (2005).

[S46] M. Curty, F. Xu, W. Cui, C. C. W. Lim, K. Tamaki, and H.-K. Lo, Finite-key analysis for measurement-device-independent quantum key distribution, *Nat Commun* **5**, 3732 (2014).

[S47] C. C. W. Lim, M. Curty, N. Walenta, F. Xu, and H. Zbinden, Concise security bounds for practical decoy-state quantum key distribution, *Phys. Rev. A* **89**, 022307 (2014).

[S48] V. Zapatero, Á. Navarrete, K. Tamaki, and M. Curty, Security of quantum key distribution with intensity correlations, *Quantum* **5**, 602 (2021).

[S49] X. Sixto, V. Zapatero, and M. Curty, Security of Decoy-State Quantum Key Distribution with Correlated Intensity Fluctuations, *Phys. Rev. Applied* **18**, 044069 (2022).

[S50] S. Nahar, T. Upadhyaya, and N. Lütkenhaus, Imperfect phase randomization and generalized decoy-state quantum key distribution, *Phys. Rev. Appl.* **20**, 064031 (2023).

[S51] X. Sixto, G. Currás-Lorenzo, K. Tamaki, and M. Curty, Secret key rate bounds for quantum key distribution with faulty active phase randomization, *EPJ Quantum Technol.* **10**, 1 (2023).

[S52] G. Currás-Lorenzo, S. Nahar, N. Lütkenhaus, K. Tamaki, and M. Curty, Security of quantum key distribution with imperfect phase randomisation, *Quantum Sci. Technol.* **9**, 015025 (2023).

[S53] M. Sandfuchs, M. Haberland, V. Vilasini, and R. Wolf, Security of differential phase shift QKD from relativistic principles, *Quantum* **9**, 1611 (2025).